



25. ULUSAL ELEKTRON  
MİKROSKOPİ KONGRESİ

1. ULUSLARARASI MİKROSKOPİ  
ve SPEKTROSKOPİ KONGRESİ

22-24 EYLÜL 2021

EMK 2021

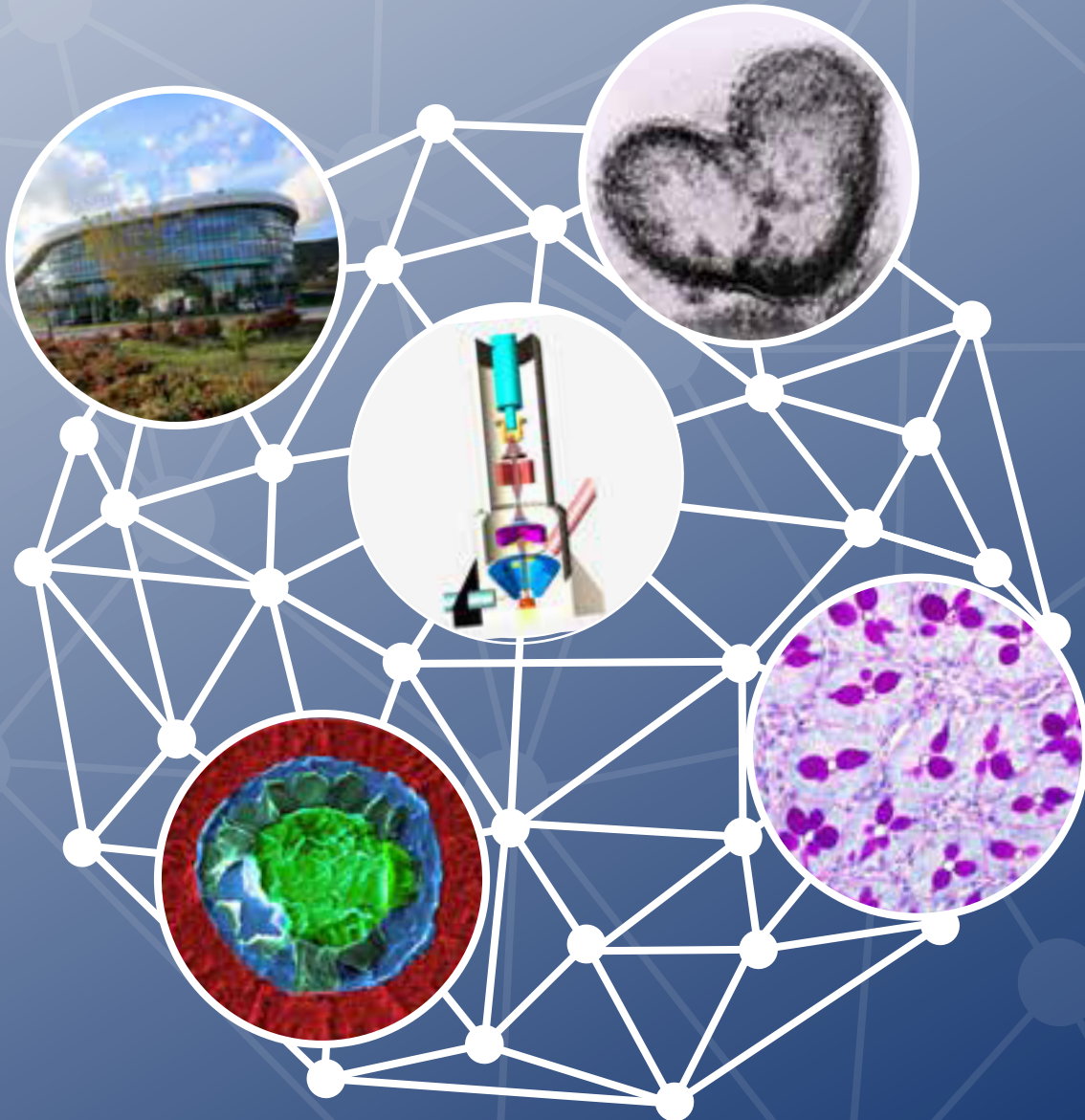
MSC 2021

1<sup>st</sup> INTERNATIONAL MICROSCOPY  
and SPECTROSCOPY CONGRESS

25<sup>th</sup> NATIONAL ELECTRON  
MICROSCOPY CONGRESS

22-24 SEPTEMBER 2021

# Book of Abstracts



[www.emk2021.com](http://www.emk2021.com)

[www.msc2021.com](http://www.msc2021.com)



25. ULUSAL ELEKTRON MİKROSKOPİ KONGRESİ  
1<sup>st</sup> INTERNATIONAL MICROSCOPY & SPECTROSCOPY CONGRESS

Publisher : Turkish Society for Electron Microscopy & Izmir Institute of Technology  
Edited by : Aziz Genç & Servet Turan  
Printing Layout : Tolga KOÇ  
Cover Design : Onur Nail Arda  
Composition : Arber Professional Congress Services

*The organizers do not have any legal liability for the contents of the abstracts.*

*Abstract Submission, reviewer evaluation and content process has been handled by  
MeetingHand Online Event Management Software.*

<https://meetinghand.com>

## Preface

Turkish Society for Electron Microscopy (TEMED) and İzmir Institute of Technology (IzTECH) are pleased to welcome you to the the 25th National Electron Microscopy Congress (EMK2021) and 1<sup>st</sup> International Microscopy and Spectroscopy Congress (MSC2021) as virtual congresses on September 22-24, 2021. This year marks the 50th anniversary of the TEMD and our national microscopy congress will be held online for the first time due to the pandemic all around the world. It would be our pleasure to welcome you in beautiful İzmir for such a monumental congress, but the health of our participants is our priority. Given the circumstances, we decided to take advantage of the convenience of an online event and organized the first ever International Microscopy and Spectroscopy Congress (MSC2021) along with the EMK2021. Such an international event would not have been possible without the international experience, community support and interest accumulated over the last 50 years. During this three-day virtual event, participants have the opportunity to hear speakers from all around the world on the wide variety of microscopy related research and technical developments in the fields of life sciences and materials sciences. The conference mainly focuses on:

- Biomaterials and regenerative medicine
- Cancer biology
- Cell death and its ramification
- Cryobiology
- Developmental and reproductive biology
- Neuroscience
- Pathology and clinical medicine
- Patogen biology
- Structure and dynamics of cell
- STEM cells
- Correlative microscopy and spectroscopy techniques for life sciences and materials sciences
- Catalysts
- Functional nanomaterials
- In-situ microscopy
- Nanofabrication
- Nano-imaging and spectroscopy
- Metals and alloys
- Thin films and interfaces

The opening plenary speech about the MINFLUX nanoscopy and related matters is given by Prof. Stefan W. Hell, who won the 2014 Nobel Prize in Chemistry for the development of super-resolved fluorescence microscopy. Three more plenary sessions comprise keynote lectures given by Prof. Toyoshi Fujimoto, Prof. Quentin Ramasse and Prof. Jordi Arbiol. The subjects of the congresses are divided into 29 sessions and 43 internationally renowned scientists have been invited to present state-of-the-art research they have been working on. The scientific program also includes contributed oral presentations and poster presentations, which are reviewed by our Scientific Committee. We are proud to mention that TEMD provided numerous registration grants to support the young scientists' contributions. In addition, several talks mentioning about the most advanced level technical developments in the fields of life sciences and materials sciences is included in the scientific program, which are given by our sponsors. Our ability to provide a high quality event would not be possible without their generous support.

We strongly believe that this conference will provide an inspiring discussion on the current issues and the state-of-the-art in the field of microscopy. We wish you a very stimulating and informative conference with a lot of excellent discussions and new insights into the various aspects of the microscopy research and technical developments. We also hope that the information shared during the congress and in this "Book of Abstracts" will stimulate new research, provide useful insights to the researchers across the fields of life sciences and materials sciences, and ultimately benefit the individuals who attended the congress.

**Aziz Genç & Servet Turan**

On behalf of the Organising Committee of MSC2021 and EMK2021

## COMMITTEES

### Organizing Committee

**Aziz GENÇ** (Chair – İzmir Institute of Technology)  
**Servet TURAN** (Co-Chair - Eskişehir Technical University)

**Serap ARBAK** (Acıbadem Mehmet Ali Aydınlar University)  
**Sevinç İNAN** (İzmir Economy University)  
**Mehtap KUTLU** (Eskişehir Technical University)  
**Nalan LİV** (University Medical Center Utrecht)  
**Gölnur KIZILAY ÖZFİDAN** (Trakya University)  
**Melek ÖZTÜRK** (İstanbul University – Cerrahpaşa)  
**Meltem SEZEN** (Sabancı University)  
**Y. Eren SUYOLCU** (Cornell University)  
**Deniz YÜCEL** (Acıbadem Mehmet Ali Aydınlar University)

### Honorary Board

**Prof. Yusuf Baran** (Rector of İzmir Institute of Technology)  
**Prof. Yurdağül CANBERK** (Honorary President of Turkish Society for Electron Microscopy)

### Local Organizing Committee – IzTECH

**Mustafa M. DEMİR** (Materials Science and Engineering)  
**Mehmet POLAT** (Director of Integrated Research Centers, Chemical Engineering Department)  
**Devrim PESEN-OKVUR** (Molecular Biology and Genetics)  
**Hasan ŞAHİN** (Photonics)  
**Serdar ÖZÇELİK** (Chemistry)  
**Cem ÇELEBİ** (Director of Center for Materials Research, Physics Department)  
**Özge TUNCEL** (Molecular Biology and Genetics)  
**Metin ÖZBEKLER** (Materials Science and Engineering)  
**Zeynep KAHRAMAN** (Photonics)

## INTERNATIONAL ADVISORY BOARD

### Life Sciences

Alper BAĞRIYANIK, **Turkey**  
John R. COUCHMAN, **Denmark**  
Özgür ÇINAR, **Turkey**  
Necdet DEMİR, **Turkey**  
Feriha ERCAN, **Turkey**  
Toyoshi FUJIMOTO, **Japan**  
Gamze GÜNEY, **Turkey**  
Pavel HOZAK, **Czech Republic**  
Bruno HUMBEL, **Japan**  
Serçin KARAHÜSEYİNOĞLU, **Turkey**  
Ümit KAYIŞLI, **USA**  
Haliem KENAR, **Turkey**  
Agnes KITTEL, **Hungary**  
Emel KOPTAGEL, **Turkey**  
Petek KORKUSUZ, **Turkey**  
Mehtap KUTLU, **Turkey**  
Nataša NESTOROVİĆ, **Serbia**  
Gülperi ÖKTEM, **Turkey**  
Kemal ÖZBİLGİN, **Turkey**  
Sait POLAT, **Turkey**  
Im Joo RHYU, **South Korea**  
Varol ŞAHİNTÜRK, **Turkey**  
Suzana ŠEGOTA, **Croatia**  
Gamze TANRIÖVER, **Turkey**  
Gamze TANRIVERDİ, **Turkey**  
A. Çevik TUFAN, **Turkey**  
José M. VALPUESTA, **Spain**  
Engin YENİLMEZ, **Turkey**  
Zahra ZAKERI, **USA**

### Materials Science

Hakan ATAPEK, **Turkey**  
Gülcan ÇORAPÇIOĞLU, **Turkey**  
Kemal DAVUT, **Turkey**  
Özgür DUYGULU, **Turkey**  
Corneliu GHICA, **Romania**  
Mehmet Ali GÜLGÜN, **Turkey**  
Y. Eren KALAY, **Turkey**  
Ali Arslan KAYA, **Türkiye**  
Pınar KAYA, **Germany**  
María de la MATA, **Spain**  
Umut SAVACI, **Turkey**  
Sašo STURM, **Slovenia**  
PengYi TANG, **People's Republic of China**  
Hilmi YURDAKUL, **Turkey**  
Kristina Žagar, **Slovenia**

### Instrumentation

Peter van AKEN, **Germany**  
Trevor ALMEIDA, **France**  
Roberto BALBONI, **Italy**  
Sinem BAŞKUT, **Turkey**  
Hasan DEMİRCİ, **Turkey**  
Martial DUCHAMP, **Singapore**  
Demie KEPAPTSOĞLOU, **UK**  
Kahraman KESKİNBORA, **USA**  
Vladislav KRZYZANEK, **Czech Republic**  
Sophie MEURET, **France**  
Ahmet ORAL, **Turkey**  
Cleva W. OW-YANG, **Turkey**  
Nick SCHRYVERS, **Belgium**  
Meltem SEZEN, **Turkey**  
Babacan UĞUZ, **Turkey**  
Burçin ÜNLÜ, **Turkey**  
Selim ÜNLÜ, **USA**  
Masashi WATANABE, **USA**

## SPONSORS

### Diamond Sponsors



### Gold Sponsors



Seeing beyond

### Other Sponsors



## Plenary / Invited Speakers



**Stefan W. Hell**

"MINIFLUX nanoscopy and related matters"

Max Planck Institute for Biophysical Chemistry,  
Germany



**Jordi Arbiol**

"Quantum nanomaterials at atomic scale: from growth mechanisms to local properties"

ICREA and Catalan Institute of Nanoscience and Nanotechnology (ICN2), CSIC & BIST  
Catalonia,



**Toyoshi Fujimoto**

"How lipid droplets go nuclear"

Juntendo University Graduate School of Medicine,  
Japan



**Quentin Ramasse**

"Recent developments in sub-100meV electron energy loss spectroscopy: from phonons to core losses in real and momentum space"

SuperSTEM Laboratory and University of Leeds,  
United Kingdom



**Peter van Aken**

"Electronic Structure Engineering Through Atomic-scale Strain Control in Complex Oxide Heterostructures"

Max Planck Institute for Solid State Research,  
Germany



**Tunç Akkoç**

"MSCs on the Road"

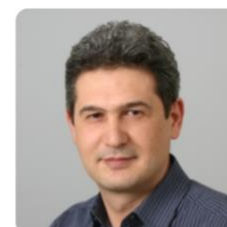
Marmara University,  
Turkey



**Cenk Oral Aktaş**

"Functional Surfaces: From Nature to Applications"

Christian-Albrechts-University · Institute of Materials Science,  
Germany



**Feridun Ay**

"Micro-Raman Spectroscopy of 2D TMDC Materials for Applications in Optoelectronics"

Eskişehir Technical University,  
Turkey



**Ömer Bayraktar**

"Mapping Human Tissue Architecture Using Spatial Genomics"

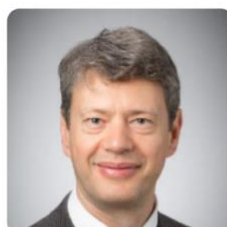
Wellcome Sanger Institute,  
UK



**Raymond Birge**

"Targeting Efferocytosis in Anti-Cancer Therapeutics"

The State University of New Jersey and New Jersey Medical School Cancer Center,  
USA



**Gianluigi Botton**

"Electron Energy Loss Spectroscopy with High Spatial and High Energy Resolution"

McMaster University,  
Canada



**Kevin Brindle**

"Imaging Tumor Metabolism with Mass Spectrometry and Magnetic Resonance Spectroscopic Imaging"

Cambridge University Cancer Research UK  
Cambridge Institute,  
UK



**Giovanna Cenacchi**

"Light and shadow in diagnostic electron microscopy of the future"

Alma Mater Università di Bologna,  
Italy



**Jerry Edward Chipuk**

"BAX-dependent Mitochondrial Outer Membrane Permeabilization: Exquisitely Regulated to the Point of Death."

Icahn School of Medicine at Mount Sinai,  
USA



**John R. Couchman**

"Emerging Roles for Syndecan Receptors in Disease"

University of Copenhagen,  
Denmark



**Hasan Demirci**

"Time-resolve Single-particle CryoEM Studies of Ribosome Complexes"

Koç University,  
Turkey



**Martial Duchamp**

"Operando and in Situ in a TEM Imaging in a Cryogenic Temperature Range"

Nanyang Technological University,  
Singapore



**Y. Murat Elçin**

"Recent Developments in Regenerative Biomaterials, Tissue Engineering and In Vitro Tissue Models"

Ankara University,  
Turkey



**Emre Erdem**

"Point Defects in Ceramics and Semiconductor Nanomaterials and Their Roles in Supercapacitors"

Sabancı University,  
Turkey



**Alev Erişir**

"Two and Three Dimensional Electronmicroscopy in Understanding Synaptic Circuits in Sensory Pathways"

University of Virginia,  
USA



**Maria de la Mata Fernandez**

"Electron Microscopy Characterization of Polymer-Based Materials"

Universidad de Cádiz  
Spain



**Vasif Hasırcı**

"Biomaterials, Microscopy and Spectroscopy"

Acibadem Mehmet Ali Aydınlar University,  
Turkey



**Pippa Hawes**

"Imaging Viruses by Electron Microscopy"

Pirbright Institute,  
UK



**Marc Heggen**

"Octahedral Pt-alloy Nanoparticle Fuel-cell Catalysts Studied by Analytical ex-and in-situ Electron Microscopy"

Ernst Ruska-Centre for Microscopy and Spectroscopy with Electrons (ER-C),  
Germany





**Pavel Hozak**

Institute of Molecular Genetics AS CR, Laboratory of Biology of the Cell Nucleus & IMG Microscopy Centre,  
**Czech Republic**



**Bruno Humbel**

"Volume Microscopy in Cell Biology: an Overview"  
Okinawa Institute of Science and Technology - OIST,  
**Japan**



**Lewys Jones**

"The STEM: a Nearly Perfect Instrument"  
Trinity College Dublin  
AMBER Research Centre,  
**Ireland**



**David Kaplan**

"Recent Advances with Silk Proteins - Functional Biomaterials for Medicine"  
Tufts University,  
**USA**



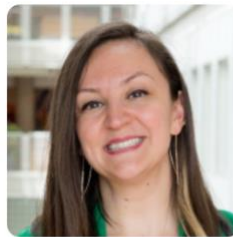
**Demie Kepaptsoglou**

"High Spatial and Energy Resolution Electron Microscopy of functional Oxides"  
SuperSTEM and University of York,  
**UK**



**Agnes Kittel**

"Electron Microscopy as the Gold Standard of the Extracellular Vesicle Research"  
Hungarian Academy of Sciences,  
**Hungary**



**Nalan Liv**

"Correlative live-cell – volume electron microscopy resolves metastasis related lysosomal subpopulations"  
University Medical Center Utrecht,  
**Netherlands**



**Mustapha Najimi**

"Immunomodulation of Inflammation: A Strategic Cell Therapy Approach to Target Acquired Liver Diseases"  
Promethera Therapeutics,  
**Belgium**



**Doğan Özkaya**

"Correlative Microscopy of Catalysts; from Device Level to Atomic Level"  
Diamond Light Source,  
**UK**



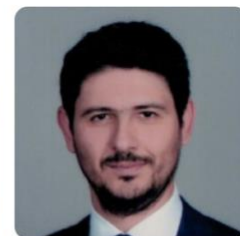
**Nurhan Özlü**

"Proteomic Analysis of Clear Cell Renal Cell Carcinoma"  
Koç University,  
**Turkey**



**Suzana Šegota**

"Nanoscale Characterisation on Functional Materials: Force Spectroscopy and Atomic Force Microscopy Beyond Imaging"  
Ruđer Bošković Institute,  
**Croatia**



**Uğur Serincan**

"Qualification of GaSb Epilayers Grown on Si Substrates"  
Eskişehir Technical University,  
**Turkey**



**Milica Manojlović-Stojanoski**

"Application of Stereology in Studying the Programming Consequences"

University of Belgrade, Serbia



**Berna Sözen**

"Deciphering Principles of Mammalian Early Embryogenesis in Development and Disease"

Yale School of Medicine, USA



**Eren Suyolcu**

"STEM as a Tool for the Design and Engineering of Functional Oxide Interfaces"

Cornell University, USA



**Umut Şahin**

"Pharmacological targeting of PML nuclear bodies in neurodegeneration"

Boğaziçi University, Turkey



**Tetsuro Takamatsu**

"Intraoperative Fluorescence Microscopy to Detect Metastatic Lesions in The Sentinel Lymph Nodes"

Kyoto Prefectural University of Medicine, Japan



**Fatih Toptan**

"Understanding the Degradation Mechanisms in Functionalized Load-bearing Metallic Biomaterials"

İzmir Institute of Technology, Turkey



**Hana Totary-Jain**

"The Role of mir-489(46) Cistron in Trophoblast Cell Lineage Specification"

University of South Florida, USA



**Peng Yi Tang**

"Engineering the Surface and Interface Structures of Catalysts for Water Splitting"

Shanghai Institute of Microsystem and Information, Chinese Academy of Sciences, People's Republic of China



**Paul Verkade**

"Cryo Fluorescence as a guide for Cellular Cryo Electron Tomography"

University of Bristol, UK



**Masashi Watanabe**

"Characterization of Single Atoms in Materials by Aberration-Corrected Scanning Transmission Electron Microscopy"

Lehigh University, USA



**Zahra Zakeri**

"Lipids and the Alteration of Viral Propagation"

Queens College of the City University of New York, USA

## TABLE OF CONTENTS

### PLENARY SPEAKERS

MINFLUX nanoscopy and related matters <i>Stefan W. Hell</i> .....	1
How lipid droplets go nuclear <i>Toyoshi Fujimoto</i> .....	2
Quantum nanomaterials at atomic scale: from growth mechanisms to local properties <i>Jordi Arbiol</i> .....	3
Recent developments in sub-100meV electron energy loss spectroscopy: from phonons to core losses in real and momentum space <i>Quentin Ramasse</i> .....	4

### INVITED SPEAKERS

Biomaterials, Microscopy and Spectroscopy <i>Vasif Hasirci</i> .....	5
Recent Advances with Silk Proteins - Functional Biomaterials for Medicine <i>David L. Kaplan</i> .....	6
Mapping human tissue architecture using spatial genomics <i>Ömer Ali Bayraktar</i> .....	7
Two and Three Dimensional Electronmicroscopy in Understanding Synaptic Circuits in Sensory Pathways. <i>Alev Erisir</i> .....	8
Electronic structure engineering through atomic-scale strain control in complex oxide heterostructures <i>Yu-Mi Wu, Ulrike Niemann, Gideok Kim, Georg Christiani, Minu Kim, Yi Wang, Y. Eren Suyolcu, Gennady Logvenov, Bernhard Keimer, Hidenori Takagi, Peter A. Van Aken</i> .....	9
High Spatial and Energy Resolution Electron Microscopy of Functional Oxides <i>Demie Kepaptsoglou</i> .....	10
The Role of mir-489(46) Cistron in Trophoblast Cell Lineage Specification <i>Ishani Wickramage, Richa Banerjee, Isabella Hetherington, Jeffrey VanWye, Umit A. Kayisli, Hana Totary-Jain</i> .....	11
Electron microscopy as the gold standard of the extracellular vesicle research <i>Agnes Kittel</i> .....	12
Pharmacological targeting of PML nuclear bodies in neurodegeneration <i>Umut ŞAHİN</i> .....	13
Engineering the Surface and Interface Structures of Catalysts for Water Splitting <i>Peng Yi Tang</i> .....	14

Octahedral Pt-alloy nanoparticle fuel-cell catalysts studied by analytical ex- and in-situ electron microscopy <i>Marc Heggen</i> .....	15
Correlative Microscopy of Catalysts; from Device Level to Atomic Level <i>Dogan Ozkaya</i> .....	16
Cryo Fluorescence as a guide for Cellular Cryo Electron Tomography <i>Paul Verkade</i> .....	17
Intraoperative fluorescence microscopy to detect metastatic lesions in the sentinel lymph nodes <i>Tetsuro Takamatsu</i> .....	18
Light and shadow in diagnostic electron microscopy of the future <i>Giovanna Cenacchi</i> .....	19
Proteomic Analysis of Clear Cell Renal Cell Carcinoma <i>Nurhan Özlü</i> .....	20
Imaging tumor metabolism with mass spectrometry and magnetic resonance spectroscopic imaging <i>Kevin M. Brindle</i> .....	21
Qualification of GaSb Epilayers Grown on Si Substrates <i>Uğur Serincan, Burcu Arpapay, Y. Eren Suyolcu, Gülcan Çorapçioğlu, Peter A. van Aken, Mehmet Ali Gülgün</i> .....	22
Application of Stereology in Studying the Programming Consequences <i>Milica Manojlović Stojanoski</i> .....	23
Nanoscale Characterisation on Functional Materials: Force Spectroscopy and Atomic Force Microscopy Beyond Imaging <i>Suzana Šegota</i> .....	24
Lipids and the Alteration of Viral Propagation <i>Zahra Zakeri</i> .....	25
Characterization of Single-Atoms in Materials by Aberration-Corrected Scanning Transmission Electron Microscopy <i>Masashi Watanabe</i> .....	26
Electron Energy Loss Spectroscopy with High Spatial and High Energy Resolution. <i>Gianluigi Botton</i> .....	27
STEM as a Tool for the Design and Engineering of Functional Oxide Interfaces <i>Y. Eren Suyolcu, Gennady Logvenov, Darrell G. Schlom, Peter A. van Aken</i> .....	28
Correlative live-cell – volume electron microscopy resolves metastasis related lysosomal subpopulations <i>Nalan Liv</i> .....	29
Emerging Roles for Syndecan Receptors in Disease <i>John R. Couchman</i> .....	30
Volume Microscopy in Cell Biology: An Overview <i>Bruno M. Humbel</i> .....	31

Imaging Viruses by Electron Microscopy <i>Pippa Hawes</i> .....	32
Operando and in situ in a TEM imaging in a cryogenic temperature range <i>M. Duchamp, E. Tiukalova, J. Vas, R. Ignatans, A.D. Mueller, R. Medwal, R.S. Rawat, V. Tileli</i> .....	33
The STEM: a nearly perfect Instrument <i>Lewys Jones</i> .....	34
MSCs on the road. <i>Tunç Akkoç</i> .....	35
Immunomodulation of Inflammation: A Strategic Cell Therapy Approach to Target Acquired Liver Diseases <i>Mustapha Najimi</i> .....	36
Recent Developments in Regenerative Biomaterials, Tissue Engineering and In Vitro Tissue Models <i>Y. Murat Elçin</i> .....	37
Point Defects in Ceramics and Semiconductor Nanomaterials and Their Roles in Supercapacitors <i>Emre Erdem</i> .....	38
Electron Microscopy Characterization of Polymer-Based Materials <i>María de la Mata Fernández</i> .....	39
Deciphering Principles of Mammalian Early Embryogenesis in Development and Disease <i>Berna Sozen</i> .....	40
Understanding the degradation mechanisms in functionalized load-bearing metallic biomaterials <i>Fatih Toptan</i> .....	41
BAX-dependent Mitochondrial Outer Membrane Permeabilization: Exquisitely Regulated to the Point of Death. <i>Jerry Edward Chipuk</i> .....	42
Micro-Raman Spectroscopy of 2D TMDC Materials for Applications in Optoelectronics <i>Feridun Ay</i> .....	43
Targeting Phosphatidylserine/TAM receptor/PD-L1 axis as a vulnerability in cancer <i>Raymond B. Birge</i> .....	44
Nuclear Phosphoinositides and Phase separation: Nuclear Lipid Islets and their importance in regulation of RNA Polymerase II driven transcription. <i>Pawel Hozak</i> .....	45
Beta Cell Golgi Stress Response to Glucolipototoxicity: Morphologic Changes After Metabolic Stress <i>Yaprak Yalçın, Neslihan Bascil Tutuncu, Hatice Pinar Baysan Cebi, Hasibe Verdi, Suleyman Erol, Figen Kaymaz</i> .....	46
Who is the ADAMTS family? <i>Tuba Parlak Ak</i> .....	47

PC-3 prostat kanseri hücrelerinde fenformin uygulamasının FGFR2 üzerine etkileri <i>Dilan Çetinavcı, Melike Özgül Önal, Gürkan Yiğittürk, Volkan Yaşar, Hülya Elbe, Feral Öztürk</i> .....	48
Effect of Melatonin on tumor growth and MDSCs in breast cancer model with circadian rhythm impairment <i>Sayra Dilmac, Sendegul Yildirim Ildem, Gamze Tanrıover</i> .....	49
Breath analysis by FTIR spectroscopy for early detection of lung cancer <i>Dilek Yonar, Deniz Köksal, Ülkü Yılmaz</i> .....	50
Reversal from Taxane-Induced apoptosis in metastatic prostate cancer cells: Molecular effect of anastasis <i>Gamze Guney Eskiler, Asuman Deveci Ozkan, Melek Ozturk, Serap Arbak</i> .....	51
Seramidaz inhibisyonunun rat glioma hücreleri üzerine etkilerinin araştırılması <i>Canan Vejselova Sezer, Hatice Mehtap Kutlu</i> .....	52
Evaluation of the cancer biology research concept: GBM and astrocyte membrane topology, morphology and chemistry <i>Berrin Ozdil Bay, Duygu Calik-Kocaturk, Cisem Altunayar-Unsalan, Eda Acikgoz, Fatih Oltulu, Volkan Gorgulu, Aysegul Uysal, Gulperi Oktem, Ozan Unsalan, Huseyin Aktuğ</i> .....	53
<i>In Vitro</i> investigation of the effect of <i>Trifolium pratense</i> L. on C6 glioblastoma cells <i>Gamze Tanrıverdi, Aynur Abdulova, Hatice Çölgeçen, Belisa Kaleci, Tuğba Ekiz-Yılmaz</i> .....	54
İnsan semen kriyoprezervasyonunda Koenzim Q10 ve Kurkuminin Spermatozoon ince yapısı üzerine etkileri <i>Derya Özdemir Taş, İ. Sinan Özkavukcu, Esra Erdemli, İrem İnanç, Kenan Köse, Kaan Aydos</i> .....	55
The potential role of Sox9 in embryo implantation and decidualization <i>Cemre Nur Balci, Nuray Acar Aydemir, Ezgi Golal, Ismail Ustunel, Ozlem Ozbey Unlu</i> .....	56
Role of hippo signaling pathway in peri-implantation period mouse uterus <i>Ezgi Golal, Nuray Acar aydemir, Cemre Nur Balci, İsmail Üstünel</i> .....	57
The Effect of DHEA on Liver and Kidney of Young Male Rats <i>Gozde Erkanli Senturk, Fatma Beyza Sag, Hakan Sahin, Zehra Sezer</i> .....	58
The Use of CRISPR/Cas9 systems for the evaluation of implantation parameters in a Three-Dimensional implantation model <i>Gizem Söyler, Gizem Nur Şahin, Mehmet Yunus Çomar, Alişan Kayabölen, Ali Cihan Taşkın, Ahmet Kocabay, Serçin Karahüseyinoğlu</i> .....	59
Linagliptinin İnsülin İle birlikte kullanımı Tip 1 diyabetik fare ovariumunda Pro-apoptotik Chop/Ddit3 mRNA ifadesini azaltır <i>Aslı Okan Oflamaz, Necdet Demir</i> .....	60
Boric acid supplementation in embryo culture medium treatment vitrified mouse embryo by Solid Surface Vitrification (SSV) <i>Ali Cihan Taskin, Ahmet Kocabay</i> .....	61
Effects of intraperitoneal and intranasal oxytocin administrated rat ovaries <i>Zehra Sezer, Gozde Erkanli Senturk, Hakan Sahin, Basak Isildar, Aynur Abdulova</i> .....	62

One step closer to lung regeneration: Detailed morphological examination of neotenic and metamorphic axolotl lungs. <i>Arzu Güneş, Duygu Gürsoy Gürgen, Arife Ahsen Kaplan, İlkay Özdemir, İlknur Keskin</i> .....	63
The healing effect of apocynin in monosodium glutamate- induced testis damage <i>Merve Acikel Elmas, Salva Asma Algilani, Ozlem Bingol Ozakpinar, Serap Arbak</i> .....	64
The effect of melatonin on TLR4 related inflammatory pathway in the Parkinson's disease model <i>Sendegul Yildirim Ildem, Gamze Tanriover, Ayse Ozkan, Aysel Agar</i> .....	65
The effects of intranasal applied oxytocin loaded nanoparticles on seizures, memory, and hippocampal regeneration <i>Hakan Sahin, Oguz Yucel, Serkan Emik, Gozde Erkanli Senturk</i> .....	66
Repurposing of PARP inhibitors as neuroprotective agents on retinal degenerations <i>Pakize Nur Akkaya, Cigdem Elmas, Eberhart Zrenner, Ayse Sahaboglu</i> .....	67
The effect of Selenium on morphological changes in hippocampus and cerebral cortex of scopolamine induced Alzheimer's <i>Alev Cumbul, Dilara Baban, Elif Çiğdem Keleş, İzem Öngünşen, Ece Genç</i> .....	68
Stereological and electron microscopic approaches for analyzing of peripheral nerve regeneration <i>Burcu Delibaş, Süleyman Kaplan</i> .....	69
Effect of melatonin and curcumin treatments on the bladder in renal ischemia/reperfusion injury: A histopathological study <i>Sude Topkaraoğlu, Tansel Sapmaz</i> .....	70
Evaluation of the effects of apocynin on kidney and bladder in high-fat diet-induced obese rats <i>Fatma Kanpalta, Büşra Ertaş, Göksel Şener, Feriha Ercan</i> .....	71
Investigation the protective effects of Quercetin on carbon tetrachloride induced hepatotoxicity with light and electron microscopy <i>Nebahat Ince, Ozlem Goruroglu Ozturk, Yasar Sertdemir, Yusuf Kenan Daglıoglu, Yurdun Kuyucu</i> .	72
Investigation of MiR-26b and MiR-27b expressions and the effect of Quercetin on Pulmonary Fibrosis <i>Çağrı Toker, Ufuk Özgü Mete, Yurdun Kuyucu, Samet Kara, Dilek Şaker, Bilge Güzelel</i> .....	73
Protective effects of rosmarinic acid against cyclophosphamide induced testicular toxicity in rats <i>Ahmet Uğur Akman, Dilan Çetinavcı, Engin Yenilmez, Ahmet Alver, Neslihan Sağlam</i> .....	74
Distribution of TNF- $\alpha$ and PCNA in Experimental Type-1 Diabetic and Nigella sativa Oil treated Rat Tongue <i>Ugur Seker, Seval Kaya, Yusuf Nergiz</i> .....	75
Effects of Rosmarinic acid against corneal toxicity of cisplatin <i>Engin Yenilmez, Abdülkadir Kutlu, Birgül Gür Kutlu</i> .....	76
The effects of dose-dependent chronic caffeine consumption in a rat burn wound model <i>Selma Aydemir, Filiz Yılmaz, Bayram Yılmaz, Orkun İlgen, Sefa Kurt, Başak Baykara</i> .....	77
The effects of pterostilbene on cyclophosphamide-induced kidney and bladder injury in rats <i>Gökçen Kerimoğlu, Tuğba Arıcı, Ayşe Firuze Bıyık, Ali Kulaber, Yüksel Aliyazıcıoğlu, Selim Demir, Nihal Turkmen, Engin Yenilmez</i> .....	78

Human amnion membrane derived MSCs can ameliorate irradiation induced testicular damage by reducing oxidative stress <i>Busra Cetinkaya Un, Burak Un, Meryem Akpolat, Yusufhan Yazir</i> .....	79
Farklı yüzey kaplamalarına ve fiziksel özelliklere sahip altın nanomateryallerin, farelerdeki histolojik değişimlere etkileri <i>İlyas Özçiçek, Nilüfer Ulaş Aytürk, Neşe Ayşit</i> .....	80
Increased differentiation efficacy of neural stem cell with the combination of three growth factors loaded nanoparticles <i>Ayşegül Açıkarsarı, Serap Mert, Zehra Seda Halbutoğulları, Deren Aslan, Yusufhan Yazir</i> .....	81
Linking microstructure and transport properties in Sm/Yb-doped AlN ceramics <i>Pinar Kaya, Eren Suyolcu, Peter A. van Aken, Servet Turan, Giuliano Gregori, Joachim Maier</i> .....	82
TEM investigations of hydrothermally synthesized pure and Al Doped Zinc Tin Oxide Nano Powders <i>Umut Savacı, Cem Açıkarsarı, Ender Suvacı, Servet Turan</i> .....	83
Synthesis of multilayer graphene encapsulated FE nanoparticles by chemical vapor deposition using ferrocene precursors <i>Siddika Mertdinç, Berk Çağatay Demiralın, Yunus Emre Sürmeli, Bilge Umay Korkmaz, Mehmet Erinç Serten, M. Lütfi Öveçoğlu, Duygu Ağaoğulları</i> .....	84
A detailed investigation on mesoporous NiS <sub>2</sub> Pre-Electrocatalyst by electron microscopy tools for a Hydrogen Evolution Reaction <i>Cüneyt Karakaya, Sarp Kaya</i> .....	85
Molibden Borür Tozlarının Sentezi ve Karakterizasyonu <i>İlayda Süzer, Esin Aysel, Siddika Mertdinç, Hasan Gökçe, Mustafa Lütfi Öveçoğlu, Duygu Ağaoğulları</i> .....	86
SEM-EDS investigation of Magnesium ZWO Alloys <i>Halil Demirtaş, Önder Tuna, Özgür Duygulu, Deniz Sultan Aydın, Metin Usta, Youngkil Jung, Wonseok Yang, Hyun Kyu Lim</i> .....	87
HRTEM-EDS-SAED Studies of Quasicrystal I-Phase in Mg-Zn-Y Alloys <i>Önder Tuna, Halil Demirtaş, Deniz sultan Aydın, Özgür Duygulu, Metin Usta, Youngkil Jung, Wonseok Yang, Hyun Kyu Lim</i> .....	88
K-Band uygulamaları için GaN temelli yüksek elektron mobiliteli transistör (HEMT) <i>Yıldırım DURMUŞ, Vahit BARIŞ, Selim ÇELİK, Gizem TENDÜRÜS, Büşra Çankaya AKAOĞLU, Doğan YILMAZ, Ekmel ÖZBAY</i> .....	89
Doku mühendisliği uygulamaları için gözenekli kompozit doku iskelelerinin üretimi ve mikroyapısal karakterizasyonu <i>Büşra Bulut, Şeyma Duman</i> .....	90
Microfluidics based single-bacterium imaging for probing role of stress factors on bacterial growth <i>Didem Rodoplu, Cheryng-Shyang Chang, Cheng-Yuan Kao, Chia-Hsien Hsu</i> .....	91
Towards “Damage-Free” TEM specimen preparation by Focused Ion Beam without Gallium <i>Chengge Jiao</i> .....	92



<i>In vitro</i> modellerde korelatif ışık ve elektron mikroskopisinin üç boyutlu olarak uygulanması <i>Mehmet Şerif AYDIN</i> .....	93
Combining crossbeam laser and X-Ray microscopy: Massive material removal and ultrafast site-specific sample preparation. <i>Jens Peter Hermann Gnauck</i> .....	94
Effects Of Carbonyl Cyanide Phenylhydrazone (CCCP) On Mitochondria in Human Hepatocellular Carcinoma (HepG2) Cell Line <i>Yaprak Yalçın, Hatice Pınar Baysan Cebi, Hasibe Verdi, Deniz Ekin Doğan, F. Figen Kaymaz, F. Belgin Atac</i> .....	95
Electron Microscopic Investigation of the Effect of Trifolium Pratense on C6 Glioblastoma Cells <i>Gamze Tanriverdi, Aynur Abdulova, Hatice Colgecen, Havva Atar, Belisa Kaleci, Tuğba Ekiz-Yılmaz</i> .....	96
Morphological evaluation of the effects of Apocynin on MSG induced liver damage in rats <i>Begum Sahin, Merve Acikel Elmas, Serap Arbak</i> .....	97
Çam kabuğu özütünün over (MDAH) kanseri hücre kültürü modelinde antikanser, antiproliferatif ve apoptotik etkilerinin incelenmesi <i>Gazi Contuk, Mücahit Seçme, Yavuz Dodurga, Meltem Taş, Gülşen Tel Çayan, Gülçin Abban Mete</i> .....	98
Activation of nesfatin-1 neurons by cytidine-5'-diphosphate choline through cholinergic receptors. <i>Gonca Topal, İlker Mustafa Kafa, Nursel Hasanoğlu Akbulut, Cenk Coşkun, Vahide Savci, Özhan Eyigör</i> .....	99
İnme modelinde arı sütü ve içeriğinde bulunan 10-HDA maddesinin astrosit reaksiyonuna etkileri <i>Nursel Hasanoğlu Akbulut, Casısu Koç, Gonca Topal, Mehmet Cansev, Özhan Eyigör</i> .....	100
Yüksek yağlı diyetle indüklenen obezitenin böbrek ve mesane hasarı üzerine myrtus communis ekstraktının koruyucu etkileri <i>Fatma Kanpalta, Büşra Ertaş, Göksel Şener, Feriha Ercan</i> .....	101
Effects of vitaminD supplementation on aorta morphology in high fat/high fructose diet induced metabolic syndrome rats <i>Betül Zorkaya, Ayşe Seda Akdemir, Fatma Kaya Dagistanli, Aynur Abdulova, Gamze Tanriverdi, Evrim Komurcu-Bayrak</i> .....	102
Effects of Resveratrol on inflammation and ER stress related apoptosis in fructose-fed streptozotocin induced diabetes <i>Fatma Kaya Dagistanli, Ayşe Seda Akdemir, Merve Anapali, Aynur Abdulova, Gamze Tanriverdi, Turgut Ulutin, Melek Ozturk</i> .....	103
Dimetiloksalilglisin ile ön koşullandırılan mezenkimal kök hücrelerden elde edilen şartlandırılmış medyum özelliklerinin incelenmesi <i>Hanife Nurdan Olcar, Başak Işıldar, Serbay Özkan, Meral Koyutürk</i> .....	104
Investigation of the TRF Conjugated Polymeric Nanoparticles Efficiency <i>In vitro</i> Blood Brain Barrier Model <i>Ayşegül Açıkşarı, Yusufhan Yazır, Serap Mert, Omur Özcan, Zehra Seda Halbutoğulları</i> .....	105
Lead Chalcogenide Quantum Dot Solar Cells <i>Selçuk Birdoğan</i> .....	106

A simple desolvation method for production of cationic albumin nanoparticles with improved drug loading <i>Tugce Özmen Egesoy, Sumeyra Cigdem Sozer, Yasar Akdogan</i> .....	107
In situ crystallization of amorphous films of Sb <sub>2</sub> S <sub>3</sub> <i>Aleksandr Bagmut, Ivan Bagmut</i> .....	108
HAADF imaging of vanadium oxide thin films: spontaneous conversion of film pores with thermal annealing <i>Emrah Dirican, Ramis Mustafa Öksüzoğlu</i> .....	109
Effect of surface treatment on the SiN passivation of AlGa <sub>N</sub> /Ga <sub>N</sub> HEMT <i>Gizem Karaca, İdil Karakuş, Elif Alagöz, Ahmet Serhat Dinçer, Doğan Yılmaz, Ekmel Özbay</i> .....	110
Çift katmanlı Si <sub>3</sub> N <sub>4</sub> dielektrik tabakası ile AlGa <sub>N</sub> /Ga <sub>N</sub> HEMT aygıtların üretimi <i>Yıldırım Durmuş, Doğan Yılmaz, Ceren Tayran, Ekmel Özbay</i> .....	111
Ex Vitro ve İn Vitro Ortamda Yetiştirilen Doğal Tetraploid <i>Trifolium pratense</i> L. Köklerinin Karşılaştırmalı İnce Yapısı <i>Havva Karahan, Hatice Çölgeçen</i> .....	112
Optimizing a workflow for cryo-TEM tomography – fabrication and transfer of frozen hydrated lamella <i>Dominik Pinkas, Samuel Zachej, Jana Havrankova, Helena Raabova, Erik Vlcek, Saskia Mimiety-Oeckler, Robert Kirmse, Pavel Hozak, Vlada Filimonenko</i> .....	113
Thermo Fisher Scientific EM workflows; Developed for the masses <i>Emine Korkmaz, Gaurav Sharma, Max Maletta, Lavery Leah, Anke Mulder</i> .....	114
A novel concept in fluorescence lifetime imaging enabling video-rate confocal FLIM <i>Jens Peter Gabriel</i> .....	115

# Plenary Speakers

## MINFLUX nanoscopy and related matters

**Stefan W. Hell**

*Max Planck Institute for Biophysical Chemistry, Göttingen &  
Max Planck Institute for Medical Research, Heidelberg*

I will show how an in-depth description of the basic principles of diffraction-unlimited fluorescence microscopy (nanoscopy) [1-3] has spawned a new powerful superresolution concept, namely MINFLUX nanoscopy [4]. MINFLUX utilizes a local excitation intensity minimum (of a doughnut or a standing wave) that is targeted like a probe in order to localize the fluorescent molecule to be registered. In combination with single-molecule switching for sequential registration, MINFLUX [4-6] has obtained the ultimate (super)resolution: the size of a molecule. MINFLUX nanoscopy, providing 1–3 nanometer resolution in fixed and living cells, is presently being established for routine fluorescence imaging at the highest, molecular-size resolution levels. Relying on fewer detected photons than popular camera-based localization, MINFLUX nanoscopy is poised to open a new chapter in the imaging of protein complexes and distributions in fixed and living cells.

- [1] Hell, S.W., Wichmann, J. Breaking the diffraction resolution limit by stimulated emission: stimulated-emission-depletion fluorescence microscopy. **Opt. Lett.** 19, 780-782 (1994).
- [2] Hell, S.W. Far-Field Optical Nanoscopy. **Science** 316, 1153-1158 (2007).
- [3] Hell, S.W. Microscopy and its focal switch. **Nat. Methods** 6, 24-32 (2009).
- [4] Balzarotti, F., Eilers, Y., Gwosch, K. C., Gynnå, A. H., Westphal, V., Stefani, F. D., Elf, J., Hell, S.W. Nanometer resolution imaging and tracking of fluorescent molecules with minimal photon fluxes. **Science** 355, 606-612 (2017).
- [5] Eilers, Y., Ta, H., Gwosch, K. C., Balzarotti, F., Hell, S. W. MINFLUX monitors rapid molecular jumps with superior spatiotemporal resolution. **PNAS** 115, 6117-6122 (2018).
- [6] Gwosch, K. C., Pape, J. K., Balzarotti, F., Hoess, P., Ellenberg, J., Ries, J., Hell, S. W. MINFLUX nanoscopy delivers multicolor nanometer 3D-resolution in (living) cells. (bioRxiv, doi: <https://doi.org/10.1101/734251>)

## **How lipid droplets go nuclear**

**Toyoshi Fujimoto**

*Juntendo University Graduate School of Medicine  
Tokyo, Japan*

Lipid droplets (LDs) are organelles related to a variety of cellular functions. In recent years, LDs in the cytoplasm have been studied intensively, whereas LDs in the nucleus have not been paid much attention because they are much fewer in number. We set out to study nuclear LDs several years ago and found that they form by two different mechanisms: that is, nuclear LDs in hepatocytes are derived from lipoprotein precursors in the ER lumen, whereas those in non-hepatocytes are generated by triglyceride synthesis in the inner nuclear membrane. These results show the unique properties of nuclear LDs, but more importantly, they indicate presence of active lipid metabolism inside the nucleus. In the present lecture, I will talk about how nuclear LDs form and what functions they may have.

## Quantum nanomaterials at atomic scale: from growth mechanisms to local properties

Jordi Arbiol<sup>1,2\*</sup>

<sup>1</sup>Catalan Institute of Nanoscience and Nanotechnology (ICN2), CSIC and BIST, Campus UAB, Bellaterra, 08193 Barcelona, Catalonia, Spain

<sup>2</sup>ICREA, Pg. Lluís Companys 23, 08010 Barcelona, Catalonia, Spain

\*arbiol@icrea.cat

Hybrid superconductor/semiconductor-based quantum devices (e.g.: for quantum computing applications) are mainly based on 3 different technologies: vapour-liquid-solid (VLS) grown vertical nanowires, selected area growth (SAG) nanowire networks and 2-dimensional electron gases (2DEG).

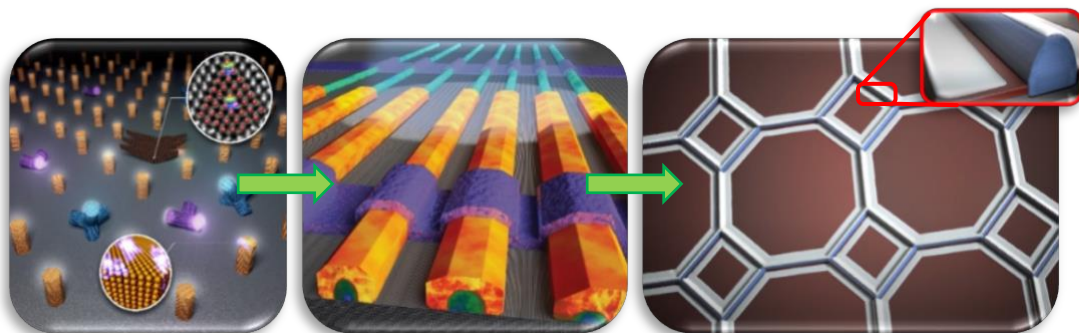
First of all, by using atomic-scale aberration corrected Scanning Transmission Electron Microscopy (AC STEM) and 3D modelling, we will study the influence of polarity on the development and properties of these complex NW-like hybrid heterostructures vertically grown by VLS.[1-5]

In a second part, we will show the natural evolution of this vertical technology to the flat growth of NW networks on III-V substrates. Developing growth techniques towards horizontally assembled semiconductor nanowire networks base on SAG is essential to promote their integration into large-scale functional circuit platforms and devices for electronic, photonic and quantum applications and more over to address a high scalability. In these complex core@shell or confined multilayer nanostructure configurations, strain relaxation mechanisms during the epitaxial growth play a key role in determining their final morphology, crystal structure and physical properties. To analyze these mechanisms, in the present work, atomic-scale Cs-corrected Scanning Transmission Electron Microscopy studies are performed on horizontal arrays of nanowires. Core morphology-dependent strain fields, involving plane bending and the resulting formation of low angle polar boundaries, are observed. The origin of this phenomenon and its consequences on the electronic band structure are discussed. Monochromated Valence Electron Energy Loss Spectroscopy is employed to spatially map the heterostructure's bandgap with sub-nanometer resolution and certify the influence of the high mismatch induced strain on the topological electronic properties at the interface of the core-shell region. These findings highlight the importance and potential of accurate sub-nanometer-level understanding of the structure-property relations in the novel SAG and guided growth mechanisms of heterostructured semiconductor nanowire networks.[6-10]

Finally, we will address the newly developed 2DEG heterostructures based on SiGe, fully compatible with CMOS technology, where the strain and composition at the Ge quantum wells will determine their final quantum properties [11,12].

### Reference:

- [1] M. de la Mata, et al., Nano Letters, **12**, 2579 (2012)
- [2] M. de la Mata, et al., Nano Letters, **14**, 6614 (2014)
- [3] M. de la Mata, et al., Nano Letters, **16**, 825 (2016)
- [4] M. de la Mata, et al., Nano Letters, **19**, 3396 (2019)
- [5] M. Zamani, et al., Advanced Materials, **32**, 2001030 (2020)
- [6] E. Oksenberg, et al., ACS Nano, **11**, 6155 (2017)
- [7] S. Vaitiekėnas, et al., Physical Review Letters, **121**, 147701 (2018)
- [8] F. Krizek, et al., Physical Review Materials, **2**, 093401 (2018)
- [9] M. Friedl, et al., Nano Letters, **18**, 2666 (2018)
- [10] P. Aseev, et al., Nano Letters, **19**, 218 (2019)
- [11] K. Aggarwal, et al., Physical Review Research, **3**, L022005 (2021)
- [12] D. Jirovec, et al., Nature Materials, <https://doi.org/10.1038/s41563-021-01022-2> (2021)



Semiconductor nanowires (*r*)evolution: from vapour liquid solid to guided growth and selected area

## **Recent developments in sub-100meV electron energy loss spectroscopy: from phonons to core losses in real and momentum space**

**Quentin Ramasse**

*SuperSTEM Laboratory and University of Leeds, United Kingdom*

The functional properties of materials are increasingly controlled and tuned through structural or chemical architectures whose engineering takes place at the nano or even atomic level. This enables emergent properties relying on the interplay between charge, spin or local atomic-scale chemistry. A particularly powerful means of characterization of these physico-chemical effects lies within a combination of high-resolution scanning transmission electron microscopy and energy-loss spectroscopy (STEM-EELS). Recent instrumentation advances have pushed the energy resolution of these instruments below 10meV while maintaining atomic sized probes, thus truly realizing the promise of placing a ‘synchrotron in a microscope’ [1].

As a result, it is now possible to fingerprint the functional chemistry of materials as diverse as organic grains in chondrites or metal organic framework glass blends at the nano-scale while simultaneously correlating it with their vibrational response in the sub 100meV energy range. This enables a direct comparison with bulk optical characterization at unprecedented length scales [2]. Further methodological developments have demonstrated the ability to balance momentum and spatial resolution to either determine the electronic band structure of materials in momentum space from nanometre-sized volumes or carry out phonon spectroscopy at the atomic scale, culminating recently in the observation of a phonon signature localized at a single atom defect [3].

It is expected that building on these recent achievements, further improvements in energy resolution and the introduction of new direct/hybrid electron detectors will widen the range of chemistries that can be spectroscopically and spatially resolved, providing the ideal spectroscopic tool to understand the nanoscale organisation of organic and metal-organic bonding and complex interfacial structures in emerging hybrid composite materials.

[1] Q.M. Ramasse, *Ultramicroscopy* 180, 41-51 (2017).

[2] S. Collins et al., *NanoLetters* 20, 1272-1279 (2020).

[3] F.S. Hage et al., *Science Advances* 4, eaar7495 (2018); F.S. Hage et al., *Science* 367, 1124 (2020).

# Invited Speakers

## Biomaterials, Microscopy and Spectroscopy

Vasif Hasirci

*Faculty of Engineering, Medical Engineering, Acibadem Mehmet Ali Aydınlar University, Istanbul, Turkey*

Biomaterials is the field where materials and devices are developed to support the function of disabled or ineffective tissues or organs. This is done by developing implants and devices without any biological components, tissue engineering products with cells, spheroids and organoids and bioactive compounds. In order to design effective devices characterization and analysis is needed with many techniques available during the design, application and post application phases. This is where microscopy using a variety of techniques and spectroscopy come into the picture. The most frequently used microscopic techniques are confocal laser scanning microscopy (CLSM), fluorescence microscopy, scanning electron microscopy (SEM), transmission electron microscopy (TEM), and atomic force microscopy (AFM). Among the almost numerous spectroscopic techniques used are Ultraviolet Visible Spectroscopy (UV-Vis), Fourier Transform Infrared Spectroscopy (FTIR), GC-MS (Gas Chromatography-Mass Spectroscopy), X-ray photoelectron spectroscopy (XPS). SEM is mostly used to study the 3D exterior of a medical device whether it is a scaffold or a contact lens and relatively simple compared TEM which requires detailed preparation protocols to be followed. TEM in the biomaterials and tissue engineering field is for highly magnified examination of tissue-material interactions and changes in cell and tissue organization. CLSM and fluorescence microscopy are mostly for cell behavior, viability, interaction, deformation and orientation studies and are applicable to cell culture studies under in vitro conditions, in vivo studies and hydrogel-based tissue engineering studies. Fig 1 shows the drastic difference in the behavior of one cell type in two chemically different natural hydrogels. The spectroscopic studies are generally for characterization during medical device preparation and chemical changes during interaction with the biological media. In this paper examples of most will be presented to give an idea as to how they are used in biomaterials and tissue engineering and also to stress their importance in our field.

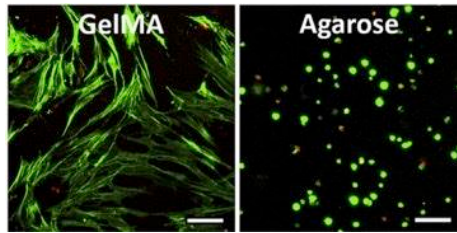


Fig 1. Fibrochondrocytes entrapped in GelMA and Agarose. (G.Bahcecioglu et al, Biomaterials 218 (2019) 119361)

## **Recent Advances with Silk Proteins - Functional Biomaterials for Medicine**

**David L. Kaplan**

*Stern Family Endowed Professor of Engineering, Professor & Chair, Department of Biomedical Engineering Distinguished University Professor, Tufts University*

[david.kaplan@tufts.edu](mailto:david.kaplan@tufts.edu)

Silk is one of the oldest biomaterials, utilized as sutures for centuries, yet undergoing a rebirth into new biomaterial formats and applications. Key to this recent emergence has been fundamental insight into mechanisms of self-assembly of this unique, high molecular weight, amphiphilic protein, along with new modes to modify the native protein using processing methods, chemistries and bioengineering approaches. Some of the recent strategies will be discussed related to fundamental aspects of controlling biomaterial structure and function, leading to new silk-based biomaterials for medicine.



## Mapping human tissue architecture using spatial genomics

**Ömer Ali Bayraktar**

*Wellcome Sanger Institute, UK*

The emerging field of spatial genomics promises transcriptomic analysis of cells within intact tissues and a spatially resolved Human Cell Atlas (HCA). Here, I will summarize our progress towards building experimental and computational approaches for spatial transcriptomic atlasing of human tissue architecture. First, I will present cell2location, a new probabilistic model that integrates single-cell and spatial transcriptomics to map cell types in situ in a comprehensive manner. We show that cell2location outperforms existing tools in accuracy and comprehensiveness and we demonstrate its utility by mapping several complex tissues. In the mouse brain, we use a new paired single nucleus and spatial RNA-sequencing dataset to map dozens of cell types and identify tissue regions in an automated manner. We discover novel regional astrocyte subtypes including fine molecularly and spatially defined subpopulations in the thalamus and hypothalamus. In the human lymph node, we resolve spatially interlaced immune cell states. We identify co-located groups of cells underlying tissue organisation and spatially map a rare pre-germinal centre B-cell population. In the human gut, we demonstrate that cell2location outperforms alternative methods in mapping transcriptionally fine lymphoid cell types. Collectively our results demonstrate how cell2location can serve as a versatile first-line analysis tool to map tissue architectures in a high-throughput manner. Second, I will present our efforts on imaging-based approaches which can deliver a single cell-resolution spatial atlas of human tissues.

## **Two and Three Dimensional Electronmicroscopy in Understanding Synaptic Circuits in Sensory Pathways.**

**Alev Erisir**

*Department of Psychology, University of Virginia, USA*

While the three-dimensional reconstructions using serial image preparations provide large scale connectomics datasets mapping local neural connectivity, quantitative transmission electron microscopy, coupled with tract-tracing and immunolabeling, continues to be a powerful tool to reveal organization of synaptic circuitries of the brain in hypothesis-based studies. In this talk, I will summarize our recent work on visual and taste thalamus using Scanning Blockface Electron Microscopy stacks and more traditional immuno-EM approaches in the rodents and the tree shrews.

## Electronic structure engineering through atomic-scale strain control in complex oxide heterostructures

Yu-Mi Wu, Ulrike Niemann, Gideok Kim, Georg Christiani, Minu Kim, Yi Wang, Y. Eren Suyolcu, Gennady Logvenov, Bernhard Keimer, Hidenori Takagi, Peter A. Van Aken

Max Planck Institute for Solid State Research, Stuttgart, Germany

In complex oxide systems, the coupling of local atomic configurations and electronic degrees of freedom play a fundamental role in understanding exotic phenomena such as formation of charge ordering, metal-insulator transition and colossal magnetoresistance. Atomic-scale thin film syntheses enable to disentangle these competing interactions and tune novel ground states of materials, which do not exist in bulk crystals. Modifying strain by depositing epitaxial thin films on substrates with different lattice spacing results in a precise control of the local physical behavior. Scanning transmission electron microscopy (STEM) combined with electron energy-loss spectroscopy (EELS) not only provides information on the local atomic structure, but also on the site-specific chemical composition and electronic structure of materials and interfaces. Such direct real-space observations are important to unveil the microscopic origins of macroscopic properties in complex oxides and are essential for possible applications in relevant electronic and spintronic devices.

Here, we demonstrate how strain locally alters physical properties in two different complex oxide systems using STEM-EELS. We will first describe our observation of epitaxial  $\text{LiV}_2\text{O}_4$  thin films grown on  $\text{SrTiO}_3$  and  $\text{MgO}$  substrates. We find that the  $\text{V-}3d$  electrons redistribute in the lattice and become confined or delocalize depending on the epitaxial strain, hereby generating ordered or disordered patterns. We reveal two competing behaviors of the thin films on the two different substrates, a metallic charge-disordered phase on  $\text{SrTiO}_3$  and an insulating charge-ordered phase on  $\text{MgO}$ . Our findings evidence that charge fluctuations can freeze into an insulating “charge-glass”-like state, when epitaxial strain is applied, which relieves the frustration in  $\text{LiV}_2\text{O}_4$ . The second part focuses on  $\text{La}_{0.5}\text{Sr}_{0.5}\text{MnO}_3$ - $\text{La}_2\text{CuO}_4$  heterostructures grown on three different substrates,  $\text{SrTiO}_3$ ,  $(\text{LaAlO}_3)_{0.3}$ - $(\text{Sr}_2\text{AlTaO}_6)_{0.7}$  and  $\text{LaSrAlO}_4$  [1]. We find that charge rearrangements in these systems give rise to two different magnetic phases, an interfacial antiferromagnetic layer and an enhanced ferromagnetic metallic region away from the interfaces. Furthermore, the epitaxial strain controls the magnitude of charge redistribution and further influences the macroscopic electronic and magnetic structures in these heterostructures differently from the strain affects reported on single-phase films. These results provide a route for understanding, controlling and designing local novel phases in complex oxides heterostructures [2].

### References:

[1] Y.-M. Wu *et al.* (submitted, 2021)

[2] This project has received funding from the European Union’s Horizon 2020 research and innovation programme under grant agreement No. 823717 – ESTEEM3.

## High Spatial and Energy Resolution Electron Microscopy of Functional Oxides

**Demie Kepaptsoglou**

*SuperSTEM Laboratory, Sci-Tech Daresbury Campus, Daresbury UK  
Department of Physics, University of York, York, UK*

Perovskite oxides are widely studied for a variety of applications, from thermoelectric heat conversion to fuel cell and solar cell applications. Part of the attraction lies in the fact that perovskite ceramics are relatively easy to dope chemically over a wide range of compositions allowing for their physical properties and functionality to be efficiently tailored. Precise control of local ordering and local or extended defects can alter the local electronic structure, affecting for instance electron transport behaviour, while the precise growth control of multilayer heterostructures can give rise to emergent properties within the interior of the multilayer structure. However, as these effects are dependent on small structural details, such as atomic arrangements at the sub-angstrom scale they are often too minute, to be detected or sufficiently characterized by bulk techniques. In this respect electron microscopy and in particular Scanning Electron Microscopy Transmission Electron Microscopy (STEM) in tandem with Electron Energy loss Spectroscopy (EELS) is probably the ultimate research tool for such systems, as it allows to probe simultaneously structural and chemical/bonding information at the atomic level. Furthermore, recent advances in instrumentation, such as the introduction of advanced, high-resolution monochromators have allowed for new exciting experiments in the electron microscope. Spectroscopic signatures of optical and acoustical phonons, excitons and defect gap states are now accessible with an atom size probe and in tandem with high precision imaging. Here, we present results on the structure and electronic structure of thermoelectric (TE) materials systems for heat recovery applications, using advanced electron microscopy. High energy resolution scanning transmission electron microscopy (STEM) and electron energy loss spectroscopy (EELS) was used to inform theoretical predictions from density functional theory electronic band-structure calculations combined with the Boltzmann transport theory.

## The Role of mir-489(46) Cistron in Trophoblast Cell Lineage Specification

Ishani Wickramage<sup>1</sup>, Richa Banerjee<sup>1</sup>, Isabella Hetherington<sup>1</sup>, Jeffrey VanWye<sup>1</sup>, Umit A. Kayisli<sup>2</sup>,  
**Hana Totary-Jain<sup>1</sup>**

<sup>1</sup> Department of Molecular Pharmacology & Physiology,

<sup>2</sup> Ob & Gyn, Morsani College of Medicine, USF Health, Tampa, FL USA

Placental dysfunction is the main cause of pregnancy complications. In early pregnancy trophoblast differentiation and invasion into the decidua is critical for the establishment of implantation and placentation. In primates, the evolution of invasive placentation coincided with the emergence of the mir-498(46) cistron. This cistron is the largest miRNA cluster in human genome that contains 46 highly homologous miRNA precursor sequences. In the term placenta, miRNAs of the mir-498(46) cistron account for ~40% of all miRNAs, suggesting their essential role in human placental development and function. We have shown that the mir-498(46) cistron is highly expressed in villous cytotrophoblasts (CTs), syncytiotrophoblasts (STs), and in proliferative trophoblastic cell columns in the anchoring villi of first trimester human placentas, but as CTs differentiate into mesenchymal extravillous trophoblasts (EVTs), and invade the decidua, the expression of the mir-498(46) cistron is greatly diminished. Hence, we hypothesize that the mir-498(46) cistron plays a central role in the regulation of trophoblast cell lineage specifications and function, and dysregulation of its expression may elicit placental dysfunction.

To gain insight into the regulatory role of the miRNAs of the mir-498(46) cistron, we employed the CRISPR/dCas9 Synergistic Activation Mediator (SAM) system and single guide RNA (sgRNA) to transcriptionally activate the entire cistron. Among the mRNA transcripts that were down-regulated in sgRNA transfected HEK293 cells compared to GFP transfected controls, 50% of them were predicted targets of mir-498(46) cistron. Gene set enrichment analysis of these genes revealed their involvement in the epithelial to mesenchymal transition (EMT), whereas the upregulated genes were involved in passive and active transport of small molecules, glucose, other sugars, amino acids, bile salts, organic acids, metal ions, and amine compounds. CRISPR/dCas9 SAM mediated mir-498(46)-activation, together with Yamanaka factors, significantly increased the efficiency of somatic cell reprogramming into iPSCs. Exposure of iPSCs to hypoxic conditions reduced miRNAs of the mir-498(46) cistron and induced EMT gene expression.

Thus, employing the CRISPR/dCas9 SAM technique to efficiently induce the expression of the mir-498(46) cistron entirely enabled us to uncover its role in maintaining the epithelial stemlike CT cells phenotype by targeting EMT genes and inducing nutrient exchange in villous trophoblasts at the maternal fetal interface. Importantly, the hypoxic conditions during early placentation reduce the expression of the mir-498(46) cistron and release its inhibition of EMT genes, leading to the acquisition of migratory and invasive characteristics of EVT. Therefore, maintaining optimal expression levels of the mir-498(46) cistron is likely critical for EVT differentiation and invasion and dysregulation of its expression may result in impaired invasion associated with either the shallow placentation of preeclampsia or the exuberant invasion of placenta accreta.

## **Electron microscopy as the gold standard of the extracellular vesicle research**

**Agnes Kittel**

*ELRN, Institute of Experimental Medicine, Budapest, Hungary*

In certain circumstances, every cell is capable to release some sort of vesicles. This heterogeneous population of extracellular vesicles (EVs) interacts with cells and conveys biological information in the neighborhood of their release or in a far distance in another tissue or organ.

Naturally, there are many ideas for the utilization of their valuable potential as a diagnostical or therapeutical tool. In the interest of this goal, the best model systems have been applied to gain EVs of different size ranges and features and almost the whole arsenal of state-of-the-art molecular biological methods has been used to investigate them.

However, in spite of almost two decades of tremendous work, we haven't solved satisfactorily the first task which is the reliable isolation and purification of the wanted group of extracellular vesicles. There are several techniques and protocols in use, but none of them provide us reliably EVs in the expected quality and purity.

We need microscopy to check the quality of our EV preparation. Due to the size range of these vesicles (between 30 nm-5  $\mu\text{m}$ ), the gold standard is electron microscopy which makes us able to investigate cells releasing the smallest exosomes and the biggest apoptotic bodies on the same micrograph of a tissue or cell culture and it also helps us to decide whether our isolated particles are extracellular vesicles or something else in the same size range.

Although the ultracryogenic electron microscopy has its unbeatable advantage in demonstrating the almost native condition of these tiny vesicles, traditional transmission electron microscopy (TEM) is also sufficient for this decision. Moreover, in several cases, the old TEM methods can be successfully applied to answer even more sophisticated questions, too.

A wide range of microscopical methods, including SMLM (Single molecule Localization Microscopy) is used for answering a given question regarding the isolated vesicles, however, to the gold standard is the electron microscopy.

## Pharmacological targeting of PML nuclear bodies in neurodegeneration

Umut ŞAHİN

*Molecular Biology and Genetics, Boğaziçi University, Istanbul, Turkey*

PML (Promyelocytic Leukemia) Nuclear Bodies (NBs) are fascinating and remarkably dynamic sub-nuclear structures organized by the scaffold PML protein. These phase separated membrane-less organelles recruit hundreds of *partner proteins*, including p53 and many of its modifying enzymes. PML NBs finely tune numerous cellular functions including stem cell self-renewal, apoptosis/senescence, DNA repair, anti-viral immunity and metabolism. PML NBs and their master organizer, the PML protein, were initially implicated in the pathogenesis of acute promyelocytic leukemia (APL). The biochemical basis of how PML NBs control diverse cellular functions has remained a mystery until very recently. According to the current model, a post-translational modification (PTM), called sumoylation, is tightly associated with PML function and underlies the biochemical basis of distinct NB-regulated activities. Like ubiquitin, SUMO is covalently conjugated onto target proteins, altering stability, subcellular localization, enzymatic activity or interactions with other proteins. Recent data indicate that PML NBs initiate in situ sumoylation of partner proteins, in turn, regulating their functions and multiple downstream cellular activities. Critically, a subset of PML NB partners are ubiquitylated and degraded following their sumoylation in situ. Because PML NB formation is highly druggable, it is possible to induce NB-dependent clearance of a variety of toxic proteins, including oncoproteins, viral proteins, or aggregation-prone proteins that are implicated in neurodegenerative diseases. ALS (amyotrophic lateral sclerosis) is a fatal neurodegenerative disease. Genetic studies identified ALS-linked mutations in a number of proteins (i.e. SOD1, TDP43, FUS and EEAT2), which aggregate in ALS neurons, leading to neuronal toxicity. Understanding the mechanisms that govern aggregation and stabilization of ALS-linked proteins is an intense area of research. Preliminary studies suggest that some ALS-linked proteins are sumoylated, suggesting that they may be perfect candidates for pharmacological targeting into PML NBs. Here, I will discuss our recent findings on how PML NBs may be manipulated to clear toxic proteins associated with ALS pathogenesis.

# Engineering the Surface and Interface Structures of Catalysts for Water Splitting

Peng Yi Tang<sup>1,2,3\*</sup>

<sup>1</sup> Shanghai Institute of Microsystem and Information Technology, Chinese Academy of Sciences, ChangNing Road 865, 200050 ShangHai, China

<sup>2</sup> Catalan Institute of Nanoscience and Nanotechnology (ICN2), CSIC and BIST, Campus UAB, Bellaterra, 08193 Barcelona, Catalonia, Spain

<sup>3</sup> Ernst Ruska-Centre Julich, Julich Research Centre, Helmholtz Association of German Research Centres, 52425 Julich, Germany

Conversion of solar energy into the form of chemical bonds is an attractive approach for efficient, economical, and convenient utilization of solar energy.[1] Among these strategies, photoelectrochemical (PEC) water splitting devices, using earth abundant semiconductors, have for long been considered to be the “Holy Grail” of the solar energy conversion revolution. [2]

Water oxidation is an important anodic half-cell process in the development of a water splitting cell. Coupling water oxidation catalysts with active photoanode materials and construction of type II heterojunctions have become the most promising methodology for PEC water oxidation. Thus, we have fabricated ITO/Fe<sub>2</sub>O<sub>3</sub>/Fe<sub>2</sub>TiO<sub>5</sub>/FeNiOOH and Fe<sub>2</sub>O<sub>3</sub>/Fe<sub>2</sub>TiO<sub>5</sub>/Prussian blue analogues (CoFe PBA) multi-layers nanowire heterostructures via combination of sputtering, hydrothermal, ALD, photo-electrodeposition and chemical bath for photoelectrochemical (PEC) oxygen evolution application. Structural, spectroscopic and electrochemical investigations disclose that the construction of type II heterojunction and coupling of water oxidation catalysts remarkably enhanced the photocurrent response of hematite photoanodes. The origin of the superior catalytic performance is owing to the interfacial coupling effect of ITO underlayer (Sn doping and conductivity promoter), ultrathin Fe<sub>2</sub>TiO<sub>5</sub> coating (Ti doping, energetics, and surface state density modulation) and FeNiOOH/CoFe PBA electrocatalyst (varying surface state energy level). [3-5]

Meanwhile, exploring low cost, highly efficient catalysts for hydrogen evolution reaction (HER) play an important role in realizing the full water splitting application. With this in mind, we have investigated the HRE reaction active sites of two dimensions (2D) MoS<sub>2</sub> material and fabrication of single atoms dispersion Pt catalysts derived from 2D PtSe<sub>2</sub> material. [6-7] Systematically structural, electrochemical, and theoretical investigation demonstrated that the HER active sites of 2D MoS<sub>2</sub> is located at the grain boundary rather than in-plane and edge regions; and the synthesized grain boundary rich 2D MoS<sub>2</sub> delivers improved HER catalytic performance.[6] Additionally, subjecting 2D PtSe<sub>2</sub> material into plasma treatment resulted in atomic dispersion amorphous Pt material, leading to excellent HER performance. [7]

**Keywords:** Surface, Interface, Catalysts, Water splitting, Mechanism.

## References

- [1] F. Urbain, P.Y. Tang, N. M. Carretero, T. Andreu, L. G. Gerling, C. Voz, J. Arbiol, J. R. Morante, *Energy & Environmental Science*, 2017, 10, 2256-2266.
- [2] P. Y.Tang, J. Arbiol,\* *Nanoscale Horizons*, 2019, 4, 1256-1276.
- [3] P.Y. Tang, H. B. Xie, C. Ros, L. J. Han, M. Biset-Peiró, Y. M. He, W. Kramer, A. Perez-Rodriguez, E. Saucedo, J. Galan-Mascaros, T. Andreu, J. R. Morante, J. Arbiol, *Energy & Environmental Science*, 2017, 10, 2124-2136.
- [4] L. J. Han, P. Y. Tang, A. Reyes-Carmona, B. Rodriguez-Garcia, M. Torrens, J. R. Morante, J. Arbiol, J. R. Galan-Mascaros, *Journal of the American Chemical Society*, 2016, 138, 16037-16045.
- [5] P. Y. Tang, L. J. Han, F. S. Hegner, P. Paciok, M. Biset-Peiró, H. C. Du, X. K. Wei, L. Jin, H. B. Xie, Q. Shi, T. Andreu, M. Lira-Cantú, M. Heggen, R. E. Dunin-Borkowski, N. López, J. R. Galán-Mascarós, J. R. Morante, J. Arbiol, *Advanced Energy Materials*, 2019, 9, 1901836.
- [6] Y. M. He, P. Y. Tang, Z. L. Hu, Q. Y. He, L. Q. Wang, Q. S. Zeng, P. Golani, G. H. Gao, C. Zhu, W. Fu, C. T. Gao, J. Xia, X. L. Wang, X. W. Wang, C. Zhu, Q. M. Ramasse, A. Zhang, J. R. Morante, L. Wang, B. K. Tay, B. Yakobson, A. Trampert, H. Zhang, M. H. Wu, Q. J. Wang, J. Arbiol, Z. Liu, *Nature Communications*, 2020, 11, 57.
- [7] Y. M. He, L. R. Liu, C. Zhu, P. Golani, B. Y. Koo, S. S. Guo, P. Y. Tang, Z. Q. Zhao, M. Z. Xu, C. Zhu, P. Yu, X. W. Wang, L. Zheng, J. F. Yang, B. Shin, J. Arbiol, Q. J. Wang, Z. H. Zhang, Z. Liu, *Nature Catalysis*, under revision.



## Octahedral Pt-alloy nanoparticle fuel-cell catalysts studied by analytical ex- and in-situ electron microscopy

Marc Heggen

Ernst Ruska-Centre for Microscopy and Spectroscopy with Electrons and Peter Grünberg Institute, Forschungszentrum Jülich GmbH, 52425 Jülich, Germany  
m.heggen@fz-juelich.de

Pt-alloy nanoparticles (NPs) with octahedral shapes are attractive as fuel cell catalysts for the oxygen reduction reaction (ORR). A deep understanding of their atomic-scale structure, degradation and formation is a prerequisite for their use as rationally-designed NP catalysts with high activity and long-term stability. Here, we present results from a comprehensive microstructural study of the growth and degradation of various octahedral Pt-alloy NPs performed using *ex situ*, *in situ* and identical location high-resolution TEM and high-angle annular dark-field STEM, combined with electron energy-loss spectroscopy and energy-dispersive X-ray spectroscopy.

We show that the NPs often show compositional anisotropy and form Ni-rich {111} facets, leading to complex structural degradation during ORR electrocatalysis. The Ni-rich {111} facets are etched preferentially, resulting in the formation of first concave octahedra and then Pt-rich skeletons that have less active facets [1,2]. We also reveal element-specific anisotropic growth as the reason for their compositional anisotropy and limited stability. During solvothermal synthesis, a Pt-rich nucleus evolves into precursor nanohexapods, followed by the slower step-induced deposition of Ni on the concave hexapod surface to form octahedral facets [3]. *In situ* thermal annealing of phase-segregated octahedral Pt-alloy NPs was performed under vacuum and under gas atmosphere to study their morphological stability and surface compositional evolution. Pristine octahedral Pt-Ni NPs, for example, show Pt-rich corners/edges and concave Ni-rich {111} facets. Time-resolved image series reveal that, on being annealed up to 800 °C, the Pt-rich surface atoms at the corners/edges diffuse onto and subsequently cover the concave Ni-rich {111} surfaces, leading to the formation of perfectly flat Pt-rich {111} surfaces with Ni-rich subsurface layers. In addition, surface doping of octahedral Pt-Ni NPs with a third element such as Mo or Rh is found to be an effective method for stabilization of the octahedral shapes of the NPs thereby improving their long-term stability during electrochemical cycling.

- [1] Heggen M, Gocyla M, Dunin-Borkowski RE, Advances in Physics X 2017; 2: 281.
- [2] Gan L, Cui CH, Heggen M, Dionigi F, Rudi S, Strasser P, Science 2014; 346: 1502.
- [3] Cui CH, Gan L, Heggen M, Rudi S, Strasser P, Nature Materials 2013; 12: 765.

## **Correlative Microscopy of Catalysts; from Device Level to Atomic Level**

**Dogan Ozkaya**

*Johnson Matthey Technology centre Blounts Court Rd Sonning Common Reading, RG4 9NH, UK  
Diamond Light Source, ePSIC Harwell Science and Innovation Campus, Fermi Ave, Didcot OX11 0DE, UK*

Autocatalysis have been around since the 70's even before the nanoscience revolution. During the nanoscience revolution, the auto catalyst design saw several orders of magnitude reduction in Platinum group metal (PGM) content originally used in the 70's. The reason for this was the ability to control nanoparticle size, composition and functionality and how it correlates with microstructure. This understanding of functionality also led to introduction of specific ingredients like ceria-zirconia into catalysts to make them more flexible for different fuel to air ratios experienced in combustion engines. There is also specific management of washcoat to make sure that they have the required porosity and interconnectivity for transport properties. This is the reason why autocatalysis needs to be characterised at various length scales, we need to understand them at the micron level as well as the atomic level both structurally and compositionally.

The device level characterisation of catalyst coating on monoliths are crucial in controlling the porosity and transport of the gases to the active sites. Characterising micron sized porosity has been carried out using X-ray Microscopy (XRM) using tomographic reconstruction routines. However, if we want to go beyond this level of characterisation, focussed ion beam (FIB) and Transmission electron microscopy (TEM) characterisation are required. FIB can be used via an image-cut-image routine over a volume followed by a reconstruction of this volume from the images. The resolution is achieved by using higher resolution imaging techniques in the SEM mode such as low voltage in-lens secondary and backscattered imaging. Another route is to cut an electron transparent transmission electron microscopy sample between 50-100nm thick and carry out a tilt series acquisition of this volume and reconstructing this volume subsequently using back projection tomography routines. It is also possible to characterise the compositions and oxidation states using (S)TEM and EELS. In this talk I will give several examples of these characterisation techniques and various ways that this gets used in understanding catalytic activity of these catalysts leading to superior catalysts.

## **Cryo Fluorescence as a guide for Cellular Cryo Electron Tomography**

**Paul Verkade**

*University of Bristol, UK*

Microtubules and actin filaments are important components to provide cells their shape and engage in migration. The complex interactions between the 2 drive many cellular processes but are largely unresolved. Cryo-electron microscopy allows us to study those interactions in great detail but does not allow for easy searching. By first analysing samples using cryo fluorescence this can be used to target the delicate cryo-EM imaging to the areas of interest.

We have used cryo fluorescence to locate and target kinosore-induced microtubular extensions out of Hap-1 cells. Once areas of interest have been identified using cryo fluorescence, these areas are then analysed at high resolution using cryo Electron Tomography.

Surprisingly we demonstrate that the microtubule lumen can be occupied by extended segments of filamentous (F-) F-actin in these small-molecule induced, microtubule-based cellular projections.

### **References:**

Paul, DM., Mantell, J., Borucu U., Coombs, J., SurrIDGE, KJ., Squire, J., Verkade, P. and Dodding MP (2020) In situ cryo-electron tomography reveals filamentous actin within the microtubule lumen. *Journal of Cell Biology*, 219(9):e201911154. doi: 10.1083/jcb.201911154.

# **Intraoperative fluorescence microscopy to detect metastatic lesions in the sentinel lymph nodes**

**Tetsuro Takamatsu**

Department of Medical Photonics, Department of Pathology and Cell Regulation, Kyoto Pref. Univ. Med., Kyoto, Japan  
\*ttakam@koto.kpu-m.ac.jp

The number of cancer patients has been increasing with worldwide growth in these past decades. Lymph node (LN) metastasis is one of the most important prognostic factors in some common malignancies, e.g. gastric cancer and breast cancer. To provide cancer patients with appropriate treatments, accurate evaluation for the presence of LN metastasis is necessary. Formalin-fixed, paraffin embedded (FFPE) tissue specimens are used as the gold-standard histopathology. This requires multiple steps and takes a few days or longer, and hence is not implementable in rapid diagnosis during surgery. Alternatively, frozen section analysis is widely used for intraoperative diagnosis. These procedures generally require about 30 minutes in total. However, there are some problems with the process, i.e. experience requirements and sample degradation.

Recently we have developed two types of intraoperative fluorescence microscopy methods to detect metastatic lesions in the sentinel LNs. The first is the deep-UV excitation fluorescence microscopy method with deep neural network (DNN) analysis (1-2). DNA and RNA were stained with DAPI and terbium ions respectively so that nuclei, nucleoli, and cytoplasm were visualized. Fluorescence images of metastasis-positive/-negative LNs of gastric cancer patients were used for patch-based training and validation with open-source DNN algorithms as well as for patch-based test of metastasis detection. The second is the highly sensitive and specific 5-aminolevulinic acid (5-ALA)-induced fluorescence imaging method (3-4). We developed a device that automatically detects LN metastasis by quantitatively evaluating the 5-ALA-induced protoporphyrin IX (PpIX) fluorescence intensity, while eliminating tissue autofluorescence.

In this paper, I will discuss the advantages of the fluorescence-based approach, which is promising for assisting pathologists in assessment of LN metastasis.

## **References**

1. Kumamoto Y, et al, *Sci Rep*, **9**, 10745 (2019).
2. Matsumoto T, et al, *Sci Rep*, **9**, 16912 (2019).
3. Koizumi N, et al, *EJSO* **42**, 1236-46 (2016)
4. Matsumoto T, et al, *Gastric Cancer* **23**, 725-733 (2020)

## **Light and shadow in diagnostic electron microscopy of the future**

**Giovanna Cenacchi**

Lab Ultrastructural Pathology and Diagnostics, Dept of Biomedical and Neuromotor Sciences, Alma Mater University of Bologna, Italy

Electron microscopy, EM, examination of pathological samples is a method to extend morphologic analysis to the ultrastructural level, providing data not discernible by the other ancillary methods. By the mid-1980s the rise of immunohistochemistry provided insight into molecular expressions that rendered mere structure seemingly obsolete. And yet, there remain areas of diagnostic pathology, and especially of diagnostic nephropathology and neuropathology, where EM provides diagnoses and also produces novel knowledges that would not be achievable by any other experimental approach. Today a resurgence of EM as an ancillary diagnostic modality is observed, however EM-diagnostic expertise due to economic and staffing issues is generally available only in larger laboratories with specific interest in ultrastructural pathology. EM, along with light and immunofluorescence microscopy, remains a vital leg in the diagnostic for renal biopsies. Primary ciliary dyskinesia is a rare genetic disorder of ciliary structure and function. The diagnosis can be challenging, particularly when using nongenetic assays. The “gold standard” diagnostic test is EM analysis of respiratory cilia obtained by nasal scrape or brush biopsy. EM has had a profound impact on our knowledge and understanding of viruses and infectious diseases. Viruses from various families exhibit distinct appearances and these morphological variations form the basis of virus identification: EM is on the front line in surveillance of new outbreaks as more recently demonstrated by the identification of the morphology of SARSCoV2 and its replicative steps. EM has been considered the most important methods in the study of nanotechnologies: the combination of nanoparticles, gene therapy, and medical imaging has given rise to a new field known as gene theranostics, in which a nanobioconjugate is used to diagnose and treat the disease. Physiological nanoparticles are the exosome, small membranous vesicle secreted by a variety of cells considered as a liquid biopsy marker. Groundbreaking advances in volume electron microscopy and specimen preparation are enabling the 3-dimensional visualisation of specimens with unprecedented detail, and driving a gratifying resurgence of interest in the ultrastructural examination of cellular systems. These changes are rapidly broadening the scope of biomedical studies to which volume EM techniques can be applied. Moreover, the introduction of integrated light and EM systems together with the ultrastructural telepathology will revolutionise correlative light and volume electron microscopy studies, by enabling the sequential collection of data from light and electron imaging modalities without intermediate specimen manipulation allowing instant and live second opinion retrieval from a remote expert worldwide.

## **Proteomic Analysis of Clear Cell Renal Cell Carcinoma**

**Nurhan Özlü**

*Koc University, Istanbul, Turkey*

Clear cell renal cell carcinoma (ccRCC) is the third most common and most malignant urological cancer. Here, we identified 10,160 unique proteins by in-depth quantitative proteomics, of which 955 proteins were significantly regulated between tumor and normal adjacent tissues. We verified four putatively secreted biomarker candidates, namely, PLOD2, FERMT3, SPARC, and SIRP $\alpha$ , as highly expressed proteins. Moreover, SPARC displayed a significant increase in urine samples of patients with ccRCC, making it a promising marker for the detection of the disease in body fluids. Based on molecular expression profiles, we propose a biomarker panel for the robust classification of ccRCC tumors into two main clusters, which significantly differed in patient outcome with an almost three times higher risk of death for cluster 1 tumors compared with cluster 2 tumors. Our rigorous proteomics approach identified promising diagnostic and tumor-discriminative biomarker candidates which can serve as therapeutic targets for the treatment of ccRCC.

# Imaging tumor metabolism with mass spectrometry and magnetic resonance spectroscopic imaging

Kevin M. Brindle

University of Cambridge, Cambridge, UK

Metabolic imaging is likely to play an increasingly important role in predicting and detecting tumor responses to treatment and thus in guiding treatment in individual patients. Nuclear spin hyperpolarization increases sensitivity in the  $^{13}\text{C}$  magnetic resonance experiment by  $>10,000\times$ . This unprecedented increase in sensitivity has allowed  $^{13}\text{C}$  magnetic spectroscopic resonance imaging of injected hyperpolarized  $^{13}\text{C}$  labelled cell substrates in vivo and, more importantly, the kinetics of their metabolic conversion into other cell metabolites<sup>1</sup>. We have used this imaging technique, which has translated to the clinic, to detect tumor treatment response<sup>2,3</sup>, to monitor disease progression<sup>4,5</sup> and to investigate the tumor microenvironment<sup>6</sup>.

The most widely used substrate, which has translated to the clinic, is  $[1-^{13}\text{C}]$ pyruvate. We have shown that exchange of hyperpolarized  $^{13}\text{C}$  label between lactate and pyruvate decreases following successful treatment and can provide an early indication of treatment response. The kinetics of this exchange may also provide prognostic information that could be used to guide treatment selection. I will describe here how we have used mass spectrometric imaging (MSI) of rapidly excised and frozen tumour sections<sup>7</sup> to obtain a mechanistic understanding of how underlying tumour metabolism influences the kinetics of hyperpolarized  $^{13}\text{C}$  label exchange between pyruvate and lactate and therefore how it can be used to provide prognostic information.

## References

1. Brindle, K.M. Imaging Metabolism with Hyperpolarized  $^{13}\text{C}$ -Labeled Cell Substrates. *J. Amer. Chem. Soc.* **137**, 6418-6427 (2015).
2. Day, S.E., *et al.* Detecting tumor response to treatment using hyperpolarized  $^{13}\text{C}$  magnetic resonance imaging and spectroscopy. *Nature Med* **13**, 1382-1387 (2007).
3. Ros, S., *et al.* Metabolic Imaging Detects Resistance to PI3K $\alpha$  Inhibition Mediated by Persistent FOXM1 Expression in ER+ Breast Cancer. *Cancer Cell* **38**, 1-18 (2020).
4. Serrao, E.M., *et al.* MRI with hyperpolarised  $[1-^{13}\text{C}]$ pyruvate detects advanced pancreatic preneoplasia prior to invasive disease in a mouse model. *Gut* **65**, 465-475 (2016).
5. Gallagher, F.A., *et al.* Imaging breast cancer using hyperpolarized carbon-13 MRI. *Proceedings of the National Academy of Sciences* **117**, 2092-2098 (2020).
6. Bohndiek, S.E., *et al.* Hyperpolarized  $[1-^{13}\text{C}]$ -ascorbic and dehydroascorbic acid: vitamin C as a probe for imaging redox status in vivo. *J Am Chem Soc* **133**, 11795-11801 (2011).
7. Fala, M., *et al.* Comparison of  $^{13}\text{C}$  MRI of hyperpolarized  $[1-^{13}\text{C}]$ pyruvate and lactate with the corresponding mass spectrometry images in a murine lymphoma model. *Magnetic Resonance in Medicine* **85**, 3027-3035 (2021).

## Qualification of GaSb Epilayers Grown on Si Substrates

**Uğur Serincan**<sup>1,2</sup>, Burcu Arpapay<sup>1,2</sup>, Y. Eren Suyolcu<sup>3,4</sup>, Gülcan Çorapçioğlu<sup>5,6</sup>, Peter A. Van Aken<sup>4</sup>, Mehmet Ali Gülgün<sup>7</sup>

<sup>1</sup>Nanoboyut Research Laboratory, Department of Physics, Eskişehir Technical University, Eskişehir, Turkey

<sup>2</sup>Advanced Technologies Application and Research Center, Eskişehir Technical University, Eskişehir, Turkey

<sup>3</sup>Department of Materials Science and Engineering, Cornell University, Ithaca, NY 14853, United States of America

<sup>4</sup>Max Planck Institute for Solid State Research, Heisenbergstrasse 1, Stuttgart 70569, Germany

<sup>5</sup>Central Research Infrastructure Directorate, Koç University, Rumelifeneri Yolu, Sariyer 34450, Istanbul, Turkey

<sup>6</sup>Sabancı University Nanotechnology Research and Application Center, Istanbul 34956, Turkey

<sup>7</sup>Sabancı University, Engineering and Natural Sciences, Istanbul 34956, Turkey

In the past two decades, GaSb based devices have been very attractive choice for a wide range of applications. However, the favorable properties of GaSb are limited by cost related factors such as the lack of large-scale, defect-free and semi-insulating GaSb substrates. Those limitations have routed researchers to develop new approaches for the fabrication of lower cost GaSb based devices. A practical way for the reduction of cost is to use an epitaxial method to grow GaSb epilayer on Si substrate, which is a remarkably cheaper and easily available substrate in large-scale. Yet, the large lattice mismatch (~12.2%) between GaSb and Si, the difference in thermal expansion coefficient between them, and polar GaSb surface versus nonpolar Si surface nature result in growing of high crystal quality GaSb epilayers on Si substrates quite difficult. In particular, considering the integration of Sb-based devices with Si, a defect-free buffer layer with atomic layer flatness is necessary. Thanks to the developments in epitaxial growth systems, the quality of GaSb epilayers on Si can be improved significantly by using various methods such as inserting AlSb quantum dot layer prior to the GaSb layer for a better initiation of GaSb, preferring miscut Si substrates instead of nominal ones to prevent antiphase domain formation and applying variable steps (superlattices, graded layers, etc.) in the buffer layer to decrease threading dislocations [1-3]. However, depending on the preferred approach and growth parameters, crystal defects will still be formed in various combinations. Hence, the growth of device-quality GaSb epilayers on Si depends to a large extent on the identification and reduction of the defect density that can reach to the surface. Therefore, in this work, the defects formed during the growth of GaSb epilayers on Si substrates and the quality of the epilayers were comprehensively studied. The analysis involved high-resolution X-ray diffraction, scanning electron microscopy, transmission electron microscopy, atomic force microscopy, and photoluminescence spectroscopy methods.

### References:

[1] B. Arpapay, Y. E. Suyolcu, G. Çorapçioğlu, P. A. van Aken, M. A. Gülgün and U. Serincan, A comparative study on GaSb epilayers grown on nominal and vicinal Si (100) substrates by molecular beam epitaxy, *Semiconductor Science and Technology*, 36, 025011, 2020.

[2] B. Arpapay, U. Serincan, The role of antiphase domain boundary density on the surface roughness of GaSb epilayers grown on Si (001) substrates, *Superlattices and Microstructures*, 140, 106450, 2020.

[3] U. Serincan, B. Arpapay, Structural and Optical Characterization of GaSb on Si (001) grown by Molecular Beam Epitaxy, *Semiconductor Science and Technology*, 34, 035013, 2019.

**Acknowledgments:** This study was supported in part by the Scientific and Technological Research Council of Turkey (TÜBİTAK) under the Grant No. 116F199 and by Eskişehir Technical University under the Project No. BAP-1305F092. This study has received funding from the European Union's Horizon 2020 research and innovation programme under Grant Agreement No. 823717-ESTEEM3. The authors thank Marion Kelsch for TEM specimen preparation.



## **Application of Stereology in Studying the Programming Consequences**

**Milica Manojlović Stojanoski**  
*University of Belgrade*

Changes during fetal development may have long-lasting consequences as Professor J. Barker observed, and defined as a concept of programming or developmental origin of health and disease. This concept implies a linkage between adverse environmental signals during prenatal development and low birth weight as a marker, along with a greater incidence of pathophysiological conditions in postnatal life. Today, the programming concept becomes increasingly important because it explains the occurrence of many diseases during adulthood and include cardiometabolic, reproductive and mental disorders. During prenatal development periods of rapid cell division have been marked as critical since the establishment of the future structure and thus the function of tissues and organs are determined at these periods. Every change during these windows of vulnerability, that are organ-specific, can influence developmental trajectory resulting in future or persistent malfunction. Glucocorticoids have been powerful modulators of gene expression and epigenetic modifications which control the proliferation and maturation of tissues to harmonize development with given environmental conditions. Acting on the tissue morphology and function in preparation for extrauterine life they promote nervous, respiratory, cardiovascular and immune system differentiation and biochemical maturation. Therefore, glucocorticoids as the main communicating signals between environment and developing organism represent a key link involved in the programming mechanism that shapes future physiology or predispositions to health or disease.

Design-based stereology remains one of the pillars of quantitative biomedical research. This modern methodological approach offers the possibility to obtain unbiased results of every aspect of an organ or tissue structure. The exact size of the structure, number and volume of cells or other constituent elements, length or surface of the studied structure can be unambiguously and accurately determined, in absolute terms by following the basic principles of stereological measurements. Combining histological analysis, and immunohistochemistry and/or immunofluorescence with quantitative microscopy as are stereological measurements and intensity of above-mentioned stainings, structural alterations can be measured and determined, enabling an understanding of the basic functional mechanisms of examined changes.

Changes that are the cause or consequence of programming in fetuses and offspring, respectively are the focus of this presentation. Prenatally, alterations of brain control centers, pituitary gland, adrenal, thyroid and reproductive axes, obtained by stereology will be presented. In offspring, the application of stereology provides physical evidence that structural changes of wide variety of tissues are the result of prenatal changes, showing that quantitative differences in early life evolve in qualitative i.e. functional problems later in life.

# Nanoscale Characterisation on Functional Materials: Force Spectroscopy and Atomic Force Microscopy Beyond Imaging

Suzana Šegota

*Division of Physical Chemistry, Ruđer Bošković Institute, POB 180, Zagreb, Croatia*

Materials and devices at the nanoscale hold vast promise for innovation in virtually every industry and public endeavor including health, electronics, transportation, the environment and national security<sup>1-3</sup>. The atomic force microscope (AFM) belongs to the broad family of scanning probe microscopes in which a proximal probe is exploited for investigating properties of surfaces with subnanometre resolution. AFM has been found to provide useful information on the multitude of its applications in fundamental and applied research (biology, chemistry and biophysics). The possibilities of spectroscopic analysis, surface modification and molecular manipulation gave rise to a real breakthrough in the realm of AFM use. The use of mild imaging conditions opened the way to dynamic studies in which conformational changes and molecular interactions could be followed in real time at single-molecule level. AFM is widely viewed as the most significant technological frontier currently being employed in material science<sup>4-7</sup>. In these cases AFM is an excellent technique to characterize morphology of obtained films, including the possibility of resolving defects on the nanometre scale. Not only structural properties can be investigated, but also mechanical or chemical and functional properties are the focus of many AFM applications<sup>8-10</sup>. The possibility of resolving phase separation, distinguishing areas with different mechanical or surface charge properties and identifying the presence of different phases is related to the high vertical resolution of AFM in a liquid environments<sup>11,12</sup>. Also, broad application of AFM stems from its ability to follow biogeochemical processes<sup>13</sup> in environment on various interfaces by monitoring the surface morphology through the surface images acquired at nanoresolution.

## References:

- 1) Aleksandr Noy, Handbook of Molecular Force Spectroscopy, Springer, 2008.
- 2) S. Amelinckx, D. van Dyck, J. van Landuyt, G. van Tendeloo, Handbook of Microscopy, Methods, VCH, Weinheim, 1997.
- 3) Pier Carlo Braga, Davide Ricci, Atomic Force Microscopy Biomedical Methods and Applications, Humana Press, 2004.
- 4) S. Šegota, L. Čurković, D. Ljubas, V. Svetličić, I. Fiamengo Houra, N. Tomašić, [Synthesis, characterization and photocatalytic properties of sol-gel TiO<sub>2</sub> films](#). *Ceramics International* 37 (2011) 1153-1160.
- 5) L. Čurković, D. Ljubas, S. Šegota, I. Bačić, [Photocatalytic degradation of Lissamine Green B dye by using nanostructured sol-gel TiO<sub>2</sub> films](#). *Journal of alloys and compounds* 604 (2014) 309-316.
- 6) K. Mehulić, V. Svetličić, S. Šegota, D. Vojvodić, I. Kovačić, D. Katanec, N. Petričević, D. Glavina, A. Čelebić, [A study of the surface topography and roughness of glazed and unglazed feldspathic ceramics](#). *Collegium antropologicum* 34 (2010) 235-238.
- 7) S. Ercegović Ražić, R. Čunko, V. Svetličić, S. Šegota, [The Application of AFM Microscopy for the Identification of Fibres Surface Changes after Plasma Treatments](#). *Material Technology* 26 (2011)146-152.
- 8) Anja Sadžak, Ignacija Vlašić, Zoran Kiralj, Marijana Batarelo, Nada Oršolić, Maja Jazvinščak Jembrek, Ines Kušen and Suzana Šegota, [Neurotoxic Effect of Flavonol Myricetin in the Presence of Excess Copper](#). *Molecules* 26 (2021) 845.
- 9) Sadžak, Anja; Mravljak, Janez; Maltar- Strmečki, Nadica; Arsov, Zoran; Baranović, Goran; Erceg, Ina; Kriechbaum, Manfred; Strasser, Vida; Příbyl, Jan; Šegota, Suzana. [The Structural Integrity of the Model Lipid Membrane during Induced Lipid Peroxidation: The Role of Flavonols in the Inhibition of Lipid Peroxidation](#). *Antioxidants*. 9 (2020) 5; 430-460.
- 10) Sadžak, Anja; Brkljača, Zlatko; Crnolatac, Ivo; Baranović, Goran; Šegota, Suzana. [Flavonol clustering in model lipid membranes: DSC, AFM, force spectroscopy and MD simulations study](#). *Colloids and surfaces. B, Biointerfaces*. 193 (2020) 111147.
- 11) S. Šegota, D. Vojta, G. Pletikapić, G. Baranović, [Ionic strength and composition govern the elasticity of biological membranes](#). *Chemistry and Physics of Lipids* 186 (2015)17-29.
- 12) A.Štimac, S. Šegota, M. Dutour Sikirić, R. Ribić, L. Frkanec, V. Svetličić, S. Tomić, B. Vranešić, R. Frkanec. [Surface Modified Liposomes by Mannosylated Conjugates Anchored via the Adamantyl Moiety in the Lipid Bilayer](#), *Biochimica et biophysica acta. Biomembranes* 1818 (2012) 2252-2259.
- 13) I. Sondi, B. Salopek-Sondi, S. Škapin, D. Srečo, S. Šegota, I. Jurina, B. Vukelić. [Colloid-chemical processes in the growth and design of the bio-inorganic aragonite structure in the scleractinian coral \*Cladocora caespitosa\*](#). *Journal of Colloid and Interface Science* 354 (2011) 181-189.

## **Lipids and the Alteration of Viral Propagation**

**Zahra Zakeri**

Department of Biology, Queens College and Graduate Center of CUNY, Flushing, NY 11367 USA

Viruses use cellular machinery to propagate, and, in doing so, they keep the cell alive until their replication is complete. To reduce viral propagation, one can use cellular elements available to the viruses. We have found that key players for viral propagation are the lipids. Viruses typically use the different types of available lipids as reservoir for construction of their own members. We have examined what happens to lipid droplets after viral infection using by RNA viruses such as influenza, Dengue and Zika viruses. We found that all the viruses alter the pattern, amounts, and distribution of lipid droplets in the infected cells. Perhaps of more importance, we have found that inhibiting synthesis of some lipids, for instance by using the HMG-CoA reductase (statin) atorvastatin, and thus restricting the availability of lipids in the infected cells, profoundly suppresses production of virus. More recently it has been also seen that lipids may also be important for propagation of COVID-19. Our data indicate that suppression of available lipid in the infected cell might be a powerful way of controlling viral propagation and hence an affective anti-viral strategy.

# Characterization of Single-Atoms in Materials by Aberration-Corrected Scanning Transmission Electron Microscopy

**Masashi Watanabe**

*Department of Materials Science and Engineering, Lehigh University, Bethlehem, PA 18015, USA.*

Identification of individual atoms randomly distributed in materials, specification of locations of them in terms of its microstructure and quantification of them, i.e. total characterizations of single atoms, are the ultimate goal in any chemical analysis. To perform such single atom characterization, atomic-scale spatial resolution is required as well as single-atom detection sensitivity. In fact, some of fundamental materials problems such as phase transformations, and dopant segregation on defects and interfaces might be controlled by a few atoms within a few atomic-layers. Thus, the single-atom characterization/analysis is essential for further understanding such phenomena toward advanced materials developments. Recently, aberration-corrected scanning transmission electron microscopy (STEM) instruments have been developed and utilized in materials characterization, which offer significant improvement in spatial resolution, even below a half Å resolution. The aberration correction for STEMs offers more probe currents while maintaining refined probe sizes. Therefore, both spatial resolution and sensitivity for analysis can also be significantly improved and atomic-resolution elemental mapping is now regularly carried out by both electron energy-loss spectrometry (EELS) and X-ray energy dispersive spectrometry (XEDS) in the latest instruments. However, single atom analysis by EELS and XEDS is still very challenging even using the latest aberration-corrected STEM instruments because signal generation is extremely limited from much smaller analyzed volumes improved by the aberration correction and signal collection is still poor. Single-atom analysis by XEDS was demonstrated in an aberration-corrected STEM with the latest advance in large solid angle silicon-drift X-ray detectors (SDDs) to improve the poor signal-collection efficiency. For evaluating single atom analysis, the X-ray signal simulation scheme was developed for an oriented crystalline specimen. This study explores challenges in single-atom characterization in terms of imaging and analysis.

## Electron Energy Loss Spectroscopy with High Spatial and High Energy Resolution.

Gianluigi Botton

*Department of Materials Science and Engineering, McMaster University, Hamilton, ON, L8S 4M1, Canada,  
Canadian Light Source, Saskatoon, Saskatchewan, Canada [gbotton@mcmaster.ca](mailto:gbotton@mcmaster.ca)*

Electron energy loss spectroscopy (EELS) is an invaluable technique to study the detailed structure and the chemical state of materials at unprecedented spatial resolution. Today, this technique is used to characterize nanoscale materials used in a myriad of applications from energy storage and conversion, to solid-state devices and biomaterials interfaces. This technique also has the potential to provide insight into much more fundamental problems where the extracting information on local unoccupied states (at atomic sites) and site occupancy are of fundamental importance.

In this presentation, I describe recent developments in electron energy loss spectroscopy to probe the changes in bonding and coordination of atoms using quantitative measurements of the energy loss spectra [1,2]. I will show that, with atomic resolved EELS, it is possible to determine ordering of cations in oxides [3] and changes in bonding at interfaces, consistent with modifications in the coordination of interface atoms. I will highlight how atomic resolved experiments with EELS near-edge fine structures (the equivalent of XANES) can be used to systematically study the local valence in high-T superconductors [4], extract the localized hole concentration in superconducting chain-ladder compounds [5] and even probe the local electronic structure of energy storage materials [6].

Finally, I will show how EELS can provide exquisite details on the plasmonic response of simple and very complex metallic nanostructures [7].

[1] G.Z. Zhu, *et al. Nature*, **490**, 384, (2012) [2] M. Bugnet, *et al., Phys. Rev. B* **88**, 201107(R) (2013), and *Phys Rev. B*, **93**, 020102 (2016) [3] S. Turner, *et al., Chem. Mater.* **24**, 1904-1909 (2012) [4] N. Gauquelin, *et al., Nature Communications* **5**, 4275 (2014) [5] M. Bugnet, *et al., Science Advances* 2016; **2**:e1501652 (2016). [6] H. S. Liu *et al. Physical Chemistry Chemical Physics* **18**, 29064-29075. (2016) and H. Liu et al, *ACS Nano*, **12** (3), pp 2708–2718 (2018) DOI: 10.1021/acsnano.7b08945 [7] D. Rossouw, *et al., Nano Letters* **11**, 1499-1504 (2011); D. Rossouw, G.A. Botton, *Phys. Rev. Letters* **110**, 066801 (2013); S. J. Barrow *et al, Nano Letters* **14**, 3799-3808. (2014); EP Bellido, *et al., ACS Photonics*, **3**, 428-433 (2016), and *ACS Photonics*, **4**, 1558-1565 (2017); E.P. Bellido, *et al., Self-similarity of plasmon edge modes on Koch fractal antennas, ACS Nano*, DOI: 10.1021/acsnano.7b05554), (2017). Bicket, IC; Bellido, EP; McRae, DM; Lagugne-Labarthe, F; Botton, GA; Hierarchical Plasmon Resonances in Fractal Structures, *ACS PHOTONICS*, **7**, 1246-1254, (2020), DoI: 10.1021/acsp Photonics.0c00110, Kapetanovic, V; Bicket, IC; Lazar, S; Lagos, MJ; Botton, GA; Tunable Infrared Plasmon Response of Lithographic Sn-doped Indium Oxide Nanostructures, *ADVANCED OPTICAL MATERIALS*, **8**, Article number 2001024, (2020), DoI: 10.1002/adom.202001024; Mousavi, MSS; Bicket, IC; Bellido, EP; Soleymani, L; Botton, GA; Electron energy-loss spectroscopy of surface plasmon activity in wrinkled gold structures, *JOURNAL OF CHEMICAL PHYSICS*, **153**, Article number 224703 (2020), DoI: 10.1063/5.0031469

# STEM as a Tool for the Design and Engineering of Functional Oxide Interfaces

**Y. Eren Suyolcu<sup>1,2\*</sup>, Gennady Logvenov<sup>2</sup>, Darrell G. Schlom<sup>1,3</sup>, Peter A. Van Aken<sup>2</sup>**

<sup>1</sup>Department of Materials Science and Engineering, Cornell University, Ithaca, New York 14853, USA

<sup>2</sup>Max Planck Institute for Solid State Research, Heisenbergstrasse 1, 70569 Stuttgart, Germany

<sup>3</sup>Leibniz-Institut für Kristallzüchtung, Max-Born-Str. 2, 12489 Berlin, Germany

\*eren.suyolcu@cornell.edu

Transition metal oxide heterostructures provide a versatile playground for prominent phenomena, including high-temperature superconductivity, magnetism, ferroelectricity, metal-to-insulator transition, thermoelectricity and piezoelectricity, as well as numerous possible applications. The origin of these phenomena is the competition between different degrees of freedom such as charge, orbital, and spin, which are interrelated with the crystal structure, the oxygen stoichiometry, and the doping dependence.

The unique combination of aberration-corrected scanning transmission electron microscopy (STEM) and oxide molecular beam epitaxy (MBE) techniques allows engineering the novel interface properties with precise control at the atomic scale<sup>[1]</sup>. Through heterostructural design, the combination of different oxide layers opens access to interface physics and leads to engineering interface properties, where the degrees of freedom can be artificially modified. IN this talk I will focus on several homo- and hetero-epitaxial interfaces with extraordinary structural quality and different functionalities, including high-temperature superconductivity, thermoelectricity, and magnetism.

The thin films and multilayers are grown in either layer-by-layer or co-deposition regimes in oxide MBE systems. To correlate the local structure and physical properties, the interfaces are extensively probed with STEM techniques, including high-angle annular dark-field (HAADF) and annular bright-field (ABF) imaging, electron energy-loss spectroscopy (EELS), and energy-dispersive X-ray spectroscopy (EDXS). High-resolution STEM investigations provide crucial feedback and further understanding of the physical properties and reveal that (i) the choice of the dopant<sup>[2,3]</sup>, (ii) the type of doping<sup>[4]</sup>, (iii) the choice of the constituent layers<sup>[5]</sup>, (iv) the individual layer thickness<sup>[6,7]</sup> directly influence the functionalities. Notably, the sharpness of the interfaces requires a meticulous definition: Structurally perfect and coherent interfaces may exhibit dissimilar chemical sharpness, which is ascribed to the elemental intermixing. The determination of the interfacial intermixing and the selective design of the interfaces are of great significance to tune the properties. Our research highlights that STEM techniques play a crucial role in understanding and engineering the novel phenomena at complex oxide interfaces.<sup>[8]</sup>

## References:

- [1] Y. E. Suyolcu, G. Christiani, P. A. van Aken, G. Logvenov, *J. Supercond. Nov. Magn.* **2020**, *33*, 107.
- [2] Y. E. Suyolcu, Y. Wang, F. Baiutti, A. Al-Temimy, G. Gregori, G. Cristiani, W. Sigle, J. Maier, P. A. van Aken, G. Logvenov, *Sci. Rep.* **2017**, *7*, 453.
- [3] Y. E. Suyolcu, Y. Wang, W. Sigle, F. Baiutti, G. Cristiani, G. Logvenov, J. Maier, P. A. van Aken, *Adv. Mater. Interfaces* **2017**, *4*, 1700737.
- [4] F. Baiutti, G. Gregori, Y. Wang, Y. E. Suyolcu, G. Cristiani, P. A. van Aken, J. Maier, G. Logvenov, *ACS Appl. Mater. Interfaces* **2016**, *8*, 27368.
- [5] F. Baiutti, G. Gregori, Y. E. Suyolcu, Y. Wang, G. Cristiani, W. Sigle, P. A. van Aken, G. Logvenov, J. Maier, *Nanoscale* **2018**, *10*, 8712.
- [6] P. Kaya, G. Gregori, F. Baiutti, P. Yordanov, Y. E. Suyolcu, G. Cristiani, F. Wrobel, E. Benckiser, B. Keimer, P. A. van Aken, H.-U. Habermeier, G. Logvenov, J. Maier, *ACS Appl. Mater. Interfaces* **2018**, *10*, 22786.
- [7] Y. E. Suyolcu, J. Sun, B. H. Goodge, J. Park, J. Schubert, L. F. Kourkoutis, D. G. Schlom, *APL Mater.* **2021**, *9*, 021117.

I kindly acknowledge all precious scientists for their significant contributions to the work presented, especially to Prof. B. Keimer, Prof. L. F. Kourkoutis, Prof. J. Maier, Dr. F. Baiutti, Dr. P. Kaya, Dr. W. Sigle, Dr. Y. Wang, B. H. Goodge, J. Sun and Y.-M. Wu. The results to be presented are the output of valuable collaborations completed in Max Planck Institute for Solid State Research, Germany, and in Cornell University, USA.

## Correlative live-cell – volume electron microscopy resolves metastasis related lysosomal subpopulations

Nalan Liv

University Medical Center Utrecht, Netherlands

Lysosomes (Lyso) are cellular organelles that regulate cellular metabolism. Alterations in the functional status and spatial distribution of lysosomes are linked to cancer cell proliferation, metastasis and invasion, and an altered energy metabolism. Malignant cells display a dramatic increase in the peripherally located population of lysosomes, which may have specific roles in the regulation of cancer cell invasion<sup>1,2</sup>. However the exact functions of this peripheral pool of lysosomes and how they differ from the perinuclear pool regarding their ultrastructure, membrane composition, hydrolytic capacity, and dynamic behavior remain as standing questions.

Correlative live-cell imaging and electron microscopy (live cell-CLEM) approaches provide elegant means to directly link molecular composition and dynamic behavior of organelles to their morphology at nanometer resolution<sup>3</sup>. A major challenge however, is to retrace single, especially small, organelles in 3 dimensions (3D). Mastering this challenge, we have recently presented an approach where we have used live-cell volume CLEM to link the dynamics and ultrastructural context of individual, highly dynamic organelles<sup>4,5</sup>. We presented that live-cell imaged lysosomes can be reliably retraced in 3D EM data, and fusion, fission and trafficking dynamics of single organelles can be linked to their ultrastructure. Here, we utilize and extend this live cell-CLEM approach to address and characterize the metastasis related peripheral subpopulation of lysosomes.

We have imaged single lysosomes located either at the periphery or the perinuclear areas of cancer cells, and analyzed their dynamic behaviors. After collection of the live-cell data, the cells are prepared for electron microscopy, the exact organelles are retraced, and imaged in EM. The (co)localization of lysosomal markers in peripheral and perinuclear populations, their motility (speed, displacement), and luminal characteristics like enzyme activity, degradative capacity, and pH gradient were assessed, and directly linked to their morphology by correlative (live-cell) fluorescence and 3D electron microscopy.

In conclusion, using live-cell CLEM, we have assessed the distinct dynamics and ultrastructure of peripheral vs. perinuclear lysosomes. Our data show the two pools exhibit significantly different functional profiles, and molecules regulating anterograde lysosome trafficking can be promising targets to prevent cancer cell invasion.

### References

1. Hämälistö, S. & Jäättelä, M. Lysosomes in cancer - living on the edge. *Curr. Opin. Cell Biol.* **39**, (2016).
2. Ballabio, A. & Bonifacino, J. S. Lysosomes as dynamic regulators of cell and organismal homeostasis. *Nat. Rev. Mol. Cell Biol.* 1–18 (2019)
3. Ando, T., Bhamidimarri, S. P., Brending, N., Colin-York, H., Collinson, L., De Jonge, N., ... Zifarelli, G. The 2018 correlative microscopy techniques roadmap. *J. Phys. D: Appl. Phys.* **51**, 443001 (2018).
4. Fermie, J., Liv, N., ten Brink, C., van Donselaar, E. G. E. G., Müller, W. H. W. H. W. H. W., Schieber, N. L. N. L. N. L., Schwab, Y., Gerritsen, H. C. H. C. & Klumperman, J. Single organelle dynamics linked to 3D structure by correlative live-cell - 3D electron microscopy. *Traffic* (2018)
5. Loginov, S., Fermie, J., Fokkema, J., Agronskaia, A. V., De Heus, C., Blab, G. A., Klumperman, J., Gerritsen, H. C. & Liv, N. Correlative Organelle Microscopy: fluorescence guided volume electron microscopy of intracellular processes. *bioRxiv* 2021.03.29.437317 (2021)

## **Emerging Roles for Syndecan Receptors in Disease**

**John R. Couchman**

*Biotech Research & Innovation Centre, University of Copenhagen, 2200 Copenhagen N, Denmark*

Heparan sulfate is one of the most complex carbohydrates occurring in animals. It comprises a repeating disaccharide of N-acetyl glucosamine and glucuronic acid that is substantially modified in the Golgi apparatus. Some of the uronic acid undergoes epimerisation to iduronic acid, while sulfation at several sites on each disaccharide creates the potential for enormous variability. In many cases, the completed heparan sulfate chain that is exported to the cell surface has domains of high sulfation interspersed with regions of low or no sulfation. These sulfated domains can interact with a wide array of proteins, including growth factors, morphogens, cytokines, chemokines, proteases and extracellular matrix macromolecules. However, overall, the fine structure of cell surface heparan sulfate is under cellular control, but the mechanisms are poorly understood.

Two families of cell surface heparan sulfate proteoglycans dominate on most cells, the transmembrane syndecans (4 in mammals) and the lipid-attached glypicans (6 in mammals). Both have a long evolutionary history. Our work and that of other groups has indicated that syndecans can function alongside other high affinity receptors, but also signal to the cytoskeleton, particularly influencing junction formation. Most recent work now indicates that syndecans-1 and -2 may be key to different cancers, while syndecan-4, about which most is understood, may be important in some forms of heart failure. Here, the structure and functions, including signaling, of the syndecans will be addressed, using microscopic, molecular and genetic evidence.



## Volume Microscopy in Cell Biology: An Overview

Bruno M. Humbel

*Okinawa Institute of Science and Technology, Onna-son, Okinawa, Japan  
Juntendo University, Tokyo, Japan*

In microscopy usually only two-dimensional images from a in reality three-dimensional object are recorded. Since a long time there was the desire to get three-dimensional information at ultrastructural level to better understand the interaction of cellular organelles. Already in 1953, with the invention of their microtome, Porter and Blum<sup>1</sup> suggested to use serial sections to understand the third dimension. The great work on the reconstruction of the nervous system of *C. elegans* is probably the summit of this technology<sup>2</sup>. Serial sectioning is a very tedious technology prone by many risks. In the beginning of 1990ies electron tomography became fashionable. By imaging the sample at many different angles, similar to x-ray computer tomography, the three-dimensional information can be retrieved. This method is, however, limited to still relatively thin sections, up to 500 – 1000 nm. More modern technologies, array tomography and focussed ion beam or serial section scanning electron microscopy have opened the way to get high-resolution three-dimensional information of much larger objects, of whole cells, even large parts of tissue. Array tomography is based serial sectioning but the sections are mounted on a support like a glass slide or a silicon wafer that allows for longer ribbons and many more sections to be retrieved. The section manipulation and also keeping the right sequence order has become much easier. Further, it can easily be correlated with light microscopy<sup>3</sup>. Serial block face scanning microscopy<sup>4</sup>, SBEM, uses a diamond knife to cut the surface of a resin embedded sample and images it with an electron beam. Focussed ion beam SEM<sup>5</sup>, FIB-tomography, uses an gallium ion beam for cutting instead of a knife. The methods are in principle very similar where usually SBEM allows for larger volumes and FIB-tomography for higher voxel resolution. These new technologies, mainly pushed by neuroscience, generate a new challenge, to model the three-dimensional organisation of the organelles of interest in such large volumes. Many different approaches have been proposed but to my opinion none is completely fulfilling our needs. In this presentation I will give an overview over the different 3D techniques along with typical examples.

### References:

- <sup>1</sup> Porter, K.R. and J. Blum, *Anat Rec* **117** (1953). p. 685-709.
- <sup>2</sup> White, J.G., et al., *Phil Trans R Soc Lond A* **314** (1986). p. 1-340.
- <sup>3</sup> Micheva, K.D. and S.J. Smith, *Neuron* **55** (2007). p. 25-36.
- <sup>4</sup> Denk, W. and H. Horstmann, *PLoS Biol* **2** (2004). p. 1900-1909.
- <sup>5</sup> Knott, G., et al., *J Neurosci* **28** (2008). p. 2959 –2964.

## **Imaging Viruses by Electron Microscopy**

**Pippa Hawes**

*Bioimaging, The Pirbright Institute  
pippa.hawes@pirbright.ac.uk*

The Pirbright Institute is a BBSRC funded research institute dedicated to studying high consequence veterinary and zoonotic viruses, with the aim of developing new, or refining existing, vaccines. It is not an exaggeration to say that virus outbreaks can have a catastrophic effect on the health of the global human and animal population, and on the economy of countries around the world. In our high containment laboratories we are able to conduct fundamental research into veterinary viruses exotic to the UK, for example foot-and-mouth disease virus and African swine fever virus, as well as zoonotic viruses including coronaviruses. The Bioimaging facility at Pirbright houses confocal, superresolution and transmission electron microscopes which makes us globally unique in the range of techniques we conduct under high containment conditions.

When viruses infect cells they hijack cellular machinery in order to replicate. This can have a dramatic effect on the ultrastructure of the cell, which can be characteristic of specific virus families. Biological samples have been prepared for electron microscopy by chemical fixation for decades, however this process introduces an extensive set of artefacts which can influence interpretation. Cryo methods of preparation preserve samples in a manner more representative of the native state, but there are other technical difficulties to address. The best preparation method depends on the type of sample and the information needed, and the key to interpreting your data is understanding what happened to your sample during preparation.

In this presentation I will give an overview of our laboratories and instrumentation, and discuss some of the most common preparation methods in the study of cell biology, within the context of high consequence virus research.

## Operando and in situ in a TEM imaging in a cryogenic temperature range

**M. Duchamp<sup>1,2</sup>, E. Tiukalova<sup>1</sup>, J. Vas<sup>1,2</sup>, R. Ignatans<sup>3</sup>, A.D. Mueller<sup>1</sup>, R. Medwal<sup>4</sup>, R.S. Rawat<sup>4</sup>, V. Tileli<sup>3</sup>**

<sup>1</sup> Laboratory for *in situ* and *operando* Electron Nanoscopy, School of Material Science and Engineering, Nanyang Technological University, Singapore 637616 Singapore.

<sup>2</sup> MajuLab, International Joint Research Unit UMI 3654, CNRS, Université Côte d'Azur, Sorbonne Université, National University of Singapore, Nanyang Technological University, Singapore, Singapore.

<sup>3</sup> Institute of Materials, École Polytechnique Fédérale de Lausanne, CH-1015 Lausanne, Switzerland.

<sup>4</sup> Natural Sciences and Science Education, National Institute of Education, Nanyang Technological University, Singapore 637616 Singapore.

We present our work on the applications of transmission electron microscopy (TEM) imaging and spectroscopy at cryogenic temperatures to delay the electron beam-induced degradation *as well as* to follow low temperature phenomena in a continuous and variable temperature range. Cryogenic imaging conditions is shown to delay the beam-induced degradation for LiMn<sub>1.5</sub>Ni<sub>0.5</sub>O<sub>4</sub> used for lithium-ion battery cathode material and ZnCo<sub>1.8</sub>Ni<sub>0.2</sub>O<sub>4</sub> used as a catalyst for oxygen evolution reaction [1]. The low temperature *TEM experiments* aim to study the evolution of ferroelectric and ferromagnetic domains walls, in BaTiO<sub>3</sub> (BTO) and Y<sub>3</sub>Fe<sub>5</sub>O<sub>12</sub> (YIG) respectively [2]. We explore the possibility to continuous imaging the samples as a function of electric or magnetic fields at different temperatures to quantify the activation energy of the specific pinning sites. Hence, we study the propagation of the domains with different stimuli like temperature, externally applied magnetic field, electric fields and currents. These studies in a continuous cryogenic temperature range will allow us to unravel the fundamental understanding of these physical phenomena at nanometer scale and for the design of future spintronics based memory.

The capability of combining *operando* TEM stimuli such as current, voltage, and/or magnetic field with *in situ* TEM imaging in a continuous cryogenic temperature range were made possible by using a MEMS-based TEM holder that allowed an electron transparent sample to be transferred and electrically contacted on a MEMS chip [3, 4]. The six-contact double-tilt holder allows alignment of the specimen into its zone-axis while simultaneously using four electrical contacts to regulate the temperature and two contacts for applying the electrical stimuli, i.e., *operando* TEM imaging. This leads to the demonstration of (i) high-resolution imaging and spectroscopy of nanoparticles oriented in the desired zone-axis direction at cryogenic temperatures to mitigate the electron beam degradation, (ii) imaging of low temperature transitions with accurate and continuous control of the temperature that allowed single-frame observation of the presence of both the orthorhombic and tetragonal phases in BTO system and (iii) magnetic domain wall propagation as a function of temperature, magnetic field and current pulses (100 ns with 100 kHz repetition rate) in the YIG system.

[1] Tyukalova, E.; Duchamp, M. Atomic Resolution Enabled STEM Imaging of Nanocrystals at Cryogenic Temperature. *J. Phys. Mater.* **2020**, 3 (3), 034006.

[2] Tyukalova, E.; Vas V.J.; Ignatans, R.; Mueller, A.D.; Medwal, R.; Imamura, M.; Asada, H.; Fukuma, Y.; Rawat, R.S.; Tileli, V.; Duchamp, M. Challenges and applications to *operando* and *in situ* TEM imaging and spectroscopic capabilities in a cryogenic temperature range. *Accounts of Chemical Research.* **2021**, doi: 10.1021/acs.accounts.1c00078.

[3] Duchamp, M.; Xu, Q.; Dunin-Borkowski, R. E. Convenient Preparation of High-Quality Specimens for Annealing Experiments in the Transmission Electron Microscope. *Microscopy and Microanalysis.* **2014**, 20 (06), 1638–1645.

[4] Jeangros, Q.; Duchamp, M.; Werner, J.; Kruth, M.; Dunin-Borkowski, R. E.; Niesen, B.; Ballif, C.; Hessler-Wyser, A. In Situ TEM Analysis of Organic–Inorganic Metal–Halide Perovskite Solar Cells under Electrical Bias. *Nano Letters.* **2016**, 16 (11), 7013–7018.

## The STEM: a nearly perfect Instrument

Lewys Jones

Trinity College Dublin AMBER Research Centre, Dublin, Ireland

The scanning transmission electron microscope (STEM) is perhaps one of the most powerful characterization tools in existence today. It is almost uniquely capable of simultaneously delivering structural, chemical, and crystallographic information in at, or close to, atomic resolution. Frequently, the planning of STEM experiments, or the interpretation of the data collected, is done with the help of image simulation. However, this partnership of two approaches necessarily triggers a conversation about the differences between them.

Simulations usually ignore the spatial and energy spread of the emission, the beam is defined within an aperture before a perfect Fourier transform represents the objective-lens and forms the probe. At the sample, the spatially pristine pixel-by-pixel interaction suffers no scan-noise, no scan-distortion, and no flyback hysteresis. After the sample, simulations require no lenses before scattered electrons fall over a perfect and homogenous detector. Perhaps simulations add Poisson noise to represent finite dose effects, while ignoring Gaussian noise, detector afterglow, or scan-speed effects.

In this talk, we will look at some of the ways that the real STEM instrument differs from our perfect intentions and look at some of the opportunities that this opens for technique and instrumentation development. We will discuss some of the cost and capability compromises that go with choosing an electron gun [1], we will review the performance and flexibility trade-offs that arise when choosing an objective-lens gap [2], and we will look at ways to use scan-strategy design to overcome several of the limitations of environmental distortion [3], flyback hysteresis [4], and of analog scintillator/photomultiplier detector technology [5,6].

### Reference:

- [1] F. Quigley, P. McBean, P. O'Donovan, and L. Jones, *Cost & Capability Compromises in STEM Instrumentation for Low-Voltage Imaging*, Arxiv (2021).
- [2] P. McBean, D. O'Mahony, and L. Jones, *Development of a User Adjustable Pole-Piece Gap Objective-Lens*, in *Proceedings of the European Microscopy Congress 2020* (Royal Microscopical Society, 2021).
- [3] L. Jones, H. Yang, T. J. Pennycook, M. S. J. Marshall, S. Van Aert, N. D. Browning, M. R. Castell, and P. D. Nellist, *Smart Align—a New Tool for Robust Non-Rigid Registration of Scanning Microscope Data*, *Adv. Struct. Chem. Imaging* **1**, 8 (2015).
- [4] T. Mullarkey, J. J. P. Peters, C. Downing, and L. Jones, *Using Your Beam Efficiently: Reducing Electron-Dose in the STEM via Flyback Compensation*, Arxiv (2021).
- [5] T. Mullarkey, C. Downing, and L. Jones, *Development of a Practicable Digital Pulse Read-Out for Dark-Field STEM*, *Microsc. Microanal.* **27**, 99 (2020).
- [6] K. E. MacArthur, L. Jones, and P. D. Nellist, *How Flat Is Your Detector? Non-Uniform Annular Detector Sensitivity in STEM Quantification*, *J. Phys. Conf. Ser.* **522**, 012018 (2014).

## **MSCs on the road.**

**Tunç Akkoç**

*Marmara University Medical Faculty Pediatric Allergy-Immunology Department, İstanbul, Turkey*

MSCs are fibroblast-like cells that have the capacity to adhere to plastic surfaces; form colonies derived from single cells (colony forming unit-fibroblasts) and can differentiate into mature cells of mesenchymal lineages, such as osteoblasts, adipocytes, and chondrocytes. Its sources include bone marrow, adipose tissue, placenta, umbilical cord, dental stem cells, and connective tissue of most organs. Oral tissues are easily accessible as a source of MSCs. Dental follicle MSCs (DF-MSCs) have considerable self-renewal capacity, doubling time, and multidifferentiation capacity with an easy lifelong accessible source of dental stem cells. They show immune-suppressive effect compared with the other dental sources.

Stem cells have special concern due to their capability to help in regenerative medicine. Broadly they are classified due to their potency as pluripotent (embryonic and inducible) and multipotent (mesenchymal). Among these, mesenchymal stem cells gain much attention because of their postnatal origin, differentiation capacity, lack of immune activity, and safety for the host. Stem cells have important immunomodulatory effect on autoimmune and allergic diseases.

Conversation and regulation of the immune system is provided by cytokines. T cell subsets are signatures with different tendencies toward cytokine secretions. Regarding their cytokine profile, they control or direct the immune system to autoimmunity or allergic disease. Inflammation is also modulated via cytokines and mainly pro-inflammatory cytokines (TNF- $\alpha$ , IL-1- $\alpha$ , IL-6) increase in that state.

As new technologies and novel strategies emerge, we are in need of more research into the mechanisms, biomarker discovery, and disease phenotyping for AIT. There will always be takehome messages for other immune tolerancerelated conditions, such as autoimmunity, organ transplantation, chronic infections, cancer, and recurrent abortion.

## **Immunomodulation of Inflammation: A Strategic Cell Therapy Approach to Target Acquired Liver Diseases**

**Mustapha Najimi**

Université Catholique de Louvain, Institute of Experimental & Clinical Research (IREC), Laboratory  
of Pediatric Hepatology & Cell Therapy, Brussels, Belgium  
mustapha.najimi@uclouvain.be

Many liver defects are still untreatable while access to the standard of care, orthotopic liver transplantation, is increasingly limited. Liver regenerative medicine using cells is a current iotechnology revolution that brings new perspectives to treat patients with unmet medical needs. Initial cell therapy clinical trials have used isolated hepatocytes to demonstrate the proof of concept. However, the significant increasing donor scarcity and poor resistance of isolated hepatocytes to cryopreservation/thawing and in vitro culture processes, have led to search for other cell sources. Stem/progenitor cells from different tissues have been investigated for their ability to support defective liver function and/or structure.

My presentation deals with mesenchymal stem/progenitor cells that are derived from healthy human liver and the main preclinical and clinical achievements that supported their current industrial development. Mainly, the analysis of their secretion profile has revealed the presence of potent bioactive molecules proposed to mediate their immuno-suppressive, immunomodulatory and anti-fibrotic modes of action. Those features have significantly supported their current clinical development for the treatment of acquired liver diseases including fibrosis, cirrhosis and cancer.

## Recent Developments in Regenerative Biomaterials, Tissue Engineering and In Vitro Tissue Models

Y. Murat Elçin

*Tissue Engineering, Biomaterials and Nanobiotechnology Laboratory, Ankara University, Ankara, Turkey*

*(www.elcinlab.org)*

*Biovalda Health Technologies, Inc., Ankara, Turkey (www.biovalda.com.tr)*

*E-mail: elcinmurat@gmail.com*

Tissue engineering has emerged as an alternative approach for the treatment of the loss or malfunction of a tissue or organ (1). The concept has been the transplantation of constructs consisting of cells (usually stem cells) grown *ex vivo* within predesigned synthetic or naturally-derived biomaterial scaffolds made up of exogenous three-dimensional (3D) extracellular matrices. The scaffolds used to guide the functional tissue development, eventually break down leaving only the cells and the stroma that they produce in the body. Decellularized native tissues have been considered as a bioactive source of biological scaffolding material for this purpose (2,3). Various tissue engineering methodologies and regenerative biomaterials have been evaluated over the years (4-6). More recently, the integration of 3D printing is expected to bring innovative solutions to engineering tissues and organs. The 3D bioprinting involves assembling cells, bioactive proteins and compatible hydrogels into living functional tissues through automated fabrication. For today, 3D bioprinting seems not to be ready for safe and widespread use in regenerative medicine. On the other hand, this technology shows significant potential for prospective use in drug development and personalized medicine, since it allows the creation of physiologically more realistic *in vitro* models (7). The talk will cover examples from the work performed in my laboratory on the mentioned topics.

### References:

- (1) Tissue Engineering, Stem Cells and Gene Therapies (Ed. Elcin YM), AEMB, Vol. 534 (2003) Kluwer-Plenum, ISBN 0-306-47788-2.
- (2) Biomed. Mater. 11(2) (2016) 022003. DOI: 10.1088/1748-6041/11/2/022003.
- (3) Adv. Exp. Med. Biol. 1249 (2020) 67-84. DOI: 10.1007/978-981-15-3258-0\_5.
- (4) Mat. Sci. Eng. C-Mater. 110 (2020) 110703. DOI: 10.1016/j.msec.2020.110703.
- (5) Stem Cell Rev. Rep. 16 (2020) 569-584. DOI: 10.1007/s12015-020-09963-y.
- (6) Mat. Sci. Eng. C-Mater. 124 (2021) 112065. DOI: 10.1016/j.msec.2021.112065.
- (7) Genes & Diseases (2021). DOI: 10.1016/j.gendis.2020.11.011.

## Point Defects in Ceramics and Semiconductor Nanomaterials and Their Roles in Supercapacitors

Emre Erdem

Sabanci University, Faculty of Engineering and Science, Materials Science and Nano Engineering, Orhanli, Istanbul, Turkey

E-mail: emre.erdem@sabanciuniv.edu

Electron paramagnetic resonance (EPR) spectroscopy is a very powerful method due to its enhanced sensitivity to unpaired electrons. In order to understand the defect structure in functional nano-materials we use multi-frequency EPR spectroscopy. In this presentation i) basics of EPR spectroscopy, ii) quantum confinement effects in ferroelectric nano-materials and iii) EPR and Photoluminescence (PL) investigations of intrinsic defect centers in semiconductor zinc oxide (ZnO) nanoparticles will be given. Starting with the introductory information about EPR spectroscopy; poling, aging, doping and nano-size effects will be discussed for the ferroelectric materials such as,  $\text{PbTiO}_3$ ,  $\text{BaTiO}_3$ ,  $\text{PbZrTiO}_3$  (PZT) etc. In the last part of the talk, surface and core defects and their reactivity under temperature and light will be presented for ZnO semiconductor nano-materials. Defect models will be discussed. Finally application of such materials as electrode materials and their electrochemical performance test results in the supercapacitor devices will be presented.

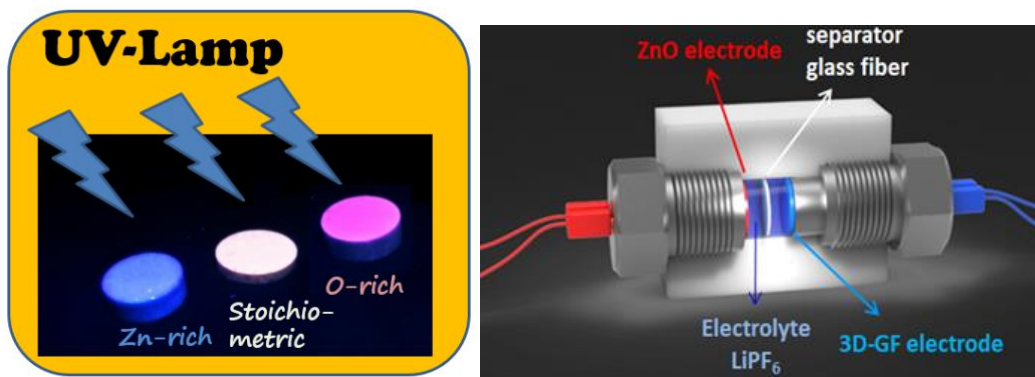


**Figure:** (left) Defect evolution of non-stoichiometric ZnO. (right) The supercapacitor device based on ZnO and 3D graphene foam electrodes.



## Electron Microscopy Characterization of Polymer-Based Materials

**María de la Mata Fernández**

*Dpto. Ciencia de los Materiales, Ing. Met. y Qca. Inorg., IMEYMAT, Universidad de Cádiz, 11510 Puerto Real (Cádiz),  
Spain  
e-mail: maria.delamata@uca.es*

Polymer-based systems are appealing candidates for the development of novel materials, allowing their blending and/or mixing with countless additives, in order to enhance their performance or provide extra functionalities. The polymer properties may be tailored to optimize either their processing or their functional applications (for instance, enhancing the electric conductivity). Among their advantages, polymers and resins are versatile lightweight systems that can be obtained through alternative synthetic routes, such as additive manufacturing.

The smart engineering of these materials requires from structural characterizations at the highest resolution attainable, which might be compromised due to sample damage during the measurements. In order to deal with hybrid composites containing soft matrices, such as polymers, and hard additives, as metal nanoparticles (NPs), specific characterization strategies may be designed based on the combined use of different electron microscopy techniques depending on the target results. The established procedures involve the use of different SEM (secondary electron, SE, images displaying topographic information, along with convergent back-scattered, CBS, electron images) and STEM techniques. Field-emission SEM measurements provide useful insights on the overall morphology of the composites, while STEM analysis allow deeper studies on nanometer size features (i.e., smaller additives) and more accurate chemical analyses. Depending on the sought information, the study may require deeper additional/alternative analysis of the components conforming the composites separately (additives/matrices).

Some examples of such analyses regard the study of metal NPs-polymer composites with optical response. On one hand, the detailed characterization of plasmonic metal nanostructures suitable as nano-additives for polymer matrices, is exemplified through the case of Ga NPs, including the plasmonic properties of individual NPs [1]. The obtained results show that single Ga NPs may support several plamon modes, whose nature is extensively discussed. On the other hand, we study hybrid Au NPs-polymer porous films with catalytic activity, addressing their microstructure and proving the thermal reduction of the Au<sup>3+</sup> within the polymer driving the formation of the Au NPs [2].

<sup>1</sup> *Small*, **15**, 1902920 (2019).

<sup>2</sup> *Colloids and Surfaces A*, **624**, 126766 (2021).

*This work has been co-financed by the 2014-2020 ERDF Operational Programme and by the Department of Economy, Knowledge, Business and University of the Regional Government of Andalusia. Project reference: FEDER-UCA18-106586.*

# Deciphering Principles of Mammalian Early Embryogenesis in Development and Disease

Berna Sozen

Assistant Professor of Developmental Stem Cell Biology  
Yale School of Medicine, Department of Genetics

There are hundreds of different cell types that make up the human body, and yet every cell is originally derived from just one - the fertilized egg. Understanding how this spectacular complexity arises during human development is a major challenge in biomedical research: it is important for understanding the origin of developmental diseases, pregnancy loss and to generate desired replacement cell types for regenerative medicine. While an incredible amount is known about the mammalian genome, physiology and anatomy, there is very little direct information about how embryonic development is regulated. Gaps in our knowledge result from the difficulty in studying embryonic development once implantation occurs and embryos become hidden within the body of the mother. To overcome this barrier, we and others have developed *in vitro* systems that recapitulate key aspects of 3-dimensional (3D) mammalian development in a dish with various types of stem cells, paving the way to a more complete understanding of the specific processes that govern embryonic development. To this end, we innovated and conceptualized transformational strategies to more faithfully model early embryogenesis *in vitro* with stem cells in mouse<sup>1-4</sup> and human<sup>5</sup> in 3D context. These series of studies, together with work from others<sup>6-12</sup>, have opened up a new experimental paradigm for advancing our knowledge of the dynamic cellular and molecular events that drive early mammalian development. These stem cell-based systems provide unprecedented access to early developing lineages and tissues, and afford insights into principles of self-organization and self-patterning during early embryogenesis as well as the intercellular signaling interactions that control dynamic cell behaviors and decisions in the developing embryo. These insights will provide the much-needed new knowledge to improve current approaches to generate distinct cell types for cell replacement therapies. Further, understanding these events will be vital for advancing developmental and reproductive health. We anticipate that our findings will be crucial in informing future studies on and possible prevention of adverse pregnancy outcomes, offering a unique opportunity to understand the cellular and molecular mechanisms behind early miscarriage and congenital pathologies.

1. Harrison, S. E., Sozen, B. *et al. Science* 356, doi:10.1126/science.aal1810 (2017).
2. Harrison, S. E., Sozen, B. *et al. Nature Protocols* 13, doi:10.1038/s41596-018-0005-x (2018).
3. Sozen, B. *et al. Nature Cell Biology* 20, 979-989, doi:10.1038/s41556-018-0147-7 (2018).
4. Sozen, B. *et al. Dev Cell* 51, 698-712 e698, doi:10.1016/j.devcel.2019.11.014 (2019).
5. Sozen, B. *et al. Nature Communications* (2021, in press).
6. Beccari, L. *et al. Nature* 562, 272-276, doi:10.1038/s41586-018-0578-0 (2018).
7. Liu, X. *et al. Nature* 591, 627-632, doi:10.1038/s41586-021-03372-y (2021).
8. Moris, N. *et al. Nature* 582, 410-415, doi:10.1038/s41586-020-2383-9 (2020).
9. Rivron, N. C. *et al. Nature* 557, 106-111, doi:10.1038/s41586-018-0051-0 (2018).
10. Veenvliet, J. V. *et al. Science* 370, doi:10.1126/science.aba4937 (2020).
11. Yanagida, A. *et al. Cell Stem Cell*, doi:10.1016/j.stem.2021.04.031 (2021).
12. Yu, L. *et al. Nature* 591, 620-626, doi:10.1038/s41586-021-03356-y (2021).

## **Understanding the degradation mechanisms in functionalized load-bearing metallic biomaterials**

**Fatih Toptan**

*Department of Materials Science and Engineering, Izmir Institute of Technology, 35430, Urla, Izmir, Turkey  
IBTN/Euro – European Branch of the Institute of Biomaterials, Tribocorrosion and Nanomedicine, Dept. Eng. Mecânica,  
Universidade do Minho, Azurém, 4800-058 Guimarães, Portugal*

Metallic materials are indispensable for load-bearing biomedical applications due to their strength, toughness, and ductility. However, their wear resistance is a major concern, especially for titanium and its alloys being the most popular metallic materials for these applications. Several functionalization (anodic treatments, mechanical treatments, and reinforcing with hard or bioactive particles) or coating approaches (plasma spraying, electrochemical deposition, and ceramic coatings) are being developed for improving the wear resistance of metallic biomaterials.

When an implant material attached to the bone, relative movements during the cyclic loading cause wear stresses. Simultaneously, surrounding corrosive body fluids cause corrosion damage that can affect the biocompatibility and mechanical integrity. This simultaneous action of corrosion and wear (i.e. tribocorrosion) leads to release of wear debris and metallic ions that can have local or systemic harmful effects. Furthermore, it is known that in tribocorrosion, total material loss may be significantly higher than that of the mechanical wear and corrosion, individually.

In order to assess the tribocorrosion behaviour, combined wear and corrosion tests are being performed in an ionic conductor, that can be a simulated physiological solution, under controlled tribological and electrochemical conditions. These tests can be performed either in tribometers or in simulators, combined with potentiostats. In order to understand the tribocorrosion mechanisms, in-situ tribological and electrochemical data should be combined with the ex-situ characterization performed on the worn mating surfaces and sub-surfaces, as well as on wear debris and testing solutions. Electron microscopy has an indispensable role in these characterization studies. Accordingly, the present communication will address the tribocorrosion mechanisms observed on various functionalized metallic biomaterials.

## **BAX-dependent Mitochondrial Outer Membrane Permeabilization: Exquisitely Regulated to the Point of Death.**

**Jerry Edward Chipuk**

*The Tisch Cancer Institute Icahn School of Medicine at Mount Sinai One Gustave L. Levy Drive, Box 1130 New York, NY 10029 USA*

The mitochondrial pathway of apoptosis is activated by the pro-apoptotic members of the BCL-2 (B cell CLL/lymphoma-2) family of proteins. Cooperation between effector proteins (e.g., BCL-2 associated x protein, BAX) and BH3-only proteins (e.g., BCL-2 interacting mediator of cell death, BIM) at the outer mitochondrial membrane (OMM) promotes its permeabilization by a process referred to as mitochondrial outer membrane permeabilization (MOMP). Once MOMP occurs, proteins within the mitochondrial inter-membrane space (IMS) gain access to the cytosol and promote caspase activation, which is ultimately responsible for rapid cellular demise and identification for phagocytosis. In the majority of cases, MOMP is the key signal committing cells to the mitochondrial pathway of apoptosis, and therefore, this process is exquisitely regulated by complex interactions among numerous proteins, lipids, membranes, and organelles. Over the years, my laboratory has contributed to the understanding of how MOMP is regulated by the development of model systems and approaches to better investigate the biochemical and biophysical requirements for BAX activation. In the upcoming presentation, we will discuss current mechanisms and pharmacological agents that control BAX-dependent MOMP and apoptosis.

## **Micro-Raman Spectroscopy of 2D TMDC Materials for Applications in Optoelectronics**

**Feridun Ay**

*Eskişehir Technical University, Department of Electrical and Electronics Engineering,  
26555 Eskişehir, Turkey  
[feridunay@eskisehir.edu.tr](mailto:feridunay@eskisehir.edu.tr)*

Following the significant interest in graphene, 2D materials and specifically Transition Metal DiChalcogenides (TMDCs) have received an ever-increasing attention in the fields of physics, materials science and optoelectronics due to their extraordinary optical and electrical properties. Here we will discuss and report on semiconductor 2D MoS<sub>2</sub>, MoSe<sub>2</sub>, and WS<sub>2</sub> TMDC growth optimization studies using CVD techniques. Specifically, a focus on the defect concentration and aging characteristics of MoS<sub>2</sub> layers and related FET devices will be presented. The discussion will have a focus specifically on use of micro-Raman spectroscopy as a tool for analysis of 2D materials and structures for investigation of defects and stability of the related TMDCs.

## **Targeting Phosphatidylserine/TAM receptor/PD-L1 axis as a vulnerability in cancer**

**Raymond B. Birge**

*Rutgers, Biomedical and Health Sciences, Department of Microbiology, Biochemistry and Molecular Genetics, New Jersey Medical School, 205 South Orange Ave, Newark, NJ 07103, USA*

The physiological fate of cells that die by apoptosis is their rapid recognition and clearance by both non-professional and professional phagocytes (efferocytosis). Apoptotic cells, by externalizing phosphatidylserine (PS) from the internal to the external surface of the plasma membrane, act as potent negative regulators of immune responses, promoting immune-suppression and the resolution of inflammation under physiological conditions to maintain tissue tolerance. In contrast to the homeostatic function of efferocytosis under physiological conditions, tumors, in particular, exist in a chronic dynamic balance of proliferation, metabolic stress, and apoptosis that magnify the post-mortem immunosuppressive effects of apoptotic cells in the tumor microenvironment (TME). In turn, persistent apoptotic cells in the TME suppress host tumor immunity by engaging a series of PS receptors called TAM receptors (Tyro3, Axl, and Mertk). While TAMs are overexpressed on a vast array of tumor types, whereby the level of expression correlates with the tumor grade and the emergence of chemo and radio resistance to targeted therapeutics, they are also implicated as inhibitory receptors expressed on infiltrating myeloid-derived cells, where they act as so-called “myeloid checkpoint inhibitors”. We have recently shown that TAMs can act as PS-sensing receptors not only to induce PS-mediated efferocytosis but also to up-regulate the immune checkpoint inhibitory ligand PD-L1 demonstrating the existing of a PS/PS-R (TAM-receptor)/PD-L1 axis that operates in the TME to drive immune escape. Finally, we will discuss the current molecular rationale that anti-PS, anti-TAM, and anti-PD-L1 based therapeutics may have therapeutic value as combinatorial checkpoint inhibitors in cancer immunotherapy.

## **Nuclear Phosphoinositides and Phase separation: Nuclear Lipid Islets and their importance in regulation of RNA Polymerase II driven transcription.**

**Pawel Hozak**

*Department of Biology of the Cell Nucleus, Institute of Molecular Genetics of the Czech Academy of Sciences, v.v.i., 142 20, Prague, Czech Republic, and Microscopy Centre, Institute of Molecular Genetics of the Czech Academy of Sciences, v.v.i., 142 20, Prague, Czech Republic*

Processes such as gene expression or DNA repair are precisely compartmentalized within eukaryotic nucleus. Nuclear environment contains dynamic membrane-less sub-compartments whose formation is prevalently driven by Phase separation. During phase separation a multivalent weak interactions lead to aggregation of molecules into liquid-behaving droplets delimited from neighboring environment. The lack of membranous barrier ensures fast intake of components. Thus formation of phase boundaries provides the surface for spatiotemporal control contributing to the high rate kinetics of crucial processes such as transcription, ribosome maturation, splicing. Our laboratory discovered a nanoscale particles - Nuclear Lipid Islets (NLIs). NLIs are up to 100 nm nucleoplasmic foci containing PI(4,5)P2 (PIP2) at their periphery which associate with key Transcription factors. We showed that NLIs are crucial for efficient Polymerase II transcription. We further observed that nuclear PIP2 distribution is affected by 1,6 hexandiol treatment. The drug disturbs a weak hydrophobic interactions and is broadly used for dissolving phase separated structures. To decipher whether the NLIs surface recruits a transcription regulatory proteins through PIP2 molecules in their surface, we employed a proteomic approach based on differential quantitative mass spectrometry (qMS). In our experimental pipeline we analyzed the PIP2-containing nuclear fraction. Our approach combines qMS analysis with super-resolution microscopy visualization of candidate proteins providing valuable information about NLIs protein composition. We identified more than 300 NLIs-associated proteins belonging to gene expression (53%) and pre-mRNA splicing (33%). Super-resolution microscopy confirmed that candidate proteins form foci in nucleoplasm and associate with sub-population of NLIs. Further, our bioinformatical analysis of putative NLIs proteins revealed that majority of them contain Intrinsically Disordered Regions (IDRs). IDRs are known feature of proteins undergoing phase separation under in vivo and in vitro conditions. Moreover, we found that the vast majority of these proteins contain K/R rich motifs, which were previously shown as recognition sites for phosphoinositide (PIPs) binding. We hypothesize that NLIs may serve as a structural platform integrating RNA Polymerase II transcription and pre-mRNA splicing. In general, PIPs may spatiotemporally orchestrate processes in nuclear environment by attracting proteins which are prone to form liquid-like particles.

Acknowledgements: This study was supported by the Czech Academy of Sciences (JSPS-20-06); Grant Agency of the Czech Republic (19-05608S, 18-19714S); IMG ASCR, v. v. i.(RVO:68378050); by the MEYS CR (COST Inter-excellence LTC19048) and the project „BIOCEV“ (CZ.1.05/1.1.00/02.0109), European Regional Development Fund (CZ.02.1.01/0.0/0.0/16\_013/0001775). Microscopy Centre - IMG ASCR the Czech-BioImaging project (LM2015062 funded by MEYS CR).

## ORAL ABSTRACTS

55 - Life Sciences - Structure and dynamics of cell organelles - Oral Presentation

### **Beta Cell Golgi Stress Response to Glucolipototoxicity: Morphologic Changes After Metabolic Stress**

**Yaprak Yalçın<sup>1,\*</sup>, Neslihan Bascil Tutuncu<sup>1</sup>, Hatice Pinar Baysan Cebi<sup>1</sup>, Hasibe Verdi<sup>1</sup>, Suleyman Erol<sup>2</sup>, Figen Kaymaz<sup>2</sup>**

<sup>1</sup> Baskent University, Ankara, Turkey

<sup>2</sup> Hacettepe University, Ankara, Turkey

In type 2 diabetes mellitus, the beta cells of the pancreas fail to produce enough insulin to meet the body's demand because of an acquired decrease in beta-cell mass and function. Glucolipototoxicity causing endoplasmic reticulum stress leads to worsening of  $\beta$ -cell function and hampers survival. Factors leading to endoplasmic reticulum stress are expected to converge adaptive and/or maladaptive changes in Golgi apparatus. Similarly lipid droplets are important organelles in cells with diverse functions in different cell types. Despite its potential importance, and being one of the prominent organelle in human beta cells, the role of lipid droplets in beta cells has been studied under metabolic stress of diabetes.

In the present study, we aimed to visualize the morphologic changes in  $\beta$ -cells under lipotoxicity and glucolipototoxicity, with special focus on the GA and lipid droplets. To evaluate the morphologic changes, electron microscopy of isolated INS-1E rat  $\beta$ -cells after 16-hour incubation with glucose (33mM) and/or palmitic acid (PA) (0.5mM) were studied.

Cells treated under 33mM glucose revealed significantly increased secretory vesicles and lipid droplets in the cytoplasm when compared to the cells processed with PA and the control cells. Golgi cisternae were more homogeneously dilated. Glycogen particles in the cytoplasm were increased. Cells incubated with 0.5mM PA had heterogeneously dilated Golgi cisternae with loss of lipid droplets in the cytoplasm and significantly decreased insulin vesicles compared to the control cells. Cells incubated both with glucose (33mMol) and PA (0,5mM) also revealed heterogeneously dilated Golgi cisternae and loss of lipid droplets.

In the present study, we showed that morphology of Golgi Apparatus and biosynthesis of lipid droplets are affected by lipotoxicity and glucolipototoxicity in  $\beta$ -cells. Golgi cisternae were dilated heterogeneously and lipid droplets were absent in the cytoplasm under lipotoxic and glucolipototoxic media. On the other hand, glucose even in high concentrations lead to a homogenous dilatation of golgi cisternae and an increase in lipid droplet biosynthesis.

#### **References:**

1. Laybutt DR, Preston AM, Akerfeldt MC et al. Endoplasmic reticulum stress contributes to beta cell apoptosis in Type 2 diabetes. *Diabetologia* 50:752-763, 2007
2. Poitout V, Amyot J, Semache M, Zarrouki B, Hagman D, Fontes G. Glucolipototoxicity of the pancreatic beta cell. *Biochimica et Biophysica Acta* 1801:289-298, 2010



## Who is the ADAMTS family?

**Tuba PARLAK AK**\*

Munzur University, Tunceli, Turkey

ADAMTS (A Disintegrin and Metalloproteinase with Thrombospondin Motifs) is a family of secreted enzymes and the ADAMTS proteins are a superfamily of 26 secreted molecules comprising two related, but distinct families. The human family includes 19 members that can be sub-grouped on the basis of their known substrates, namely the aggrecanases or proteoglycanases (ADAMTS1, 4, 5, 8, 9, 15 and 20), the procollagen N-propeptidases (ADAMTS2, 3 and 14), the cartilage oligomeric matrix protein-cleaving enzymes (ADAMTS7 and 12), the von-Willebrand Factor proteinase (ADAMTS13) and a group of orphan enzymes (ADAMTS6, 10, 16, 17, 18 and 19). The members have a pro-domain, and a metalloproteinase, disintegrin, and cysteine-rich domain, but they lack a transmembrane domain and instead have characteristic thrombospondin motifs. The ADAMTS proteases are multi-domain matrix-associated zinc metalloendopeptidases, most of whose substrates are extracellular matrix (ECM) components, whereas ADAMTS-like proteins lack a metalloprotease domain, reside in the ECM, and have regulatory roles vis-à-vis ECM assembly and/or ADAMTS activity. Control of the structure and function of the ECM is a central theme of the biology of the ADAMTS, as exemplified by the actions of the procollagen-N-propeptidases in collagen fibril assembly and of the aggrecanases in the cleavage or modification of ECM proteoglycans. Evolutionary conservation and expansion of ADAMTS proteins in mammals are suggestive of crucial embryologic or physiological roles in humans. Also, the ADAMTS enzymes play diverse important roles in the turnover of ECM proteins in various tissues, in tissue morphogenesis and pathophysiological remodeling, and in vascular biology. Their dysregulation has been implicated in disease-related processes such as inflammation and fibrosis. These enzymes are critical in many pathological situations such as cancers, musculoskeletal disorders, and autoimmune events as well as they have numerous potential connections to other human disorders that were identified by genome-wide association studies. Recent studies about the roles of these enzymes have produced new perspectives for the molecular mechanisms behind regenerative biology with clinical potential to generate therapeutic targets to resolve tissue injury. Finally, because the ADAMTS family members have the potential to alter tissue architecture and regulate cellular function, they can serve as important diagnostic biomarkers and potential therapeutic tools for the management of various disorders.

**Keywords:** ADAMTS family , extracellular matrix , biological biomarker , regenerative biology , metalloproteinases

### References:

1. Armutcu F, Demircan K. Emerging roles of ADAMTS metalloproteinases in regenerative medicine and restorative biology. *Turk J Biol* 2016;40: 308-15.
2. Kelwick R, Desanlis I, Wheeler GN, Edwards DR. The ADAMTS (A Disintegrin and Metalloproteinase with Thrombospondin motifs) family. *Genome Biol* 2015;16:113
3. Zhong, S, Khalil, RA. A Disintegrin and Metalloproteinase (ADAM) and ADAM with thrombospondin motifs (ADAMTS) family in vascular biology and disease. *Biochem Pharmacol.* 2019;164:188–204.

## PC-3 prostat kanseri hücrelerinde fenformin uygulamasının FGFR2 üzerine etkileri

**Dilan Çetinavcı<sup>1\*</sup>, Melike Özgül Önal<sup>2</sup>, Gürkan Yiğittürk<sup>2</sup>, Volkan Yaşar<sup>2</sup>, Hülya Elbe<sup>2</sup>, Feral Öztürk<sup>2</sup>**

<sup>1</sup> Muğla Sıtkı Koçman Üniversitesi, Eğitim ve Araştırma Hastanesi, Histoloji ve Embriyoloji, Muğla, Turkey

<sup>2</sup> Muğla Sıtkı Koçman Üniversitesi, Tıp Fakültesi, Histoloji ve Embriyoloji, Muğla, Türkiye, Muğla, Turkey

**Amaç:** Prostat kanseri, gelişmiş ülkelerde görülen önemli bir sağlık sorunu olmakla birlikte erkeklerde, ikinci en sık kansere bağlı ölüm nedenidir (1). Kanser tedavisinde kemoterapötik ajanlar kullanılır, ancak çoğu durumda hastalarda direnç gelişir. Bu sebeple prostat kanseri tedavisi için kullanılabilir yeni ilaçların bulunmasına ihtiyaç vardır. Fenformin, biguanid antidiyabetik ajandır. AMP ile aktive protein kinaz (AMPK) yolu ve mTOR düzenleyici kompleksin blokörü olarak antikanser etkileri bulunmaktadır (2). Fenforminin; rektal, over, meme ve mesane gibi çeşitli kanser tiplerinde antikanser aktivitesi çeşitli çalışmalar ile gösterilmiştir (3,4). Fibroblast büyüme faktörü reseptörü 2 (FGFR2), hücre proliferasyonunu ve farklılaşmasını destekleyen bir membran reseptörüdür. İnsan prostat kanseri vakalarından radikal prostatektomi ile elde edilen kanserli dokularda FGFR2 proteininin ortalama konsantrasyonu, kontrol dokusuna göre belirgin şekilde arttığı bilinmektedir (5). Çalışmamızın amacı; PC-3 insan prostat kanseri hücre hattında fenformin'in antikanserojen etkilerini FGFR2 üzerinden incelemektir.

**Gereç-Yöntem:** PC-3 insan prostat kanseri hücre hattı %10 FBS, 2 mM L-Glutamin ve %1 Penisilin/Streptomisin içeren RPMI-1640 besiyeri içerisinde ve 37°C, %5 CO2 koşullarını sağlayan nemli inkübatörde çoğaltıldı. 96 ve 24 kuyucuklu kültür kaplarına ekim yapıldı. Deneysel grupları kontrol grubu (uygulama yapılmamış), 1 mM, 2 mM, 5 mM ve 10 mM fenformin uygulaması gerçekleştirilmiş gruplar olacak şekilde planlandı. Uygulamalardan 24 saat sonra 96 kuyucuklu kültür kabının her kuyucuğuna içinde bulundurduğu besiyerinin 1:10' u kadar WST-1 (Water-soluble tetrazolium salt) çözeltisi eklendi. Hücreler 3 saat 37°C %5 CO2 optimum nemli koşullarda inkübe edildi. İnkübasyon sonunda 450 nm/650 nm dalga boylarında absorbans ölçümleri yapıldı. 24 kuyucuklu kültür kabında %4'lük paraformaldehit ile tespit edilen hücrelerde immunositokimyasal olarak FGFR2 dağılımlarının analizi gerçekleştirildi. İmmunoreaktivite boyanma sonuçları; boyanma yok (0), zayıf (1), orta (2) ve kuvvetli (3) olarak değerlendirildi. Her grup için rastgele seçilmiş 5 alanda her 100 hücre içinde pozitif boyanan hücreler sayılarak semi-kantitatif H-SCORE değerleri hesaplandı. (H-SCORE:  $\sum Pi (i+1)$  (Pi: % pozitif boyanmış hücre sayısı; i: boyanma şiddeti)). Sonuçlar "ortalama  $\pm$  standart sapma" olarak hesaplandı ve SPSS (Windows version 23.0) yazılımı kullanılarak değerlendirildi ve p<0.05 olan değerler istatistiksel olarak anlamlı kabul edildi.

**Bulgular ve sonuç:** WST sonuçlarında hücre canlılık yüzdelere %100 (kontrol), %92.533 (1 mM), %85.074 (2 mM), %11.252 (5 mM), %6.464 (10 mM) olduğu tespit edildi. WST sonuçlarının istatistiksel analizlerine göre kontrol ile 5 mM Fenformin grupları arasındaki azalma (p=0.019), kontrol ile 10 mM Fenformin grupları arasındaki azalma (p=0.002) ve 1 mM Fenformin ile 10 mM Fenformin grupları arası azalma (p=0.034) anlamlı çıktı. FGFR2 immunositokimyasal analizi sonuçlarına göre grupların H-SCORE değerleri sırası ile; 250.83 $\pm$ 9.06 (Kontrol), 249 $\pm$ 15.01 (1 mM), 239.33 $\pm$ 7.11 (2 mM), 219.5 $\pm$ 8.78 (5 mM) ve 218.5 $\pm$ 10.15 (10 mM) olarak hesaplandı. FGFR2 H-SCORE sonuçlarının istatistiksel analizlerine göre kontrol ile 5 mM Fenformin grupları arasındaki azalma (p=0.019), kontrol ile 10 mM Fenformin grupları arasındaki azalma (p=0.012), 1 mM Fenformin ile 5 mM Fenformin grupları arası azalma (p=0.028) ve 1 mM Fenformin ile 10 mM Fenformin grupları arası azalma (p=0.018) anlamlı bulundu.

Fenformin uygulanmış prostat kanseri hücrelerinde FGFR2 ekspresyonunu ve canlılığı azaltan en etkili dozun 10 mM fenformin olduğu ortaya konulmuştur. Bu çalışmanın farklı dozlar ve yöntemler kullanılarak in vitro ve in vivo fenformin ile yapılacak yeni çalışmalara yol gösterici olması ve literatüre katkı sağlaması beklenmektedir.

**Keywords:** Prostat kanseri , FGFR2 , PC3

### References:

1. Szliszka E, Krol W. Polyphenols isolated from propolis augment TRAIL-induced apoptosis in cancer cells. Evid Based Complement Alternat Med 2011; doi: 10.1155/2013/731940.
2. García Rubiño, M., Carrillo, E., Ruiz Alcalá, G., Domínguez-Martín, A., A Marchal, J., & Boulaiz, H. (2019). Phenformin as an anticancer agent: challenges and prospects. International journal of molecular sciences, 20(13), 3316.
3. Park, J. H., Kim, Y. H., Park, E. H., Lee, S. J., Kim, H., Kim, A., ... & Kim, M. J. (2019). Effects of metformin and phenformin on apoptosis and epithelial-mesenchymal transition in chemoresistant rectal cancer. Cancer science, 110(9), 2834.
4. Huang, Y., Zhou, S., He, C., Deng, J., Tao, T., Su, Q., ... & Yang, X. (2018). Phenformin alone or combined with gefitinib inhibits bladder cancer via AMPK and EGFR pathways. Cancer Communications, 38(1), 1-14.
5. Lee, J. E., Shin, S. H., Shin, H. W., Chun, Y. S., & Park, J. W. (2019). Nuclear FGFR2 negatively regulates hypoxia-induced cell invasion in prostate cancer by interacting with HIF-1 and HIF-2. Scientific reports, 9(1), 1-12.

## Effect of Melatonin on tumor growth and MDSCs in breast cancer model with circadian rhythm impairment

**Sayra Dilmac** , Sendegul Yildirim Ildem , Gamze Tanriover \*

Akdeniz University, School of Medicine, Department of Histology and Embryology, Antalya, Turkey

**Objectives:** Breast cancer is the second common cancer in women [1]. Circadian rhythm refers to changes in the organism's approximately daily physiological and biological processes [2]. Melatonin synthesis and secretion by the pineal gland is under the control of the suprachiasmatic nucleus and consequently has a profound circadian rhythm [3]. Melatonin inhibits tumor signal transduction and metabolic activity of cancer cells [4]. Myeloid-derived suppressor cells (MDSCs) are heterogeneous group of immune cells from the myeloid lineage which are positive for Gr1 and CD11b in the mouse. Presence of MDSCs in the tumor microenvironment reflects poor prognosis and likely to have a role in immune suppression [5]. In this study, we aimed to see the effect of melatonin on tumor progression and metastasis and its effect on MDSCs in the tumor microenvironment in mouse breast cancer model with circadian rhythm impairment. The aim of this study, to demonstrate how melatonin plays a role in the suppression of metastasis in mouse breast cancer model with circadian rhythm impairment.

**Method:** 8-weeks female BALB/c mice were randomly divided into 7 groups; Control (C), Circadian rhythm impairment (CR), 4TBM injected (TM), Circadian rhythm impairment and 4TBM injected (CR+TM+CR), 4TBM injected and melatonin treatment (TM+M), Circadian rhythm impairment, 4TBM injected and melatonin treatment (CR+TM+M+CR), Circadian rhythm impairment and vehicle injected (CR+ EtOH) for melatonin. 4T1-Brain Metastatic cells (4TBM) were injected into female BALB/c mice's mammary pad with orthotopically. Melatonin was administered (30 mg/kg) by intraperitoneally two times a day to TM+M and CR+TM+M+CR groups. Breast tumor sizes were measured twice a week. Tumor, lung, and liver tissue samples were removed 26 days after the inoculation of tumor cells, and also metastasis assays were performed. CD11b, GR1, TNF- $\alpha$  expressions were evaluated with immunohistochemically in primary tumors.

**Results:** In the CR+TM+CR group, it was seen that tumor size increased compared to TM group. These tumor growths decreased in melatonin treatment groups as; TM+M and CR+TM+M+CR. Also, TM+M group's tumor sizes were smaller than CR+TM+M+CR groups. Malignant cells metastasized to liver and lung were increased in circadian rhythm impairment groups compare that the others. According to our results, with the effect of melatonin, MDSC expressions and increased TNF- $\alpha$  expression due to inflammatory response decreased.

**Conclusion:** In conclusion, tumor growth and metastasis were significantly suppressed in the melatonin administration groups. Despite the administration of melatonin in breast cancer model, it was observed that circadian rhythm impairment increased for tumor growth and metastasis. In addition, melatonin suppresses the inflammatory response and MDSCs, which is thought to be one of the factors that inhibit tumor growth.

**Keywords:** Circadian rhythm , breast cancer , melatonin , metastasis , MDSC

### References:

1. Bray F, et al. (2018) Global cancer statistics 2018: GLOBOCAN estimates of incidence and mortality worldwide for 36 cancers in 185 countries. *CA Cancer J Clin* 68 (6): 394-424
2. Buttgerit F, et al. (2015) Clocking in: chronobiology in rheumatoid arthritis. *Nat Rev Rheumatol* 11 (6): 349-56
3. Haim A, Zubaidat AE (2015) Artificial light at night: melatonin as a mediator between the environment and epigenome. *Philos Trans R Soc Lond B Biol Sci* 370 1667)
4. Reiter RJ, et al. (2017) Melatonin, a Full Service Anti-Cancer Agent: Inhibition of Initiation, Progression and Metastasis. *Int J Mol Sci* 18 (4)
5. Tanriover G, et al. (2018) Presence of S100A8/Gr1-Positive Myeloid-Derived Suppressor Cells in Primary Tumors and Visceral Organs Invaded by Breast Carcinoma Cells. *Clin Breast Cancer* 18 (5): e1067-e76

## Breath analysis by FTIR spectroscopy for early detection of lung cancer

**Dilek Yonar**<sup>1,\*</sup>, **Deniz Köksal**<sup>2</sup>, **Ülkü Yılmaz**<sup>3</sup>

<sup>1</sup> Yüksek İhtisas University, Ankara, Turkey

<sup>2</sup> Hacettepe University, Ankara, Turkey

<sup>3</sup> Atatürk Chest Diseases and Chest Surgery Training and Research Hospital, Ankara, Turkey

Lung cancer is the leading cause of cancer and cancer related death worldwide [1]. The overall 5-year survival rate of lung cancer is 19% with a median survival time of 12 months [2]. The reason of this poor survival rate is its diagnosis at advanced stages. Thus, screening and early diagnosis are key issues for improving lung cancer survival rates [3].

Breath analysis is one of the most noninvasive screening approaches for early diagnosis of lung cancer. It has been reported that the presence and concentration of some volatile compounds in exhaled breath may be different in lung cancer patients than in healthy individuals [4]. This volatile organic compounds (VOCs) can be considered as biomarkers within the breath matrix for clinical diagnosis and disease monitoring since they represent different metabolic processes of body. Therefore, their identification is essential for clinical application of breath VOCs. Fourier transform infrared spectroscopy (FTIR) has recently gained clinical importance, since it is a fast, non-invasive and operator independent method. It gives information at molecular level and enables early diagnosis of the disease long before they become visible to pathologist [5]. In the present study, FTIR spectroscopy coupled with multivariate analysis methods were utilized to develop a new approach for breath analysis, the diagnosis of lung cancer and its differentiation from healthy individuals. The study included 94 patients with lung cancer aged from 24 to 85 years and 68 healthy controls aged from 22 to 82 years. Lung cancer patients were all treatment-naïve, newly diagnosed patients with Eastern Cooperative Oncology Group (ECOG) performance status  $\geq 2$ . IR gas phase spectra obtained from control and patients' breath samples were compared with current gas libraries, and VOCs over 70% correlation for both groups were determined. Although no different chemical substance was observed between healthy individuals and lung cancer patients, it was observed that there were quantitative differences in some spectral bands and a decrease in the intensities of out-of-plane C-H bending bands at 893, 910 and 990  $\text{cm}^{-1}$ , which are the most typical intense bands of alkenes. Moreover, unsupervised methods such as hierarchical cluster analysis (HCA) and principal component analysis (PCA) were performed to categorize groups and extract the meaningful information from complex and large spectral datasets. Based on the spectral differences, lung cancer differentiation from healthy individuals with 71% sensitivity and 65% specificity were obtained by HCA of breath IR spectra. PCA results showed that there are successful clustering for control and lung cancer group, the best variation is observed for the spectral region of 1300-800  $\text{cm}^{-1}$  when the variations in principal components, expressing the differences between the groups, are examined, and there are changes in VOC content of lung cancer patients' breath from higher loading values. This study demonstrated that FTIR spectroscopy coupled with multivariate analysis methods has a good potential in the diagnosis of lung cancer and its success can be increased by increasing the number of samples and selecting more demographically specific groups (This research was funded by TUBITAK-Project No: 115E046).

**Keywords:** lung cancer , exhaled breath , FTIR spectroscopy , multivariate analysis

### References:

1. Bray F, Ferlay J, Soerjomataram I, Siegel R L, Torre L A and Jemal A 2018 Global cancer statistics 2018: GLOBOCAN estimates of incidence and mortality worldwide for 36 cancers in 185 countries CA. Cancer J. Clin. 68
2. N H, AM N, M K, D M, A B, M Y, J R, Z T, A M, DR L, HS C, EJ F and KA C 2019 SEER Cancer Statistics Review, 1975-2016.
3. Bade B C, Brasher P B, Luna B W, Silvestri G A and Tanner N T 2018 Reviewing Lung Cancer Screening: The Who, Where, When, Why, and How Clin. Chest Med. 39
4. Peng G, Tisch U, Adams O, Hakim M, Shehada N, Broza Y Y, Billan S, Abdah-Bortnyak R, Kuten A and Haick H 2009 Diagnosing lung cancer in exhaled breath using gold nanoparticles Nat. Nanotechnol. 4
5. Yonar D, Ocek L, Tiftikcioglu B I, Zorlu Y and Severcan F 2018 Relapsing-Remitting Multiple Sclerosis diagnosis from cerebrospinal fluids via Fourier transform infrared spectroscopy coupled with multivariate analysis Sci. Rep. 8 1025

## Reversal from Taxane-Induced apoptosis in metastatic prostate cancer cells: Molecular effect of anastasis

Gamze Guney Eskiler<sup>1,\*</sup>, Asuman Deveci Ozkan<sup>1</sup>, Melek Ozturk<sup>2</sup>, Serap Arbak<sup>3</sup>

<sup>1</sup> Sakarya University, Sakarya, Turkey

<sup>2</sup> Istanbul-Cerrahpasa University, Istanbul, Turkey

<sup>3</sup> Acibadem University, Istanbul, Turkey

Anastasis is defined as the escape of dying cells from the death threshold and their return to life and therefore leads to recurrence, metastasis and the development of drug resistance. Taxanes are currently used as chemotherapy drugs in the treatment of different types of cancer and inhibit cell division by binding to microtubules and dynein microtubule motor proteins. We, for the first time, aimed to elucidate the relationship between cabazitaxel (CAB) and anastasis at the molecular level in metastatic prostate cancer cells. In this context, Annexin V, acridine orange (AO)/propidium iodide (PI) staining, oxidative stress analysis and mitochondrial staining were performed to detect anastasis in late apoptotic cells at different recovery time-dependent after treatment with 1 and 5 mM CAB for 72 h in PC-3 cells. While the total apoptotic cell death was 65.9% in PC-3 cells treated with 5 mM CAB for 72 h, the apoptosis rates were analyzed as 50.9%, 39.5% and 25.5% at recovery times of 12, 24 and 48 h, respectively and these findings were supported by AO/PI staining. Additionally, the amount of intracellular reactive oxygen species (ROS) and mitochondrial aggregation were lower depending on the recovery times compared with PC-3 cells following treatment with 5 mM CAB. Within the scope of the preliminary data of this study, it was concluded that anastasis might play a role in escape from apoptotic cell death and possible drug-resistance development in metastatic prostate cancer cells upon treatment with CAB.

**Keywords:** Metastatic prostate cancer , Taxane , Anastasis

## Seramidaz inhibisyonunun rat glioma hücreleri üzerine etkilerinin araştırılması

**Canan Vejselova Sezer\*, Hatice Mehtap Kutlu**

Eskişehir Teknik Üniversitesi, Eskişehir, Turkey

Kanser hastalığı günümüzde yüksek ölüm oranları ve görülme sıklığı nedenleriyle önemli toplum sağlığı tehditleri arasında yer almaktadır. Kanser genetik ve çevresel gibi farklı nedenlerle ortaya çıkabilmektedir. Bu hastalık hücrelerin anormal bir şekilde büyümesi, çoğalması ve düzensiz apoptoz geçirmesi nedenlerinin sonucunda oluşabilmektedir. İnsan vücudunda çok farklı kanser türleri mevcuttur. Gliomalar beyin dokularında sıklıkla meydana gelen kanser türlerindedir. Dünya Sağlık Örgütü gliomaları malignite seviyelerine göre derecelendirmiştir. Glioblastoma, beyin dokularında meydana gelen ve hızlıca yayılma özelliğine sahip ölümcül tümör tipi olup primer beyin tümörlerinin yaklaşık %30'unu teşkil etmektedir. Kanser araştırmalarında son yıllarda insan beyin tümörleri ve hayvan beyin tümör modelleri arasındaki benzerliklerden faydalanılmaktadır. Rat glioma hücre hattı olan C6, in vitro araştırmalarda kullanılan beyin tümör modeli olarak kaynaklarda yer almaktadır.

Son yıllarda kanser çalışmalarında çok farklı apoptoz tetikleme mekanizmaları olabilecek olan moleküller kullanılmaktadır. Böyle proapoptotik mekanizmaları tetikleme özelliği olan moleküllerden olan seramid yolağı üyeleri, kanser çalışmalarında anti-kanser etkinlik araştırmalarında yer almaktadır. Seramidler, sfingolipid metabolik yolağında yer alan, hücre içerisindeki seviyeleri arttığında apoptozu indükleyen moleküllerdir. Hücre içi seramidleri arttırmanın farklı yolları mevcuttur. Bu yollardan en etkili olanlardan birisi de seramidaz enzimlerinin inhibisyonudur. Seramidazları inhibe edebilen farklı inhibitörler mevcuttur ve farklı hücre hatlarında gerçekleştirilen kanser araştırmalarında kullanılmışlardır. LCL521 bir seramidaz inhibitörü olup C6 rat glioma hücreleri üzerindeki anti-kanser etkileri henüz aydınlatılmamıştır. Bu çalışmada LCL521 molekülünün C6 hücreleri üzerindeki sitotoksik, antiproliferatif ve proapoptotik etkileri araştırılmıştır.

Bulgular LCL521'in C6 glioma hücreleri üzerinde düşük dozlarda sitotoksikite gösterip, hücrelerin ince yapısını da değiştirerek apoptozu tetiklediğini göstermiştir. Tüm bulgular sonucunda, LCL521 ileri mekanistik ve teranostik çalışmalarda araştırılmak üzere önerilmiş olup in vitro düzeyde C6 hücrelerinde sitotoksikite, antiproliferatif ve proapoptotik etkileri aydınlatılmıştır.

**Keywords:** Sitotoksikite , Glioma , Seramidaz

### References:

1. Çiftçi, G. A., Işcan, A., & Kutlu, M. (2015). *Cytotechnology*, 67(5), 893–904.
2. Sonoda, Y., Kumabe, T., Watanabe, M., Nakazato, Y., Inoue, T., Kanamori, M., & Tominaga, T. (2009). 151(11), 1349–1358.
3. Furuya, H., Shimizu, Y., Kawamori, T. (2011). 30(3-4), 567–576.
4. Saied, E. M., and Arenz, C. (2016). 197, 60–68.

## Evaluation of the cancer biology research concept: GBM and astrocyte membrane topology, morphology and chemistry

**Berrin Ozdil Bay**<sup>1</sup>, **Duygu Calik-Kocaturk**<sup>2</sup>, **Cisem Altunayar-Unsalan**<sup>3</sup>, **Eda Acikgoz**<sup>4</sup>, **Fatih Oltulu**<sup>1</sup>, **Volkan Gorgulu**<sup>1</sup>, **Aysegul Uysal**<sup>1</sup>, **Gulperi Oktem**<sup>1</sup>, **Ozan Unsalan**<sup>5</sup>, **Huseyin Aktuğ**<sup>1,\*</sup>

<sup>1</sup> Department of Histology and Embryology, Faculty of Medicine, Ege University, İzmir, Turkey

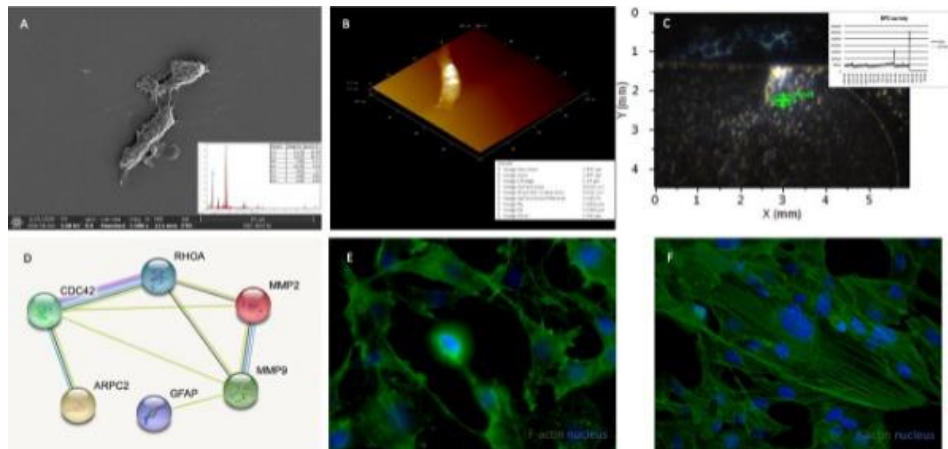
<sup>2</sup> Ismail Fehmi Cumalıoğlu Tekirdağ City Hospital, Tekirdag, Turkey

<sup>3</sup> Ege University Central Research Testing and Analysis Laboratory Research and Application Center (EGE-MATAL), İzmir, Turkey

<sup>4</sup> Department of Histology and Embryology, Faculty of Medicine, Van Yüzüncü Yıl University, Van, Turkey

<sup>5</sup> Department of Physics, Faculty of Science, Ege University, İzmir, Turkey

Astrocytes are the most abundant cells in the central nervous system and play critical roles for the organization and homeostasis of the brain. Glioblastoma multiforme (GBM) is astrocytic cancer which is the most common and aggressive primary brain tumour and is classified as a grade IV astrocytoma. Histologically, GBM consists of pleomorphic cells and shows high mitotic activity, intravascular microthrombus, necrosis, and/or microvascular proliferation. Although the characteristics of healthy and cancer cells and their responses to chemotherapeutic drugs have been clearly demonstrated in drug-based cancer approaches, studies investigating the differences and similarities of cancer cells from normal cells through a multidisciplinary perspective are still limited. Here, we presented a contribution to the cancer biology field by identifying the morphology, topology, and chemistry of cancer (GBM) and healthy (astrocyte) cells with different multi-analytical techniques. From this point of view, we performed immunofluorescence/RT-PCR test for cytoskeletal structure, Atomic Force Microscopy (AFM) for topological roughness, Scanning Electron Microscopy-Electron Dispersive Spectroscopy (SEM-EDS) for morphological and elemental assessment, and finally X-ray Photoelectron Spectroscopy (XPS) for the chemical composition of the cell membranes. GBM and astrocytes showed differential expression of cell cytoskeleton-related molecules at the gene and protein level. Besides, GBM and astrocytes both formed a membranous structure with cellular extensions and were firmly attached to the surface astrocyte cells which were also observed as more spread and dispersed morphology than GBM cells. Astrocyte cells had a distinct elevation in the nucleus region, spreading morphology in other cell parts. However, the heights of the astrocyte cells were slightly higher than GBM cells in general. AFM results showed that GBM and astrocyte cells presented relatively close roughness and these findings were consistent with the SEM-EDS results together with the elemental weight ratios which were statistically comparable in both cells. XPS results revealed the similar composition of the cell membrane. The abundance of C and O elements were close to each other in these cells. Our research demonstrates that the spectroscopic and microscopic techniques as a candidate of diagnostic tool in cell biology at molecular level should be considered in a combinatorial approach to further identify the membrane topology, morphology, and chemistry. This work was supported by Ege University Scientific Research Projects Coordination Office (grant number 18-TIP- 013).



**Keywords:** GBM , Astrocyte , AFM , XPS , SEM

## In Vitro investigation of the effect of *Trifolium pratense* L. on C6 glioblastoma cells

Gamze Tanriverdi <sup>1</sup>, Aynur Abdulova <sup>1,\*</sup>, Hatice Çölgeçen <sup>2</sup>, Belisa Kaleci <sup>1</sup>, Tuğba Ekiz-Yılmaz <sup>3</sup>

<sup>1</sup> Istanbul University-Cerrahpasa, Istanbul, Turkey

<sup>2</sup> Bülent Ecevit University, Zonguldak, Turkey

<sup>3</sup> Istanbul University, Istanbul, Turkey

**Introduction:** Glioblastoma multiforme (GBM) is the most common type of primary brain tumors in adults, characterized by its ability to proliferate rapidly and its tendency to aggressively and strongly spread into the surrounding brain tissue. The standard treatment approach of GBM is surgical resection followed by simultaneous chemotherapy and radiation. However, a significant number of GBM cases develop resistance to currently used chemotherapeutic drugs. Therefore, there is a need for the development of new chemotherapeutic agents. *Trifolium Pratense* L. is an endemic plant containing various isoflavones such as biochanin A, genistein, daidzein and formononetin in high concentrations, and it has been shown in various studies that these molecules can function as anticancer agents. The present study was designed to determine the effect of the possible anticarcinogenic effects of the "*Trifolium Pratense* L." plant which grown in our country and to obtain new treatment approaches alternative to the classical treatment protocols applied in the treatment of GBM.

**Material-Method:** C6 glioblastoma cells were cultured with increasing doses (0, 7, 12.5, 25, 50 and 100 µl) of *Trifolium Pratense* L. prepared by dissolving 22.5 µg in 100 µl ethanol for during 24 hour. Cell proliferation, apoptotic index and cell microtubule structure were evaluated with CCK-8, Annexin V and Beta-tubulin labeling respectively.

**Results and Discussion:** Decreased cell proliferation and increased number of apoptotic cells were observed depending on the increasing doses of *Trifolium Pratense* L. In addition, morphological changes and deformation in cells, deterioration both in tubule structure and in intercellular connections were detected depending on increasing doses. In this context, we believe that the plant *Trifolium Pratense* L., which is endemic in our country, may be a new alternative agent for the treatment of GBM.



## İnsan semen kriyoprezervasyonunda Koenzim Q10 ve Kurkuminin Spermatozoon ince yapısı üzerine etkileri

**Derya Özdemir Taş<sup>1,\*</sup>, İ.Sinan Özkavukcu<sup>2</sup>, Esra Erdemli<sup>2</sup>, İrem İnanç<sup>2</sup>, Kenan Köse<sup>2</sup>, Kaan Aydos<sup>2</sup>**

<sup>1</sup> Ankara City Hospital, Ankara, Turkey

<sup>2</sup> Ankara University School of Medicine, Ankara, Turkey

**Giriş:** Spermatozoonların sıvı azot buharındaki kriyoprezervasyonu diğer vitrifikasyon yöntemlerinden daha iyi sonuçlar vermesine rağmen hücrelerin hareketlilik (motilite), canlılık, akrozom bütünlüğü, DNA ve kromatin yapısında hasar oluşturmaktadır. Bu çalışmada insan sperm kriyoprezervasyonunda antioksidan maddeler olan kurkuminin ve koenzim Q10 (CoQ10)'un spermatozoonlar üzerindeki etkileri araştırılmıştır.

**Materyal Metod:** Ankara Üniversitesi Tıp Fakültesi Yardımcı Üreme Ünitesine semen analizi için başvuran 18 - 45 yaşları arasındaki 40 sağlıklı erkekte semen örneği alındı. Çalışma protokolü Ankara Üniversitesi Tıp Fakültesi Klinik Araştırmalar Etik Kurulu tarafından onaylandı (No: 07-429-18; Tarih: 16 Nisan 2018). Yıkama sonrası spermatozoonların bazal motilitesi, canlılığı, DNA fragmentasyonu ve ayrıntılı morfolojisi değerlendirildi. Daha sonra hücre süspansiyonları 4 gruba ayrıldı: Kontrol (antioksidan ilavesiz), Kurkumin (0.25 mM), Koenzim Q10 (25 µM) ve Kurkumin (0.25 mM) + Koenzim Q10 (25 µM). Sperm süspansiyonları, kriyoviyallerde 1:1 oranında antioksidan takviyeli veya takviyesiz sperm dondurma medyumunu ile karıştırıldı. Kriyoviyaller sıvı nitrojen buharında 30 dakika tutuldu ve ardından sıvı nitrojene yerleştirildi. Numuneler sıvı nitrojenden alınıp buz eriyene kadar sıcak suda çözüldü. Çözülme işlemi yapılan örneklerin canlılığı, motilitesi, DNA fragmentasyonu ve ayrıntılı morfolojisi değerlendirildi.

**Bulgular:** Kontrol grubu ile karşılaştırıldığında kurkuminin, canlılık ve motilite üzerine etkisinin olmadığı belirlendi. CoQ10 grubundaki spermatozoon canlılığı kontrol grubuna benzerdi ve CASA (Bilgisayar Destekli Sperm Analizi) spermatozoonun ileriye doğru hareket etme yüzdesinin özellikle arttığını gösterdi ( $p \leq 0.05$ ). İmmünofloresan ve akış sitometri analizleri, kurkumin (%22.2) ve kurkumin + CoQ10 (%18.9) gruplarında DNA fragmentasyonunun hem kontrol (%11.9) hem de CoQ10 (%10.7) gruplarıyla karşılaştırıldığında önemli ölçüde arttığını gösterdi ( $p < 0.05$ ). Geçirimli elektron mikroskopuyla ayrıntılı morfolojiye bakıldığında tüm gruplarda çözündürme sonrası akrozomal değişiklikler saptandı. Aynı zamanda subakrozomal bölgede şişme izlendi. Özellikle kurkumin grubunda, spermatozoonların hücre zarı bütünlüğü ve baş bölge morfolojisindeki değişiklikler belirgindi. CoQ10 grubunda orta parçadaki mitokondriyon yapısı ve baş bölgesinin hücre zarı yapısı bütünlüğünün korunduğu gözlemlendi.

**Sonuç:** Kriyoprezervasyon sürecinde CoQ10 grubunda spermatozoon morfolojisinin ve motilitesinin daha iyi korunduğunu göstermektedir. Bu sonuç, özellikle elektron taşıma zincirinde spermatozoonun mitokondriyondan zengin orta parçası ile CoQ10 arasında bir ilişki olabileceğini göstermektedir. Kurkumin ve kurkumin + CoQ10 gruplarında yüksek oranda DNA fragmentasyonu ve baş bölgesinde kusurlar gözlemlenmiştir. Bu nedenle özellikle kurkuminin kriyoprezervasyon işleminde doza bağımlı kullanımı konusunda daha ileri çalışmalara ihtiyaç vardır.

Bu çalışma Ankara Üniversitesi tarafından finanse edilmiştir (BAP No: 18L0230011).

**Keywords:** Spermatozoon hücresi, kriyoprezervasyon, koenzim Q10, kurkumin

### References:

1. CONNELL, M., MCCLURE, N. & LEWIS, S. E. 2002. The effects of cryopreservation on sperm morphology, motility and mitochondrial function. *Hum Reprod*, 17, 704-9.
2. OZKAVUKCU, S., ERDEMLI, E., ISIK, A., OZTUNA, D. & KARAHUSEYINOGLU, S. 2008. Effects of cryopreservation on sperm parameters and ultrastructural morphology of human spermatozoa. *J Assist Reprod Genet*, 25, 403-11.
3. WANG, S., WANG, W., XU, Y., TANG, M., FANG, J., SUN, H., SUN, Y., GU, M., LIU, Z., ZHANG, Z., LIN, F., WU, T., SONG, N., WANG, Z., ZHANG, W. & YIN, C. 2014. Proteomic characteristics of human sperm cryopreservation. *Proteomics*, 14, 298-310.
4. LIU, T., GAO, J., ZHOU, N., MO, M., WANG, X., ZHANG, X., YANG, H., CHEN, Q., AO, L., LIU, J., CUI, Z. & CAO, J. 2016. The effect of two cryopreservation methods on human sperm DNA damage. *Cryobiology*, 72, 210-5.

## The potential role of Sox9 in embryo implantation and decidualization

**Cemre Nur Balci, Nuray Acar Aydemir<sup>\*</sup>, Ezgi Golal, Ismail Ustunel, Ozlem Ozbey Unlu**  
Akdeniz University, Antalya, Turkey

**Objective:** Embryo development, implantation and decidualization are critical for healthy pregnancy in mammals. Successful implantation requires communication between competent blastocyst and receptive uterus. Sox genes have key roles on cell identities, reprogramming cell fates and are critical factors on developmental and physiological mechanisms. Twenty Sox genes are encoded by human and mouse genomes. Member of the Sox family have high mobility group DNA binding domain that are conserved. One member of the Sox family, Sox9 (SRY-Box transcription factor 9) is a transcriptional activator of target genes and contains an activation domain. In previous studies, expressions of SOX9 were detected in epithelium of many organs. SOX9 expression was shown to be in human endometrium and this expression was significantly increased in proliferative phase compared to secretory phase. In addition, Sox9 expressions have been shown in human endometrial cell lines and endometrial tumors. There are no studies in the literature showing whether Sox9 has a role in implantation and decidualization. In this study, we aimed to evaluate the expression and localization of Sox9 in peri-implantation period mouse uteri and implantation sites.

**Methods:** We used Balb/C mice for our study. 6-8 weeks old female and 12-16 weeks old male mice were mated. Next day females with vaginal plaque were accepted on first day of pregnancy. Uteri of mice on estrous phase, uteri and implantation sites of mice on days 1, 4, 5, 6 and 8 of pregnancy were collected. In addition, inter-implantation sites between implantation sites of mice on day 5 of pregnancy were taken. Localization of SOX9 was determined by immunohistochemistry and analysed via H-SCORE, SOX9 expression was determined quantitatively by Western blot and analysed via Image J software (NIH, USA).

**Results:** Sox9 was expressed at different intensities in luminal epithelium, gland epithelium and stroma layers of all experimental groups. According to Western blot analysis, Sox9 expression increased in D4 group compared to oestrus ( $p<0.05$ ) and D1 ( $p<0.005$ ) groups. Sox9 expression was at highest in D6 group. Although there is no significant difference between D6 and D8 groups, Sox9 expression decreased in D8 group ( $p>0.05$ ).

**Conclusion:** Our findings suggest that SOX9 may be involved in implantation and decidualization processes. We believe that our study will guide further studies and may help to understand roles of Sox9 in peri-implantation period and elucidate the underlying causes of various pathologies such as implantation failure, pregnancy loss and in the clinic.

**Keywords:** SOX9, mouse, uterus, implantation, decidualization

## Role of hippo signaling pathway in peri-implantation period mouse uterus

**Ezgi Golal , Nuray Acar aydemir \* , Cemre Nur Balcı , İsmail Üstünel**

Akdeniz University, Antalya, Turkey

**Objective:** The events in uterus during peri-implantation period are critical for healthy progression and termination of pregnancy. These include development of embryo, acquisition of uterine receptivity, implantation and decidualization. Hippo signaling pathway was first discovered in *Drosophila melanogaster* that regulates organ size and then was demonstrated in mammals too. Hippo signaling pathway regulates cell number by regulating cell proliferation, apoptosis and differentiation. In this study, we aimed to determine localization and expressions of YAP (Yes-Associated Protein), TEAD1 (Tea Domain 1) and CTGF (Connective Tissue Growth Factor) which are members of Hippo signaling pathway in peri-implantation mouse uteri and implantation sites.

**Methods:** One male and two female Balb/C mice were kept in same cage overnight, following day female with vaginal plaque were accepted on first day of pregnancy. Uteri and implantation sites of mice on days 1, 4, 5, 6 and 8 of pregnancy were obtained. Expressions of YAP (Yes-Associated Protein), TEAD1 (Tea Domain 1) and CTGF (Connective Tissue Growth Factor) in these tissues were quantitatively determined by Western blot, localizations were determined by immunohistochemistry and were evaluated via H-SCORE.

**Results:** YAP (Yes-Associated Protein), TEAD1 (Tea Domain 1) and CTGF (Connective Tissue Growth Factor) were expressed at different densities in the uteri and implantation sites of different days of pregnancy. According to our Western blot findings, YAP, TEAD1 and CTGF expressions increased on days that proliferation was high. We observed that expressions of YAP, TEAD1 and CTGF decreased on days that differentiation was high. According to our immunohistochemistry findings, expressions of YAP and CTGF were low in lumen epithelium of implantation sites on day 5 of pregnancy where embryo implants. Also we observed that expressions of YAP and CTGF was high in implantation sites on day 6 of pregnancy, when decidualization takes place.

**Conclusion:** It is known that Hippo signaling pathway has a role in the regulation of cell proliferation, apoptosis and differentiation. We have shown different expressions of members of Hippo signal pathway-YAP, TEAD1 and CTGF- in uteri and implantation sites on different days of pregnancy. We conclude that Hippo signaling pathway may play a role in implantation and decidualization processes in mouse.

**Keywords:** mouse , implantation , YAP , TEAD1 , CTGF

### References:

1. Bao, Y., et al., Mammalian Hippo pathway: from development to cancer and beyond. *J Biochem*, 2011. 149(4): p. 361-79.
2. Croy, A., *The Guide to Investigation of Mouse Pregnancy*. Elsevier, 2014.
3. Yu, F.X. and K.L. Guan, The Hippo pathway: regulators and regulations. *Genes Dev*, 2013. 27(4): p. 355-71.

## The Effect of DHEA on Liver and Kidney of Young Male Rats

Gozde Erkanli Senturk \* , Fatma Beyza Sag , Hakan Sahin , Zehra Sezer

Department of Histology and Embryology, Cerrahpasa Faculty of Medicine, Istanbul University-Cerrahpasa, Istanbul, Turkey

Dehydroepiandrosterone (DHEA) is a steroidal hormone classified as an adrenal androgen, acting as a precursor of androgens and estrogens. DHEA has been marketed as an over-the-counter nutritional supplement. Recently published data displays DHEA has dual effects as protective and detrimental effects for cells, particularly liver and kidney cells. We investigated the effect of DHEA on young male rats and possible detrimental effects treated with vitamin E (Vit E) as a popular anti-oxidant. In order to remark to the importance of our study due to the increasing use of DHEA as a dietary supplement for body-building in young people, especially young men, we aimed to reveal the possible detrimental effects of chronically high doses of DHEA intake by young men. For this purpose, male 21-days old Sprague-Dawley rats (pre-puberty) were randomly divided into three groups as control (n=4), DHEA (n=8), and DHEA+Vit E (n=8). Since our aim is to study chronic and high dose of DHEA's effects, it was decided that the best method to adopt for this investigation to apply 60 mg/kg/day subcutaneously DHEA for a total of 28 days on DHEA and DHEA+Vit E groups. Additionally, DHEA+Vit E group were given 200 mg/kg/day Vit E by oral way for total 28 days starting by the after day of last DHEA application. Control group was given with the same method and amount of sesame oil parallel to both DHEA and Vit E applications. Kidney and liver morphologies were investigated by hematoxylin and eosin staining. As subsequent histomorphological examinations, periodic acid schiff (PAS) technique was used to estimate the thickness of parietal layer of bowman capsules and glycocalyx layer of proximal tubules in kidney. Moreover, PAS technique was used to investigate liver in terms of glycogen storages of hepatocytes. Furthermore, Gomori's silver stain was used to show reticular fibers and cleaved caspase-3 which is an apoptosis marker was used on liver tissue by immunohistochemistry. Consequently, as a result of PAS technique, it was indicated that thickness of parietal layer of bowman capsule got thicker in DHEA group (p=0.027). Along with this, there was no significant difference in liver tissue of rats in terms of total glycogen positive areas, although control group showed higher levels of positive areas comparing to the other groups. On the other hand, while apoptosis increased significantly in DHEA group (p=0.005), DHEA+Vit E group showed decrement of apoptosis (p=0.022) according to immunohistochemical results. Moreover, Gomori's silver stain showed that detrimental effect of DHEA in liver structure (p=0.010) is alleviated by the treatment with vit E (p=0.011) compared to the control group.

**Keywords:** dehydroepiandrosterone , vitamin E , kidney , liver , histology

## The Use of CRISPR/Cas9 systems for the evaluation of implantation parameters in a Three-Dimensional implantation model

**Gizem Söyler \*** , Gizem Nur Şahin , Mehmet Yunus Çomar , Alişan Kayabölen , Ali Cihan Taşkın , Ahmet Kocabay , Serçin Karahüseyinoğlu  
Koç University, Istanbul, Turkey

**Background:** Implantation is a highly complex biological event, and any disruptions may cause recurrent implantation failure or pregnancy loss. The aim of this study is to knock out p53, a tumor suppressor gene crucial for embryo implantation, by CRISPR/Cas9 genome edition technology, separately in endometrial epithelial and stromal cells to detect the effect of silenced p53 on the other implantation related genes in a three-dimensional blastocyst culture system.

**Methods:** Zygotes from superovulated mice were harvested and cultured up to the blastocyst stage (4AA, Gardner's classification). A three-dimensional culture construction was prepared by application of endometrial stromal cells into and endometrial epithelial cells onto Matrigel. Blastocysts were placed on the culture systems for incubation of 24 and 72 hours. Three groups of cultures were prepared: i. wild stromal cells, wild epithelial cells, wild blastocysts; ii. mutant stromal cells, wild epithelial cells, wild blastocysts, iii. wild stromal cells, mutant epithelial cells, wild blastocysts, iv. routine drop IVF culture Mutant cells were obtained by knocking out the p53 gene in these group of cells via the use of CRISPR/Cas9. Briefly, in 293T cells lentivirus particles that possess the cloning plasmid for p53 gRNA and Cas9 gene sequences were obtained, and the endometrial cells were transfected separately for different experimental groups. Following the incubation, qPCR analysis was accomplished to detect the effect of knocked out p53 gene on the other implantation genes as MMP9, E-cadherin, fibronectin, Wnt, Hoxa10, LIF, estrogen receptor (ER), progesterone receptor (PR). Immunofluorescent stainings were also performed for MMP9, LIF, ER, PR, e-cadherin, entactin, and fibronectin for the evaluation of adhesion, invasion, and functional properties. The imaging was obtained by STED equipped Leica dmi8/sp8 confocal microscope.

**Results:** In both mutant groups silencing p53 has caused a significant increase in MMP9 expression ( $p < 0.05$ ). The expressions of ER, PR, fibronectin, and LIF were decreased significantly in these groups ( $p < 0.05$ ). Although there were some alterations in the expression of developmental genes of Hoxa10 and Wnt, the difference was non-significant. Although non-significant the decrease in Hoxa10 was seen in both mutant groups, to give a clue about the role of p53 in development, as well. A differential effect between stromal and epithelial cells was revealed for entactin (nidogen-1) which is an essential component of the basement membrane. The effects were also revealed significantly by microscopic imaging.

**Conclusion:** It has been revealed that p53 has an important role especially in the controlled invasion of the blastocyst and both epithelial and stromal cells take part in this effect. CRISPR/Cas9 can be used differentially to detect the effects of different genes in separate cells in three-dimensional culture systems.

**Acknowledgment:** Part of this study has been supported by TUBİTAK 118S676.

**Keywords:** implantation , p53 , CRISPR/Cas9 , 3D culture

### References:

1. Psychoyos A. Uterine receptivity for nidation. Ann N Y Acad Sci. 1986;476:36–42. doi: 10.1111/j.1749-6632.1986.tb20920.x.
2. Paria B C, Reese J, Das S K, Dey S K. Deciphering the crosstalk of implantation: advances and challenges. Science. 2002;296:2185–2188. doi: 10.1126/science.1071601

## Linagliptinin İnsülin İle birlikte kullanımı Tip 1 diyabetik fare ovaryumunda Pro-apoptotik Chop/Ddit3 mRNA ifadesini azaltır

**Aslı Okan Oflamaz<sup>1</sup>, Necdet DEMİR<sup>2,\*</sup>**

<sup>1</sup> Yozgat Bozok Üniversitesi, Tıp Fakültesi, Histoloji ve Embriyoloji Anabilim Dalı, Yozgat, Turkey

<sup>2</sup> Akdeniz Üniversitesi, Tıp Fakültesi, Histoloji ve Embriyoloji Anabilim Dalı, Antalya, Turkey

Endoplazmik retikulum (ER) stresinin ve katlanmamış protein yanıt sinyalinin ovaryen fizyolojisindeki işlevlerine ek olarak, ovaryen hipersitümlasyon sendromu [1], polikistik over sendromu [2], over kanseri [3] ve tip 1 diyabetes mellitus (T1DM) [4] gibi ovaryen patolojisinde de rolleri vardır. İnsülindeki ve uygulamadaki gelişmelere rağmen, T1DM'li hastaların çoğu insülin tedavisi ile optimal glikoz kontrolüne erişmede zorluk yaşamaya devam etmektedir [5]. Tedavi hedeflerine ulaşmak için, insüline tamamlayıcı olan ilaçların kullanıldığı kombinasyon terapisi uygun olabilir. Dipeptidil peptidaz-4 (DPP-4) inhibitörleri (Vildagliptin, linagliptin, saxagliptin, alogliptin ve dutogliptin)[6], hiperglisemi tedavisi için yeni bir ilaç sınıfıdır. Linagliptinin diğer iki DPP-4 inhibitörde (sitagliptin ve vildagliptin) olmayan glikozdaki herhangi bir düşüşten bağımsız olarak NADPH oksidaz aktivitesi ve malondialdehid (MDA) seviyeleri incelenerek antioksidan aktivite gösterdiği kanıtlanmıştır [7, 8]. Özellikle, hiperglisemi ER stresine paralel olarak oksidatif strese de neden olur [9, 10]. Dolayısıyla, linagliptin ER stresi sonucu oluşan reaktif oksijen türlerinin (ROT) üretimini azaltarak hiperglisemik koşullar altında kalan ovaryumun apoptozdan kaçınmalarını sağlayabilir. Hipoglisemi riskini artırmadan kan şekerini düşürücü etkileri ve yüksek antioksidan aktivitesi olan linagliptinin, insülin ile birlikte uygulanmasının tip 1 diyabetik fare ovaryumlarında ER stresi ilişkili yanıtta rol oynayan genlerin ekspresyon düzeylerini nasıl etkilediğini incelemeyi amaçladık.

Bu çalışmada, 6 haftalık her grupta 12 hayvan olmak üzere toplamda 84 adet Balb/C dişi fare yedi gruba ayrıldı: 1) Kontrol, 2) Çözgen, 3) İnsülin, 4) Linagliptin, 5) Linagliptin+İnsülin, 6) TUDCA ve 7) TUDCA+İnsülin grupları. Streptozotosin (STZ, 150 mg/kg/bw), kontrol ve çözgen grupları dışında tip 1 diyabetik fare modelini oluşturmak için tek doz olarak ip olarak enjekte edildi. Linagliptin (3 mg/kg/gün) ve Tauroursodeokisikolik (TUDCA, 100 mg/kg/gün) iki hafta boyunca oral gavaj yoluyla uygulandı. Deneyin sonunda fareler servikal dislokasyon ile sakrifiye edildi ve ovaryum dokuları çıkartıldı. Farelerden alınan kan serum örneklerinde linagliptinin etkinliğini teyit etmek amacıyla ELISA yöntemi ile DPP-4 aktivitesi ölçüldü. Buna ek olarak, alınan ovaryum örneklerinde linagliptinin antioksidan aktivitesini belirlemek için ELISA yöntemi ile reaktif oksijen türleri olan MDA ve NOX1 değerlerinin ölçümü yapıldı. qRT-PCR yöntemi ile ER stresi belirteçleri olan Grp78 ve pro-apoptotik Ddit3 genlerinin ekspresyon seviyeleri incelendi.

İncelenen serum örneklerinde İnsülin grubunda incelenen DPP-4 değeri diğer tüm gruplardan daha yüksek çıkmıştır (P<0.05). Linagliptin ve TUDCA uygulaması bu gruplara ait kan serumlarındaki DPP-4 değerlerini düşürdüğü gözlenmiştir (P<0.05). MDA ve NOX1 değerleri İnsülin gruplarında artarken, Linagliptin uygulanan gruplarda ise bu değerler azalmıştır. Fakat hem MDA (P=0.4826) hem de NOX1 (P=0.2129) açısından gruplar arasında istatistiksel olarak anlamlı bir farklılık olmadığı tespit edilmiştir (P>0.05). Grp78/Bip mRNA ekspresyonu İnsülin grubunda artmış olmasına rağmen gruplar arasında istatistiksel olarak anlamlı bir farklılık tespit edilmemiştir (P= 0.4146). Chop/Ddit3 mRNA ekspresyonu İnsülin ve TUDCA gruplarında artmıştır (P<0.0001). Linagliptin, Linagliptin+İnsülin ve TUDCA+İnsülin gruplarında Chop/Ddit3 mRNA ekspresyonu İnsülin grubuna göre anlamlı miktarda düşmüştür (P<0.05).

TUDCA hem glukoz homeostazi üzerine yararlı etkisinin olması [11] hem de ER stresini azaltan bir kimyasal şaperon [12] olması nedeniyle linagliptinin ER stresi ve diyabet ile olan ilişkisini değerlendirmek açısından önem taşımaktadır. Bulgularımıza göre, Linagliptin ve İnsülinin birlikte kullanımı, TUDCA+İnsülin grubundaki verilerle paralel olarak ER stresi ilişkili apoptotik yanıtta etkin olan Chop/Ddit3 mRNA ekspresyonunu azaltmıştır. Çalışmamızın bulgularının diyabete bağlı gelişen ovaryen başarısızlıkların tedavisinde kullanılabilir yeni yaklaşımlara katkıda bulunacağına inanmaktayız.

**Keywords:** DPP-4, Linagliptin, Fare, Diyabet, Chop

### References:

1. Takahashi N, Harada M, Hirota Y, Zhao L, Yoshino O, Urata Y, et al. A potential role of endoplasmic reticulum stress in development of ovarian hyperstimulation syndrome. *Mol Cell Endocrinol.* 2016;428:161-9. doi: 10.1016/j.mce.2016.03.032. PubMed PMID: 27032713.
2. Takahashi N, Harada M, Hirota Y, Nose E, Azhary JM, Koike H, et al. Activation of Endoplasmic Reticulum Stress in Granulosa Cells from Patients with Polycystic Ovary Syndrome Contributes to Ovarian Fibrosis. *Sci Rep.* 2017;7(1):10824. doi: 10.1038/s41598-017-11252-7. PubMed PMID: 28883502; PubMed Central PMCID: PMC5589802.
3. Hu JL, Hu XL, Guo AY, Wang CJ, Wen YY, Cang SD. Endoplasmic reticulum stress promotes autophagy and apoptosis and reverses chemoresistance in human ovarian cancer cells. *Oncotarget.* 2017;8(30):49380-94. doi: 10.18632/oncotarget.17673. PubMed PMID: 28537902; PubMed Central PMCID: PMC5564776.
4. Okan A, Demir N, Sozen B. Unfolded protein response triggers differential apoptotic mechanisms in ovaries and early embryos exposed to maternal type 1 diabetes. *Sci Rep.* 2021;11(1):12759. doi: 10.1038/s41598-021-92093-3. PubMed PMID: 34140543; PubMed Central PMCID: PMC58211688.
5. Livingstone R, Boyle JG, Petrie JR, Team RS. A new perspective on metformin therapy in type 1 diabetes. *Diabetologia.* 2017;60(9):1594-600. doi: 10.1007/s00125-017-4364-6. PubMed PMID: 28770327; PubMed Central PMCID: PMC5552844.
6. Deacon CF, Holst JJ. Dipeptidyl peptidase-4 inhibitors for the treatment of type 2 diabetes: comparison, efficacy and safety. *Expert Opin Pharmacother.* 2013;14(15):2047-58. doi: 10.1517/14656566.2013.824966. PubMed PMID: 23919507.
7. Salheen SM, Panchapakesan U, Pollock CA, Woodman OL. The Dipeptidyl Peptidase-4 Inhibitor Linagliptin Preserves Endothelial Function in Mesenteric Arteries from Type 1 Diabetic Rats without Decreasing Plasma Glucose. *PLoS One.* 2015;10(11):e0143941. doi: 10.1371/journal.pone.0143941. PubMed PMID: 26618855; PubMed Central PMCID: PMC4664283.
8. Kroller-Schon S, Knorr M, Hausding M, Oelze M, Schuff A, Schell R, et al. Glucose-independent improvement of vascular dysfunction in experimental sepsis by dipeptidyl-peptidase 4 inhibition. *Cardiovasc Res.* 2012;96(1):140-9. doi: 10.1093/cvr/cvs246. PubMed PMID: 22843705.
9. Basha B, Samuel SM, Triggler CR, Ding H. Endothelial dysfunction in diabetes mellitus: possible involvement of endoplasmic reticulum stress? *Exp Diabetes Res.* 2012;2012:481840. doi: 10.1155/2012/481840. PubMed PMID: 22474423; PubMed Central PMCID: PMC3299342.
10. Mooradian AD, Haas MJ. Glucose-induced endoplasmic reticulum stress is independent of oxidative stress: A mechanistic explanation for the failure of antioxidant therapy in diabetes. *Free Radic Biol Med.* 2011;50(9):1140-3. doi: 10.1016/j.freeradbiomed.2011.02.002. PubMed PMID: 21320588.
11. Vettorazzi JF, Kurauti MA, Soares GM, Borck PC, Ferreira SM, Branco RCS, et al. Bile acid TUDCA improves insulin clearance by increasing the expression of insulin-degrading enzyme in the liver of obese mice. *Sci Rep.* 2017;7(1):14876. doi: 10.1038/s41598-017-13974-0. PubMed PMID: 29093479; PubMed Central PMCID: PMC565899.

## Boric acid supplementation in embryo culture medium treatment vitrified mouse embryo by Solid Surface Vitrification (SSV)

Ali Cihan Taskin \*, Ahmet Kocabay  
Koc University, Istanbul, Turkey

Boric acid (BA) is an essential trace element for plants, humans and animals to support metabolic events(1). Reproductive biotechnology studies focus on the long-term storage of embryos (cryopreservation), embryo cultures, genome editing of embryos and embryo transfer. Micromanipulation techniques in reproduction biotechnologies have an important role especially in studies investigating assisted reproductive technology in laboratory animals. Importantly, the quality of the produced blastocysts and may vary depending on the culture conditions (2-3). The specific culture conditions in which embryos are cultured can affect the blastocyst quality, cell numbers. Embryo and embryos are exposed to severe oxidative stress at in vitro culturing conditions (4). Oxidative stress is also a critical factor in mortality animal derived cells and tissues during vitrification process. Most effective way to overcome this issue is supplementation anti-oxidants to culture media. The previous studies of BA have a potential beneficial effect on sertoli cells, leydig cells, fetal embryo development of lab animals due to antioxidant activity (5-7). In the literature, there is no publication about boric acid effect on preimplantation mouse embryo about in vitro developments of cryopreservation embryo. In this presented study, in vitro propagated oocytes were vitrification by Solid Surface Vitrification (SSV) method and after thawing, their in vitro development and embryo qualities in boric acid added media were investigated. Superovulated C57Bl6/6j female mice (5–6 weeks of age) were killed ~18 to 20 h after hCG administration. Single-cell embryos were flushed from the oviducts of the dead mice with human tubal fluid medium supplemented with HEPES and 3 mg/mL of BSA (A3311). The single-cell embryos were randomly divided into 3 groups and cultured in LifeGlobal blastocyst medium supplemented with 4 mg/mL BSA +0 (control), SSV and SSV+10-5 ppm BA+LifeGlobal Embryo Culture medium+4 mg/mL of BSA in 5% CO<sub>2</sub>, 37°C until 96-120 h at the blastocyst stage(8). The results were evaluated using one-way ANOVA with Bonferroni post-hoc test in SPSS 22.0. The P-values <0.05 were considered statistically significant. Each experiment was repeated at least 3 times. The blastocyst development rates of 0, SSV, and SSV+10-5 ppm BA were 68.11% (36/59), 40.16% (16/48) and 64.92% (28/48), respectively. The in vitro development rates were no significantly in the 10-5 ppm compared with 0 (control) (P≥0.05). Our results indicated that boric acid supplementation of embryo culture increased development rates embryos vitrification by SSV method.

**Keywords:** Boric acid , Mouse , Emrbyo , Cryopreservation

### References:

1. Sogut, I., Oglakci, A., Kartkaya, K., Ol, K. K., Sogut, M. S., Kanbak, G., & Inal, M. E. (2015). Effect of boric acid on oxidative stress in rats with fetal alcohol syndrome. *Experimental and therapeutic medicine*, 9(3), 1023-1027.
2. Smith AG (2001) Embryo-derived stem cells: of mice and men. *Annu Rev Cell Dev Biol* 17: 435-462.
3. Iijima S, Tanimoto Y, Mizuno S, Daitoku Y, Kunita S, Sugiyama F and Yagami KI (2010) Effect of different culture conditions on establishment of embryonic stem cells from BALB/cAJ and NZB/BINJ mice. *Cell Reprogram* 12: 679-688.
4. Nagina, G., Asima, A., Nemat, U., & Shamim, A. (2016). Effect of melatonin on maturation capacity and fertilization of Nili-Ravi buffalo (*Bubalus bubalis*) embryo. *Open veterinary journal*, 6(2), 128-134.
5. Sinan, İ. N. C. E., DEMİREL, H. H., ERDOĞAN, M., Cevdet, U. Ğ. U. Z., Yuksel, A. G. C. A., & Gamze, D. A. L. Borun ratlarda embriyo morfolojisi üzerine etkisi/The effect of boron on embryo morphology in rats. *Journal of Boron*, 1(2), 60-65.
6. Lu, L., Zhang, Q., Ren, M., Jin, E., Hu, Q., Zhao, C., & Li, S. (2020). Effects of boron on cytotoxicity, apoptosis, and cell cycle of cultured rat Sertoli cells in vitro. *Biological trace element research*, 196(1), 223-230.
7. Yalcin, C. O., & Abudayyak, M. (2020). Effects of boric acid on cell death and oxidative stress of mouse TM3 Leydig cells in vitro. *Journal of Trace Elements in Medicine and Biology*, 61, 126506.
8. Taskin AC, Kocabay A, Ebrahimi A, Karahuseyinoglu S, Sahin GN, Ozcimen B, Ruacan A & Onder TT (2019) Leptin treatment of in vitro cultured embryos increases outgrowth rate of inner cell mass during embryonic stem cell derivation. *In Vitro Cell Dev Biol Anim* 1-9.

### Effects of intraperitoneal and intranasal oxytocin administrated rat ovaries

**Zehra Sezer** , **Gozde Erkanli Senturk \*** , **Hakan Sahin** , **Basak Isildar** , **Aynur Abdulova**

Istanbul University-Cerrahpasa, Cerrahpasa Faculty of Medicine, Department of Histology and Embryology, Istanbul, Turkey

Oxytocin (OT) is a neuropeptide and its receptors are distributed widely both central nervous system (CNS) and periphery. Its role in labor and lactation is well-defined and it is also widely distributed throughout the CNS. However, it has been reported that OT is found in the gonads of mammals and is a locally produced hormone that acts on the ovary. Some studies have suggested that OT administration exogenously can have therapeutic effects on the uterus and ovary. Since OT has a low ability to pass brain-blood barrier, many studies applied this neuropeptide intranasal way to be more effective instead of other systemic ways like intraperitoneal method. Although there are many studies applied OT intranasal way to be more effective comparing to the intraperitoneal method in the brain research, there are very limited studies which compare intranasal and intraperitoneal administration method of OT on the female reproductive system. This study aims to investigate the effects of intraperitoneal (ip) and intranasal (in) OT administration on ovary of female rats.

All rats were divided randomly into four groups: The control group (n = 8) received no treatment. Rats in OT-ip group were treated with 0,1mg/100 ml of OT intraperitoneally for 28 days. Rats in OT-in/1 and OT-in/2 groups, were treated with 0,05 mg/ 100 ml and 0,1 mg/100 ml OT for 28 days, respectively. Subsequently, blood samples were collected for biochemical analysis; follicle-stimulating hormone (FSH), Luteinizing hormone (LH), anti-müllerian hormone (AMH), 17- $\beta$  estradiol (E2), oxytocin (OT), and testosterone (TT) were analyzed by ELISA in serum samples. Ovariectomy was performed for histopathological examination. Statistical results were obtained by SPSS software.

AMH levels in OT administrated rats were higher than the control group. In contrast, E2 levels in OT-ip group decreased compared to the control group. There were no statistically significant differences for LH, GNRH, OT, and TT levels among the groups. The histological evaluation of the ovarian sections has currently being proceeded by the investigators.

On the basis of our findings, the exogenous application of OT may have supporting effects on ovarian functions of rats.

**Keywords:** Oxytocin , ovary , rat , intranasal , intraperitoneal



## One step closer to lung regeneration: Detailed morphological examination of neotenic and metamorphic axolotl lungs.

**Arzu Güneş** , Duygu Gürsoy Gürgen , Arife Ahsen Kaplan , İlkay Özdemir , İlnur Keskin \*

Department of Histology and Embryology, Istanbul Medipol University, Istanbul, Turkey

**Objectives:** *Ambystoma mexicanum* (Axolotl), known as Mexican salamander, is an endemic amphibian species in Xochimilco Valley, Mexico. Axolotl can extraordinarily regenerate their internal organs, limb, spinal cord, tail, and brain in comparison with other vertebrates. This remarkable potential has been attributed to axolotl life-long neoteny, characterized by the exhibition of embryonic characteristics at the adult stage. Unlike most amphibians, axolotls never metamorphose naturally into pulmonary respiration. In mammal lungs, it is known that Type 2 pneumocytes (PN2) have the ability of self-renewal and differentiate into type 1 pneumocytes (PN1) during lung development. Additionally, PN2 produces and stores surfactant (composed of 90% lipid and 10% protein) as lamellar bodies. PN1 is responsible for gas changing and air-blood barrier forming. Although PN1 and PN2 are identical in number, they occupy 96% and 4% of the alveolar surface area, respectively. The ratio of alveolar epithelial cells changes in case of lung injuries; the number of PN1 decreases and PN2 increases. Another progenitor cell, interstitial lipofibroblast cells (ILC), are located in the walls of the alveoli and store lipids to provide when PN2 needs for surfactant production.

**Materials and Methods:** Neotenic axolotls were induced to metamorphosis by adding thyroid hormone to their aquarium for 3 months. Neotenic and metamorphic axolotls (n=3 for each group) were maintained in individual aquaria within Holtfreter's solution at 18°C. Under the 0,1 % benzocaine anesthesia animals were sacrificed and lung samples were dissected. For morphological examination, lung tissues were cryo-sectioned and stained with Scharlach Biebrich for lipids (surfactant), Safranin-Mallory for elastic fibers and hematoxylin-eosin after 4% paraformaldehyde fixation. Slides were visualized and scored to count PN2 (surfactant-containing) ratio to total pneumocytes under the light microscope. For ultrastructural examination, samples were fixed in 2% glutaraldehyde solution and then postfixed in 1% osmium tetroxide. The samples were embedded in epon resin after dehydrated by increasing acetone series. Thick sections were stained with toluidine blue. Thin sections were contrasted and examined by scanning transmission electron microscopy (STEM).

**Results:** The ratio of lipid-containing (Scharlach Biebrich positive) pneumocytes to total alveolar epithelial cells was significantly different between groups. Also, interstitial lipofibroblasts were observed in both groups but the number of them could not reach the statistical level to analyze the difference. In both groups, the first micrographs of the lamellar bodies that consist of concentrated surfactant were recorded. The alveolar wall thickness and elastic fiber densities of both groups were also different.

**Conclusion:** The ratio of PN2 to total pneumocytes was higher in neotenic lung made us think that neotenic tended to be developing and regenerating more than metamorphic. When considering the PN2 are progenitors of PN1, neotenic axolotl shows the early saccular phase of lung development. According to qualitative observations, ILCs have a higher incidence in neotenic may mean higher regeneration potential. During pulmonary respiration, it is reasonable that more elastic fiber infers more expansion in metamorphic lungs. This study enhances our understanding of lung regeneration by revealing detailed morphological differences in neotenic and metamorphic axolotl lungs.

**Keywords:** axolotl , lung , ultrastructure , type 2 pneumocytes , lamellar body

### References:

1. Tanaka EM, Reddien PW. The Cellular Basis for Animal Regeneration. *Dev Cell* 2011; 21:172–85. <https://doi.org/10.1016/j.devcel.2011.06.016>.
2. Joven A, Elewa A, Simon A. Model systems for regeneration: Salamanders. *Dev* 2019;146:0–2. <https://doi.org/10.1242/dev.167700>.
3. Herriges M, Morrisey E. Lung development: orchestrating the generation and regeneration of a complex organ. *Development*. 2014 Feb;141(3):502-13. doi: 10.1242/dev.098186
4. Liu X, Rowan SC, Liang J, et al. Categorization of lung mesenchymal cells in development and fibrosis. *iScience* 2021 May 19;24(6):102551. doi: 10.1016/j.isci.2021.102551.
5. Nguyen TM, Jimenez J, Rending LE, et al. The proportion of alveolar type 1 cells decreases in murine hypoplastic congenital diaphragmatic hernia *PloS One* 2019 Apr 17;14(4): e0214793. doi: 10.1371/journal.pone.0214793.
6. Opitz L, Kling KM, Brandenberge C, et al, Lipid-body containing interstitial cells (lipofibroblasts) in the lungs of various mouse strains. *J Anat*. 2017 Dec;231(6):970-977. Doi 10.1111/joa.12677.

## The healing effect of apocynin in monosodium glutamate- induced testis damage

Merve Acikel Elmas<sup>1</sup>, Salva Asma Algilani<sup>1</sup>, Ozlem Bingol Ozakpinar<sup>2</sup>, Serap Arbak<sup>1,\*</sup>

<sup>1</sup> Acibadem Mehmet Ali Aydinlar University, İstanbul, Turkey

<sup>2</sup> Marmara University, İstanbul, Turkey

**Introduction:** Monosodium L- glutamate (MSG) is widely used in food industry as a flavor enhancer which is derived from glutamic acid that is found in protein foods naturally. Recent experiments show that MSG has unhealthful effects in many organ systems (1). Apocynin (APO) is a constituent of *Picrorhiza kurroa*. Studies suggested to the antioxidant activity of APO in variety of animals(2). The aim of this study is to evaluate the effects of the Apocynin on male reproductive system using biochemical and histological methods.

**Material and Method:** Thirty-two adult male Sprague-Dawley rats were randomly divided into four groups (150-200 g; n=8/group) Control (C), APO, MSG and MSG+APO. Distilled water was given to C group orally for 28 days. MSG (120 mg/kg ) group was given orally to MSG for 28 consecutive days. APO (25 mg/kg) was given to MSG+ APO and APO groups for 5 days starting from 24th day of the experiment to 28th day. At the end of the experiment the rats were sacrificed under anesthesia and testis tissues were dissected. These tissues were processed for biochemical and light, fluorescent and transmission electron microscopical evaluations. (FSH), luteinizing hormone (LH) and testosterone levels were analyzed biochemically from blood serum. Malondialdehyde (MDA), superoxide dismutases (SOD), and glutathione (GSH) levels were determined by tissue samples. For histological evaluations, paraffin-embedded samples were stained with hematoxylin-eosin and periodic acid-Schiff (PAS). ZO-1, Occludin and NOX-2 immunoreactivities in testis tissue were evaluated by fluorescent microscopy Cell proliferation and apoptosis were also evaluated by immunohistochemical methods. All data were statistically analyzed.

**Results:** C and APO groups presented a regular organization of seminiferous tubules whereas MSG group had the most damaged seminiferous tubules with vacuolizations and degenerations in the germinal epithelial cells. Morphology of seminiferous tubular cells had slightly degenerated in MSG + APO group compared to MSG group. Transmission electron microscopical examination of the testis tissue revealed the parallel results in all groups as in the light microscopical level. C and APO groups had a higher immunoreactivity of ZO-1 and Occludin compared to MSG+ APO and MSG groups where MSG group showed the weakest immunoreactivity. NOX-2 immunoreactivity was the strongest in MSG compared to the other experimental groups. TUNEL- positive cells were fewer in C, APO MSG+APO groups compared to the MSG group. Biochemical results were consistent with histopathological results.

**Conclusion:** MSG increased oxidative damage and degenerated testis tissue morphology, changed blood-testis barrier protein immunoreactivity. It is thought that Apocynin was ameliorated testicular degeneration by regulating oxidant/antioxidant balances and preserving blood-testis barrier integrity.

**Acknowledgments:** This study was financed by The Scientific and Technological Research Council of Turkey (TUBITAK) - Project number 220S350.

**Keywords:** Monosodium glutamate , Apocynin , Blood testis barrier , Ultrastructure

### References:

1. Zanfirescu A, Ungurianu A, Tsatsakis AM, Nitulescu GM, Kouretas D, Veskoukis A, et al. A review of the alleged health hazards of monosodium glutamate. *Compr Rev Food Sci Food Saf.* 2019;18(4):1111-34.
2. Stefanska J, Pawliczak R. Apocynin: molecular aptitudes. *Mediators Inflamm.* 2008;2008:106507.

## The effect of melatonin on TLR4 related inflammatory pathway in the Parkinson's disease model

**Sendegul Yildirim Ildem , Gamze Tanriover \* , Ayse Ozkan , Aysel AGAR**

Akdeniz University, Faculty of Medicine, Antalya, Turkey

Parkinson's disease (PD) is a progressive disabling neurodegenerative disease. Neuroinflammation has an important role in various neurodegenerative diseases including PD. Microglial activation due to neuroinflammation also leads to the pathology of the disease. In 1-methyl-4-phenyl-1,2,3,6-tetrahydropyridine (MPTP) induced PD, accumulation of alpha-synuclein ( $\alpha$ -synuclein) caused by the toxic effect, triggers dopaminergic neuron death. Toll-like receptor 4 (TLR4) stimulates cytokine release through NF- $\kappa$ B by activating glial cells, and thus initiates the death of dopaminergic neurons. Melatonin can cross the blood-brain barrier and provide neuronal protection through anti-inflammatory properties. We hypothesized that melatonin could suppress TLR4-mediated neuroinflammation and inhibit the release of cytokines due to the inflammatory response and reduce dopaminergic neuron loss in experimental MPTP-induced PD model. Thus, we aimed to evaluate the neuroinflammatory responses caused by TLR4 activation and the effect of melatonin on these responses in the MPTP-induced PD model.

Three-month-old male C57BL/6 mice were randomly divided into 5 groups; Control (Group-C), Sham (Group-S), Melatonin-treated (Group-M), MPTP-injected (Group-P), and MPTP+melatonin-injected (Group-P+M). Melatonin was administered (20mg/kg) intraperitoneally to Group-M and Group-P+M two times a day for 5 days. Motor activities of mice were evaluated by locomotor activity tests on the 8th day. The SNPC area of the brain were determined by the tyrosine hydroxylase (TH). TLR4,  $\alpha$ -synuclein, and p65 expression was evaluated by immunostaining and TNF- $\alpha$  in total brain were evaluated by western blot analysis.

Locomotor activity was lower in the Group-P compared to the Group-C, however, melatonin treatment improved this impairment. MPTP caused decrease in TH positive dopaminergic neurons viability. Melatonin treatment was decreased TLR4 ( $p < 0.001$ ),  $\alpha$ -synuclein ( $p < 0.001$ ), and p65 ( $p < 0.01$ ) expressions in dopaminergic neurons compared to the Group-P. TNF- $\alpha$  expression was lower in the Group-C, Group-S, Group-M, and Group-P+M, when compared to the Group-P ( $p < 0.0001$ ). In conclusion, our study revealed that melatonin administration reduced  $\alpha$ -synuclein aggregation and TLR4-mediated inflammatory response, in MPTP induced PD model.

**Keywords:** Parkinson's disease, MPTP, dopaminergic neuron, TLR4, melatonin

### References:

1. Zhang, Q.S., Heng, Y., Mou, Z., Huang, J.Y., Yuan, Y.H., Chen, N.H., 2017. Reassessment of subacute MPTP-treated mice as animal model of Parkinson's disease. *Acta Pharmacol Sin* 38(10), 1317-1328
2. Yildirim, F.B., Ozsoy, O., Tanriover, G., Kaya, Y., Ogut, E., Gemici, B., Dilmac, S., Ozkan, A., Agar, A., Aslan, M., 2014. Mechanism of the beneficial effect of melatonin in experimental Parkinson's disease. *Neurochem Int* 79, 1-11
3. Cui, B., Guo, X., You, Y., Fu, R., 2019. Ferrerol attenuates MPP(+)-induced inflammatory response by TLR4 signaling in a microglia cell line. *Phytother Res* 33(4), 1134-1141.
4. Gagliano, S.A., Gandhi, S., Bryant, C., Klenerman, D., 2019. Picomolar concentrations of oligomeric alpha-synuclein sensitizes TLR4 to play an initiating role in Parkinson's disease pathogenesis. *Acta Neuropathol* 137(1), 103-120.

## The effects of intranasal applied oxytocin loaded nanoparticles on seizures, memory, and hippocampal regeneration

**Hakan Sahin**<sup>1,\*</sup>, **Oguz Yucel**<sup>2</sup>, **Serkan Emik**<sup>2</sup>, **Gozde Erkanli Senturk**<sup>1</sup>

<sup>1</sup> Department of Histology and Embryology, Cerrahpasa Faculty of Medicine, Istanbul University-Cerrahpasa, Istanbul, Turkey

<sup>2</sup> Department of Chemical Engineering, Faculty of Engineering, Istanbul University-Cerrahpasa, Istanbul, Turkey

Temporal lobe epilepsy (TLE) related to hippocampus is characterized with seizures. Memory-related cognitive abnormalities are important problems with this disorder. Pentilentetrazol (PTZ)-kindling is one of the models which is applied on rodents in order to investigate TLE. Findings for the histopathology of hippocampus are like, decrease of neurogenesis, and short-time memory alterations are seen in PTZ-kindling model which are also related to human TLE. It is known that oxytocin (OT) application exogenously may impact seizures, memory, and neurogenesis. Although, exogenously applications of OT studies are increasing for the effects of brain and related pathophysiologicals, epilepsy related studies are highly limited. According to previous data about OT application for non-invasive and efficiently passing through the brain, it is seen that intranasal (IN) pathway and OT loaded nanoparticles (OT&NPs) are prominent methods for that issue. In this study, we aimed to investigate whether low dose but chronic administration of OT/NP-OTs may have potential effects on PTZ-kindling rats in terms of adult neurogenesis, memory and seizures. Ethical approval was provided for this study from Bezmialem Vakif University Animal Experiments Local Ethics Committee with the given number of 2019/226. We used male adult Sprague-Dawley rats for this study. Rats were divided into Ctrl (n=6), Ctrl+OT (n=5), Ctrl+NP-OT (n = 5), PTZ (n = 8), PTZ+OT (n = 8), and PTZ+NP-OT (n = 8) groups. Subconvulsive PTZ solution (35-40 mg/kg/48 hours i.p.) was given to the PTZ, PTZ+OT, and PTZ+NP-OT groups for total of 25 dosages while only saline was given to the Ctrl/Ctrl+OT/Ctrl+NP-OT groups. After injections, time for seizure latency and severity were calculated in the 20-min observation period. One hour before the PTZ injections, Ctrl+NP-OT and PTZ+NP-OT groups received NP-OT (containing <10 µg OT), Ctrl+OT and PTZ+OT groups received OT (20 µg) while Ctrl and PTZ groups received only saline by intranasal pathway. The next day of the last injection of PTZ, spatial working memory evaluation test (SWMET) was applied in Y-maze. Next, all animals were anesthetized and brain samples were collected for further histological analyses. Hippocampus histopathology, neurogenesis, and apoptosis rates were also demonstrated by histological methods. Statistical results were obtained nonparametric Kruskal Wallis test and Dunn's post hoc test was used to see any difference between the groups. Statistical significance was accepted as  $p < 0.05$ . Our findings showed that OTs and NP-OTs have positive effects on seizure severity and latency. In addition, recovery of some SWMET related behaviors was observed in PTZ+OT and PTZ+NP-OT groups. Increment of neurogenesis and decrement of apoptosis were only statistically significant in hippocampus for PTZ+NP-OT group. Also, the protective effects of OTs and NP-OTs against PTZ induced damaged of hippocampal neurons were shown. Our results indicate that low dosage but chronic application of OT&NPs may have positive effects on spatial working memory by protective effects for hippocampal damage, increasing neurogenesis, and decreasing apoptosis.

**Keywords:** PTZ-kindling , hippocampus , oxytocin , nanoparticle , histology

## Repurposing of PARP inhibitors as neuroprotective agents on retinal degenerations

**Pakize Nur Akkaya**<sup>1,\*</sup>, **Cigdem Elmas**<sup>2</sup>, **Eberhart Zrenner**<sup>3</sup>, **Ayse Sahaboglu**<sup>3</sup>

<sup>1</sup> Gazi University Health Sciences Institute Department of Histology-Embryology (Fac. of Med.), Ankara, Turkey

<sup>2</sup> Gazi University Faculty of Medicine Department of Histology-Embryology, Ankara, Turkey

<sup>3</sup> University of Tuebingen Institute for Ophthalmic Research, Tuebingen, Germany

**Purpose:** In hereditary retinal degenerations, rod and cone photoreceptors lose their functions and as a result irreversible vision loss occurs. Retinitis pigmentosa (RP) is a group of hereditary retinal degenerative diseases leading to photoreceptor cell death. Poly-ADP-ribose Polymerase (PARP) is the key factor for a novel form of cell death which involves several diseases such as cancer and neurodegenerative diseases including RP. PARP dependent cell death, PARthanatos, is distinct from apoptosis and necrosis and has special features such as PARP1 activation, PAR accumulation, mitochondrial depolarization, early nuclear AIF translocation, cellular NAD<sup>+</sup> and ATP depletion (1). Our previous studies showed that excessive PARP activity is involved in photoreceptor degeneration in different mice and rat model for inherited retinal diseases (2). The PARP inhibitors under clinical trial for some types of cancer can be used as a therapeutic agent in retinal degenerations. Here, we compared the effects of clinically used PARP inhibitors on fast rod photoreceptor degeneration in rd1 mice and slow rod-cone photoreceptor degeneration in rd2 mice model.

**Methods:** rd1 and rd2 mouse retinæ were explanted together with retinal pigment epithelium (RPE) at postnatal day (PN) 5 and 9. Retinal explants were treated with different concentrations of PARP inhibitors (*PI1*, *PI2*, *PI3*) starting at PN7 (rd1) and PN11 (rd2). One eye was used for the treatment, while the other eye was used as control. Treatment was terminated at PN11 (rd1) and PN18 (rd2). TUNEL, PAR, Cone-Arrestin (CAR), GSH, GFAP staining were performed for the assessment of dying cells, PAR accumulation, number of Cone photoreceptors, glutathione level.

**Results:** The TUNEL assay assessment of dying photoreceptors showed that all PARP inhibitors (PI1, PI2, PI3) decreased the number of dying photoreceptors in rd2 retinæ. The maximal level of photoreceptor protection was detected with 100nM PI1, 3nM PI2 and 10nM PI3 (untreated:  $1.3 \pm 0.6$  SEM, n=9, *PI1*:  $0.6 \pm 0.04$  SEM, n=4, *PI2*:  $0.4 \pm 0.04$  SEM, n=5, *PI3*:  $0.9 \pm 0.1$  SEM, n=7,  $p \leq 0.0001$ ). The most effective doses for PARP inhibition were assessed by the number of PAR<sup>+</sup> cells in ONL (PAR; untreated:  $0.2 \pm 0.01$  SEM, n=4, *PI1*:  $0.1 \pm 0.01$  SEM, n=5, *PI2*:  $0.1 \pm 0.03$  SEM n=5,  $p \leq 0.01$ ). In addition, 100nM *PI1* treatment led to a significant increase in CAR density and percentage in ONL (CAR density; untreated:  $1.1 \pm 0.1$  SEM n=4, *PI1*:  $1.4 \pm 0.1$  SEM n=4  $p \leq 0.05$ , CAR percentage; untreated:  $4.1 \pm 0.4$  SEM n=4, *PI1*:  $5.6 \pm 0.2$  SEM n=4,  $p \leq 0.05$ ).

**Conclusions:** PARP may have important functions as it regulates the cellular components during photoreceptor degeneration. Excessive PARP activation is occurred during photoreceptor cell death. Repurposing of PARP inhibitors might facilitate a translation into a treatment for inherited retinal degenerations. PARP inhibition could open new treatment strategies for a variety of hereditary photoreceptor dystrophies.

**Keywords:** Retinal degenerations , PARP inhibitors , neuroprotective agents.

### References:

1. Hassa, P.O., et al., Nuclear ADP-ribosylation reactions in mammalian cells: where are we today and where are we going? Microbiology and Molecular Biology Reviews, 2006. 70(3): p. 789-829.
2. Arango-Gonzalez, B., et al., Identification of a common non-apoptotic cell death mechanism in hereditary retinal degeneration. PloS one, 2014. 9(11): p. e112142.

## The effect of Selenium on morphological changes in hippocampus and cerebral cortex of scopolamine induced Alzheimer's

Alev Cumbul<sup>1,\*</sup>, Dilara Baban<sup>1</sup>, Elif Çiğdem Keleş<sup>1</sup>, İzem Öngünşen<sup>2</sup>, Ece Genç<sup>3</sup>

<sup>1</sup> Medicine School of Yeditepe University, Istanbul, Turkey

<sup>2</sup> Medicine School of Yeditepe University, Istanbul, Turkey

<sup>3</sup> Medicine School of Medicine, Istanbul, Turkey

Alzheimer's Disease is one of the neurodegenerative diseases which cause severe memory loss, and it is very common worldwide. Amyloid plaques and neurofibrillary tangles, which are important symptoms of the disease, cause progressive neuronal losses in the hippocampus and cerebral cortex regions of the brain. Neuronal death occurs due to some pathological changes in the brain such as amyloid plaque formation and tau hyperphosphorylation. These pathological changes increase mitochondrial damage, causing oxidative stress and neuroinflammation. The pathology of the disease progresses with the release of proinflammatory cytokines from microglia that stimulate neurons. Similarly, proinflammatory cytokines, reactive oxygen species, and chemokines increase cell death to initiate Alzheimer's. Inflammation mediators of microglia play a protective role in the acute activation of astrocytes and neurons, while chronic activation of microglia causes neurotoxic effects, leading to the death of neurons, especially cholinergic ones.

Scopolamine substance creates Alzheimer's-like pathology; therefore, it is one of the common neurotoxins used to model Alzheimer's. Scopolamine-induced Alzheimer's models cause memory loss and cognitive loss by blocking muscarinic receptors of cholinergic neurons.

In recent years, there have been many studies investigating a potential treatment for Alzheimer's, and many studies show that selenium is one of the most promising substances in Alzheimer's pathology. Selenium binds to the active sites of catalytic enzymes, which are responsible for protecting cells from oxidative damage. It is also a trace element with antioxidant potential that our body needs. It protects cells from oxidative damage and is present on the active surfaces of catalyst enzymes. As a result of this relationship, cognitive decline is prevented. Meanwhile, selenium is found in the structure of selenoproteins, which provides the balance between free radical production and antioxidant effect. Studies show that selenoproteins co-occur with neurofibrillary tangles and amyloid plaques in Alzheimer's brain. Based on this information, it is suggested that selenium can prevent amyloid plaque formation and hyperphosphorylation of tau protein. In this study, the effect of selenium on the hippocampus and cerebral cortex was evaluated in a scopolamine-induced Alzheimer's model to examine morphological changes by histological analysis.

First, it was observed by locomotor activity test that scopolamine caused an Alzheimer's-like locomotor movement loss, and it was understood that selenium caused some improvement in these movements. Hematoxylin-eosin staining was performed to observe the pathological findings, and as expected, less pathological findings were observed in the selenium treatment group compared to the scopolamine Alzheimer model group. Amyloid-Beta immunohistochemistry staining showed extensive amyloid plaque formation in the scopolamine group and rare amyloid plaque formation in the test group. Finally, the apoptosis level was determined by calculating the apoptotic index with the TUNEL experiment. According to the apoptotic index, the highest values were obtained in the scopolamine group, the second highest values in the test group, and the lowest values in the control and selenium groups.

In conclusion, as expected in this study, selenium caused improvement in Alzheimer's model pathology simulated by scopolamine. In the future, this study may be a guide in Alzheimer's drug studies of selenium substance.

**Keywords:** neurodegenerative diseases , Alzheimer's Disease , rat model , Selenium , Scopolamine-induced

### References:

1. Querfurth HW, Laferla FM. Alzheimer's Disease. Clin Trials. 2010;9:329-344. doi:10.1056/NEJMra0909142
2. Harrington CR. The Molecular Pathology of Alzheimer's Disease. Neuroimaging Clin N Am. 2012;22(1):11-22. doi:10.1016/j.nic.2011.11.003
3. Glass CK, Saijo K, Winner B, Marchetto MC, Gage FH. Review Mechanisms Underlying Inflammation in Neurodegeneration. Cell. 2010;140(6):918-934. doi:10.1016/j.cell.2010.02.016
4. Sarlus H, Heneka MT, Sarlus H, Heneka MT. Microglia in Alzheimer's disease Find the latest version : Microglia in Alzheimer's disease. 2017;127(9):3240-3249.

## **Stereological and electron microscopic approaches for analyzing of peripheral nerve regeneration\***

**Burcu DELİBAS \* , Süleyman KAPLAN**

Ondokuz Mayıs University Faculty of Medicine Histology and Embryology Department, SAMSUN, Turkey

Qualitative histopathology has been used as a gold standard for evaluating morphological changes in the tissue and organ systems, including the peripheral and central nervous systems. However, such an approach may not show real changes in the organ and tissues since it may have biased results based on observer variation or unknown reasons. On the other hand, it does not fully show quantitative changes in tissue volume, neuron size, number, diameter, or nerve fiber numbers. Therefore, unbiased and reliable techniques are needed. Such techniques are named design-based stereological techniques. The main bases of these techniques are unbiased and systematic random sampling (SRS). Unbiased sampling means evaluating items in three-dimensional using two-dimensional images of them, and SRS means giving an equal chance to each part of evaluated structures to be sampled.

In this study, we present some empirical experiences on how we have evaluated the dorsal root ganglia that have sciatic nerve injury obtained from rats, using light and electron microscopic images. By means of these approaches, estimation of sensory neuron numbers, sensory neuron volume, and total tissue volume parameters would be possible.

The physical disector method is commonly used for cell/particle counts and is an ideal method for dorsal root ganglia tissue. Total ganglion volume can be estimated using the Cavalieri principle. The cell diameter can be measured in sections sampled at specific intervals using the nucleator method.

The stereological approach is becoming a gold standard for quantitative studies. Because of the simple applicability and reliability of these methods, take more attention in immunohistochemical, electron microscopic, and confocal microscopic studies. As the application of stereological techniques becomes simpler, quantitative evaluations of items would be performed more quickly and effectively.

(\* ) This study was supported by the Ondokuz Mayıs University Project Management Office with the Project number PYO.TIP.1904.20.006.

**Keywords:** stereology , dorsal root ganglion , peripheral nerve regeneration , electron microscopy

### **References:**

1. Krames, E.S., 2015. The dorsal root ganglion in chronic pain and as a target for neuromodulation: a review. *Neuromodulation*. 18, 24–32.
2. Mirabile, R., Boyce, R. W., Gundersen, H. J. G., 2020. A metric fractionator for estimation of total cell number in paraffin-embedded flat or hollow organs. *Toxicol. Pathol.* 48(6), 784-790.
3. Murotori, L., Ronchi, G., Raimondo, S., Geuna, S., Giacobini-Robecchi, M.G., Fornaro, M., 2015. Generation of new neurons in dorsal root ganglia in adult rats after peripheral nerve crush injury. *Neural Plast.* 860546.
4. Napper, R., 2018. Total number is important: Using the disector method in design-based stereology to understand the structure of the rodent brain. *Front. Neuroanat.* 12, 16.
5. Schiønning, J., Larsen, J. A., 1997. stereological study of dorsal root ganglion cells and nerve root fibers from rats treated with inorganic mercury. *Acta Neuropathol.* 94, 280–286.
6. Tandrup, T., 2004. Unbiased estimates of number and size of rat dorsal root ganglion cells in studies of structure and cell survival. *J. Neurocytol.* 33, 173–192.

## 2 - Life Science - Pathology and clinical medicine - Oral Presentation

### Effect of melatonin and curcumin treatments on the bladder in renal ischemia/reperfusion injury: A histopathological study

**Sude Topkaraoğlu , Tansel Sapmaz \***  
University of Health Sciences, Istanbul, Turkey

**Introduction:** Renal ischemia-reperfusion injury (IR) results in acute kidney injury (AKI), which causes severe morbidity and mortality. AKI has been reported to be associated with distant organ dysfunction in the lung, heart, brain, and liver. Inflammatory cell infiltration, tubular dilatation, and endothelial injury occur in AKI. These injuries explain the physiological and molecular mechanisms of distant organ dysfunction. Oxidative stress caused by the production of reactive oxygen species (ROS) is also an important mechanism of distant organ dysfunction. Many antioxidants are used in the treatment of IR injury. Melatonin is a hormone with antioxidant properties and has been shown to reduce cellular injury caused by oxidative stress. Curcumin, a spice with antioxidant properties, is a preferred substance in the treatment of IR injury.

**Objective:** In this study, the effect of melatonin and curcumin treatments on the bladder (distant organ dysfunction) in kidney IR injury was investigated histologically.

**Method:** 42 rats were divided into 6 groups. Renal ischemia for 45 minutes followed by 2 hours of reperfusion was applied to all groups except the control group. IR, IR+PLACEBO, IR+MEL (20 mg/kg melatonin), IR+CUR (200 mg/kg curcumin), IR+MEL-KUR (20 mg/kg melatonin+200 mg/kg curcumin). All injections were given intraperitoneally. Kidney tissue is stained with Hematoxylin & Eosin, PAS, Masson Trichrome, and Toluidine Blue.

**Results:** On IR and IR+PLACEBO groups, we observed increased Inflammatory cell infiltration, number of mast cells, edema, and vascular congestion. Acute phase markers of all treatment groups (IR+MEL, IR+CUR, and IR+MEL-CUR) decreased compared to IR and IR+PLACEBO groups.

**Discussion and Conclusion:** Our results showed that IR injury is harmful to kidney function, so it caused significant impairment in bladder tissue. The histological structure of the bladder tissue of the melatonin and curcumin applied group was similar to the control group. We observed that the acute phase markers of these groups decreased ( $p < 0.05$ ) which consist of edema, inflammatory cell infiltration, number of mast cells, and vascular congestion.

**Keywords:** Bladder, Curcumin, Kidney Ischemia/Reperfusion, Melatonin, Rats

#### References:

1. Shi, S., Lei, S., Tang, C., Wang K., Xia, Z. (2019). Melatonin attenuates acute kidney ischemia/reperfusion injury in diabetic rats by activation of the SIRT1/Nrf2/HO-1 signaling pathway. *Bioscience Reports*, 39(1), BSR20181614.
2. Rogers, N.M., Stephenson, M.D., Kitching, A.R., Horowitz J.D., Coates, P.T.H. (2012). Amelioration of renal ischaemia–reperfusion injury by liposomal delivery of curcumin to renal tubular epithelial and antigen-presenting cells. *Br J Pharmacol*, 166(1), 194-209.
3. Keskin-Aktan, A., Akbulut, K.G., Yazıcı-Mutlu, Ç., Sonugur, G., Ocal, M., Akbulut, H. (2018). The effects of melatonin and curcumin on the expression of SIRT2, Bcl-2 and Bax in the hippocampus of adult rats. *Brain Res Bull*, 137, 306-310.
4. Muratoğlu, S., Akarca Dizakar, O.S., Keskin Aktan, A., Ömeroğlu, S., Akbulut, K.G. (2019). The protective role of melatonin and curcumin in the testis of young and aged rats. *Andrologia*, 51(3), e13203.
5. Ali, B.H., Abdelrahman, A., Suleimani, Y.A., Manoj, P., Ali, H., Nemmar, A., Za'abi, M.A. (2020). Effect of concomitant treatment of curcumin and melatonin on cisplatin-induced nephrotoxicity in rats. *Biomed Pharmacother*, 131, 110761.
6. Mercantepe, F., Mercantepe, T., Topcu, A., Yılmaz, A., Tumkaya, L. (2018). Protective effects of amifostine, curcumin, and melatonin against cisplatin-induced acute kidney injury. *Naunyn Schmiedebergs Arch Pharmacol*, 391(9), 915-931
7. Faeq Husain-Syed, Mitchell H. Rosner, Claudio Ronco. (2019). Distant organ dysfunction in acute kidney injury. *Acta Physiologica*, 1-10.
8. Ricardo Cavalheiro Cavalli, Renato Tambara Filho, Regina de Paula Xavier Gomes, Djanira Aparecida da Luz Veronez, Julio Slongo, Rogério de Fraga. (2014). Analysis of the histology of the scar bladder and biochemical parameters of rats with a solitary kidney undergoing immunosuppression with tacrolimus. *Experimental Urology*, Vol. 29 (8).
9. Sul A Lee, M.D.1,2, Martina Cozzi, M.D.3, Errol L. Bush, M.D.4, and Hamid Rabb. (2018). Distant Organ Dysfunction in Acute Kidney Injury: A Review. *Am J Kidney Dis*. 72(6): 846–856.



## Evaluation of the effects of apocynin on kidney and bladder in high-fat diet-induced obese rats

**Fatma Kanpalta**<sup>1,\*</sup>, **Büşra Ertaş**<sup>2</sup>, **Göksel Şener**<sup>3</sup>, **Feriha Ercan**<sup>1</sup>

<sup>1</sup> Marmara University, Faculty of Medicine, Istanbul, Turkey

<sup>2</sup> Marmara University, Faculty of Pharmacy, Istanbul, Turkey

<sup>3</sup> Fenerbahçe University, Vocational School of Health Service,, Istanbul, Turkey

**Introduction:** The prevalence of obesity, which is common in developed and developing countries, is increasing. Obesity is in the etiopathogenesis of many diseases such as cardiovascular diseases, diabetes, metabolic syndrome, chronic kidney disease and over active bladder (1, 2). It has been shown that obesity is a risk factor for chronic kidney disease independent of diabetes or hypertension, and causes urinary system pathologies through reactive oxygen species and inflammation (3). NADPH oxidase(NOX)-2 has a role in oxidative stress mechanisms. Apocynin (APC), a NOX-2 inhibitor, has been shown to reduce the negative effects of obesity on the cardiovascular system (4).

**Objective:**The aim of this study was to investigate the possible protective effects of APC on kidney and bladder damage in high-fat-diet(HFD) induced obesity.

**Materials and Methods:**Wistar albino male rats were divided into four equal (n=8) groups: Control, high-fat diet (HFD), HFD+dimethylsulfoxide (HFD+DMSO) and HFD+APC. Experimental groups were fed with standard (control group; 6% fat) or HFD (HFD, HFD+DMSO, HFD+APCgroups; 45% fat) for 16 weeks. In the last 4 weeks of the experiment, DMSO (15%) to the HFD+DMSO group and APC (25 mg/kg, dissolved in DMSO) to the HFD+APC group were administered via orogastric gavage. Rat weights were measured every week during the experimental period. At the end of the experiment, rats were decapitated under light ether anesthesia. Leptin, cholesterol, high-density-lipoprotein (HDL) and triglyceride values were measured in blood serum. Kidney and bladder tissues were prepared for light microscopic examinations. NOX-2 and NFκ-B protein localisation were evaluated using immunohistochemistry method. Malondialdehyde (MDA), 8-hidroksideoksiguanozin (8-OHdD), glutathione (GSH) and myeloperoxidase(MPO) levels were evaluated biochemically. All of the parameters were evaluated statistically. P < 0.05 was considered significant.

**Results:**The body weight was increased in the HFD and HFD+DMSO groups. Leptin, cholesterol and triglyceride levels increased in these groups. Enlargement of Bowman's space and glomerular damage, increased interstitial collagen, degenerated tubules with luminal cell debris in kidney; shedding of apical urothelial cells, vascular congestion and increase of collagen in muscular layer in urinary bladder were seen. Increased NOX-2 and NFκ-B immunoreactive cells were present in both kidney and bladder. Parallel to the morphological findings, MDA, 8-OHdG and MPO levels increased, GSH level decreased in these groups. All these histologic and biochemical results were better in the HFD+APCgroup.

**Conclusion:** High-fat diet causes kidney and bladder damage by increasing NOX-2 activity and inflammation through oxidative stress. Apocynin may ameliorate kidney and bladder damage by inhibiting oxidative stress.

**Acknowledgement:** This study was supported by the Marmara University Scientific Research Project Commission (TTU-2020-10107).

**Keywords:** High fat diet, Kidney, Urinary bladder, Oxidative stress, Apocynin

### References:

1. Ejerblad E, Fored CM, Lindblad P, Fryzek J, McLaughlin JK, Nyrén O. Obesity and risk for chronic renal failure. *J Am Soc Nephrol.* 2006;17(6):1695-702.
2. Li N, Ding H, Li Z, Liu Y, Wang P. Effect of high-fat diet-induced obesity on the small-conductance Ca(2+)-activated K(+) channel function affecting the contractility of rat detrusor smooth muscle. *Int Urol Nephrol.* 2019;51(1):61-72
3. Ninomiya T, Kiyohara Y. Albuminuria and chronic kidney disease in association with the metabolic syndrome. *J Cardiometab Syndr.* 2007;2(2):104-7.
4. Du J, Li J-M. BAS/BSCR23 Apocynin treatment reduces high-fat diet-induced obesity and hypertension but has no significant effect on hyperglycaemia. *Heart.* 2010;96(17):e19-e

## Investigation the protective effects of Quercetin on carbon tetrachloride induced hepatotoxicity with light and electron microscopy

**Nebahat Ince, Ozlem Goruroglu Ozturk, Yasar Sertdemir, Yusuf Kenan Daghoglu, Yurdun Kuyucu\***  
Cukurova University, Adana, Turkey

Hepatotoxicity is induced by inhalation, oral or intravenous administration of many pharmacological and chemical substances. Treatment of liver diseases is applied according to the underlining reason. In hepatotoxicity, toxic substance must be stopped and supportive treatment is applied. Nowadays, natural antioxidants within the diet is becoming popular in studies to prevent liver damage. Quercetin is an antioxidant and is found in many plants. In this study, effects of Quercetin on carbon tetrachloride (CCl<sub>4</sub>) induced hepatotoxicity were investigated with light and electron microscopy. 30 adult Wistar male rats were divided into 5 groups (n=6).

In group 1 (Control group), 0.3 ml saline i.p. for 14 days and on 14th day 1 ml/kg olive oil i.p. were injected.

In group 2 (Quercetin control group), 50 mg/kg Quercetin (dissolved in 0.3 ml saline) for 14 days i.p. and on 14th day 1 ml/kg olive oil i.p. were injected.

In group 3 (CCl<sub>4</sub> group), 0.3 ml saline i.p. for 14 days and on 14th day 1 ml/kg CCl<sub>4</sub> (50 % diluted in olive oil) i.p. were injected.

In group 4 (Quercetin + CCl<sub>4</sub> group), 50 mg/kg Quercetin (dissolved in 0.3 ml saline) for 14 days i.p. and on 14th day 1 ml/kg CCl<sub>4</sub> (50 % diluted in olive oil) i.p. were injected.

In group 5 (Quercetin + CCl<sub>4</sub> + Quercetin group), 50 mg/kg Quercetin (dissolved in 0.3 ml saline) for 14 days i.p. and on 14th day 1 ml/kg CCl<sub>4</sub> (50 % diluted in olive oil) i.p. were injected. For 7 days after 14th day 50 mg/kg Quercetin (dissolved in 0.3 ml saline) injection i.p. was continued.

Anesthesia was performed to the rats in the first four groups on the 15th day, and in the fifth group on the 22th day. Intracardiac blood samples were taken from the rats and serum ALT, AST, TAS, TOS values and oxidative stress index (OSI) were measured. Liver specimens were prepared for light microscopic and electron microscopic examination. Serum ALT, AST, TOS and OSI were increased and TAS was decreased in CCl<sub>4</sub> group. It was observed that serum ALT, AST, TOS and OSI were decreased and TAS was increased in Group 4 and 5 when compared to CCl<sub>4</sub> group. In CCl<sub>4</sub> group inflammatory cell infiltration, enlarged sinusoidal capillaries, ballooning degeneration and fat degeneration characterized by microvesicular steatosis in hepatocytes, and the presence of lytic areas were seen. CCl<sub>4</sub> group also revealed enlargement of the perinuclear cisternae and swelling of endoplasmic reticulum cisternae, decrease in cytoplasmic organelles and glycogen particles, and cytoplasmic vacuoles with membranous structures. It was observed that inflammatory cell infiltration, lytic areas, ballooning degeneration, cytoplasmic organelle degeneration, vacuoles and microvesicular steatosis in hepatocytes were decreased in the Quercetin + CCl<sub>4</sub> group. We found that the Quercetin + CCl<sub>4</sub> + Quercetin group had similar morphological characteristics to the control group and normal structure.

As a result, it was concluded that Quercetin decreases the oxidative stress in liver, and has protective and therapeutic effects on hepatocytes in CCl<sub>4</sub> induced hepatotoxicity.

**Keywords:** Liver, Quercetin, Transmission Electron Microscopy, Carbon Tetrachloride, Oxidative Stress

### References:

1. Weber LWD, Boll M, Stampfl A. Hepatotoxicity and Mechanism of Action of Haloalkanes: Carbon Tetrachloride as a Toxicological Model. *Critical Reviews in Toxicology*, 2003; 33(2): 105-136.
2. Boll M, Weber LW, Becker E, Stampfl A. Mechanism of carbon tetrachloride-induced hepatotoxicity. Hepatocellular damage by reactive carbon tetrachloride metabolites. *Z Naturforsch C J Biosci*. 2001; 56(7-8): 649-659.
3. Boots AW, Haenen GRMM, Bast A. Health effects of quercetin: from antioxidant to nutraceutical. *Eur J Pharmacol*, 2008; 585(2-3): 325-37.
4. Lackner C. Hepatocellular ballooning in nonalcoholic steatohepatitis: the pathologist's perspective. *Expert Rev Gastroenterol Hepatol*, 2011; 5(2): 223-31.
5. Poli G, Parola M. Oxidative damage and fibrogenesis. *Free Radic Biol Med*, 1997; 22 (1-2): 287-305.

## Investigation of MiR-26b and MiR-27b expressions and the effect of Quercetin on Pulmonary Fibrosis

**Cağrı Toker, Ufuk Özgü Mete, Yurdun Kuyucu, Samet Kara, Dilek Şaker, Bilge Güzelel\***  
Cukurova University, Adana, Turkey

Idiopathic Pulmonary Fibrosis (IPF) is a chronic, progressive disease characterized by destruction of the alveolar wall, myofibroblast hyperplasia, extracellular matrix deposition, and remodeling of the lung interstitium. Although the pathogenesis is not fully elucidated, alveolar epithelial cell damage and abnormal repair are the main mechanisms leading to pulmonary fibrosis. Currently, there are limited treatment options with unproven efficacy in IPF. Quercetin, a flavonoid found in various plants, has been noted by researchers to prevent cell damage caused by free radicals thanks to its strong antioxidant property, and there are studies reporting that it alleviates bleomycin-induced pulmonary fibrosis. Recently, many studies have reported that microRNAs (miRNAs) are effective in organ development, normal physiology and the pathogenesis of various diseases and play an important role in IPF. As a result of these studies, miR-27b was determined as an anti-fibrotic miRNA that inhibits fibroblast activation. In our study, it was aimed to evaluate the therapeutic effects of Quercetin in pulmonary fibrosis using electron microscopic methods and to compare the expression levels of miR-26b and 27b.

In this study, 48 Wistar rats were randomly distributed and initially 4 experimental groups were formed. Groups 3 and 4 were further divided into 2 subgroups according to the treatment and life expectancy (n=8). Group 1 was administered saline intratracheally on day 0 of the experiment, and then saline was administered intraperitoneally (i.p.) for 21 days. Quercetin was given intraperitoneally to Group 2 for 21 days, starting from the 8th day of the experiment. Group 3 received a single intratracheal dose of Bleomycin Sulfate on day 0. These animals are divided into 2 subgroups; half were sacrificed on the 22nd day (Group 3A) and the remaining half (Group 3B) on the 29th day. Group 4B received a single intratracheal dose of Bleomycin Sulfate on day 0. These animals were divided into 2 subgroups and Quercetin was given intraperitoneally to half of them (Group 4A) for 14 days and to the other half (Group 4B) for 21 days, starting from day 8. Lung tissues obtained after sacrifice were examined using electron microscopic, immunohistochemical and molecular biological methods.

In electron microscopic examinations, it was observed that the alveolar structure was deteriorated by dense collagen accumulation in the interalveolar septum in the damage groups, while the fibrotic response was decreased and the alveolar structure improved with Quercetin treatment. Immunohistochemically,  $\alpha$ -SMA expressions were higher in the damage groups, but lower in the treatment groups compared to the damage groups, while E-Cadherin expressions were decreased in the damage groups and showed stronger immunoreactivity in the treatment groups compared to the damage groups. It was found that miR-26b and miR-27b expressions were lower in the damage groups than in the control groups, and higher in the treatment groups than in the damage groups and approached the levels of the control groups.

When the findings were evaluated, it was concluded that Quercetin can be considered as a new treatment agent in the Idiopathic Pulmonary Fibrosis.

**Keywords:** pulmonary fibrosis, ultrastructure, miR-26b, miR-27b, Quercetin

### References:

1. Zhang X, Cai Y, Zhang W, Chen X. Quercetin ameliorates pulmonary fibrosis by inhibiting SphK1/S1P signaling. *Biochem. Cell Biol.* 2018;96(6):742–751
2. Hohmann MS, Habel DM, Coelho AL, Verri WA, Hogaboam CM. Quercetin enhances ligand-induced apoptosis in senescent idiopathic pulmonary fibrosis fibroblasts and reduces lung fibrosis in vivo. *Am. J. Respir. Cell Mol. Biol.* 2019;60(1):28–40.
3. Díaz-Peña R, Castro-Santos P, Sannino G, Marchetto A, Kirchner T, Grünwald TGP, et al. MicroRNAs in development and cancer. *Clin. Exp. Metastasis* 2017;9(5):685–693.
4. Sayed D, Abdellatif M. MicroRNAs in development and disease. *Physiol. Rev.* 2011;91(3):827–887
5. Zeng X, Huang C, Senavirathna L, Wang P, Liu L. miR-27b inhibits fibroblast activation via targeting TGF $\beta$  signaling pathway. *BMC Cell Biol.* 2017;18(1). doi:10.1186/s12860-016-0123-7.

## Protective effects of rosmarinic acid against cyclophosphamide induced testicular toxicity in rats

**Ahmet Uğur Akman**<sup>1\*</sup>, **Dilan Çetinavcı**<sup>2</sup>, **Engin Yenilmez**<sup>3</sup>, **Ahmet Alver**<sup>4</sup>, **Neslihan Sağlam**<sup>4</sup>

<sup>1</sup> Amasya University, Faculty of Medicine, Department of Histology and Embryology, Amasya, Turkey

<sup>2</sup> Mugla Sıtkı Kocman University, Mugla Training and Research Hospital, Department of Histology and Embryology, Mugla, Turkey

<sup>3</sup> 3 Karadeniz Technical University, Faculty of Medicine, Department of Histology and Embryology, Trabzon, Turkey

<sup>4</sup> Karadeniz Technical University, Faculty of Medicine, Department of Medical Biochemistry, Trabzon, Turkey, Trabzon, Turkey

**Introduction:** Cyclophosphamide (CP) is an alkylating antineoplastic agent and it's very cytotoxic (1). Various side effects are observed in CP treatment and testicular toxicity is a common side effect (2). Rosmarinic acid (RA) is a polyphenol and ester of caffeic acid (3,4). RA is naturally found in plants like thyme, sage tea, rosemary and sweet basil. It has anti-inflammatory, anti-apoptotic and antioxidant effects (5).

**Materials and Methods:** The aim of our study was to investigate the effects of RA against CP-induced testicular damage in rats. 18 Sprague Dawley rats were randomly divided into three groups. Sham group was given physiological saline (PS) (1 ml) by gavage for 8 days from the 1st day of the experiment and PS (1 ml) was administered intraperitoneally (i.p.) on the 8th day of the experiment. The CP group was given PS by gavage from the 1st day to the 8th day and a single dose of 200 mg/kg CP was administered on the 8th day of the experiment (i.p.). The CP+RA group was given 100 mg/kg RA by gavage for 8 days from first day and 200 mg/kg CP intraperitoneally on the 8th day. On the 9th day of the experiment, the rats were sacrificed by exsanguination and the blood samples were taken. Right testicles were taken for histopathological analysis.

**Results:** Histopathologically, testicular tissues were normal in the sham group. In the CP group, Johnson score levels were lower compared to the sham group. Johnson's score was higher in CP+RA group compared to the CP group. In hematoxylin and eosin stain with CP group seminiferous tubule epithelium exhibited dehiscence in some parts of the basal membrane. Leydig cell atrophy was observed in the interstitial area. Number of immature cells in the lumen increased compared to the sham group. In the CP+RA group dehiscence of seminiferous tubules decreased compared to the CP group, Leydig cell atrophy was decreased in the interstitial area and again immature cell in the lumen decreased compared to the CP group. In Masson-trichrome stain histopathological findings were similar to hematoxylin and eosin stain. Also biochemical parameters of oxidative stress were investigated. In the CP group malondialdehyde (MDA) levels increased to 149.69±18.10 and in the CP+RA group MDA levels decreased to 124.97±2.5 (p<0.05). In the CP group superoxide dismutase (SOD) levels decreased to 1.39±0.28 and in the CP+RA group SOD levels increased to 3.32±1.77 (p<0.05). SOD levels were nearly similar to sham group in the CP+RA group.

**Conclusion:** As a result, with our histopathological and biochemical findings, rosmarinic acid has beneficial effects on cyclophosphamide-induced testicular toxicity.

**Keywords:** Rosmarinic acid, Cyclophosphamide, Toxicity, Antioxidant, Testis

### References:

1. Ilbey YO, Ozbek E, Simsek A, Otuncemur A, Cekmen M, Somay A. Potential chemoprotective effect of melatonin in cyclophosphamide- and cisplatin-induced testicular damage in rats. *Fertil Steril*. 2009 Sep;92(3):1124-1132. doi: 10.1016/j.fertnstert.2008.07.1758. Epub 2008 Oct 1. PMID: 18829000.
2. Shittu SA, Shittu ST, Akindele OO, Kunle-Alabi OT, Raji Y. Protective action of N-acetylcysteine on sperm quality in cyclophosphamide-induced testicular toxicity in male Wistar rats. *JBRA Assist Reprod*. 2019 Apr 30;23(2):83-90. doi: 10.5935/1518-0557.20180079. PMID: 30633472; PMCID: PMC6501750.
3. Min J, Chen H, Gong Z, Liu X, Wu T, Li W, Fang J, Huang T, Zhang Y, Zhao W, Zhu C, Wang Q, Mi S, Wang N. Pharmacokinetic and Pharmacodynamic Properties of Rosmarinic Acid in Rat Cholestatic Liver Injury. *Molecules*. 2018 Sep 7;23(9):2287. doi: 10.3390/molecules23092287. PMID: 30205454; PMCID: PMC6225135
4. Tsai CF, Wu JY, Hsu YW. Protective Effects of Rosmarinic Acid against Selenite-Induced Cataract and Oxidative Damage in Rats. *Int J Med Sci*. 2019 May 10;16(5):729-740. doi: 10.7150/ijms.32222. PMID: 31217741; PMCID: PMC6566745
5. Georgy GS, Maher OW. Ellagic acid and rosmarinic acid attenuate doxorubicin-induced testicular injury in rats. *J Biochem Mol Toxicol*. 2017 Sep;31(9). doi: 10.1002/jbt.21937. Epub 2017 Jun 6. PMID: 28586512

## Distribution of TNF- $\alpha$ and PCNA in Experimental Type-1 Diabetic and *Nigella sativa* Oil treated Rat Tongue

Ugur Seker <sup>1,\*</sup>, Seval Kaya <sup>2</sup>, Yusuf Nergiz <sup>2</sup>

<sup>1</sup> Harran University, Faculty of Medicine, Department of Histology and Embryology, Sanliurfa, Turkey

<sup>2</sup> Dicle University, Faculty of Medicine, Department of Histology and Embryology, Diyarbakir, Turkey

Until today, studies that are investigated the effects of hyperglycemia on lingual morphology and gustatory functions are limited (1,2). In this study, we aimed to examine the distribution TNF- $\alpha$  and PCNA in hyperglycemic and *Nigella sativa* treated rat tongue. Eighteen Sprague Dawley rats were divided into 3 groups; control (G1), diabetes (G2), and diabetes + *Nigella sativa* (G3) of 6 animals in each. Diabetes was induced with intraperitoneally administration of 45 mg/kg streptozotocin to the animals in G2 and G3. Animals in G3 received 2.5 ml/kg *Nigella sativa* oil daily per os. All animals were sacrificed 56 days following induction of diabetes and tongues were received for examination of TNF- $\alpha$  and PCNA immunoeexpression. Immunopositivity ratio of PCNA was evaluated with considering dorsal surface epithelium cells either positive or negative. Randomly selected 3 regions from each tongues of animals with regular magnification were evaluated for PCNA positive cell ratio. TNF- $\alpha$  immunopositivity was evaluated at randomly selected 3 lingual epithelial and lamina propria part of each tongue sample with h-scoring system, and h-scoring system was designed as follows; no staining in lamina propria and surface epithelium (0), weak immunopositivity in lamina propria (1), moderate staining in lamina propria and surface epithelium (2), dense staining all over the lingual tissue (3). Microscopic examinations indicated that basal, parabasal and taste bud cells of G1 group were positive for PCNA alone, but cellular structures in lamina propria were negative. Slightly immunopositivity for TNF- $\alpha$  was observed in the epithelium and lamina propria of this group. PCNA positivity ratio in G1 group was % 80.99  $\pm$  15.69. Positive cell ratio in G2 and G3 groups were % 48.29  $\pm$  22.39, and % 67.38  $\pm$  17.29 respectively. The difference in G1 - G3 and G2 - G3 groups were significant ( $p < 0.05$ ), but positive cell ratio between G1 and G3 groups were similar ( $p > 0.05$ ). TNF- $\alpha$  h-scoring results were 0.56  $\pm$  0.62, 1.33  $\pm$  0.91 and 0.67  $\pm$  0.59 in G1, G2 and G3 groups respectively. The highest h-score in G2 was significantly different than G1 and G3 groups ( $p < 0.05$ ), and the distribution of TNF- $\alpha$  was similar among the G1 and G3 groups ( $p > 0.05$ ). Results of this study indicated that streptozotocin decreased PCNA immunopositive cell ratio, but upregulated TNF- $\alpha$  immunoeexpression positivity. In literature the effects of streptozotocin induced diabetes on lingual morphology and function is limited, but the results of previous studies in literature are conflicting. In a previous study it was reported that PCNA positive cell ratio to be decreased in streptozotocin induced diabetic rat tongue (3). Our results is consistent with this study. Additionally our study indicated that anti-hyperglycemic *Nigella sativa* treatment is ameliorative on lingual PCNA expression. Also we haven't reached any study which reported TNF- $\alpha$  expression in hyperglycemic and *Nigella sativa* treated rat tongue. We believe our results may be related with altered taste function and morphological alterations in diabetic tongue and increased TNF- $\alpha$  immunopositivity may be a result of imbalance in immune response and apoptotic cell death induction in diabetic tongue which are also can be considered as observed diabetic oral manifestations.

**Keywords:** streptozotocin , rat , tongue , PCNA , TNF- $\alpha$

### References:

1. Rohani, B. (2019). Oral manifestations in patients with diabetes mellitus. World journal of diabetes, 10(9), 485-489.
2. Altundag, A., Ay, S. A., Hira, S., Salihoglu, M., Baskoy, K., Deniz, F., ... & Hummel, T. (2017). Olfactory and gustatory functions in patients with non-complicated type 1 diabetes mellitus. European Archives of Oto-Rhino-Laryngology, 274(6), 2621-2627.
3. Mohsen, R. O. M., Halawa, A. M., & Hassan, R. (2019). Role of bone marrow-derived stem cells versus insulin on filiform and fungiform papillae of diabetic albino rats (light, fluorescent and scanning electron microscopic study). Acta histochemica, 121(7), 812-822.

## Effects of Rosmarinic acid against corneal toxicity of cisplatin

Engin Yenilmez \*, Abdülkadir Kutlu , Birgül Gür Kutlu

Karadeniz Technical University Faculty of Medicine, Trabzon, Turkey

Cisplatin is an antineoplastic drug that is actively used in the treatment of many cancer types today. However, its various side effects on many systems and eyes limit its use. Oculotoxic effects of cisplatin due to oxidative damage include retinal ischemia and toxicity, pigment changes, bleeding, cone cell dysfunction, visual impairment and blindness. Rosmarinic acid, which has strong antioxidant and antiapoptotic effects, is a natural phenolic compound present in many plants. In our study, it was aimed to determine the possible toxic effects of cisplatin on the rat cornea and to determine the capacity of rosmarinic acid to eliminate these effects.

In this study, 24 adult male Sprague Dawley rats weighing between 200-250 g were divided into 4 equal groups. No application was made to the control group (K) during the 7-day experiment. On the 3rd day of the experiment, a single intraperitoneal dose of 7 mg/kg cisplatin were given to Cisplatin (C) and treatment (C+R) groups. 50 mg/kg rosmarinate was administered by oral gavage for 7 days to the treatment (C+R) and antioxidant (R) groups. At the end of the experiment, ocular tissues of rats sacrificed under anesthesia were excised and standard procedures were applied for histopathological analysis. General morphology, total corneal thickness, corneal epithelial thickness, the ratio of epithelial thickness to corneal thickness, and the number of keratocyte layers forming the epithelium were determined in hematoxylin-eosin (H&E) stained preparations. Apoptotic indices in the epithelium and stroma were evaluated with the TUNEL technique. In statistical analyses,  $p < 0.05$  was accepted as significant.

In the evaluation of H&E stained preparations, it was observed that cisplatin and rosmarinate had a slight negative effect on the general morphology. It was determined that cisplatin decreased both corneal epithelial thickness and stromal thickness. It was determined that it thinned the epithelium more than the stroma and decreased the epithelial/corneal ratio. The most pronounced effect of rosmarinate was on the epithelium. Rosmarinate increased the thickness and number of layers of the epithelium and partially thinned the stroma. Thus, it decreased the total corneal thickness and increased the epithelial/corneal ratio. While cisplatin significantly increased the apoptotic index in the epithelium and stroma, it was found that rosmarinate partially increased it when given alone, but decreased it in the treatment group. In the statistical analysis of all findings, the differences between the groups were significant ( $p < 0.05$ ).

**Keywords:** cisplatin , cornea , rosmarinic acid , microscopy , apoptosis

### References:

1. Langevin S, Chang JS, Chang S. Serous retinopathy associated with cisplatin treatment. *Retin Cases Brief Rep* 2019;13:211–214.
2. Gul Baykalir B, Ciftci O, Cetin A, et al. The protective effect of fish oil against cisplatin induced eye damage in rats. *Cutan Ocul Toxicol* 2018;37:151–156.
3. Ahiskali I, Ferah Okkay I, Mammadov R, et al. Effect of taxifolin on cisplatin-associated oxidative optic nerve damage in rats. *Cutan Ocul Toxicol* 2020;40(1):1–6.
4. Ben Ayed W, Ben Said A, Hamdi A, et al. Toxicity, risk factors and management of cisplatin-induced toxicity: a prospective study. *J Oncol Pharm Pract* 2020;26:1621–1629.
5. Polat N, Ciftci O, Cetin A, et al. Toxic effects of systemic cisplatin on rat eyes and the protective effect of hesperidin against this toxicity. *Cutan Ocul Toxicol* 2016;35:1–7.
6. Sadzuka Y, Shoji T, Takino Y. Mechanism of the increase in lipid peroxide induced by cisplatin in the kidneys of rats. *Toxicol Lett* 1992;62:293–300.
7. Petersen, M., & Simmonds, M. S. (2003). Rosmarinic acid. *Phytochemistry*, 62(2), 121-125.
8. Domitrović, R., Potočnjak, I., Crnčević-Orlić, Ž., & Škoda, M. (2014). Nephroprotective activities of rosmarinic acid against cisplatin-induced kidney injury in mice. *Food and chemical toxicology*, 66, 321-328.

### The effects of dose-dependent chronic caffeine consumption in a rat burn wound model

Selma AYDEMİR<sup>1</sup>, Filiz YILMAZ<sup>2</sup>, Bayram YILMAZ<sup>3</sup>, Orkun ILGEN<sup>4</sup>, Sefa KURT<sup>4</sup>, Başak BAYKARA<sup>5,\*</sup>

<sup>1</sup> Health Science Dokuz Eylül University, Faculty of Medicine, Department of Histology and Embryology, Izmir, Turkey

<sup>2</sup> Hitit University, Training and Research Hospital, IVF Center, CORUM, Turkey

<sup>3</sup> Hitit University, Training and Research Hospital, Pathology Department, CORUM, Turkey

<sup>4</sup> Dokuz Eylül University, Faculty of Medicine, Department of Obstetrics and Gynecology, Izmir, Turkey

<sup>5</sup> Dokuz Eylül University, Faculty of Medicine, Department of Histology and Embryology, Izmir, Turkey

**Aim:** Thermal injury is one of the most severe forms of trauma affecting an organism. Burn wound healing is highly dynamic, with complex interactions between numerous cell types, cytokines and proteins. The effects of caffeine consumption on wound healing have been documented in vitro, but little is known about the wound healing mechanism in vivo after burns. We aim to examine the dose-dependent effects of chronic caffeine consumption on the burn wound healing process in an in-vivo rat model using histopathological and immunohistochemical methods.

**Materials and Methods:** The burn model was created in rats. Forty-five (200-220g) female Wistar rats were randomly assigned to a chronic high caffeine group (20mg/kg per day for 8 weeks via oral gavage; n=15), a chronic low caffeine group (10mg/kg per day for 8 weeks via oral gavage; n=15) and control group (n=15). Each group was divided into three subgroups (n=5) according to the sacrifice day (7th, 14th, 21st day). The wound area, the wound closure percentage, the histopathological and immunohistochemical reactivity were evaluated. **Result:** Delayed healing process was observed in the high dose group compared to the control and low dose groups. Successful wound healing was noted in the low dose group, similar to the control group. The pathological findings observed in the high dose group were insufficient re-epithelization, inflammation and increased granulation. Besides,  $\alpha V\beta 3$  integrin, VEGF and MMP-9 immunohistochemical reactivity showed a statistically significant difference compared to the control group.

**Conclusion:** Chronic caffeine consumption in rats has been shown to adversely affect burn wound healing in a dose-dependent manner, and it is possible to suggest that this occurs by causing delayed wound healing via MMP-9,  $\alpha V\beta 3$  integrin and VEGF molecules. The treatment that modulates these factors can lead to a better and faster recovery of skin damage in caffeine addicts.

**Keywords:** caffeine, integrin, MMP-9, VEGF, wound healing

#### References:

1. Quain AM, Khardori NM. Nutrition in Wound Care Management: A Comprehensive Overview. Wounds. 2015 Dec;27(12):327-35. PMID: 27447105.
2. Shirakata Y, Kimura R, Nanba D, Iwamoto R, Tokumaru S, Morimoto C, et al. Heparin-binding EGF-like growth factor accelerates keratinocyte migration and skin wound healing. J Cell Sci. 2005;118(Pt 11):2363-70
3. DiPietro LA. Angiogenesis and wound repair: when enough is enough. J Leukoc Biol. 2016 Nov;100(5):979-984. doi: 10.1189/jlb.4MR0316-102R. Epub 2016 Jul 12. PMID: 27406995; PMCID: PMC6608066.

## The effects of pterostilbene on cyclophosphamide-induced kidney and bladder injury in rats

Gökçen Kerimoğlu<sup>1\*</sup>, Tuğba Arıcı<sup>2</sup>, Ayşe Fırıze Bıyık<sup>1</sup>, Ali Kulaber<sup>1</sup>, Yüksel Aliyazıcıoğlu<sup>1</sup>, Selim Demir<sup>1</sup>, Nihal Turkmen<sup>1</sup>, Engin Yenilmez<sup>1</sup>

<sup>1</sup> Karadeniz Technical University Faculty Of Medicine, Trabzon, Turkey

<sup>2</sup> Başakşehir Çam and Sakura City Hospital, Istanbul, Turkey

Cyclophosphamide (CYP) is a toxic drug used in chemotherapy that targets normal cells as well as cancer cells. CYP can cause side effects such as hemorrhagic cystitis and renal toxicity. Metabolic conversion of CYP leads to the formation of two cytotoxic metabolites: phosphoramidate mustard and acrolein. Acrolein is thought to be responsible for essential tissue damage caused by CYP. Acrolein produces highly reactive oxygen species (ROS), interferes with the tissue antioxidant defense system.

In our study, the possible curative and protective effect of Pterostilbene (Ptr), which is the primary antioxidant component of blueberry, against the damage caused by CYP in the kidney and bladder were investigated.

In this study, 21 adult male Sprague Dawley rats were randomly divided into three equal groups. The Control Group (CG) was given 1 ml/kg of sunflower oil by oral gavage for 14 days from the first day of the experiment and a single dose of 10 ml/kg saline (SF) intraperitoneally (ip) on the ninth day of the experiment. The Cyclophosphamide Group (CYPG) was administered 1 ml/kg sunflower oil by oral gavage for 14 days from the beginning of the experiment and CYP was administered ip at a dose of 200 mg/kg in a single dose of 10 ml/kg saline on the ninth day of the experiment. In the Cyclophosphamide and Pterostilbene Group (CYP+PtrG), 40 mg/kg Ptr was administered in 1 ml/kg sunflower oil by oral gavage for 14 days from the first day of the experiment and on the ninth day of the experiment a single dose of CYP was administered ip at a dose of 200 mg/kg in 10 ml/kg saline. At the end of the experiment, while the rats were under anesthesia the kidneys and bladder were removed. Half of the kidneys and bladders were used for biochemical analysis, while the other halves were used for histopathological assessments.

In the renal tissue stained with hematoxylin-eosin of the CYPG, extensive renal tubular dilatation, degeneration of the tubule epithelium, and abundant epithelial cells shed into the tubule lumen were observed. Atrophy/degeneration in certain glomerular structures, dilatation of Bowman's capsule and separation of parietal layer were examined. In the CYP+PtrG, tubular dilatation and epithelial cells shed into the lumen were still present yet at a lower level. Degeneration in the glomeruli and tubular epithelium were mostly improved, and the dilatation and separation observed in Bowman's capsule significantly ameliorated. In bladder mucosa belonging to the CYPG; significant edema, hemorrhage and inflammatory cell infiltration were observed that enlarged the lamina propria more than twice the size. There were significant loss and hemorrhage in the mucosal epithelium. In the CYP+PtrG; hemorrhage, inflammatory cell infiltration, epithelial loss, and edema significantly decreased. While an increase in MDA, TOS, Caspase-3 and OSI values of CYPG was observed, SOD values of CYPG decreased compared to CG in renal biochemical parameters. TOS and OSI values of CYPG increased compared to CG in the biochemical parameters of the bladders.

In conclusion, pterostilbene may reduce cyclophosphamide-induced oxidative injury in kidney and bladder in rats.

**Keywords:** Pterostilbene , cyclophosphamide , rat , kidney , bladder

### References:

1. Bhat, N., Kalthur, S. G., Padmashali, S., & Monappa, V. (2018). Toxic Effects of Different Doses of Cyclophosphamide on Liver and Kidney Tissue in Swiss Albino Mice: A Histopathological Study. *Ethiopian journal of health sciences*, 28(6), 711–716. <https://doi.org/10.4314/ejhs.v28i6.5>
2. Sakthivel KM, Guruvayoorappan C (2015) Acacia ferruginea inhibits cyclophosphamide-induced immunosuppression and urotoxicity by modulating cytokines in mice. *J Immunotoxicol* 12(2):154–163. <https://doi.org/10.3109/1547691X.2014.914988>
3. Gunes, S., Sahinturk, V., Uslu, S. et al. Protective Effects of Selenium on Cyclophosphamide-Induced Oxidative Stress and Kidney Injury. *Biol Trace Elem Res* 185, 116–123 (2018). <https://doi.org/10.1007/s12011-017-1231-8>
4. McCormack D, McFadden D. A review of pterostilbene antioxidant activity and disease modification. *Oxid Med Cell Longev*. 2013;2013:575482. doi: 10.1155/2013/575482. Epub 2013 Apr 4. PMID: 23691264; PMCID: PMC3649683.



## Human amnion membrane derived MSCs can ameliorate irradiation induced testicular damage by reducing oxidative stress

**Busra Cetinkaya Un** <sup>1\*</sup>, **Burak Un** <sup>2</sup>, **Meryem Akpolat** <sup>3</sup>, **Yusufhan Yazir** <sup>4</sup>

<sup>1</sup> Zonguldak Bulent Ecevit University Medicine Faculty, Zonguldak, Turkey

<sup>2</sup> Department of Gynecology and Obstetrics, University of Health Sciences Adana City Training and Research Hospital, Adana, Turkey, Adana, Turkey

<sup>3</sup> Department of Histology and Embryology, Medicine Faculty, Zonguldak Bulent Ecevit University, Zonguldak, Turkey, Zonguldak, Turkey

<sup>4</sup> Department of Histology and Embryology, Medicine Faculty, Kocaeli University, Kocaeli, Turkey, Kocaeli, Turkey

**OBJECTIVES:** Today, infertility affects 15% of couples and half of this rate is due to reproductive problems in men. Oxidative stress caused by excessive increase of reactive oxygen species (ROS) plays a role in the pathogenesis of radiation-induced male infertility. In this study, the effect of human amnion membrane derived mesenchymal stem cells (hAMSCs) and conditioned medium (hAMSCs-CM) on testicular damage induced by ionizing radiation is aimed to be elucidated through oxidative stress mediated MAPK pathways.

**METHODS:** 6 Gy scrotal irradiation was used to create a testicular injury model. While  $2,5 \times 10^5$  hAMSCs isolated from placental amnion membrane were transplanted into testis in one group, hAMSCs-CM was applied to the other group. Johnsen scoring was made. Seminiferous tubule diameter and seminiferous epithelial height were measured. Immunoreactivities of p38, JNK, NFκB, Parp-1 were determined. TUNEL test was performed. Serum 8OHdG level was measured as an oxidative stress marker.

**RESULTS:** After hAMSCs transplantation and administration of hAMSCs-CM, offsprings were obtained. Seminiferous tubule diameter and seminiferous epithelial height increased. The expression of p38, JNK, NFκB, Parp-1 decreased. Percentages of tunel positive cells decreased. Level of 8OHdG decreased.

**CONCLUSION:** After irradiation, both hAMSCs transplantation and paracrine activity of hAMSCs may have a role in reducing oxidative stress. hAMSCs transplantation after irradiation inhibits JNK/p38MAPK signaling by reducing oxidative stress. The results of the hAMSCs-CM applied group were similar to the results of the hAMSCs group, suggesting that the factors and cytokines in the conditioned medium may have reduced oxidative stress, oxidative stress-mediated JNK/p38MAPK pathways and apoptosis. Thus, it can be said that MSCs derived from placental amniotic membrane can improve ionized radiation-induced testicular damage by reducing oxidative stress, JNK/p38MAPK signaling and apoptosis.

**Keywords:** Radiation , Testicular damage , Mesenchymal stem cells

## Farklı yüzey kaplamalarına ve fiziksel özelliklere sahip altın nanomateryallerin, farelerdeki histolojik değişimlere etkileri

İlyas Özçiçek <sup>1,\*</sup>, Nilüfer Ulaş Aytürk <sup>2</sup>, Neşe Aysit <sup>1</sup>

<sup>1</sup> İstanbul Medipol Üniversitesi, Tıp Fakültesi, Tıbbi Biyoloji Anabilim Dalı, Sağlık Bilim ve Teknolojileri Araştırma Enstitüsü (SABİTA), İstanbul, Turkey

<sup>2</sup> Çanakkale Onsekiz Mart Üniversitesi, Tıp Fakültesi, Histoloji ve Embriyoloji Anabilim Dalı, Çanakkale, Turkey

**Giriş ve Amaç:** Altın nanopartiküller ve altın nanoçubuklar oldukça popüler metalik nanomateryaller olup; eşsiz fiziksel, kimyasal ve optik özelliklere sahiptirler. Son zamanlarda, fototermaal terapi, hedefleme, ilaç aktarımı, DNA/RNA aktarımı, biyosensör ve görüntüleme gibi geniş bir yelpazedeki biyomedikal alanlarda uygulamaları bulunmaktadır. Nanomateryallerin yüzey kaplaması ve boyutu; toksisite, biyodağılım, hücresel lokalizasyon ve terapötik potansiyel gibi konularla yakından ilgilidir. Bu çalışma kapsamında yüzeyleri polietilenimin (PEİ) ve polietilen glikol (PEG) ile kaplanmış altın nanopartiküllerin ve altın nanoçubukların sentezlenmesi sonrası, Balb-c ırkı farelerdeki histolojik etkilerinin incelenmesi amaçlanmıştır.

**Gereç ve Yöntemler:** İki farklı boyuttaki altın nanopartiküller (20 nm ve 50 nm) ile yaklaşık 15 nm-90 nm boyutlarındaki nanoçubuklar yüksek stabilitede sentezlenerek, yüzeyleri PEİ ve PEG kullanılarak kaplanmıştır. Sentezlenen tüm altın nanomateryallerin, taramalı elektron mikroskobu (SEM) görüntüleri alınmış ve gerekli diğer tüm fizikokimyasal karakterizasyonlar yapılmıştır. Farelere iki farklı konsantrasyonda (0.5 ve 5 mg Au/kg hayvan ağırlığı) kuyruk veninden enjeksiyondan 48 saat sonra, materyallerin çeşitli organlardaki (karaciğer, beyin, böbrek ve dalak) genel histolojik etkileri Hematoksilen-Eozin (H&E) boyamalarıyla araştırılmıştır. Farklı olarak, tek yüksek konsantrasyondaki (5 mg Au/kg hayvan ağırlığı) materyal enjeksiyonundan 14 gün sonra, karaciğer için geçirimli elektron mikroskobu (TEM) incelemeleri yapılarak, toksik etkileri ve dağılımları değerlendirilmiştir.

**Bulgular:** Oldukça yüksek stabilitede, PEİ/PEG kaplı nanopartiküller ve nanoçubuklar başarıyla sentezlenmiştir. Altın nanomateryallerin boyutları ve yüzey kaplamaları; SEM görüntüleri ve UV-görünür spektrumlarındaki kaymalarla ortaya konulmuştur. PEİ modifikasyonu materyallere pozitif yönde bir zeta potansiyel artışı sağlarken, PEG kaplı olanlarda zeta potansiyel değerleri negatif olarak kalmıştır. Histolojik incelemelerde, karaciğer nanotoksikolojik açıdan en fazla etkilenen organ olmuştur. Nanomateryallerin PEİ ya da PEG yüzey kaplamaları, olumsuz yöndeki histolojik değişimleri önemli ölçüde indirgeyerek, biyoyumluluğu artırmıştır. Karaciğer TEM kesitleri incelendiğinde, özellikle yüzey fonksiyonize gruplarda, hepatositlerin sitoplazmik bölgelerinde ve çekirdek içinde fazlaca nanomateryal dağılımı ortaya konulmuştur. Histolojik değişimler üzerinde, partiküllerin yüzey özellikleri boyuttan daha belirleyici bir parametre olarak ön plana çıkmıştır. Genel toksik etki açısından, PEİ ve PEG arasında önemli farklılıklar gözlenmezken, hepatositlerdeki dağılım açısından PEİ yüzey modifikasyonu ön plana çıkmıştır.

**Tartışma ve Sonuç:** Altın nanopartiküllerin ve nanoçubukların PEİ ve PEG yüzey kaplamaları, histolojik açıdan biyoyumluluğu önemli ölçüde artırmıştır. Özellikle nanoçubuklar için bu durum oldukça önemlidir. Nanopartiküller için, toksikolojik etki açısından yüzey kimyası, boyuttan daha belirleyici bir parametredir. Karaciğer histolojik değişimlerin gerçekleştiği majör organ olarak değerlendirilmiştir. Sentezlenen yüzey fonksiyonize altın nanomateryaller; biyoyumlulukları, stabiliteleri ve diğer fizikokimyasal özellikleri göz önüne alındığında; gelecekteki potansiyel biyomedikal uygulamalar için umut vaat edicidir. Bu çalışma, Türkiye Bilimsel ve Teknolojik Araştırma Kurumu (TÜBİTAK) tarafından, 217S135 proje numarası ile desteklenmiştir.

**Keywords:** altın nanopartiküller , altın nanoçubuklar , PEİ/PEG yüzey modifikasyonu , histopatoloji , nanotoksisite

### References:

1. Wang, X.; Shao, M.; Zhang, S.; Liu, X., Journal of Nanoparticle Research 2013, 15 (9).

## Increased differentiation efficacy of neural stem cell with the combination of three growth factors loaded nanoparticles

Avşegül Açıkşarı<sup>1\*</sup>, Serap Mert<sup>2</sup>, Zehra Seda Halbutoğulları<sup>2</sup>, Deren Aslan<sup>1</sup>, Yusufhan Yazır<sup>2</sup>

<sup>1</sup> Department of Stem Cell, Institute of Health Sciences, Kocaeli University, Kocaeli, Turkey

<sup>2</sup> Center for Stem Cell and Gene Therapies Research and Practice, Kocaeli University, Kocaeli, Turkey

Neural stem cells (NSCs) are self-renewing, proliferating multipotent cells and can generate somatic cell lines of neuronal origin (1). NSCs can differentiate into dopaminergic (DA) neurons by induction with growth factors (GFs) so this provides promising treatment of Parkinson's disease (PD) caused by loss of DA neurons (2). In recent years, a variety of polymeric nanoparticles (NPs) that carry therapeutic compounds to the brain have been formulated (3). GF-loaded poly(lactic-co-glycolic acid) (PLGA) NPs have been shown to suitable candidate for the treatment of neurodegeneration in lesioned PD rat model (4).

The aim of this study is to develop the new approach for the differentiation of NSCs into DA neurons by the usage of GF-NPs. For this reason brain-derived neurotrophic factor (BDNF), glial-derived neurotrophic factor (GDNF) and transforming growth factor- $\beta$ 3 (TGF- $\beta$ 3) loaded PLGA-NPs was formulated and used for NSCs. By this way, GF loaded PLGA-NPs can release their content into the NSCs and their microenvironment steering them into DA neurons.

BDNF, GDNF and TGF- $\beta$ 3 loaded PLGA-NPs were prepared by double emulsion technique as defined by Herrán et al. (4). The size, surface zeta potential and polydispersity index of NPs were found as 230 nm, -22 mV and 0.13 with Malvern Zeta Sizer respectively. The loading efficiencies and release profiles of GFs were determined by a Micro BCA Protein Assay analysis after 30 days release of NPs. Morphological structures of NPs were examined by electron microscopy. Then, NSCs were cultured as neurospheres and seeded on poly-ornithine/laminin coated dishes to induce DA neuron differentiation with NPs for 10 days. The phenotype of differentiated cells was examined by immunofluorescence microscopy for the DA neuron markers; tyrosine hydroxylase (TH) and microtubule-associated protein (Map2). The expression levels of TH and Tubb3 genes were analyzed by RT-PCR.

As a result of this study, it can be ensured that the therapeutic substance is transferred to the NSCs or affects them indirectly as it is released from NPs in the microenvironment. Moreover, it has been shown that it is possible for NSCs to form DA-like neurons, not with the help of a single agent, but with the use of different agents that will trigger many different pathways. Consequently, it can be claimed that a new approach has been developed for a possible use of GF loaded PLGA-NPs and NSCs in the permanent treatment of Parkinson's disease.

Acknowledgements: Financial support was received from KOU-BAP (2019/036).

**Keywords:** Neural stem cells , Nanoparticles , Parkinson's disease

### References:

1. Tang, Y., Yu, P. ve Cheng, L. (2017). Current progress in the derivation & therapeutic application of neural stem cells. *Cell Death and Disease*, 8(10). doi:10.1038/cddis.2017.504
2. Yang, H., Wang, J., Wang, F., Liu, X., Chen, H., Duan, W. ve Qu, T. (2016). Dopaminergic Neuronal Differentiation from the Forebrain-Derived Human Neural Stem Cells Induced in Cultures by Using a Combination of BMP-7 and Pramipexole with Growth Factors. *Frontiers in Neural Circuits*, 10(April), 1–6. doi:10.3389/fncir.2016.00029
3. Saraiva, C., Praça, C., Ferreira, R., Santos, T., Ferreira, L. ve Bernardino, L. (2016). Nanoparticle-mediated brain drug delivery: Overcoming blood-brain barrier to treat neurodegenerative diseases. *Journal of Controlled Release*, 235, 34–47. doi:10.1016/j.jconrel.2016.05.044
4. Herrán, E., Pérez-González, R., Igartua, M., Pedraz, J. L., Carro, E. ve Hernández, R. M. (2013). VEGF-releasing biodegradable nanospheres administered by craniotomy: A novel therapeutic approach in the APP/Ps1 mouse model of Alzheimer's disease. *Journal of Controlled Release*, 170(1), 111–119. doi:10.1016/j.jconrel.2013.04.028

## Linking microstructure and transport properties in Sm/Yb-doped AlN ceramics

**Pinar Kaya**<sup>1,\*</sup>, **Eren Suyolcu**<sup>2</sup>, **Peter A. van Aken**<sup>3</sup>, **Servet Turan**<sup>4</sup>, **Giuliano Gregori**<sup>3</sup>, **Joachim Maier**<sup>3</sup>

<sup>1</sup> Materials Research Institute (IMFAA), Aalen University, Aalen, Germany

<sup>2</sup> Cornell University, Ithaca, United States

<sup>3</sup> Max Planck Institute for Solid State Research, Stuttgart, Germany

<sup>4</sup> Eskişehir Technical University, Eskişehir, Turkey

Aluminium nitride (AlN) ceramics have received increased attention not only in the field of ceramics research but also in semiconductor technology due to their very high thermal conductivity and excellent electrical insulation properties. However, densification of the starting powder is challenging due to the strong covalent bonding between Al and N, which challenges manufacturing with high densities. One way to improve densification is implementing sintering aids, such as rare-earth and/or alkaline earth oxides that could contribute to the transport behaviour<sup>1</sup>. Moreover, it is known that the electrical transport along the grain boundaries, designed interfaces and particular crystallographic directions can be tuned, even by several orders of magnitudes. Several examples such as LaAlO<sub>3</sub>/SrTiO<sub>3</sub><sup>2</sup> and La<sub>2</sub>CuO<sub>4</sub>-based interfaces<sup>3,4</sup>, TiCN/SiAlON composites<sup>5</sup>, mesoscopic SrTiO<sub>3</sub><sup>6</sup> and polycrystalline PdCoO<sub>2</sub><sup>7</sup> have been extensively studied. Relatedly, microstructural design, particularly the utilization of the grain boundaries and interfaces, can be critical for tailoring the transport properties. From this point of view, we have investigated the microstructural effects on the electrical and thermal transport properties of the AlN ceramics in terms of cation size and nature of sintering aids (i.e. Sm<sub>2</sub>O<sub>3</sub> and Yb<sub>2</sub>O<sub>3</sub>)<sup>8</sup>.

**Keywords:** Grain boundary , Electrical conductivity , Thermal conductivity , Microstructure , AlN

### References:

1. Qiao, L., Zhou, H., Xue, H., & Wang, S., *J. Eur. Ceram. Soc.*, 23(1), 61-67 (2003).
2. Ohtomo, A. & Hwang, H. Y., *Nature* 427, 423–426 (2004).
3. Suyolcu, Y. E., Christiani, G., van Aken, P. A., et al., *J. Supercond. Nov. Magn* 33 1 107-120 (2020).
4. Kaya, P., Gregori, G., Baiutti, F. et al., *ACS Appl. Mater. Interfaces* 10, 22786–22792 (2018).
5. Kaya, P., Gregori, G., Yordanov, P. et al., *J. Eur. Ceram. Soc.* 37, 3367–3373 (2017).
6. Lupetin, P., Gregori, G. & Maier, J., *Angew. Chem. Int. Ed.* 49, 10123–10126 (2010).
7. Yordanov, P., Gibbs, A. S., Kaya, P., et al., *Physical Review Materials* 5 1 015404 (2021).
8. Kaya, P., Suyolcu, Y. E., van Aken, P. A., et al., *J. Eur. Ceram. Soc.* 41 9 4870-4875 (2021).

## TEM investigations of hydrothermally synthesized pure and Al Doped Zinc Tin Oxide Nano Powders

**Umut Savacı<sup>\*</sup> , Cem Açıkşarı , Ender Suvacı , Servet Turan**  
Eskisehir Technical University, Eskisehir, Turkey

Metal oxide-based materials are used in various electronic applications such as digital screens, transparent thin film transistors and various kinds of sensors thanks to their physical and electrical properties. In recent years, there has been a significant interest to the metal oxide thin films due their potential application areas such as thin film transistors (TFT) used inside the digital screen panels. For the TFT applications, amorphous oxide semiconductor (AOS) materials have been considered as an excellent material due to their ease of production and processing. Amorphous indium gallium zinc oxide (IGZO) has been considered as one of the best compositions and it has been commercially used in thin film transistors due to its high carrier mobility, optical transparency and good uniformity. Despite the excellent properties of the IGZO TFT's, AOS researches have been focused on development of new indium and gallium free compositions due to their limited and expensive resources. For this purpose, researches have been carried out on the new possible compositions of zinc based amorphous oxide compositions and it has been shown that zinc tin oxide (ZTO-Zn<sub>2</sub>SnO<sub>4</sub>) ternary composition is the best possible candidate due to its high electron mobility, electrical conductivity, environmental stability and relatively lower production costs. Oxide TFT's are produced with sputtering methods over a substrate and for this purpose high density ceramic targets having a small grain size are required to obtain uniform ZTO thin films. These ceramic sputtering targets are produced by the sintering of ZTO powders; therefore, particle characteristics have a significant role on the performance of TFT's. In this study hydrothermal synthesis method was chosen to produce nano scale ZTO powders for sputtering targets. With this method, synthesis conditions can change particle characteristics which can also affect the sputter target performance; therefore, it is important to characterize effects of processing conditions on particle size, morphology and purity.

In the literature electrical and optical properties of ZnO amorphous oxide semiconductors were improved with an incorporation of dopant elements, such as Al, In and Ga, inside the crystal structure. With a similar approach, it has been reported that Al doping can also improve the electrical and optical properties of ZTO phase having Zn<sub>2-x</sub>Sn<sub>1-x</sub>Al<sub>2x</sub>O<sub>4</sub> (AZTO) chemical formula. In the literature only solid-state synthesis method was utilized and reported for the production of AZTO particles; however, hydrothermal synthesis method, which can allow to produce nano scale particles with controlled characteristics has not been reported. Therefore, effects of Al doping during the hydrothermal synthesis and particle characteristics are not clear.

The aim of this study is the characterization of nano sized pure and Al-doped ZTO particles synthesized with hydrothermal synthesis method to understand effects of processing conditions on the particle characteristics. For these purposes, ZTO and AZTO particles were characterized by means of X-ray diffraction, scanning electron microscopy and (scanning) transmission electron microscopy techniques to understand the effects of process parameters on the particle size, morphology as well as chemical composition of the produced materials. In this presentation the obtained results will be given and discussed.

**Keywords:** Hydrothermal synthesis , Zinc Tin Oxide

## **Synthesis of multilayer graphene encapsulated FE nanoparticles by chemical vapor deposition using ferrocene precursors**

**Siddika Mertdinc \* , Berk Çağatay Demiralın , Yunus Emre Sürmeli , Bilge Umay Korkmaz , Mehmet Erinç Serten , M. Lütfi Öveçoğlu , Duygu Ağaoğulları**

Istanbul Technical University, Chemical and Metallurgical Engineering Faculty, Metallurgical and Materials Engineering Department, Graphene & 2D Materials Laboratory, Istanbul, Turkey

In this study, chemical vapor deposition (CVD) was used to synthesize Fe@C core-shell nanoparticles from Ferrocene ( $C_{10}H_{10}Fe$ ) based precursors. First, ferrocene and fumed silica ( $SiO_2$ ) powders were mixed in ethanol to prepare Ferrocene loaded fumed silica powders that used as precursor for CVD studies. Prepared precursor powders placed in quartz boats located at the heating zones of the furnace. Then, CVD system was performed under flows of Hydrogen ( $H_2$ ) and methane ( $CH_4$ ) gases. Hydrogen ( $H_2$ ) was used for Ferrocene reduction and also methane ( $CH_4$ ) led to graphitic layer formation on the Fe nanoparticles. CVD temperature and gas flows were investigated as variables of this study. Both CVD temperature was changed between 850 and 1000°C and the flow rates of gases were changed ( $H_2/CH_4 = 100/100, 50/50, 50/100$  ml/min). Purification of synthesized powders after CVD studies were performed using 2 M HF and 4 M HCl acid solutions. Silica content and uncoated Fe nanoparticles were removed using HF and HCl acid solutions. After that, characterization investigations of synthesized and purified powders were conducted with X-ray diffractometer (XRD), transmission electron microscope (TEM), scanning electron microscope (SEM), particle size analyzer, Raman spectroscopy and vibrating sample magnetometer (VSM). Raman and XRD investigations show that 950°C was optimum condition for multi layer graphene formations on Fe nanoparticles reduced from Ferrocene based precursors. Moreover, TEM images revealed that the core/shell morphologies of synthesized powders. According to the VSM results, synthesized powders have soft magnetic properties with saturation magnetisation (between 22.39 and 150.27 emu/g) and coercivity (between 82.34 and 278.26 Oe) values.

**Acknowledgements.** This study was supported by a research project financed by The Scientific and Technological Research Council of Turkey (TUBITAK) under the project number of 118F430.

**Keywords:** Chemical vapor deposition , Graphene encapsulation , Core-shell nanoparticles

## **A detailed investigation on mesoporous NiS<sub>2</sub> Pre-Electrocatalyst by electron microscopy tools for a Hydrogen Evolution Reaction**

**Cüneyt Karakaya** , Sarp Kaya \*  
Koç University, İstanbul, Turkey

Developing active, durable, and inexpensive electrocatalysts is critical for hydrogen production to meet ever-growing sustainable energy needs. Nickel sulfides offer significant potential as electrocatalysts for a hydrogen evolution reaction (HER); however, the active phase governing the electrochemical conversion is still under debate. We show that mesoporous thin-film NiS<sub>2</sub> synthesized by a novel soft-templating method without post-sulfurization exhibits superior HER activity in alkaline media after a preconditioning step that results in sulfur leaching, amorphization of the surface, and collapse of the mesoporous structure. A comparative analysis with scanning electron microscopy (SEM), transmission electron microscopy (TEM), energy-dispersive X-ray spectroscopy (EDX) and X-ray photoelectron spectroscopy (XPS) reveals that partial hydroxylation of the under-coordinated Ni sites is responsible for the superior HER activity.

**Keywords:** NiS<sub>2</sub>, HER, mesoporous

**References:**

1. <https://doi.org/10.1021/acscatal.0c03094>

## Molibden Borür Tozlarının Sentezi ve Karakterizasyonu

**İlayda Süzer \*** , Esin Aysel , Sıddıka Mertdinç , Hasan Gökçe , Mustafa Lütfi Öveçoğlu , Duygu Ağaoğulları  
İstanbul Teknik Üniversitesi, İstanbul, Turkey

Bu çalışma molibden oksit ( $\text{MoO}_3$ ), yerli bor oksit ( $\text{B}_2\text{O}_3$ ) ve magnezyum (Mg) redükleyici ajanının varlığında mekanokimyasal sentezleme ile molibden borür ( $\text{MoB}_2$ ,  $\text{Mo}_2\text{B}_5$ ,  $\text{MoB}_4$ ,  $\text{Mo}_2\text{B}$ , MoB) tozlarının üretimini ve karakterizasyonunu içermektedir. İlk olarak, stokiyometrik oranlarda hazırlanan tozlar farklı sürelerde (2, 4, 6, 8 sa) Spex 8000D karıştırıcı/öğütücü (1200 devir/dk) ile öğütülmüştür. Daha sonra, saflaştırma amacı ile 4 M HCl asit liçi yapılmıştır. Sentezlenen ve liç yapılan tozların faz karakterizasyonu X-ışınları difraktometresi, taramalı elektron mikroskobu/enerji dağılımlı spektroskopu (SEM/EDS) ve geçirimli elektron mikroskobu (TEM) ile gerçekleştirilmiştir. Ayrıca sentezlenen ve liç yapılan tozların partikül boyut ölçümleri de yapılmıştır. Faz analiz sonuçlarına göre 6 sa ideal süre olarak belirlenmiştir. İlâveten, ağırlıkça stokiyometrik orandan fazla  $\text{B}_2\text{O}_3$  ve Mg tozları kullanılarak da çalışmalar yapılmıştır. Tüm analizler sonucunda, optimum sentez parametresinin 6 sa öğütülen ve liç yapılan ağı. %100 fazla  $\text{B}_2\text{O}_3$  ile birlikte ağı. %50 fazla Mg içeren tozlarda elde edildiği tespit edilmiştir. Bu çalışma "Ulusal Bor Araştırma Enstitüsü (BOREN)" tarafından 2019-31-07-15-001 proje numarasıyla desteklenmektedir.

**Keywords:** Mekanokimyasal sentezleme , Liç , Borür



### SEM-EDS investigation of Magnesium ZWO Alloys

**Halil Demirtas**<sup>1</sup>, **Önder Tuna**<sup>1</sup>, **Özgür Duygulu**<sup>2\*</sup>, **Deniz Sultan Aydın**<sup>2</sup>, **Metin Usta**<sup>2</sup>, **Youngkil Jung**<sup>3</sup>, **Wonseok Yang**<sup>3</sup>, **Hyun Kyu Lim**<sup>3</sup>

<sup>1</sup> Gebze Technical University, Kocaeli, Turkey

<sup>2</sup> TÜBİTAK-MAM, KOCAELİ, Turkey

<sup>3</sup> KITECH, Songdo, Republic of Korea

The use of magnesium alloys in civil aircraft has been banned to minimize the risk of passengers. Recently, the application of magnesium alloys to aircraft parts has been actively studied due to the development of fire-resistant magnesium alloys. In 2015, the Federal Aviation Administration (FAA) approved the use of magnesium alloys that meet FAA's flammability regulations by changing the regulations that prohibit the use of magnesium alloys in civil aircraft. Therefore, it is necessary to develop and study fire-resistant magnesium alloys which can satisfy the flammability regulation of FAA. In the present study, fire resistant wrought magnesium ZWO (Mg-Zn-Y-Ca) alloy system was studied. By changing the element ratios of Zn and Y elements and by adding Ca element in different ratios, 10 different magnesium alloys were developed by gravity casting. Warm rolling was applied on six different alloys and 1 mm thick magnesium alloy sheets were achieved. Extrusion was performed on four different alloys and 8 mm diameter rods have been developed. Heat treatments such as homogenization, annealing and aging were also performed. The effect of Zn, Y and especially Ca on microstructure, mechanical properties and ignition temperature were investigated. Detailed scanning electron microscopy (SEM) and energy dispersive spectrometry (EDS) analyses were performed after casting and also thermomechanical processes. The phases observed by x-ray diffraction were characterized with the help of SEM-EDS. The phases observed were Mg<sub>3</sub>YZn<sub>6</sub> and Mg<sub>3</sub>Y<sub>2</sub>Zn<sub>3</sub> in the alloys without Ca and additionally Ca<sub>2</sub>Mg<sub>6</sub>Zn<sub>3</sub> and small amount of Mg<sub>2</sub>Ca phases. These phases were larger than 20 microns in the cast samples while the sizes were as small as nano-scale in the rolled or extruded samples. It was observed that size, distribution and type of the phases observed with SEM-EDS were effective in mechanical and physical properties of Mg ZWO alloys.

**Keywords:** Magnesium alloys, Fire-resistance, Extrusion, Rolling, Civil aircraft, SEM, EDS

### HRTEM-EDS-SAED Studies of Quasicrystal I-Phase in Mg-Zn-Y Alloys

Önder Tuna<sup>1</sup>, Halil Demirtaş<sup>1</sup>, Deniz sultan Aydın<sup>2\*</sup>, Özgür Duygulu<sup>2</sup>, Metin Usta<sup>2</sup>, Youngkil Jung<sup>3</sup>, Wonseok Yang<sup>3</sup>, Hyun Kyu Lim<sup>3</sup>

<sup>1</sup> Gebze Technical University, Kocaeli, Turkey

<sup>2</sup> TUBITAK MAM, Kocaeli, Turkey

<sup>3</sup> KITECH, Songdo, Republic of Korea

The magnesium alloys have the lowest density among the structural alloys. High specific strength and stiffness, good castability and machining properties, good energy absorbance capacity, electromagnetic shielding property, effective heat dissipation makes magnesium alloys as one of the top candidates. It is sixth most abundant metal and eighth element on the earth. Moreover, it is recyclable. Mg-Zn-Y alloys system attracted great interest from researchers. The main aim of this study is to provide the use of light materials in civil aviation in order to reduce the consumption of fuel and energy, protect the limited fuel reserves and reduce to amount of CO<sub>2</sub> gas emission which accelerates global warming. In this study, it is aimed to develop wrought magnesium alloys with high fire resistance in billet and sheet form for civil aviation. Fire resistant wrought magnesium Mg-Zn-Y-Ca alloy system has been studied. By changing the element ratios of Zn and Y elements and by adding Ca element in different ratios, 10 different magnesium alloys were developed by gravity casting. Zn/Y ratio was arranged in order to form quasicrystal icosahedral phase (I phase). Quasicrystals have unique properties. It is known that the Mg-Zn-Y alloys containing icosahedral phase (I-phase) have very good mechanical properties and good formability at room temperature. Warm rolling was applied on six different alloys and 1 mm thick magnesium alloy sheets were achieved. Extrusion was performed on four different alloys and 8 mm diameter rods have been developed. Heat treatments such as homogenization, annealing and aging were also performed. Detailed transmission electron microscopy (TEM) examinations were performed. Quasicrystal I-phase was observed with the help of selected area electron diffraction (SAED) and also atomic lattice imaging. Five-fold symmetry which is characteristic for icosahedral quasicrystal and also, three-fold and two-fold symmetries were observed. Mechanical properties of the samples were determined by tensile tests. In extrusion alloys, UTS value has been reached to over 330 MPa and elongation value has been reached to 15-27%. For rolled alloys, UTS values were in between 215-250 MPa with elongation values of 20-27 %. It was observed that quasicrystal I-phase was effective to achieve high strength and also high ductility. These results indicate that these alloys have great potential for civil aircraft applications.

## K-Band uygulamaları için GaN temelli yüksek elektron mobiliteli transistör (HEMT)

**Yıldırım DURMUŞ, Vahit BARIŞ<sup>\*</sup>, Selim ÇELİK, Gizem TENDÜRÜS, Büşra Çankaya AKAOĞLU, Doğan YILMAZ, Ekmele ÖZBAY**

Bilkent Üniversitesi, ANKARA, Turkey

Son yıllarda SiC temelli AlGaIn/GaN yüksek elektron temelli transistörler yüksek RF frekanslarda güç uygulamaları için öncelikli aday konumundadırlar. Yüksek elektron mobilitesi ve kırılma gerilimleri sayesinde 8 GHz'de 30.6 W/mm [1], 40 GHz'de 10 W/mm [1], 75 GHz'de 3.1 W/mm [2] ve 85 GHz'de 1.5 W/mm [3] güçler elde edilmiştir. AlGaIn/GaN HEMT'lere üretim ile kazandırılan düşük omik kontak direnci ve düşük gate uzunluğu sayesinde 100 GHz ft (birim akım kazanç frekansı) ve 128 GHz fmax (maksimum güç kazancı kesim frekansı) performansı ortaya çıkmıştır [4]. Özellikle Ka band (26.5-40 GHz) ve daha yukarıdaki bantlarda çalışan AlGaIn/GaN HEMT'ler uydu haberleşme, dijital radyo uygulamaları ve yeni nesil araba teknolojisinde büyük öneme sahiptirler [5].

Bu çalışmada ilk olarak AlGaIn/GaN yapısı MOCVD yöntemi ile SiC alttaş üzerine farklı sıcaklıklarda ve kalınlıklarda büyütülerek bu iki farklı yapı arasında polarizasyon oluşması sağlanmıştır. Bu polarizasyon ile iki farklı tabaka arasında 2 boyutlu elektron gazı (2 DEG) ortaya çıkmıştır. AlGaIn/GaN yapıların büyütülmesinden sonra HEMT aygıtlarına üretime geçilmiştir. 3 numune olarak başlanılan üretimde ilk olarak HEMT aygıtların omik kontak metalleri Ti/Al/Ni/Au (20/100/40/50nm) kaplanarak oluşturulmuştur. N<sub>2</sub> atmosferinde 850 C'de 30 s tavlansarak metallere omik özelliği kazandırılmıştır. Aygıtların izolasyonu için RIE sisteminde Cl tabanlı gazlar ile yüzey aşındırılmıştır. PECVD sisteminde 1. numune üzerine 100, 3. numune üzerine 30 nm SiN kaplanmıştır. Bu işlemde hemen sonra 3. numune üzerine 100 nm kalınlıkta Ge metali kaplanmıştır. Elektron demeti litografi sisteminde 3 numune için farklı yapılarda T-gate litografisi yapılmıştır. 1. numune için SiN üzerinde duran T-gate, 2. numune için havada duran T-gate ve 3. numune için SiN ve Ge üzerinde T-gate litografisi yapılmıştır. Bu üç numune içinde Ni/Au (50/400 nm) metalleri kaplanmıştır. En son olarak elektriksel kontak alınacak yerlere Ti/Au (100/1000 nm) kaplanarak üretim tamamlanmıştır. Üretim sonunda numunelerdeki iletkenlik (gm), ft ve fmax değerleri ölçülmüş ve karşılaştırılmıştır. En yüksek gm 310 mS/mm, ft 46.9 GHz ve fmax 104.2 GHz olarak T-gate yapısı SiN ve Ge üzerinde olan 3. numunedeki ölçülmüştür.

**Keywords:** GaN, SiC, T-gate, MOCVD, Yüksek frekans uygulamaları

### References:

1. I.Y. -Fu. Wu, A. Saxler, M. Moore, R. P. Smith, S. Sheppard, P. M. Chavarkar, T. Wisleder, U. K. Mishra, P. Parikh, "30-W/mm GaN HEMTs by Field Plate Optimization," IEEE Electron Device Lett., vol. 25, pp. 117-119, March 2004.
2. A. Brown, et al., "High power, high efficiency E-Band GaN amplifier MMICs," IEEE Int. Conference on Wireless Information Technology and Systems, Nov. 2012
3. Dirk Schwantuschke, Peter Brückner, Sandrine Wagner, Michael Dammann, Michael Mikulla, Rüdiger Quay, "Enhanced GaN HEMT Technology for E-Band Power Amplifier MMICs with 1W Output Power" Asia Pacific Microwave Conference Dec. 2017
4. Durmus Y, Yilmaz D, Toprak A, Turhan AB, Sen OA, Ozbay E (2015) AlGaIn/GaN HEMT with ft:100 GHz and fmax:128 GHz. 10th European Microwave Integrated Circuits Conference (EuMIC), Paris, 2015, pp 199-202
5. T Palacios, U K Mishra, G.K. Sujan "GaN-Based Transistors for High-Frequency Applications" Comprehensive Semiconductor Science and Technology Volume 5, 2011, Pages 242-298

## **Doku mühendisliği uygulamaları için gözenekli kompozit doku iskelelerinin üretimi ve mikroyapısal karakterizasyonu**

**Büşra Bulut , Şeyma Duman \***  
Bursa Teknik Üniversitesi, Bursa, Turkey

Hastalıklar, yaralanmalar ve anormal iskelet gelişimi gibi durumlar nedeniyle oluşan kemik kusurları, hastaların yaşam kalitesini büyük ölçüde etkileyen önemli sağlık sorunlarıdır. Kemik kusurlarının tedavisinde geleneksel yöntemlerin sınırlamalarının üstesinden gelebilmek amacıyla alternatif bir yaklaşım olarak ortaya çıkan doku iskeleleri, biyomalzeme, hücre ve biyosinyal moleküllerin etkileşimini temel alarak dokuların en iyi şekilde taklit edilmesini ve fonksiyonel kemik yenilenmesini amaçlamaktadır. İdeal doku iskelesi, kemik hücrelerinin büyümesini teşvik edecek, kemiğin üç boyutlu yapısının oluşmasını sağlayacak osteokondüktif bir matris, hücrelerin farklılaşmasını ve daha sonra kemiği oluşturmasını sağlamak için osteoindüktif ajanlar içermelidir. Doku iskelelerinin vücut içerisine yerleştirildiğinde istenmeyen tepkilere yol açmaması için biyoyumlu, biyolojik olarak parçalanabilmesi için biyobozunur ve kemik dokuda hücre canlılığı için gerekli besinlerin ve oksijenin başarılı bir şekilde difüzyonunun sağlanması için içsel bağlantılı ve kontrol edilebilir gözenekliliğe sahip olması istenen diğer özelliklerdir. Bu özelliklerin başarılı bir şekilde elde edilebilmesi için malzeme seçiminin ve üretim yönteminin belirlenmesinin hayati önemi haizdir. Bu çalışmada, çok çeşitli malzemeler kullanılarak farklı yöntemlerle üretilen doku iskelelerinin mikroyapısal, mekanik ve biyolojik özellikleri üzerine malzeme türünün ve üretim yönteminin etkilerinin tartışılması amaçlanmıştır. Bu amaca yönelik olarak, üretilen doku iskelelerinin yapısal özellikleri taramalı elektron mikroskobu (SEM) ve fourier transform kızılötesi spektroskopisi (FTIR) ile karakterize edilmiş, mekanik özellikleri basma dayanımı ölçülerek belirlenmiştir. Doku iskelelerinin biyolojik özellikleri ise, yapay vücut sıvısı (SBF) içerisinde in vitro biyoaktivitesi incelenerek değerlendirilmiştir. Elde edilen sonuçlar üretilen doku iskelelerinin mikroyapısal, mekanik ve biyolojik özelliklerinin görülen sınırlar içerisinde kemik yenilenmesini destekleyecek özelliklere sahip olduğunu doğrulamıştır. Sonuç olarak, içsel bağlantılı, açık ve yüksek gözenekliliğe sahip olarak çeşitli malzemelerin bir arada kullanılmasıyla ve farklı yöntemlerle üretilen kompozit doku iskelelerinin doku mühendisliğinde uygulama için önemli bir potansiyele sahip olduğu düşünülmektedir.

**Keywords:** doku mühendisliği , kemik doku iskeleleri , kompozit malzemeler

## Microfluidics based single-bacterium imaging for probing role of stress factors on bacterial growth

**Didem Rodoplu**<sup>1</sup>, **Cherng-Shyang Chang**<sup>2</sup>, **Cheng-Yuan Kao**<sup>2</sup>, **Chia-Hsien Hsu**<sup>1,\*</sup>

<sup>1</sup> Institute of Biomedical Engineering and Nanomedicine, National Health Research Institutes, Zhunan, Taiwan

<sup>2</sup> Immunology Research Center, National Health Research Institutes, Zhunan, Taiwan

In bacteriology, conventional imaging techniques including Gram staining, optical and electron microscopy are insufficient to provide quantitative and real-time investigation at the individual bacterium level. Microfluidic devices are emerging tools to enhance real-time monitoring of microorganisms under microscope [1, 2]. The recent advances in microfluidics facilitates single-cell trapping, and probing cell-cell communication and time-dependent morphostructural variabilities of individual bacterium under drug treatment [2, 3]. Herein, we have developed a microfluidic based stress-free culture environment that enables monitoring morphostructural variabilities of *Escherichia coli* (*E. coli*) with green fluorescence expressing genes during 36 hours of long incubation time using inverted fluorescence microscopy. The effect of stress on the proliferation of *E. coli* were demonstrated by exposing chemical stress using water including 0.4–1 ppm chlorine and 100–1000 µg/ml of ampicillin treated culture medium, and physical stress using continuous light during incubation, respectively. The fluorescence intensity was measured quantitatively using an analysis software and the morpho-structural changes were evaluated by fluorescence imaging. For individual bacterium imaging, magnetic microparticle captured bacterium and physically trapped bacterium were found advantageous. Our results showed that a transparent and shallow microfluidic chamber enables high-resolution imaging of individual bacterium, and nano/picoliter volume of devices provide a stress-free culture environment during long-incubation time. Under applied intensive stress factors, bacteria cells enter an injured or dormant state that results with a non-motile and non-dividing phase of live bacteria. Our results revealed that microfluidic based time-dependent image acquisition is promising for fast phenotypic characterization and broad antibiotic susceptibility testing of individual bacterium that can aid personalized medicine in the future.

**Keywords:** microfluidics , bacterium , stress factors , phenotypic characterization

### References:

1. H. Etayash, M.F. Khan, K. Kaur, T. Thundat, Microfluidic cantilever detects bacteria and measures their susceptibility to antibiotics in small confined volumes, *Nat Commun* 7 (2016) 12947-12947.
2. D. Rodoplu, C.-S. Chang, C.-Y. Kao, C.-H. Hsu, A simple magnetic-assisted microfluidic method for rapid detection and phenotypic characterization of ultralow concentrations of bacteria, *Talanta* 230 (2021) 122291.
3. K. Hsieh, H.C. Zec, L. Chen, A.M. Kaushik, K.E. Mach, J.C. Liao, T.-H. Wang, Simple and Precise Counting of Viable Bacteria by Resazurin-Amplified Picoarray Detection, *Analytical Chemistry* 90(15) (2018) 9449-9456.

## Towards “Damage-Free” TEM specimen preparation by Focused Ion Beam without Gallium

**Chengge Jiao \***

ThermoFisher Scientific, Eindhoven, Netherlands

Focused ion beam (FIB) has been widely used in materials science. Different types of ions (Argon, Gallium, Xenon, Oxygen, Nitrogen) have their unique characteristics for various applications. Plasma Xenon ion beam has been greatly accepted by the FIB microscopy community providing the advantages of high sputtering yield, high current milling at 30 keV for a large 3D volume data acquisition, and correlated microscopy applications. Reactive oxygen ion beam dramatically improves sample milling quality for carbon-carbon bonding hard or soft materials by smoothing the cut-face very effectively during sputtering.

The focus of this presentation is on FIB TEM specimen preparation. Preparation of "damage-free" TEM specimen is one of the challenges of traditional gallium (Gallium FIB, G-FIB). Our question is, if ions other than the gallium ion are used, what will happen to the specimen besides gallium-free ion implantation? How can we predict the damage of Argon, Gallium, and Xenon ions to the sample?

In this presentation, we start with introducing ion solid interactions, followed by defining ion beam application domains classified by ion projected range. We explain sample amorphous material formation induced by ion-atom knock-on damage effect before presenting a TEM specimen sidewall damages by analysis of the simulation data.

During FIB sample preparation, the ions bombards solid materials over a wide energy range from a few hundred electron-volts to 30 keV. By analyzing the simulation data generated by SRIM (Stopping and Range of Ions in Matter), including Ion range, sputter yield, atomic displacement, and vacancy damage density, this report provides clear guidance on which ion species to choose for what application domain.

With actual experimental trials guided by investigation of ion-solid interaction SRIM data, we have shown results of really close to “damage-free” TEM specimen preparation for HR (S)TEM by multi-ion source plasma FIB Hydra low energy argon ion beam at 500 eV.

We hope this presentation encourages gallium-focused ion beam and even TEM user groups to explore a new FIB application domain by applying multi-ion sources plasma ion beam DualBeam microscopy for gallium-free TEM specimens preparation. With introduce high-performance low energy focused argon ion beam to DualBeam, we are approaching to “damage-free” TEM specimen preparation domain.

**Keywords:** ion solid interaction, FIB, Focused Ion Beam, plasma ion beam, FIB TEM specimen preparation, , low energy ion beam, argon ion beam, multi-ion source

## **İn vitro modellerde korelatif ışık ve elektron mikroskopisinin üç boyutlu olarak uygulanması**

**Mehmet Serif AYDIN**\*

Istanbul Medipol University, Regenerative and Restorative Medicine Research Center (REMER), Istanbul, Turkey

Biyolojik yapılar ve hücrelerin incelenmesinde mikroskoplar önemli bir yer tutmaktadır. İncelenen bu örneklerin üç boyutlu yapıları göz önünde bulundurulduğunda mikroskopik incelemelerin de üç boyutlu olarak yapılması önem kazanmaktadır. Işık mikroskopisinde uzun yıllardır stereolojik yöntemler ve konfokal mikroskopisi gibi tekniklerle hücrelerin üç boyutlu yapıları incelenebilmektedir. Geçirimli elektron mikroskobu (TEM) ile örneklerden alınan kesitler ile numunenin iç yapısı detaylı olarak incelenebilmekte ancak bu iki boyutlu düzlemde mümkün olmaktadır. Taramalı elektron mikroskobu (SEM) numunelerin üç boyutlu yapısını görüntüleyebilmekte ancak bu örneklerin topografik özellikleri ile sınırlı kalmaktadır. Son yıllarda yaşam bilimleri alanında kullanımı giderek yaygınlaşan odaklanmış iyon tabanlı-SEM (FIB-SEM), dizi tomografisi (array tomography) ve seri blok yüzeyi görüntülemesi (SBF-SEM) teknikleriyle numunenin iç yapısının elektron mikroskobu ile üç boyutlu olarak incelenebilmektedir. Elektron mikroskobu ile ilgili bu teknikler, standart ekipmanların dışında yüksek maliyetli altyapı ve teçhizat gerektirmektedir.

Çalışmamızda, in vitro ortamdaki hücrelerin SEM ve konfokal mikroskobu kullanılarak korelatif mikroskopi yöntemiyle üç boyutlu görüntülenmesini sağlayan, kolay ve tekrarlanabilir bir teknik ortaya koyulmaktadır. Bu tekniğin temel aşamaları; (i) petri içerisinde in vitro kültürü yapılmış hücrelerin fiksasyon sonrasında konfokal mikroskobu ile üç boyutlu (z-stack) görüntülerinin alınması ve lokasyonlarının işaretlenmesi, (ii) petri içerisindeki hücrelerin elektron mikroskopik doku takibi işleminin tamamlanması ve Epon içerisinde gömülmesi, (iii) işaretlenen hücrelerin Epon blok içerisinde çıkarılarak ultramikrotom ile cam üzerine 50 nm kalınlıkta seri ince kesitlerinin alınması, (iv) alınan seri kesitlerde belirlenen hücrelere ait tüm kesitlerin SEM ile görüntülenmesi, (v) elde edilen elektron mikroskobu ve konfokal mikroskop görüntülerinin bilgisayar yazılımı ile bir araya getirilmesidir.

Elektron mikroskobu ile üç boyutlu görüntüleme imkanı sunan sistemler (FIB-SEM, SBF-SEM) yüksek altyapı maliyetleri sebebiyle kullanım imkanları kısıtlı olan tekniklerdir. Çalışmamızda uygulanan bu teknik ile, standart elektron ve konfokal mikroskoplarıyla, yüksek maliyetli ekipmanlara ihtiyaç olmaksızın üç boyutlu görüntüleme imkanı sunulmaktadır. Bu teknik ile Işık mikroskopunda belirlenen bir hücrenin elektron mikroskobu ile üç boyutlu ince yapısı görüntülenebilmektedir. Bu sayede, hücrelerde ışık mikroskopi teknikleri ile belirlenmesi mümkün olmayan yapılar ve olaylar ortaya çıkarılabilmektedir.

**Keywords:** Korelatif mikroskopi , Konfokal mikroskobu , taramalı elektron mikroskobu

## **Combining crossbeam laser and X-Ray microscopy: Massive material removal and ultrafast site-specific sample preparation.**

**Jens Peter Hermann Gnauck** \*

Carl Zeiss Microscopy GmbH, Berlin, Germany

Development of novel alloys and materials in combination with innovative fabrication and processing techniques such as additive manufacturing have enabled advanced components for new age technologies and are pushing new frontiers in numerous research fields. Focused ion beam scanning electron microscopes (FIB-SEMs) have become integral tools for characterizing sub-surface and internal features, understanding and optimizing microstructure, failure analysis in various components and materials for subsequent optimization in various applications.

With more complex materials and components high resolution imaging and analysis of large area cross-sections in the millimeter scale are required where FIB-SEMs are not effective. Conventional techniques employing mechanical grinding and polishing methods introduce cracks, deformations and introduce artifacts further damaging the samples. Here we introduce the integration of a femtosecond (fs) laser system with the ZEISS Crossbeam FIB-SEM. The massive material ablation using laser milling is highly efficient in large volume bulk material removal and provides high throughput capabilities for fast cross-sectional preparation of large volume samples.

A novel workflow by combining with a non-destructive submicron 3D X-Ray Microscopy (XRM) and fs-Laser FIB-SEM has been developed to enable higher throughput sample preparation and to access buried structures and features at desired locations with high precision. The femto-second laser fills the missing link for fast and accurate sample preparation to access the sub-surface features of interest identified using the XRM which are then polished and prepared by FIB-SEM for high resolution cross-sectional imaging.

In this presentation, the details of the fs laser, integration of the system and the workflow using the Crossbeam laser together with an XRM will be presented along with application examples focusing on geoscience, electronics, battery research, life science and additive manufacturing.



## POSTER ABSTRACTS

54 - Life Sciences - Structure and dynamics of cell organelles - Poster Presentation

### Effects Of Carbonyl Cyanide Phenylhydrazone (CCCP) On Mitochondria in Human Hepatocellular Carcinoma (HepG2) Cell Line

Yaprak Yalçın<sup>1\*</sup>, Hatice Pınar Baysan Cebi<sup>1</sup>, Hasibe Verdi<sup>1</sup>, Deniz Ekin Doğan<sup>2</sup>, F. Figen Kaymaz<sup>2</sup>, F. Belgin Atac<sup>1</sup>

<sup>1</sup> Baskent University, Ankara, Turkey

<sup>2</sup> Hacettepe University, Ankara, Turkey

**Aim:** Carbonyl cyanide phenylhydrazone (CCCP); a mitochondrial uncoupler can cause depolarization and trigger mitophagy. Here we present the 10 $\mu$ M CCCP induced cellular stress response in the HepG2 cell line. **Methods:** Following 0, 1, 2, 24 and 48 hours of 10 $\mu$ M CCCP stress into the human hepatocellular carcinoma cell line (HepG2) (ATCC-HB8065) the cytotoxicity of the cells was evaluated with MTT while the expression of p62, LC3-II, PARK2 genes were determined by the qRT-PCR method. Changes in the mitochondrial ultrastructure were observed by electron microscopy.

**Results:** Our results reveal that the CCCP caused mitotoxicity in HepG2 cells without causing cytotoxicity. The gene expression of P62 and LC3-II genes involved in mitophagy increased at 24th hour while PARK2 gene expression has been increased in the 48th hour. As a result, it was observed that cellular stress response at the gene expression level has started at 24th hour and driven up to 48th hour. However, the ultrastructural changes in the mitochondria are observed very early with more round and elongated form than the control groups, especially at the 1st and 2nd hours. C-shaped and ring-shaped mitochondria were observed at the 2nd hour and some mitochondria were smaller. At the 24th and 48th hours, C-shaped mitochondria, mitophagic vacuoles, and spherical mitochondria were observed.

**Discussion:** The preliminary results of our study may indicate that although the ultrastructural changes in mitochondria are started at the preliminary time to the CCCP exposure, the mitophagic gene expression is started at later hours. This finding may implicate that mitophagy is not the first cellular response choice of the HepG2 cells. Therefore, further studies are required for the explanation of cellular preference in managing mitochondrial quality control.

## Electron Microscopic Investigation of the Effect of Trifolium Pratense on C6 Glioblastoma Cells

**Gamze Tanrıverdi**<sup>1,\*</sup>, **Aynur Abdulova**<sup>2</sup>, **Hatice Colgecen**<sup>3</sup>, **Havva Atar**<sup>3</sup>, **Belisa Kaleci**<sup>4</sup>, **Tuğba Ekiz-Yılmaz**<sup>5</sup>

<sup>1</sup> Istanbul University-Cerrahpasa, Cerrahpasa Medical Faculty, Istanbul, Turkey

<sup>2</sup> Istanbul University-Cerrahpasa, Cerrahpasa Faculty of Medicine, Istanbul, Turkey

<sup>3</sup> Bulent Ecevit University, Faculty of Arts and Sciences, Zonguldak, Turkey

<sup>4</sup> Istanbul University-Cerrahpasa, Cerrahpasa Faculty of Medicine, Istanbul, Turkey

<sup>5</sup> Istanbul University, Istanbul Faculty of Medicine, Istanbul, Turkey

**Introduction and purpose:** Glioblastoma multiforme (GBM) is the most common brain tumor in adults. It is an aggressive primary brain tumor capable of rapid proliferation. The standard treatment approach of GBM is surgical resection followed by simultaneous chemo and radiation therapy. Unfortunately, a significant number of GBM cases develop resistance to the used chemotherapeutic drugs. Therefore, there is an urgent need for the development of new chemotherapeutic agents. Red clover, also known as Trifolium Pratense is an endemic plant containing various isoflavones such as biochanin A, genistein, daidzein, and formononetin in high concentrations. Also, it has been shown in different studies that these molecules can function as anticancer agents. Trifolium Pratense is a naturally tetraploid plant grown in our country. In this study, using electron microscopy, we aimed to examine the effects of the "Trifolium Pratense" on GBM cells.

**Material and Method:** C6 glioblastoma cells were exposed for 24 hours to increasing doses (0, 7, 12.5, 25, 50, and 100 µl) of Trifolium Pratense extract. This extract was prepared by dissolving 22.5 µg of Trifolium Pratense in 100 µl of ethanol. The cell proliferation indexes of the experimental groups were calculated using the CCK-8 assay kit. It was determined that Trifolium Pratense reached IC50 at 25nM dose and IC25 value at 12.5nM dose. After the determination of the effective dose, the cells were prepared for electron microscopic examinations. After fixation with glutaraldehyde and osmium tetroxide, it was passed through a series of ascending alcohols and embedded in araldite. Sections taken with an ultramicrotome were evaluated with Jeol 1011 electron microscope.

**Conclusion and Discussion:** It was determined that the control groups consisted of spindle-shaped elongated cells with mitochondria in normal morphology, well-developed Golgi, and a prominent GER and SER. In the 12.5nM and 25nM effective dose groups, the cells have lost their elongated form and show round or polygonal shapes. Mitochondria were damaged, and cristae structures were degenerate. The GER and SER cisternae were highly enlarged and with irregular shapes. The cells have abnormal morphology and cytoplasmic appearance, and the number of vesicular structures in their cytoplasm has increased markedly. In parallel with the increasing doses of Trifolium Pratense, autophagic vacuoles increased in the cells. In addition, it was observed that there were many extra vesicles closely related to the cells. Microscopic evaluations revealed numerous cells with cytoplasmic membrane blebs and numerous apoptotic cell bodies. These findings suggest that the plant Trifolium Pratense, a natural tetraploid endemic in our country, has an apoptotic cell death-inducing effect on GBM cells and maybe a new alternative to classical treatment for GBM treatment.

## Morphological evaluation of the effects of Apocynin on MSG induced liver damage in rats

**Begum Sahin** , Merve Acikel Elmas , Serap Arbak \*

Acibadem Mehmet Ali Aydinlar University, Istanbul, Turkey

**Introduction:** Monosodium glutamate (MSG) is used as a flavour enhancer that processed food and home cooking in the whole world in recent years. Although MSG has been reported by The Food and Drug Administration (FDA) as a safe material, several animal experiments demonstrated its negative effects following its chronic consumption. These negative effects have been associated with several diseases such as obesity, hypertension, and neurotoxicity. Apocynin, obtained from the roots of *Apocynum cannabinum* and *Picrorhiza kurroa*, has NOX (Nicotinamide adenine dinucleotide phosphate oxidase) inhibitory effect. The present study intended to demonstrate protective/healing effect of apocynin (APO) against MSG-induced hepatotoxicity.

**Material and Methods:** Thirty-two adult male Sprague-Dawley rats were randomly split into four groups (150-200 g; n=8/group). MSG was given orally as 120 mg/kg to MSG and MSG +APO group for 28 consecutive days. APO was given to MSG+ APO and APO groups as 25 mg/kg dose for 5 days starting from 24th day of the experiment till 28th day. Distilled water was given to control group orally for 28 days. At the end of the experiment the rats were sacrificed under anesthesia where liver tissues were dissected and processed for light, fluorescent and transmission electron microscopical evaluations. Paraffin sections were stained with Hematoxylin-eosin, Masson's trichrome and Periodic-Schiff reaction. Histopathological scoring has been performed in all sections. TUNEL immunocytochemistry was used to detect apoptotic cells. NOX-2 immunoreactivity in liver tissue was evaluated by fluorescent microscopy.

**Results:** The light microscopical examinations revealed normal morphology of liver parenchyme in control and APO groups while steatosis and vacuolization in hepatocytes, leukocyte infiltration and increased amount of collagen fibers in the parenchyme were detected in MSG group. Based on histopathological scoring, liver tissue damage was in less degree in MSG+APO group. PAS-positivity of hepatocytes was decreased in MSG group while this reaction was in normal levels in the MSG+APO and APO groups. TUNEL-positivity was increased in MSG group compared to control, MSG+APO and APO groups. NOX-2 positive cells were highest in MSG group. Transmission electron microscopy presented the parallel ultrastructural data as in light microscopy.

**Conclusion:** Based on the presented data, we could conclude that APO has a protective/ healing role against MSG-induced hepatotoxicity at histopathological levels.

This study was supported by Acibadem Mehmet Ali Aydinlar University Scientific Research Projects Commission (ABAPKO) (2021/01/07).

**Keywords:** Monosodium glutamate , apocynin , oxidative damage , microscopy

### References:

1. El-Meghawry El-Kenawy, A., H.E. Osman, and M.H. Daghestani, The effect of vitamin C administration on monosodium glutamate induced liver injury. An experimental study. *Exp Toxicol Pathol*, 2013. 65(5): p. 513-21.
2. Hajihasani, M.M., et al., Natural products as safeguards against monosodium glutamate-induced toxicity. *Iran J Basic Med Sci*, 2020. 23(4): p. 416-430.

## Çam kabuğu özütünün over (MDAH) kanseri hücre kültürü modelinde antikanser, antiproliferatif ve apoptotik etkilerinin incelenmesi

**Gazi Contuk**<sup>1,\*</sup>, **Mücahit Seçme**<sup>2</sup>, **Yavuz Dodurga**<sup>2</sup>, **Meltem Taş**<sup>3</sup>, **Gülşen Tel Çayan**<sup>4</sup>, **Gülçin Abban Mete**<sup>5</sup>

<sup>1</sup> Muğla Sıtkı Koçman Üniversitesi Fethiye Sağlık Bilimleri Fakültesi, Muğla, Turkey

<sup>2</sup> Pamukkale Üniversitesi Tıp Fakültesi, Denizli, Turkey

<sup>3</sup> Muğla Sıtkı Koçman Üniversitesi Fen Fakültesi, Muğla, Turkey

<sup>4</sup> Muğla Sıtkı Koçman Üniversitesi Muğla Meslek Yüksek Okulu, Muğla, Turkey

<sup>5</sup> Pamukkale Üniversitesi Tıp Fakültesi, Muğla, Turkey

Kanser, günümüzün en önemli sağlık sorunlarından birisidir. Dünyada jinekolojik kanserler en yaygın olarak görülen dördüncü kanser türüdür. Yumurtalık kanseri, rahim ağzı ve rahim kanserinden sonra üçüncü sırada yer alan en yaygın jinekolojik kanserlerden biridir. Çam kabuğu özleri, kateşin, epikateşin, taksifolin ve fenolik asitler gibi çok sayıda fenolik bileşik içerir. Çam kabuğu özleri antimutajenik, antikarsinojenik ve yüksek antioksidan aktivitelere sahip özütler içerirler. Bu etkilerinden dolayı kanser çalışmalarında etkileri araştırılmaya başlanmıştır. Bu çalışmanın amacı Kızılcım (Pinus brutia) kabuğu özütünün insan Over kanser hücre hattı (MDAH-2774) üzerindeki antiproliferatif ve apoptotik etkilerinin değişik yolaklar kullanılarak araştırılmasıdır.

Muğla Kızılcım ormanlarından toplanan Kızılcım (Pinus brutia) kabuklarından özüt elde edilmiştir. Over kanser hücre hattı (MDAH-2774) üzerine çam kabuğu özütü farklı konsantrasyonlarda uygulanmış ve XTT yöntemi ile IC50 değeri tespit edilmiştir. Gen ekspresyonları Real-time RT-PCR yöntemiyle tespit edilirken, apoptoz tayini için TUNEL testi yapılmıştır. MDAH hücrelerinde invazyonu göstermek için matrigel-invazyon testi yapılmış ve mikroskopik görüntüleri için krsital viole ile boyanmıştır. Kanser hücre migrasyonuna olan etkisi yara wound-healing yöntemi ile gösterilirken koloni oluşumu için koloni formasyon testi uygulanmıştır.

MDAH 2774 hücrelerinde IC50 dozu 48. Saate 117.6 µg/ml olarak belirlenmiştir. Programlı hücre ölümü olayında rol alan genlerden kaspaz 3,9,10 ve yine mitokondriyal iç apoptoz yolağının önemli düzenleyicilerinden olan Bax, Bcl-2, Bcl-X1 gibi genlerin ekspresyonlarındaki anlamlı değişimler görülmüştür. Doz grubunda apoptotik hücre yüzdesinde belirgin bir artış görülürken invazyon kapasitelerinde belirgin düşüş belirlenmiştir. Ayrıca çam kabuğu ekstraktının over kanser hücrelerinin migrasyon kapasitelerinde ve koloni formasyonu oluşumunda düşüş sağladığı bulunmuştur.

Çam kabuğu özütünün over kanser hücre hattı (MDAH-2774) üzerinde antikanserojen, antiproliferatif ve apoptotik etkilerinin olduğu bulunmuştur.

### References:

1. WHO <https://www.who.int/cancer/PRGLOBOCANFinal.pdf> (last access date:30.03.2021)
2. Yoneda A, Lendorf ME, Couchman JR, Mulhaupt HA. Breast and ovarian cancers: a survey and possible roles for the cell surface heparan sulfate proteoglycans. J Histochem Cytochem. 2012;60 (1):9–21. doi:10.1369/0022155411428469
3. Bray F, Ferlay J, Soerjomataram I, Siegel RL, Torre LA, Jemal A. Global cancer statistics 2018: GLOBOCAN estimates of incidence and mortality worldwide for 36 cancers in 185 countries. CA Cancer J Clin. 2018;68(6):394–424.
4. Coburn S, Bray F, Sherman M, Trabert B. International patterns and trends in ovarian cancer incidence, overall and by histologic subtype. Int J Cancer. 2017;140(11):2451–2460. doi:10.1002/ijc.30676
5. Fahrioglu U, Dodurga Y, Elmas L, Seçme M. Ferulic Acid Decreases Cell Viability and Colony Formation While Inhibiting Migration of MIA PaCa-2 Human Pancreatic Cancer Cells in Vitro". Gene . 2016 Jan 15;576(1 Pt 3):476-82. doi: 10.1016/j.gene.2015.10.061

### Activation of nesfatin-1 neurons by cytidine-5'-diphosphate choline through cholinergic receptors.

**Gonca Topal<sup>1</sup>, İlker Mustafa Kafa<sup>2</sup>, Nursel Hasanoğlu Akbulut<sup>1</sup>, Cenk Coşkun<sup>3</sup>, Vahide Savci<sup>4</sup>, Özhan Eyigör<sup>5,\*</sup>**

<sup>1</sup> Bursa Uludağ University Institute of Health Science, Department of Medical Histology and Embryology, Bursa, Turkey

<sup>2</sup> Bursa Uludağ University Faculty of Medicine, Department of Anatomy, Bursa, Turkey

<sup>3</sup> Düzce University Faculty of Medicine, Department of Medical Pharmacology, Bursa, Turkey

<sup>4</sup> Bursa Uludağ University Faculty of Medicine, Department of Medical Pharmacology, Bursa, Turkey

<sup>5</sup> Bursa Uludağ University Faculty of Medicine, Department of Histology and Embryology, Bursa, Turkey

**Aim:** Nesfatin-1 is a centrally active peptide regulating the food intake in addition to its effects on cardiovascular system, energy metabolism and stress. Exogenous administration of cytidine-5'-diphosphate choline (CDP-choline) produces several effects on cardiovascular and endocrine systems. A recent report has shown that CDP-choline causes an increase in the peripheral levels of nesfatin-1 peptide. We aimed to demonstrate the activation of nesfatin-1 neurons following CDP-choline administration and the effect of cholinergic antagonist atropine sulfate on this activation using c-Fos immunohistochemistry as the marker of neuronal activation.

**Materials and Methods:** Male rats (n=5/ group) were used and CDP-choline (1.0 g/kg) was intravenously administered (CDP-choline group). Control group received saline injections and the antagonist group received intracerebroventricular atropine sulfate (10 µl/5 µl saline) injections 15 minutes before the CDP-choline administration. Ninety minutes after last injections animals were sacrificed by perfusion fixation and brain sections were collected with vibratome. Double immunohistochemistry was employed for nesfatin-1 and c-Fos. Double-labeled neurons were counted in the supraoptic nucleus (SON) of the hypothalamus and percentages of these neurons to all nesfatin-1-positive neurons were calculated. Data were statistically analyzed between groups.

**Results:** In contrast to the control group, CDP-choline administration activated most of the nesfatin-1 neurons in SON. The number of c-Fos-positive neurons was calculated as about 6% in the control group, while the CDP-choline injection statistically increased this number to 82% (p<0.01). The number of activated nesfatin-1 neurons significantly decreased by the effect of the antagonist, atropine sulfate (26%), when compared to the CDP-choline group (p<0.05).

**Conclusion:** This study showed that CDP-choline effectively increased the number of activated nesfatin-1 neurons in the SON. The results also suggested that CDP-choline exerts this effect partly through acetylcholine receptors, since the pre-injection of muscarinic acetylcholine receptor antagonist atropine sulfate significantly blocked the neuronal activation. It is not known, at this time, if CDP-choline directly affects nesfatin-1 neurons, since no report is available in the literature demonstrating the expression of acetylcholine receptors by the nesfatin-1 neurons. It is thought that this effect might also be regulated by interneurons that can receive CDP-choline signal and in turn convey this signal to nesfatin-1 neurons using a different neurotransmitter system. Nevertheless, the results of this study strongly suggest that the cholinergic system plays an important role in the regulation of nesfatin-1 neurons. It is also plausible to suggest that CDP-choline can modulate food intake at the level of hypothalamus through a central mechanism.

## İnme modelinde arı sütü ve içeriğinde bulunan 10-HDA maddesinin astrosit reaksiyonuna etkileri

**Nursel Hasanoğlu Akbulut<sup>1</sup>, Casnsu Koç<sup>2</sup>, Gonca Topal<sup>1</sup>, Mehmet Cansev<sup>3</sup>, Özhan Eyigör<sup>4,\*</sup>**

<sup>1</sup> Bursa Uludağ Üniversitesi, Sağlık Bilimleri Enstitüsü, Histoloji ve Embriyoloji Anabilim Dalı., BURSA, Turkey

<sup>2</sup> Bursa Uludağ Üniversitesi, Sağlık Bilimleri Enstitüsü, Tıbbi Farmakoloji Anabilim Dalı, BURSA, Turkey

<sup>3</sup> Bursa Uludağ Üniversitesi, Tıp Fakültesi, Tıbbi Farmakoloji Anabilim Dalı, BURSA, Turkey

<sup>4</sup> Bursa Uludağ Üniversitesi, Tıp Fakültesi, Histoloji ve Embriyoloji Anabilim Dal, BURSA, Turkey

İnme, tüm dünyada mortalite ve morbiditenin başta gelen nedenleri arasında bulunan ve 65 yaş üstü popülasyonu ilgilendiren önemli bir hastalıktır. İskemik veya hemorajik inme olarak iki şekilde ortaya çıkar. Daha sık karşılaşılan (%85-90) iskemik inme genelde bir beyin damarının sateroskleroz/embolizm nedeniyle geçici veya kalıcı olarak tıkanması sonucu ortaya çıkıp, kanlanmanın azalmasına veya ortadan kalkmasına neden olur. Bu durum inflamasyon, oksidasyon, eksitotoksinite ve apoptoz gibi çeşitli patofizyolojik süreçlerin başlamasına neden olarak sinir hücrelerinin nekrozuna ilerler. Bu çalışmada inme patofizyolojisinde yer alan önemli bazı süreçleri baskıladığı bildirilen arı sütünün ve içeriğinde bulunan 10-hidroksi-2-dekanoik asit 10-HDA maddesinin inme sonrası ilk hasarı en aza indirmek ve onarmak için bir savunma mekanizması olan Astroglizis üzerine etkisi incelenmiştir.

Bu amaçla, orta serebral arter oklüzyonu ile deneysel iskemik inme modeli oluşturulan sıçanlar (n:21) kontrol, arı sütü (100mg/kg/gün) ve 10-HDA (3,1 mg/kg/gün) uygulanan grup olmak üzere 3 gruba ayrılmıştır. Sıçanlar tedavi sonunda (28 gün) sıçanlar transkardial yolla verilen fosfat tamponlu %4 paraformaldehid ile fikse edilmiştir. Çıkarılan beyinlerden vibratom ile 40 mikrometre kalınlığında koronal kesitler 5 seri olarak alınmıştır. Astroglizis alanları immünohistokimyasal olarak GFAP boyaması ile belirlenmiştir. GFAP ile boyanan kesitlerde öncelikle astroglizis alanlarının kontralateral hemisfer alanına oranı hesaplanması yapılmış, ipsilateral alanda da reaktif astrositlerin bulunduğu alanların toplamı elde edilerek kontralateral hemisfer alanı ile karşılaştırılmış ve astroglizisin içerdiği alanın yüzdesi belirlenmiştir. Eldes edilen veriler deney gruplarında istatistiksel olarak karşılaştırılmıştır. Elde edilen veriler 10-HDA tedavisinin (%30,06±3,93) kontrol grubuna (%18,03±2,39) kıyasla astrosit reaksiyonunu anlamlı olarak arttırdığını göstermiştir (p=0,019). Arı sütü tedavisinin de (% 21,81±2,18) kontrol grubuna göre astrosit reaksiyonunu artırma yönünde etkisi olduğu görülmesine rağmen bu artışın istatistiksel olarak anlam taşımadığı belirlenmiştir (p>0,05 p=0,126).

Bu çalışmada arı sütünün ve içeriğinde bulunan 10-HDA maddesinin deneysel inme modeli oluşturulan hayvanlarda iskemik inme hasarı sonrasında olan Astroglizisi indüklediği belirlenmiştir. Reaktif astrosit artışının, iskemi sonrası doku iyileşmesi sürecinde olumlu etkiler gösterebileceği değerlendirilmiştir.

**Keywords:** Arı sütü , 10-HDA , İnme , İmmünohistokimya , GFAP

## Yüksek yağlı diyetle indüklenen obezitenin böbrek ve mesane hasarı üzerine myrtus communis ekstraktının koruyucu etkileri

**Fatma Kanpalta**<sup>1,\*</sup>, **Büşra Ertaş**<sup>2</sup>, **Göksel Şener**<sup>3</sup>, **Feriha Ercan**<sup>1</sup>

<sup>1</sup> Marmara Üniversitesi Tıp Fakültesi, Histoloji ve Embriyoloji AD, İstanbul, Turkey

<sup>2</sup> Marmara Üniversitesi Eczacılık Fakültesi, Farmakoloji AD, İstanbul, Turkey

<sup>3</sup> Fenerbahçe Üniversitesi, Sağlık Hizmetleri Meslek Yüksekokulu, İstanbul, Turkey

**Giriş:** Obezite sıklığı tüm dünyada artmaktadır, kardiyovasküler hastalıklar, tip 2 diyabet, metabolik sendrom, kronik böbrek hastalığı gibi pek çok hastalığın etyolojisinde rol oynamaktadır [1]. Obezitenin hipertansiyon, diyabet veya önceden var olan böbrek hastalığı olmayan kişilerde böbreklere zarar verebildiği, reaktif oksijen türleri(ROT) ve enflamasyon aracılığıyla üreter sistem patolojilerine sebep olduğu gösterilmiştir [2]. Myrtus communis (MC) endemik bir bitkidir ve ekstraktının anti-obezite, antioksidan ve antiinflamatuvar etkilere sahip olduğu belirtilmiştir[3-5].

**Amaç:** Bu çalışmada YYD ile indüklenmiş obezitenin böbrek ve mesane hasarı üzerine MC ekstraktının olası koruyucu etkilerini araştırmak amaçlandı.

**Materyal ve Metod:**Wistar albino erkek sıçanlar kontrol, yüksek yağlı diyet(YYD) ve YYD+MC olmak üzere üçdeney grubuna (n=8) ayrıldı. Deney grupları, 16 hafta boyunca standart (kontrol grubu; %6 yağ) veya YYD (YYD, YYD+MC grupları; %45 yağ) ile beslendiler. YYD ve YYD+MC gruplarına serum fizyolojik ya da serum fizyolojik içinde çözünmüş MC (100 mg/kg) ekstraktı deneyin son 4 haftası boyunca orogastrik gavajla uygulandı. Deney süresi boyunca sıçan ağırlıkları her hafta ölçüldü. Deney sonunda hafif eter anestezisi altında dekapite edilen sıçanlardan alınan kan serumunda leptin, kolesterol, yüksek yoğunluklu lipoprotein(HDL) ve trigliserit değerlerine bakıldı. Böbrek ve mesane dokuları histolojik olarak değerlendirildi. NADPH oksidaz-2 (NOX-2), NFκ-B proteinlerinin dokuda lokalizasyonu immünohistokimyasal yöntemlerle gösterildi. Oksidan/antioksidan hasar parametreleri olan malondialdehit(MDA), glutatyon(GSH) ve 8-hidroksideoksiguanozin(8-OHdD); enflamasyonda rol oynayan miyeloperoksidaz(MPO) düzeyleri dokuda biyokimyasal olarak değerlendirildi. Gruplar arasındaki farklılıklar istatistiksel olarak değerlendirildi. P < 0.05 anlamlı olarak kabul edildi.

**Bulgular:** YYD grubunda vücut ağırlığının arttığı, serum kolesterol, trigliserid, HDL ve leptin seviyelerinin kontrol grubuna göre arttığı gözlemlendi. Böbrekte, Bowman kapsülü epitelyumunda hasar, genişleme, yer yer glomerül hasarı ve bazı tübüllerin lümeninde hücre artıkları, bazal membran kalınlaşması, fırçamsı kenar kaybı, kollajen artışı gözlemlendi. Mesanede ise ürotelyumda yer yer açılma ve dökülme, vasküler konjesyon ve müsküler tabakada kas demetleri arasında kollajen artışı görüldü. Hem böbrek hem mesanede NOX-2 ve NFκ-B immunpozitif hücre sayısında ve boyanma yoğunluğunda artış görüldü. Morfolojik bulgulara paralel olarak, bu grupta MDA, 8-OHdG ve MPO seviyelerinin yükseldiği, GSH seviyesinin ise düştüğü gözlemlendi. YYD+MC grubunda ise tüm bu morfolojik ve biyokimyasal bulguların kontrol düzeylerine yaklaştığı gözlemlendi.

**Sonuç:** Yüksek yağlı diyet ile indüklenmiş obezitede böbrek ve mesane hasarı oksidatif ve enflamatuvar hasarın artışına bağlı olarak gelişmiş olabilir. Myrtus communis ekstraktının antioksidan etkileriyle böbrek ve mesane hasarının düzelmesinde rol oynayabilir

**Keywords:** Yüksek yağlı diyet , böbrek , mesane , myrtus communis , oksidatif stres

### References:

1. Ejerblad E, Fored CM, Lindblad P, Fryzek J, McLaughlin JK, Nyrén O. Obesity and risk for chronic renal failure. J Am Soc Nephrol. 2006;17(6):1695-702.
2. Ninomiya T, Kiyohara Y. Albuminuria and chronic kidney disease in association with the metabolic syndrome. J Cardiometab Syndr. 2007;2(2):104-7.
3. Sen A, Ozkan S, Recebova K, Cevik O, Ercan F, Kervancıoğlu Demirci E, Bitis L, Sener G. Effects of Myrtus communis extract treatment in bile duct ligated rats. J Surg Res. 2016 Oct;205(2):359-367. doi: 10.1016/j.jss.2016.06.094
4. Ahmed AH. Flavonoid content and antiobesity activity of leaves of Myrtus Communis. Asian J Chem. 2013; 25(12): 6818-22
5. Sen A, Yuksel M, Bulut G, Bitis L, Ercan F, Ozyilmaz-Yay N, Akbulut O, Cobanoğlu H, Ozkan S, Şener G. Therapeutic potential of myrtus communis subsp. Communis extract against acetic acid-induced colonic inflammation in rats. J Food Biochem. 2017;41(1):e12297.

## Effects of vitaminD supplementation on aorta morphology in high fat/high fructose diet induced metabolic syndrome rats

**Betül Zorkaya<sup>1</sup>, Ayse Seda Akdemir<sup>2</sup>, Fatma Kaya Dagistanli<sup>2</sup>, Aynur Abdulova<sup>3</sup>, Gamze Tanriverdi<sup>3</sup>, Evrim Komurcu-Bayrak<sup>4,\*</sup>**

<sup>1</sup> Istanbul University, Aziz Sancar Institute of Experimental Medicine, Department of Genetics, Istanbul, Turkey

<sup>2</sup> Istanbul University-Cerrahpasa, Cerrahpasa Faculty of Medicine, Department of Medical Biology, Istanbul, Turkey

<sup>3</sup> Istanbul University-Cerrahpasa, Cerrahpasa Faculty of Medicine, Department of Histology and Embryology, Istanbul, Turkey

<sup>4</sup> Istanbul University, Istanbul Faculty of Medical, Department of Medical Genetics, Istanbul, Turkey

Atherosclerosis, which is the most important cause of mortality and morbidity in adults, is a chronic vascular disease due to inflammation that develops against endothelial damage (1). Chronic diseases or clinical conditions such as hypertension, obesity, dyslipidemia, diabetes mellitus caused by high fat and sugar diet are among the risk factors for the development of cardiovascular disease due to atherosclerosis(2). In this study, it was aimed to determine the effect of Vitamin D (VitD) supplementation on aortic tissue morphology and vascular senescence (3) during the development of atherosclerosis in a rat model of metabolic syndrome (4,5,6) induced by a high fatty and fructose diet.

In this study, 29 male Sprague Dawley rats were randomly divided into four groups as Control (K), Control+VitD (K+VitD), Metabolic Syndrome (MetS) and Metabolic Syndrome+VitD (MetS+VitD). For 16 weeks, MetS groups were fed high fat (17%)-fructose (17%) chow and 20% fructose water, while control groups fed standard mouse chow and normal water. Skin thickness, waist circumference, weight and fasting blood glucose levels were monitored in all rats. VitD (170 IU/week) was administered to the Control and MetS groups, once a week for 12 weeks starting from the 3<sup>rd</sup> week. At the end of the 16<sup>th</sup> week, all of the rats were sacrificed and aortic tissues were taken and embedded in paraffin. Aortic tissue sections were stained using Hematoxylin-Eosin, Masson Trichrome Stain, and Von Kossa Staining, as well as immunohistochemically with p16Ink4a antibody. All obtained results were evaluated statistically.

It was determined that VitD had a significant effect on blood glucose and waist circumference values in the experimental groups at the 16<sup>th</sup> week compared to the beginning ( $p < 0.05$ ). While mean blood glucose levels were  $75.1 \pm 29.5$  in all groups at the beginning, these values decreased with the effect of vitD at the 16th week (K;  $110.4 \pm 26.8$ , K+VitD;  $93.3 \pm 39.7$ , MetS;  $198.8 \pm 34.8$ , MetS+VitD;  $157.7 \pm 34.7$  mg/dl,  $p = 0.0001$ ) was found. In histopathological examination, in the vessel sections of the control group, elastic fibers were found to be convoluted, the epithelium intact, and the muscle cells in the tunica media retained their fusiform spindle shape in a healthy appearance. In the MetS group, it was determined that the elastic fibers lost their convoluted properties and became significantly flatter, and the smooth muscle cells between them were vacuolized in some areas and moved away from their healthy appearance. In this group, pycnotic nuclei were also seen between epithelial cells in some places. It was thought that the high-fat and high-fructose diet might have caused endothelial damage. Von Kossa histochemical staining revealed calcified areas in atheroma plaques in the MetS group. Although some flattening continued in the vitD administered group, it was determined that the vascular morphology showed similar characteristics to the control group. An increase in the number of p16 immune positive cells was observed in the MetS group when compared to the other groups.

As a result, it was determined that the metabolic syndrome model caused by high-fat and high-fructose diet disrupted the vascular structure, and this damage was largely corrected vitD supplementation.

**Keywords:** Atherosclerosis , metabolic syndrome , vitamin D , p16Ink4a

### References:

1. Gancheva S, Zhelyazkova-Savova M, Galunska B, Chervenkov T. Experimental Models Of Metabolic Syndrome In Rats. Scripta Scientifica Medica 2015 47; 2:14-21.
2. Rebane A, Akdis CA: MicroRNAs: Essential players in the regulation of inflammation. J Allergy Clin Immunol 2013, 132:15-26.
3. Katsuumi G, Shimizu I, Yoshida Y, Minamino T. Vascular Senescence in Cardiovascular and Metabolic Diseases. Front Cardiovasc Med. 2018 5;18.
4. Cardellini M, Menghini R, Martelli E, et al. TIMP3 is reduced in atherosclerotic plaques from subjects with type 2 diabetes and increased by SirT1. Diabetes 2009; 58(10): 2396-401.
5. Grundy SM, Cleeman JI, Daniels SR, et al; American Heart Association; National Heart, Lung, and Blood Institute. Diagnosis and management of the metabolic syndrome: an American Heart Association/National Heart, Lung, and Blood Institute Scientific Statement. Circulation 2005 25;112(17):2735-52.
6. Surks HK, Riddick N, Ohtani K. M-RIP targets myosin phosphatase to stress fibers to regulate myosin light chain phosphorylation in vascular smooth muscle cells. J Biol Chem 2005; 280(52): 42543-51.



## Effects of Resveratrol on inflammation and ER stress related apoptosis in fructose-fed streptozotocin induced diabetes

Fatma Kaya Dagistanli <sup>1</sup>, Ayse Seda Akdemir <sup>1</sup>, Merve Anapali <sup>2</sup>, Aynur Abdulova <sup>3</sup>, Gamze Tanriverdi <sup>3</sup>, Turgut Ulutin <sup>1</sup>, Melek Ozturk <sup>1,\*</sup>

<sup>1</sup> Istanbul University-Cerrahpasa, Cerrahpasa Faculty of Medicine, Medical Biology Department, Istanbul, Turkey

<sup>2</sup> Atatürk University, Faculty of Medicine, Medical Biology Department, Erzurum, Turkey

<sup>3</sup> Istanbul University-Cerrahpasa, Cerrahpasa Faculty of Medicine, Histology and Embryology Department, Istanbul, Turkey

Oxidative stress and inflammation play an important role in the pathogenesis of Diabetes Mellitus (DM). The increase of cytokines in serum is associated with insulin resistance and diabetes [1]. The proinflammatory cytokine, IL-1 $\beta$ , plays a crucial role in negatively regulating  $\beta$ -cell function in Type 2 DM. Proinflammatory cytokines such as interleukin-1 $\beta$  (IL-1 $\beta$ ), tumor necrosis factor- $\alpha$  (TNF- $\alpha$ ), and interferon- $\gamma$  (IFN- $\gamma$ ) stimulate  $\beta$ -cell dysfunction and apoptosis. It has been suggested that cytokines induce Endoplasmic Reticulum (ER) stress, which causes  $\beta$ -cell dysfunction and death [2-4]. However, the mechanisms have not been fully elucidated. Resveratrol is a phytoestrogen with antioxidant, anti-inflammatory, and anti-tumor properties. It has been shown to prevent IL-1 $\beta$ -mediated destruction in several cell types [5]. We aim to investigate the effects of resveratrol treatment on inflammation and endoplasmic reticulum stress-mediated apoptosis in the pancreas of 10% fructose diet and low dose Streptozotocin (STZ) induced diabetic rats.

In this study, 8 week old male Sprague-Dawley rats were randomly divided into 4 groups; 1) Diabetic group was supplied with a 10% fructose solution ad libitum, two weeks later, rats were injected with streptozotocin (40 mg/kg) and supplied with 10% fructose solution for three weeks. 2) Diabetic rats treated with resveratrol (1mg/kg/day, bw) for four weeks. 3) Non-diabetic rats treated with resveratrol (1mg/kg/day, bw) 4) Control group. At the end of 9 weeks, the rats were sacrificed and pancreas tissues were taken. During the experiment, body weight and blood glucose (BG) levels were measured. All the animals were sacrificed and their pancreas tissues were removed and prepared for light and electron microscopic examinations. The pancreas tissue sections were immunostained with Insulin, IL-1 $\beta$ , TNF- $\alpha$ , IL-6, GRP78, and active caspase-3 antibodies. TUNEL assay was used to detect apoptotic cells. All values were analyzed by statistical methods.

BG levels were significantly decreased in resveratrol treated diabetic group compared to the diabetic group. It was determined that the  $\beta$ -cells number decreased and the expressions of IL-1 $\beta$ , TNF- $\alpha$ , IL-6, GRP78, and active caspase-3 were increased in islets of the diabetic group compared to the other groups. TNF- $\alpha$  immune positive cells were also detected in the exocrine tissue of the diabetic group. In a few islet cells of the resveratrol-treated group, TNF- $\alpha$  stained weakly. The decreased insulin granules, dilated endoplasmic reticulum and autophagic vacuoles were seen in  $\beta$ -cells of the diabetic group. TUNEL positive apoptotic cells were also found in both islet cells and exocrine tissue in the diabetic group. Only a few (1-2) apoptotic cells were detected in the islets of the resveratrol treated group. It was observed that diabetes-induced glucose toxicity and inflammation caused  $\beta$ -cell loss and apoptotic cell death in both islet cells and exocrine cells.

We concluded that resveratrol administration protects  $\beta$ -cells from both glucose toxicity and cytokine damage with its anti-inflammatory effect by providing regulation of blood glucose.

**Keywords:** Diabetes , Fructose , Endoplasmic Reticulum Stress , Inflammation , Resveratrol

### References:

1. Oguntibeju OO. *Int J Physiol Pathophysiol Pharmacol.* 2019;11(3):45-63.
2. Eizirik DL, Colli ML, Ortis F. *Nat Rev Endocrinol.* 2009;5(4):219-26.
3. Rabinovitch A, Suarez-Pinzon WL. *Rev Endocr Metab Disord.* 2003;4(3):291-9.
4. Thomas HE, McKenzie MD, Angstetra E, Campbell PD, Kay TW. *Apoptosis.* 2009;14(12):1389-404.
5. Chen F, Zhou X, Lin Y, et al. *J Biomed Res.* 2010;24(5):381-388.

## Dimetiloksalilglisin ile ön koşullandırılan mezenkimal kök hücrelerden elde edilen şartlandırılmış medyum özelliklerinin incelenmesi

**Hanife Nurdan Olcar , Başak Işıldar , Serbay Özkan , Meral Koyutürk \***

Istanbul Üniversitesi-Cerrahpaşa Cerrahpaşa Tıp Fakültesi Histoloji ve Embriyoloji Anabilim Dalı, İstanbul, Turkey

İnsan umbilikal kord kaynaklı mezenkimal kök hücrelerin (MKH) hipoksimitetik bir ajan olan dimetiloksalilglisin (DMOG) ile ön koşullandırılmasıyla elde edilen şartlandırılmış medyum (DMOG-ŞM) özelliklerinin, koşullandırma yapılmayan normal ŞM (N-ŞM) ile karşılaştırılması ve terapötik önem taşıyabilecek olası değişikliklerin incelenmesi amaçlanmıştır. Primer kültür ile izole edilen MKH'lerde flow sitometri ile immünofenotipik karakterizasyon, adipojenik ve osteojenik farklılaşma deneyleri yapıldı (1). MKH'lerde immünohistokimya yöntemi ile hipoksi ile indüklenebilir faktör-1 $\alpha$  (HIF-1 $\alpha$ ) ekspresyon seviyelerine bakılarak etkin DMOG ön koşullandırma doz ve süresine karar verildi. DMOG ile ön koşullandırılan MKH'lerden elde edilen DMOG-ŞM grubu ile N-ŞM grubu karşılaştırmalı olarak incelendi. ŞM'lerin içeriğindeki büyüme faktörlerinden vasküler endotelial büyüme faktörü (VEGF), beyin kaynaklı nörotrofik faktör (BDNF), glial hücre hattı kaynaklı nörotrofik faktör (GDNF), nöral büyüme faktörü (NGF) ile proinflamatuvar sitokinlerden interferon-gama (IFN- $\gamma$ ), interlökin-17 (IL-17) ve anti-inflamatuvar sitokinlerden interlökin-10 (IL-10), interlökin-4 (IL-4) düzeylerine ELISA yöntemi ile bakıldı(2,3). Ayrıca her iki gruptaki MKH'ler geçirimli elektron mikroskobu ile morfolojik olarak incelendi (4). MKH'lerin immünofenotipik değerlendirilmesinde CD44 ve CD90 ekspresyonu >%95, CD34 ve CD45 ise <%5 olarak tespit edildi. Mikroskobik olarak MKH'lerin adipojenik ve osteojenik farklılaşmaları gösterildi. HIF-1 $\alpha$  ekspresyonunun 24 saat ve 1000  $\mu$ M DMOG uygulanan MKH'lerde arttığı tespit edildi. DMOG-ŞM'lerin içerdiği VEGF, NGF ve IL-4 düzeylerinde N-ŞM grubuna kıyasla artış olduğu saptandı. Her iki grup ŞM içeriğinde BDNF, GDNF, IFN- $\gamma$ , IL-10, IL-17'ye rastlanmadı. Elektron mikroskobik incelemede DMOG ile ön koşullandırılmış MKH'lerin daha aktif ultrastrüktürel görünüme sahip oldukları izlendi. MKH'lerin DMOG ile ön koşullandırılabilmesi ve ön koşullandırma sonucu bu hücrelerden salınan parakrin faktör içeriklerinin geliştirilebileceği gösterilmiştir. Bu bilgiler doğrultusunda hedefe yönelik terapötik ürün eldesinin DMOG ön şartlandırması ile mümkün olabileceği düşünülmektedir.

**Keywords:** Mezenkimal Kök Hücre , Şartlandırılmış Medyum , Hipoksi ile İndüklenebilir Faktör , Dimetiloksalilglisin , Geçirimli Elektron Mikroskobu

### References:

1. Isildar, B., Ozkan, S., Oncul, M., Baslar, Z., Kaleli, S., Tasyurekli, M., & Koyuturk, M. (2019). Comparison of different cryopreservation protocols for human umbilical cord tissue as source of mesenchymal stem cells. *Acta Histochemica*, 121(3), 361–367. <https://doi.org/10.1016/j.acthis.2019.02.008>
2. Esmailzade, B., Artimani, T., Amiri, I., Najafi, R., Shahidi, S., Sabec, M., Farzadinia, P., Zare, M., Zahiri, M., & Soleimani Asl, S. (2019). Dimethylxalylglycine preconditioning enhances protective effects of bone marrow-derived mesenchymal stem cells in A $\beta$ - induced Alzheimer disease. *Physiology and Behavior*, 199(November 2018), 265–272.
3. Oses, C., Olivares, B., Ezquer, M., Acosta, C., Bosch, P., Donoso, M., Léniz, P., & Ezquer, F. (2017). Preconditioning of adipose tissue-derived mesenchymal stem cells with deferoxamine increases the production of pro-angiogenic, neuroprotective and anti-inflammatory factors: Potential application in the treatment of diabetic neuropathy.
4. Ozkan, S., Isildar, B., Oncul, M., Baslar, Z., Kaleli, S., & Koyuturk, M. (2018). Ultrastructural analysis of human umbilical cord derived MSCs at undifferentiated stage and during osteogenic and adipogenic differentiation. *Ultrastructural Pathology*, 42(3), 199–210. <https://doi.org/10.1080/01913123.2018.1453905>

## Investigation of the TRF Conjugated Polymeric Nanoparticles Efficiency in vitro Blood Brain Barrier Model

**Aysegül Açıksarı**<sup>1\*</sup>, **Yusufhan Yazır**<sup>2</sup>, **Serap Mert**<sup>2</sup>, **Onur Özcan**<sup>1</sup>, **Zehra Seda Halbutoğulları**<sup>2</sup>

<sup>1</sup> Department of Stem Cell, Institute of Health Sciences, Kocaeli University, Kocaeli, Turkey

<sup>2</sup> Center for Stem Cell and Gene Therapies Research and Practice, Kocaeli University, Kocaeli, Turkey

The blood-brain barrier (BBB) is a dynamic structure that effectively separates the central nervous system (CNS) from the circulatory system and controls the passage of many substances to the brain, including most therapeutics. This is an important limiting factor in the development of new drugs for the treatment of diseases related to the CNS. The most important feature of the BBB is the existence of tight junctions between endothelial cells, which are arranged in a single cell layer. Receptors on the endothelial cells such as insulin, transferrin (TRF), low-density lipoproteins, and leptin provide receptor-mediated transport across the BBB (1). In recent years, polymeric nanoparticle (NP)-mediated drug delivery systems, particularly TRF-conjugated NPs, have been frequently studied for use in specific imaging or treatment of CNS diseases, as they can transport therapeutic compounds to the brain by crossing the BBB (2).

The aim of this study is to observe the TRF conjugated PLGA-COOH-NPs transition efficiency from in vitro BBB model. In vitro BBB models offer an opportunity in research as a tool to understand the delivery capabilities, transport mechanism, cytotoxicity of therapeutic ingredients, and to identify and evaluate optimal formulations for in vivo studies.

In order to mimic in vitro BBB model, pericytes from rat brain tissue and HUVECs were seeded on an insert, which allows cell cultivation in a different layer in 12-well plates. It was ensured that the upper part of the insert imitates the blood (apical region), and the NSCs seeded under the barrier on the bottom of the culture dish represent the brain region (basolateral region) (3). PLGA-COOH NPs, carrying Coumarin 6 as a fluorescent marker, were prepared by double emulsion technique (4) and conjugated with recombinant Anti-Transferrin (TRF) receptor antibody after functionalization with EDC (1-ethyl-3-[3-dimethylaminopropyl]-carbodiimide) and NHS (N-hydroxysuccinimide) (5). The size, surface zeta potential and polydispersity index of NPs (before and after TRF conjugation) were determined with Malvern Zeta Sizer. The in vitro BBB transition and cellular uptake efficiency of the TRF conjugated NPs were observed by immunofluorescence microscopy and flow cytometer after the 3 and 24 hours incubation.

As a result, it has been observed that the NPs can cross the BBB and the transition efficiency of TRF-conjugated ones were found higher. By this way, NPs provide stability and high efficiency of therapeutics by reaching the desired site in sufficient quantities when conjugated with TRF. In conclusion, the delivery of many different drugs or therapeutics to the brain and their use in the treatment of many different neuronal diseases will be enabled with the development of targeted NPs crossing the BBB.

Acknowledgements: Financial support was received from KOU-BAP (2019/036).

**Keywords:** Nanoparticles, Blood-brain barrier

### References:

1. Mc Carthy, D. J., Malhotra, M., O'Mahony, A. M., Cryan, J. F. ve O'Driscoll, C. M. (2015). Nanoparticles and the Blood-Brain Barrier: Advancing from In-Vitro Models Towards Therapeutic Significance. *Pharmaceutical Research*, 32(4), 1161–1185. doi:10.1007/s11095-014-1545-6
2. Saraiva, C., Praça, C., Ferreira, R., Santos, T., Ferreira, L. ve Bernardino, L. (2016). Nanoparticle-mediated brain drug delivery: Overcoming blood-brain barrier to treat neurodegenerative diseases. *Journal of Controlled Release*, 235, 34–47. doi:10.1016/j.jconrel.2016.05.044
3. Stone, N. L., England, T. J. ve O'Sullivan, S. E. (2019). A novel transwell blood brain barrier model using primary human cells. *Frontiers in Cellular Neuroscience*, 13(June), 1–11. doi:10.3389/fncel.2019.00230
4. Herrán, E., Pérez-González, R., Igartua, M., Pedraz, J. L., Carro, E. ve Hernández, R. M. (2013). VEGF-releasing biodegradable nanospheres administered by craniotomy: A novel therapeutic approach in the APP/Ps1 mouse model of Alzheimer's disease. *Journal of Controlled Release*, 170(1), 111–119. doi:10.1016/j.jconrel.2013.04.028
5. Sari, E., Tunc-Sarisozen, Y., Mutlu, H., Shahbazi, R., Ucar, G. ve Ulubayram, K. (2015). ICAM-1 targeted catalase encapsulated PLGA- b -PEG nanoparticles against vascular oxidative stress. *Journal of Microencapsulation*, 32(7), 687–698. doi:10.3109/02652048.2015.1073384

## Lead Chalcogenide Quantum Dot Solar Cells

Selçuk Birdođan \*

Gebze Technical University, Kocaeli, Turkey

In this study, PbSe, PbS and PbTe quantum dots (QDs) were synthesized. TiO<sub>2</sub> nanoparticles were coated on conductive coated glass using the Dr. Blade technique. Ligand exchange was made to quantum dots and p-n junction was formed on the TiO<sub>2</sub> structure by chemical bath technique. 5 different ionic liquids (IL) were prepared for the redox reaction. The TEM, FT-IR, PL and UV characteristics of the quantum dots were examined. SEM and EDS spectra of TiO<sub>2</sub> structures were performed. Solar cell parameters between lead chalcogen quantum dots and ionic liquids were investigated. Lead Chalcogenide QDs were observed to be more compatible with organic ILs, the efficiency of the solar cell prepared with 960 organic IL and PbSe QD was calculated as 8.257 %.

## A simple desolvation method for production of cationic albumin nanoparticles with improved drug loading

**Tugce ÖZMEN EGESÖY**, Sumeyra Cigdem Sozer, Yasar Akdogan  
*Materials Science and Engineering Department, Izmir Institute of Technology, Izmir*

The transport protein albumin has been used as a drug nanocarrier for a long time due to its versatility. Albumin is negatively charged at physiological conditions limiting its anionic drug loading capacity. However, loading of anionic drugs in the albumin nanoparticles (NPs), can be facilitated by albumin cationization. A simple desolvation method for preparation of cationic albumin NPs with improved anionic drug loading. First, bovine serum albumin was cationized with ethylenediamine molecule. Next, salicylic acid (SA) was added to the cationic bovine serum albumin (cBSA) solution prior to the desolvation. Among different desolvating agents tested, acetonitrile allowed the highest nanoparticle formation yield (54.8%) and cBSA NPs with an average size around 200 nm were obtained. SEM analyses showed that the average size of cBSA NPs decreased from ~200 nm to ~100 nm upon SA loading. Moreover, the drug loading capacity of cBSA NPs was found to increase ~2 fold, and drug release was slower compared to BSA NPs. Finally, a significant increase in cellular uptake of cBSA NPs compared to that of native BSA NPs showed the potential for improved drug delivery. Finally, a significant increase in cellular uptake of cBSA NPs compared to that of native BSA NPs showed the potential for improved drug delivery.

**Keywords:** Desolvation , Salicylic acid , Drug loading , Cationic albumin nanoparticles

### References:

1. Y. Akdogan, M. J. N. Junk, and D. Hinderberger, "Effect of ionic liquids on the solution structure of human serum albumin," *Biomacromolecules*, vol. 12, no. 4, pp. 1072–1079, 2011, doi: 10.1021/bm1014156.
2. Y. Akdogan, Y. Wu, K. Eisele, M. Schaz, T. Weil, and D. Hinderberger, "Host-guest interactions in polycationic human serum albumin bioconjugates," *Soft Matter*, vol. 8, no. 43, pp. 11106–11114, Nov. 2012, doi: 10.1039/c2sm26511g.
3. S. C. Sozer, T. O. Egesoy, M. Basol, G. Cakan-Akdogan, and Y. Akdogan, "A simple desolvation method for production of cationic albumin nanoparticles with improved drug loading and cell uptake," *J. Drug Deliv. Sci. Technol.*, vol. 60, Dec. 2020, doi: 10.1016/j.jddst.2020.101931.
4. A. Saha et al., "Fatty-Amine-Conjugated Cationic Bovine Serum Albumin Nanoparticles for Target-Specific Hydrophobic Drug Delivery," *ACS Appl. Nano Mater.*, vol. 2, no. 6, pp. 3671–3683, 2019, doi: 10.1021/acsanm.9b00607.
5. M. Jahanshahi and Z. Babaei, "Protein nanoparticle: A unique system as drug delivery vehicles," *African J. Biotechnol.*, vol. 7, no. 25, pp. 4926–4934, 2008, doi: 10.4314/ajb.v7i25.59701.

## In situ crystallization of amorphous films of Sb<sub>2</sub>S<sub>3</sub>

**Aleksandr Bagmut** , **Ivan Bagmut** \*

National Technical University "Kharkiv Polytechnic Institute", Kharkiv, Ukraine

Amorphous films of Sb<sub>2</sub>S<sub>3</sub> with stoichiometric composition were formed on substrates at room temperature in the process of thermal evaporation of powder of Sb<sub>2</sub>S<sub>3</sub> with S additives. Amorphous films of Sb<sub>2</sub>S<sub>3</sub> with the excess of Sb were formed on substrates at room temperature in the process of thermal evaporation of powder of pure antimony sulfide. Electron beam irradiation of amorphous film of Sb<sub>2</sub>S<sub>3</sub> with stoichiometric composition causes phase transformation that occurs according to the scheme of layer polymorphous crystallization. A single flat ellipse-shaped crystal of Sb<sub>2</sub>S<sub>3</sub> nucleates and grows in the film region under investigation. The dependence on time of the length of major and minor ellipse axis of this crystal has a linear character. As the ellipse-shaped crystal grows, its eccentricity decreases exponentially with time. This corresponds to decreasing in its elongation along the major axis. The dependence on time of the area of S of ellipse-shaped crystal and of the fraction crystallized  $x$  at layer polymorphous crystallization of Sb<sub>2</sub>S<sub>3</sub> has a quadratic character. Wherein the relative length  $\delta_0 \approx 4992$  [1]. A similar dependence of  $S(t)$  and  $x(t)$ , as well as the value of  $\delta_0$ , amounting to several thousand, are characteristic of electron-beam crystallization of stoichiometric films of Cr<sub>2</sub>O<sub>3</sub>, V<sub>2</sub>O<sub>3</sub> and HfO<sub>2</sub> [2].

Electron beam irradiation of amorphous non-stoichiometric films with excess of antimony initiates the predominant crystallization of Sb during the first stage of the process, and subsequent matrix Sb<sub>2</sub>S<sub>3</sub> crystallization during the second stage. As the film warms up, the density  $n$  and average value of the diameter  $\langle D \rangle$  of antimony particles monotonically increases and at saturation  $n \approx 7.5 \cdot 10^9 \text{ cm}^{-2}$  and  $\langle D \rangle \approx 0.029 \text{ }\mu\text{m}$ . Then in the amorphous matrix with inclusions of micro-crystals of Sb a single flat ellipse-shaped crystal of Sb<sub>2</sub>S<sub>3</sub> is growing. At the same time Sb particles are not nucleation centres of Sb<sub>2</sub>S<sub>3</sub> crystals. Growth of Sb<sub>2</sub>S<sub>3</sub> crystal practically does not change the spatial distribution of Sb particles. In rare cases, a displacement of particles in the direction of motion of the crystallization front was observed. The dependence on time of the length of major and minor ellipse axis of this crystal has a non linear character. So, the growth rate of the major axis and of the minor axis is not constant, but decreases with time. As the ellipse-shaped crystal grows, its eccentricity decreases exponentially with time. This corresponds to decreasing in its elongation along the major axis. The dependence on time of the area of S of ellipse-shaped crystal and of the fraction crystallized  $x$  at secondary polymorphous crystallization of Sb<sub>2</sub>S<sub>3</sub> described by a power function with the exponent of 0.68. Wherein the relative length  $\delta_0 \approx 9725$ .

**Keywords:** Amorphous state , Kinetics , Antimony sulfide , Crystallization , Electron microscopy

### References:

1. I. Bagmut, A. (2019). Functional Materials, 26, 6.
2. I. Bagmut, A.G., Bagmut, I.A. (2018). Mol. Cryst. Liquid Cryst., 673 20.

## HAADF imaging of vanadium oxide thin films: spontaneous conversion of film pores with thermal annealing

**Emrah Dirican** , **Ramis Mustafa Öksüzoğlu** \*

Department of Materials Science and Engineering, Faculty of Engineering, Eskişehir Technical University, Eskişehir, Turkey

Understanding the influence of processing parameters on thin-film structure is essential to govern the electrical properties of vanadium oxide thin films<sup>[1]</sup>. Thermal annealing is a well-known procedure to improve the electrical properties of the films. Annealing can also introduce defects into the film structure or alter the defective structure imposed by deposition conditions. High-angle annular dark field (HAADF) imaging operated in scanning transmission electron microscopy (STEM) mode provides convenience on the observation of defects<sup>[2]</sup>. It can also give hints at the growth mechanism of thin films.

In TEM, a number of electrons passing through the sample scatter at high angles as a result of interactions with the nuclei of the atoms. These electrons are strongly associated with the atomic number  $Z$  accordingly. The collection of such electrons for HAADF imaging enables the generation of images based on  $Z$  contrast. In a HAADF image, the regions constituted of high-density atoms (high  $Z$ ) are reflected in bright contrast, whereas the regions with low-density atoms (low  $Z$ ) appear in dark contrast. Since the defects, i.e., nanopores in thin films, are regions deprived of material atoms, such regions emerge in dark contrast and can be easily distinguished from the other part of the material.

In the present study, three groups of vanadium oxide thin film samples have been prepared on Si/SiO<sub>2</sub>/Si<sub>3</sub>N<sub>4</sub> substrates. As-deposited films, the first group, have been deposited at room temperature by reactive pulsed DC magnetron sputtering. The second and third groups have been obtained by annealing the as-deposited films at 200 °C and 300 °C under nitrogen gas flow. HAADF imaging unveils the structural features of the as-deposited film and the evolution of these features with annealing. In the HAADF image of the as-deposited film, the nanopores distributed uniformly over the cross-section resemble fiber-like morphology. After annealing the as-deposited film at 200 °C, the pores contract and their morphology turn into sphere. With 300 °C annealing of the as-deposited film, the pores reach their largest dimensions. The HAADF image of this film also reveals the crack formation due to stress. It is known that improvement in the crystallinity and phase transformation lead to film densification and built-in stress in turn<sup>[3,4]</sup>. This stress is annihilated by nanopore formation. In conclusion, the HAADF method has facilitated monitoring the film pores and tracking their change with thermal annealing, so that explaining the films' electrical properties.

**Keywords:** High-angle annular dark field, vanadium oxide, annealing, nanopores

### References:

1. R. Mustafa Öksüzoğlu, P. Bilgiç, M. Yildirim, and O. Deniz, "Influence of post-annealing on electrical, structural and optical properties of vanadium oxide thin films," *Opt. Laser Technol.*, vol. 48, pp. 102–109, 2013
2. K. Ide et al., "Effects of working pressure and annealing on bulk density and nanopore structures in amorphous In-Ga-Zn-O thin-film transistors," *Jpn. J. Appl. Phys.*, vol. 56, no. 3, 2017
3. S. Karwal et al., "Tailoring nanopore formation in atomic layer deposited ultrathin films," *J. Vac. Sci. Technol. A Vacuum, Surfaces, Film.*, vol. 36, no. 1, p. 01A103, 2018
4. M. G. Blanchin, B. Canut, Y. Lambert, V. S. Teodorescu, A. Barău, and M. Zaharescu, "Structure and dielectric properties of HfO<sub>2</sub> films prepared by a sol-gel route," *J. Sol-Gel Sci. Technol.*, vol. 47, no. 2, pp. 165–172, 2008

## Effect of surface treatment on the SiN passivation of AlGaIn/GaN HEMT

**Gizem Karaca**\*, İdil Karakuş, Elif Alagöz, Ahmet Serhat Dinçer, Doğan Yılmaz, Prof. Dr. Ekmel Özbay  
Bilkent University-AB MikroNano, ANKARA, Turkey

Semiconductor technology is promising in wireless communication, radar, and satellite applications that require high temperature and high voltage. High electron mobility transistors (HEMT) fabricated with wide-bandgap AlGaIn/GaN heterostructures provide advantages such as high sheet carrier concentration, high electron mobility, large electron saturation velocity and in particular high breakdown voltage in high frequency and high-power applications [1]. However, AlGaIn/GaN HEMTs have surface/interface-related problems such as large gate leakage current [2], collapse in drain current [3], aging of Schottky and Ohmic contacts [4], etc. To prevent these problems and increase its performance and reliability, AlGaIn/GaN surface chemistry is emphasized. In this direction, oxygen and ammonia treatment processes before the passivation step were compared and their effects on chemical and electrical results were investigated.

In this study, AlGaIn/GaN structure on SiC substrate is grown by the MOCVD method and 2-DEG region was formed by polarization between these materials. The fabrication of basic AlGaIn/GaN submicron transistors start with the deposition of a Ti/Al/Ni/Au (15/90/50/50 nm) multilayer by e-beam evaporation to form the ohmic contacts. After the metallization of the ohmic contacts, especial alignment marks for the e-beam lithography are etched down in the AlGaIn by using the ohmic metal as a mask. Then the ohmic metal on top of these alignment marks is removed by a combination of several wet etches. After the e-beam alignment marks have been defined, the ohmic contacts are annealed at 850°C in N<sub>2</sub> atmosphere for 30 s. A Cl<sub>2</sub>-based reactive ion etching (RIE) is used for mesa isolation. After the mesa isolation process, the 1st dielectric (SiN) coating is applied with the PECVD system to prevent electron entrapment caused by imperfections on the active surfaces of the devices, ion-induced surface degradation, and creation of the foot width in the T-Gate structure. Before 1st dielectric (SiN) coating, surface-controlled wet treatment is applied with ammonia solution to remove the oxide layer formed on the GaN surface after O<sub>2</sub> plasma to reduce the gate and drain leakage levels before this coating. After the fabrication steps were completed, electrical measurements were made of the samples that received and did not receive the native oxygen layer. It was concluded that this wet treatment performed before the passivation step reduces the leakage of gate and drain.

**Keywords:** AlGaIn/GaN Heterostructures, Passivation, High Electron Mobility Transistor, MOCVD

### References:

1. M. A. Khan et al., "AlGaIn/GaN metal oxide semiconductor heterostructure field effect transistor," *IEEE Electron Device Lett.*, vol. 21, no. 2, pp. 63–65, Feb. 2000, doi: 10.1109/55.821668.
2. S. L. Romyantsev et al., "Effect of gate leakage current on noise properties of AlGaIn/GaN field effect transistors," *J. Appl. Phys.*, vol. 88, no. 11, pp. 6726–6730, Nov. 2000, doi: 10.1063/1.1321790.
3. B. M. Green, K. K. Chu, E. M. Chumbes, J. A. Smart, J. R. Shealy, and L. F. Eastman, "Effect of surface passivation on the microwave characteristics of undoped AlGaIn/GaN HEMT's," *IEEE Electron Device Lett.*, vol. 21, no. 6, pp. 268–270, Jun. 2000, doi: 10.1109/55.843146.
4. J. Hilsenbeck et al., "Aging behaviour of AlGaIn/GaN HFETs with advanced ohmic and Schottky contacts" *Electron. Lett.*, vol. 41, no. 2, pp. 40–41, 2005, doi: 10.1049/el.



## Çift katmanlı Si<sub>3</sub>N<sub>4</sub> dielektrik tabakası ile AlGa<sub>N</sub>/Ga<sub>N</sub> HEMT aygıtların üretimi

Yıldırım DURMUS<sup>1,\*</sup>, Doğan YILMAZ<sup>1</sup>, Ceren TAYRAN<sup>2</sup>, Ekmel ÖZBAY<sup>1</sup>

<sup>1</sup> Bilkent University/AB Mikronano A.Ş, Ankara, Turkey

<sup>2</sup> Gazi University/Physics Department, Ankara, Turkey

AlGa<sub>N</sub>/Ga<sub>N</sub> HEMT aygıtlar yüksek elektron mobilitesi, elektron yoğunluğu ve yüksek kırılma gerilimleri[1] sayesinde yüksek güç ve yüksek çalışma frekansı sağlamaktadır[2,3]. Bu özellikleri sayesinde AlGa<sub>N</sub>/Ga<sub>N</sub> HEMT'ler yüksek güç, yüksek frekans ve yüksek voltaj uygulamalarında oldukça ümit veren aygıtlar olarak görülmektedir[4,5]. Bu çalışmada; Çift katmanlı Si<sub>3</sub>N<sub>4</sub> dielektrik tabakası kullanılarak AlGa<sub>N</sub>/Ga<sub>N</sub> HEMT aygıtları üretilmiş, çift katmanlı Si<sub>3</sub>N<sub>4</sub> tabakanın AlGa<sub>N</sub>/Ga<sub>N</sub> HEMT aygıtlarda elektriksel ve mekaniksel özelliklerine bakıldı. AlGa<sub>N</sub>/Ga<sub>N</sub> yapısı MOCVD yöntemi ile SiC alttaş üzerine farklı sıcaklıklarda ve kalınlıklarda büyütülerek elektriksel ve optiksel olarak karakterize edildi. Elektriksel ve optiksel karakterizasyon için XRD, Pl,Hall ve SEM ölçümleri yapıldı. AlGa<sub>N</sub>/Ga<sub>N</sub> HEMT üretiminde ilk olarak PVD yöntemi akaç ve kaynak kontaktları oluşturuldu. Daha sonra EBL tekniği ile G(gama) yapılı kapı kontağı oluşturuldu. Kapı kontağı oluşturulmadan önce yüksek büyütme sıcaklığında birinci Si<sub>3</sub>N<sub>4</sub> dielektrik tabakası akaç ve kaynak kontaktları üzerine PECVD yöntemi ile kaplandı. G(gama) kapı kontağı oluşturulduktan sonra düşük büyütme sıcaklığındaki ikinci Si<sub>3</sub>N<sub>4</sub> dielektrik tabakası G(gama) kapı ,akaç ve kaynak kontaktları üzerine kaplandı. AlGa<sub>N</sub>/Ga<sub>N</sub> HEMT aygıtların üretimi tamamlandıktan sonra DC ölçümü, RF Ölçümü ve RF güç ölçümü yapılmıştır. Mekaniksel olarak da birinci Si<sub>3</sub>N<sub>4</sub> tabakası ile ikinci Si<sub>3</sub>N<sub>4</sub> tabakasının stress ölçümleri yapıldı. Üretilen AlGa<sub>N</sub>/Ga<sub>N</sub> HEMT aygıtlarda 1.5 GHz'de 45.56dBm (35.90 W) çıkış gücü ve %69.85 verimlilik elde edildi. Stress olarak birinci Si<sub>3</sub>N<sub>4</sub> tabakasında 300 Mpa, ikinci Si<sub>3</sub>N<sub>4</sub> tabakasında ise 240 Mpa stress değeri görüldü.

**Keywords:** AlGa<sub>N</sub>, Ga<sub>N</sub>, HEMT,XRD,Pl,Hall,SEM, Gamma kapı kontağı, Si<sub>3</sub>N<sub>4</sub>,Stress,RF ölçümü

### References:

1. S. Sze, K. Ng, "Physics of Semiconductor Devices," John Wiley& Sons, (2006).
2. J. Zolper, "A review of junction field effect transistors for hightemperature and high power electronics," Solid State Electron 42, 2153-2156 (1998).
3. M. Alim, M. Ali, A. Rezazadeh, C. Gaquiere, "Thermal response for intermodulation distortion components of GaN HEMT for lowand high frequency applications," Microelectronic Engineering209, 53-59 (2019).
4. A. Chvala, J. Marek, P. Pribytnya, A. Satka, S. Stoffels, N.Posthuma, S. Decoutere, D. Donoval, "Analysis of multifinger power HEMTs supported by effective 3-D device electrothermalsimulation," Microelectronics Reliability 78, 148-155 (2017)
5. A. Mojab, Z. Hemmat, H. Riazmontazer, A. Rahnamaee, "Introducing optical cascode GaN HEMT," IEEE Transactions on Electron Devices 64, 796-804 (2017).

## Ex Vitro ve İn Vitro Ortamda Yetiştirilen Doğal Tetraploid Trifolium pratense L. Köklerinin Karşılaştırmalı İnce Yapısı

**Havva Karahan \* , Hatice Çölgeçen**

Department of Biology, Faculty of Arts and Sciences, Zonguldak, Turkey

Bu çalışmada, doğal tetraploid Trifolium pratense L.'nin tohumları Zonguldak Bülent Ecevit Üniversitesi Biyoloji Bölümüne ait deneme bahçesinde çimlendirilmiştir. Diğer taraftan doğal tetraploid T. pratense L.'nin tohumları yüzey sterilizasyonu gerçekleştirildikten sonra bitki büyüme düzenleyicisi içermeyen Murashige ve Skoog (1962) ortamında çimlendirilmiştir. Ex vitro ve İn vitro yetiştirilen bir aylık fidelerin köklerinden diseksiyon yapılmıştır. Her iki ortamda yetiştirilen köklerin ince kesitleri alınarak TEM ile karşılaştırmalı ince yapısının incelenmesi amaçlanmıştır. Alınan ince kesitler, SATO kurşun boyaması yapıldıktan sonra, geçirimli elektron mikroskopunda incelenmiştir. Parankimatik hücrelerin ince yapıları bakımından her iki örnekte de hücreler benzer olarak dairesel ve büyüktür. Aynı zamanda hücrelerde vakuol, ribozomlar ve az sayıda mitokondri vardır. Deneme bahçesinde yetiştirilmiş bitkiden alınan kök kesitlerinde farklı olarak, hücre duvarı daha kalın, sitoplazma ise hücre duvarlarına paralel olarak vakuolün etrafında belli belirsiz bir tabaka halindedir. Hücreler çok büyük merkezi vakuollere sahiptir. Vakuollerde tonoplast net olarak ayırt edilebilmektedir. Vakuoller içinde az sayıda zar parçaları vardır.

İn vitro besin ortamında yetiştirilmiş bitkiden alınan kök kesitlerinde ise hücre duvarı daha incedir. Sitoplazma hücre duvarlarına paralel olarak vakuolün etrafında belirgin bir tabaka halindedir. Hücreler daha küçük vakuollere sahiptir ve tonoplasta yapışık çok fazla sayıda elektron yoğun damlacıklar görülmüştür. Vakuoller içinde çok sayıda zar parçaları vardır. Merkezi vakuoller çok büyük olduğundan sitoplazma hücre zarı ve tonoplast arasına sıkışmış durumdadır. Aynı zamanda kloroplastlar mevcuttur.

**Keywords:** Aseptik fide , Doğal tetraploid Trifolium pratense L. , Ex vitro , İnce yapı , İn vitro

### References:

1. Coon J.T., Pittler M.H., Ernst E. (2007) Trifolium pratense isoflavones in the treatment of menopausal hot flushes: A systematic review and meta-analysis. *Phytomedicine*, 2(3), 153-159.
2. Çölgeçen H., Koca U., Büyükkartal H.N. (2011) Sayfa 975-980. Nuts and Seeds in Health and Disease Prevention. Use of Red Clover (Trifolium pratense L.) seeds in Human Therapeutics. Editors: Preedy, V.R., Watson, R.R., Patel, V.B. USA: Academic Press.
3. Çölgeçen H., Büyükkartal H.N., Koca-Çalışkan U. (2016) Ultrastructural observations in somatic embryogenesis of natural tetraploid Trifolium pratense L.. *Turk J Bot*, 40: 496-505.
4. Kaurinovic B., Popovic M., Vlajsavljevic S., Schwartzova H., Vojinovic-Miloradov M. (2012) Antioxidant Profile of Trifolium pratense L.. *Molecules*, 17(9): 11156-11172.
5. van de Wewijer P., Barentsen R. (2002) Isoflavones from red clover (Promensil (R)) significantly reduce menopausal hot flush symptoms compared with placebo. *Maturitas*, 42, 187-193.

## Optimizing a workflow for cryo-TEM tomography – fabrication and transfer of frozen hydrated lamella

**Dominik Pinkas<sup>1</sup>, Samuel Zachej<sup>3</sup>, Jana Havrankova<sup>3</sup>, Helena Raabova<sup>1</sup>, Erik Vlcek<sup>1</sup>, Saskia Mimietz-Oeckler<sup>4</sup>, Robert Kirmse<sup>4</sup>, Pavel Hozak<sup>2</sup>, Vlada Filimonenko<sup>1,2 \*</sup>**

<sup>1</sup>Electron Microscopy Core Facility, Institute of Molecular Genetics ASCR, Prague, Czech Republic, vlada@img.cas.cz

<sup>2</sup>Department of Biology of the Cell Nucleus, Institute of Molecular Genetics ASCR, Prague, Czech Republic;

<sup>3</sup>TESCAN ORSAY HOLDING, a.s., Libušina třída 21, 623 00 Brno, Czech Republic

<sup>4</sup>Leica Mikrosysteme GmbH, Hernalser Hauptstraße 219, 1170 Vienna, Austria

Electron microscopy provides unique insight into the ultrastructure of cells and tissues. Preservation of sensitive biological samples in close-to-native state is crucial for obtaining quality data. Vitrification with subsequent observation in cryo conditions in an electron microscope is a valuable approach. Cryo-electron tomography is a method of choice to gain volume information about the object. A serious technical limitation is the thickness of the object. While small objects, like bacteria, viruses, isolated cellular organelles, or thin areas of cytoplasm at the edge of a eukaryotic cell can be imaged directly, bigger parts of cells or tissues need to be thinned before observation. Fabrication of a thin FIB-milled lamellae from a frozen hydrated sample with subsequent cryo-transfer and tilt series acquisition in cryoTEM is currently the best workflow introducing minimal artefacts into the sample compared to other available techniques. The workflow is technically challenging and needs significant skills and optimization of all steps to produce homogeneously thin lamella and to avoid heat damage, mechanical damage, and surface contamination of the lamella.

We demonstrate optimization of the semi-automated cryo TEM lamella preparation workflow on yeast, mammalian and plant samples using TESCAN FIB-SEM Cryo AMBER system equipped with the Leica VCT500 cryo transfer stage for operation in cryogenic conditions. The use of a side-entry TEM cryoholder makes the workflow more universal and accessible for a broader range of microscopy workplaces, compared to autoloader-equipped systems that are currently used in most cases.

Acknowledgements: This project is supported by MEYS CR (LRI Czech-BioImaging LM2018129, COST Inter-excellence internship LTC19048), OPVVV (CZ.02.1.01/0.0/16\_013/0001775), IMG grant (RVO: 68378050)

**Keywords:** cryo FIB-SEM, cryo-TEM, biological sample preparation

## Thermo Fisher Scientific EM workflows; Developed for the masses

**Emine Korkmaz\*, Gaurav Sharma, Max Maletta, Lavery Leah, Anke Mulder**

Materials and Structural Analysis, Analytical Instruments Group, Thermo Fisher Scientific Achtseweg Noord 5651 GG, Eindhoven, Netherlands

As cryo-electron microscopy (cryo-EM) continues to mature, an increasing number of researchers from around the world use this cutting-edge technique to gain insight into many of today's leading scientific research. Scientists use cryo-EM because of its unique ability to examine samples at high resolution in their near-native state, which is leading to breakthrough discoveries. As cryo-EM instruments become easier to use while generating higher resolution results, these discoveries are taking place at an unprecedented pace.

From neurodegenerative diseases such as Alzheimer's and Parkinson's to infectious diseases such as COVID-19, cryo-EM is leading to new discoveries that are pushing the boundaries of research.

Several recent studies have used cryo-EM to uncover structures related to SARS-CoV-2, the strain of coronavirus that causes the COVID-19 disease. Scientists at Regeneron used cryo-EM to determine the structural features of individual antibodies (REGN10933 and REGN10987) that simultaneously bind the receptor-binding domain of the spike protein, accelerating the development of a SARS-CoV-2 therapeutic antibody cocktail that has moved into human trials.

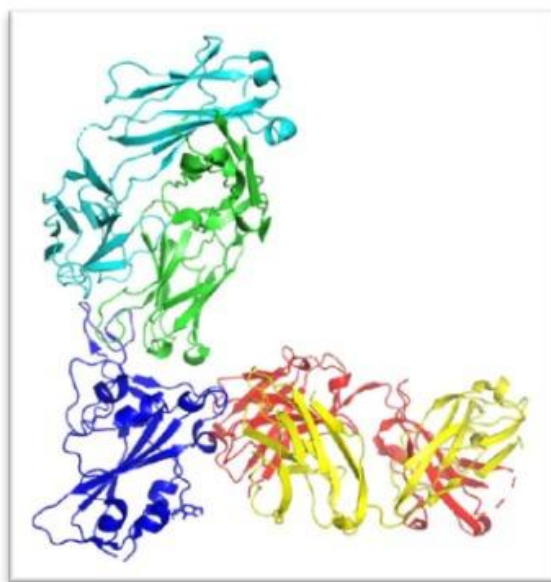


Figure 1. a) SARS CoV-2 receptor binding domain (in dark blue) in complex with potential therapeutic antibodies REGN10933 (heavy and light chains in green and cyan) and REGN10987 (heavy and light chains in yellow and red).

Understanding complex 3D architecture of cells and tissues is essential for the investigation of biological structure-function relationships. That is why biologists rely on 3D imaging techniques, such as physical sectioning or optical serial imaging, to study cellular ultrastructure and morphology. Traditional microtomy, however, relies on the production and imaging of individual sample sections, which can be challenging and time consuming.

Large volume analysis (LVA) performed in scanning electron microscopes (SEMs), is an increasingly popular technique for the high-resolution imaging of cellular ultrastructure. Using these instruments, scientists can study cellular structures at nanometers resolution across millimeters of volume. The Volumescope Apreo 2 System<sup>TM</sup> offers an improved axial resolution by combining the mechanical microtome with optical sectioning. After each section is cut from the block face, the exposed sample is imaged with a series of increasing accelerating voltages. This generates a 3D subset of optical subsurface layers that provide isotropic information with 10 nm Z-resolution. The ability to quickly remove the microtome allows you to switch the system back to normal 2D SEM operation or even to automated tomography through the addition of optional Thermo Scientific Maps<sup>TM</sup> Software.

**A novel concept in fluorescence lifetime imaging enabling video-rate confocal FLIM**

**Jens Peter Gabriel**

Leica Microsystems, Mannheim, Germany

Confocal Microscopy is the gold standard for imaging 3-dimensional fluorescent samples with high spatial resolution. Advanced confocal applications demand multicolor flexibility, sensitivity to capture dim signals, and/or speed to allow acquisition of fast and dynamic events in living samples. In addition to spectral and intensity-based information, Fluorescence Lifetime Imaging (FLIM) adds a new dimension of contrast to your imaging, opening the door to biosensing and tracking of interactions between proteins.”

## Author Index

Abban Mete, G.	98	Bayraktar, A.	7
Abdulova, A.	54, 62, 96, 102, 103	Baysan Cebi, H.	46, 95
Acar Aydemir, N.	56, 57	Bingol Ozakpinar, O.	64
Acikel Elmas, M.	64, 97	Birdođan, S.	106
Acikgoz, E.	53	Birge, B. R.	44
Açıksarı, A.	81, 105	Bıyık, F. A.	78
Açıksarı, C.	83	Botton, G.	27
Ađaođulları, D.	84, 86	Brindle, K.	21
Agar, A.	65	Bulut, B.	90
Akaođlu, B.	89	Calik-Kocaturk, D.	53
Akdemir, A.	102, 103	Cansev, M.	100
Akkaya, P.	67	Çelik, S.	89
Akkoç, T.	35	Cenacchi, G.	19
Akman, A.	74	Çetinavcı, D.	48, 74
Akpolat, M.	79	Cetinkaya Un, B.	79
Aktuđ, H.	53	Chang, C.	91
Alagöz, E.	110	Chipuk, J.	42
Algilani, S.	64	Christiani, G.	9
Aliyazicioglu, Y.	78	Çölgeçen, H.	54, 96, 112
Altunayar-Unsalan, C.	53	Çomar, M.	59
Alver, A.	74	Contuk, G.	98
Anapali, M.	103	Çorapçıođlu, G.	22
Arbak, S.	51, 64, 97	Coşkun, C.	99
Arbiol, J.	3	Couchman, J.	30
Arıcı, T.	78	Cumbul, A.	68
Arpapay, B.	22	Daghoglu, Y.	72
Aslan, D.	81	Delibaş, B.	69
Atac, F.	95	Demir, N.	60
Atar, H.	96	Demir, S.	78
Ay, F.	43	Demiralın, B.	84
Aydemir, S.	77	Demirtaş, H.	87, 88
Aydin, M.	93	Deveci Ozkan, A.	51
Aydın, D.	87, 88	Dilmac, S.	49
Aydos, K.	55	Dinçer, A.	110
Aysel, E.	86	Dirican, E.	109
Ayşit, N.	80	Dodurga, Y.	98
Baban, D.	68	Dođan, D.	95
Bagmut, A.	108	Duchamp, M.	33
Bagmut, I.	108	Duman, Ş.	90
Balci, C.	56, 57	Durmuş, Y.	89, 111
Banerjee, R.	11	Duygulu, Ö.	87, 88
Bariş, V.	89	Ekiz-Yılmaz, T.	54, 96
Bascil Tutuncu, N.	46	Elbe, H.	48
Baykara, B.	77	Elçin, Y.	37

Elmas, C.	67	Jung, Y.	87, 88
Emik, S.	66	Kafa, M.	99
Ercan, F.	71, 101	Kaleci, B.	54, 96
Erdem, E.	38	Kanpalta, F.	71, 101
Erdemli, E.	55	Kao, C.	91
Eriřir, A.	8	Kaplan, A.	63
Erkanli Senturk, G.	58, 62, 66	Kaplan, D.	6
Erol, S.	46	Kaplan, S.	69
Ertař, B.	71, 101	Kara, S.	73
Eyigör, Ö.	99, 100	Karaca, G.	110
Fernández, M.	39	Karahan, H.	112
Filimonenko, V.	113	Karahüseyinođlu, S.	59
Fujimoto, T.	2	Karakaya, C.	85
Gabriel, J.	115	Karakuř, İ.	110
Genç, E.	68	Kaya Dagistanli, F.	102, 103
Gnauck, J.	94	Kaya, P.	82
Gökçe, H.	86	Kaya, S.	85
Golal, E.	56, 57	Kaya, S.	75
Gorgulu, V.	53	Kayabölen, A.	59
Gorurođlu Ozturk, O.	72	Kayıřlı, Ü.	11
Gregori, G.	82	Kaymaz, F.	95
Gülgün, M.	22	Kaymaz, F.	46, 95
Güneř, A.	63	Keimer, B.	9
Guney Eskiler, G.	51	Keleř, E.	68
Gür Kutlu, B.	76	Kepaptsoglou, D.	10
Gürsoy Gürgen, D.	63	Kerimođlu, G.	78
Güzelel, B.	73	Kim, G.	9
Halbutođulları, Z.	81, 105	Kim, M.	9
Hasanođlu Akbulut, N.	99, 100	Kirmse, R.	113
Hasırcı, V.	5	Kittel, A.	12
Havrankova, J.	113	Koç, C.	100
Hawes, P.	32	Kocabay, A.	59, 61
Heggen, M.	15	Köksal, D.	50
Hell, S. W.	1	Komurcu-Bayrak, E.	102
Hetherington, I.	11	Korkmaz, B.	84
Hozak, P.	113	Korkmaz, E.	114
Hozak, P.	45	Köse, K.	55
Hsu, C.	91	Koyutürk, M.	104
Humbel, B.	31	Kulaber, A.	78
Ignatans, R.	33	Kurt, S.	77
Ilgen, O.	77	Kutlu, A.	76
İnanç, İ.	55	Kutlu, H.	52
Ince, N.	72	Kuyucu, Y.	72, 73
Iřıldar, B.	62, 104	Leah, L.	114
Jiao, C.	92	Lim, H.	87, 88
Jones, L.	34	Liv, N.	29

Logvenov, G.	9, 28	Sahin, B.	97
Maier, J.	82	Şahin, G.	59
Maletta, M.	114	Sahin, H.	58, 62, 66
Manojlović Stojanoski, M	23	Şahin, U.	13
Medwal, R.	33	Şaker, D.	73
Mert, S.	81, 105	Sapmaz, T.	70
Mertdinç, S.	84, 86	Savaci, U.	83
Mete, U.	73	Savci, V.	99
Mimietz-Oeckler, S.	113	Schlom, D.	28
Mueller, A.	33	Seçme, M.	98
Mulder, A.	114	Şegota, S.	24
Najimi, M.	36	Seker, U.	75
Nergiz, Y.	75	Şener, G.	71, 101
Niemann, U.	9	Serincan, U.	22
Okan Oflamaz, A.	60	Sertdemir, Y.	72
Öksüzoğlu, R.	109	Serten, M.	84
Oktem, G.	53	Sezer, Z.	58, 62
Olcar, H.	104	Sharma, G.	114
Oltulu, F.	53	Söyler, G.	59
Öngünşen, İ.	68	Sözen, B.	40
Öveçoğlu, M.	84, 86	Sürmeli, Y.	84
Özbay, E.	89, 110, 111	Suvacı, E.	83
Ozbey Unlu, O.	56	Suyolcu, Y.E.	9, 22, 28, 82
Özcan, O.	105	Süzer, İ.	86
Özçiçek, İ.	80	Takagi, H.	9
Özdemir Taş, D.	55	Takamatsu, T.	18
Özdemir, İ.	63	Tang, P.	14
Ozdil Bay, B.	53	Tanriover, G.	49, 65
Özgül Önal, M.	48	Tanrıverdi, G.	54, 96
Ozkan, A.	65	Taş, M.	98
Özkan, S.	104	Taskin, A.	59, 61
Özkavukcu, S.	55	Tayran, C.	111
Özkaya, D.	16	Tel Çayan, G.	98
Özlu, N.	20	Tendürüs, G.	89
Özmen Egesoy, T.	107	Tileli, V.	33
Öztürk, F.	48	Tiukalova, E.	33
Ozturk, M.	51, 103	Toker, Ç.	73
Parlak Ak, T.	47	Topal, G.	99, 100
Pinkas, D.	113	Topkaraoğlu, S.	70
Raabova, H.	113	Toptan, F.	41
Ramasse, Q.	4	Totary-Jain, H.	11
Rawat, R.	33	Tuna, Ö.	87, 88
Rodoplu, D.	91	Turan, S.	82, 83
Sag, F.	58	Turkmen, N.	78
Sağlam, N.	74	Ulaş Aytürk, N.	80
Sahaboglu, A.	67	Ulutin, T.	103



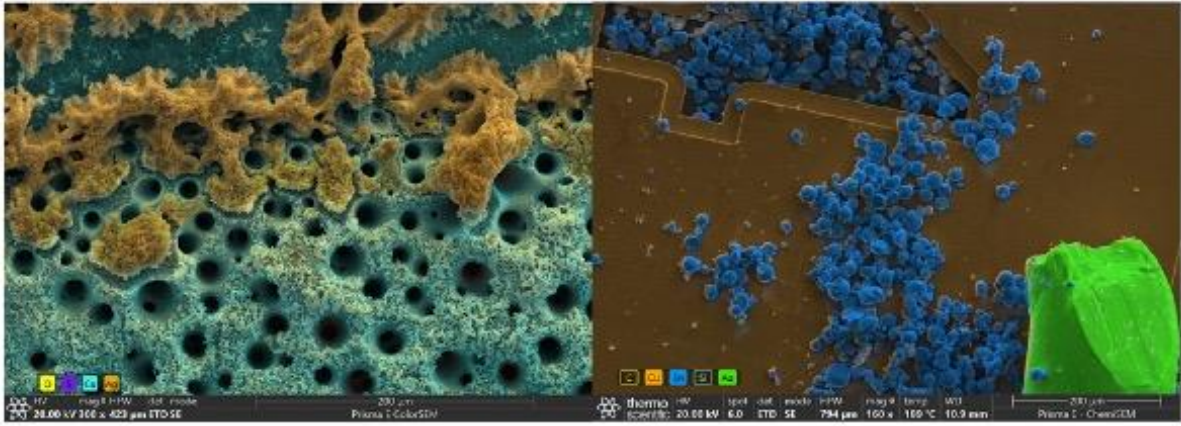
<b>Un, B.</b>	79	<b>Yang, W.</b>	87, 88
<b>Unsalan, O.</b>	53	<b>Yaşar, V.</b>	48
<b>Usta, M.</b>	87, 88	<b>Yazır, Y.</b>	79, 81, 105
<b>Ustunel, I.</b>	56, 57	<b>Yenilmez, E.</b>	74, 76, 78
<b>Uysal, A.</b>	53	<b>Yiğittürk, G.</b>	48
<b>Van Aken, P.</b>	9, 22, 28, 82	<b>Yildirim Ildem, S.</b>	49, 65
<b>VanWye, J.</b>	11	<b>Yilmaz, B.</b>	77
<b>Vas, J.</b>	33	<b>Yilmaz, D.</b>	89, 110, 111
<b>Vejselova Sezer, C.</b>	52	<b>Yilmaz, F.</b>	77
<b>Verdi, H.</b>	95, 46	<b>Yılmaz, Ü.</b>	50
<b>Verkade, P.</b>	17	<b>Yonar, D.</b>	50
<b>Vlcak, E.</b>	113	<b>Yucel, O.</b>	66
<b>Wang, Y.</b>	9	<b>Zachej, S.</b>	113
<b>Watanabe, M.</b>	26	<b>Zakeri, Z.</b>	25
<b>Wickramage, I.</b>	11	<b>Zorkaya, B.</b>	102
<b>Wu, Y.</b>	9	<b>Zrenner, E.</b>	67
<b>Yalçın, Y.</b>	46, 96		

## Apreo 2 S Color SEM



<b>High Vac</b>	
15kV (BD)	0.5 nm
0.5 kV	0.8 nm
0.2 kV	1.2 nm
<b>Low Vac</b>	
15kV (30 Pa)	1.2nm

- Özel kolon tasarımı sayesinde 500V' da 0.8 nm çözünürlük.
- T1, T2 ve T3 dedektörleri ile benzersiz kontrast. 8 segmentli DBS ve GAD imkanı, 11 Segmentli STEM dedektörü ve 12 portlu Numune Odası.
- Tam entegre EDS dedektörü ve ColorSEM teknolojisi ile element dağılımının anlık renkli SEM görüntüsü.
- Eucentric numune tablası özelliği ile odak ve çalışılan bölge kaybedilmeksizin 90 derece tilt imkanı.
- "Flash" ve "Smart Align" teknolojisi ile kullanıcı dostu sistem.
- MAPS yazılımı ile tüm optik mikroskoplar (Konfokal, Raman, IR vb.) ile korelasyon imkanı + otomasyon.
- 500 Pa' a kadar Düşük Vakum Opsiyonu.
- Özel PLA donanımı ile düşük vakumda en doğru ve en güvenilir EDS ölçümü.
- 18 düz, 3 ön eğimli, cross section örnek kısmına ek 12 TEM gridi tutucusu içeren özel numune tablası ile bir seferde 30' dan fazla numune yükleme imkanı...



## Axia ChemiSEM



- 2021' de Thermo Fisher' in piyasaya sunduğu, element dağılım bilgisine göre çok hızlı Renkli SEM görüntüsü verebilen Tungsten kaynaklı SEM sistemi
- Undo/Redo, Kolon ve Tarama ayarları, Sürüklenme Düzeltme vb. gelişmiş yazılım özellikleri ve ayarlar ile en kolay ve en hızlı kullanımına imkan tanıyan temel SEM sistemi.
- 10 kg' a kadar ağırlıkta ve yaklaşık 13 cm yükseklikte örnekle çalışabilen tek SEM sistemi.
- 90 derece tilt imkanı.
- R-BSE, R-CL gibi birçok opsiyona destek veren SEM sistemleri içerisinde fiyat/performans olarak benzersiz.
- Beam Deceleration, Düşük Vakum gibi opsiyonel modlar.



## Spectra Ultra S/TEM



Spectra Ultra S/TEM	Energy spread*	Information limit	STEM resolution
Probe corrector + X-EDG	0.4 eV or 0.2 eV**	100 ppm	30 pm (30 pm @ 30 kV with 100 pA of probe current)
Probe + image corrector + X-EDG	0.4 eV or 0.2 eV**	70 ppm	30 pm (30 pm @ 30 kV with 100 pA of probe current)
Probe + image corrector + X-EDG Mono	0.2-0.3 eV***	50 ppm	• 30 pm (with 30 pA of probe current) • 125 pm at 30 kV (with 20 pA of probe current)
Probe + image corrector + X-EDG UltraMono	0.025 eV****	30 ppm	• 30 pm (with 30 pA of probe current) • 125 pm at 30 kV (with 20 pA of probe current)

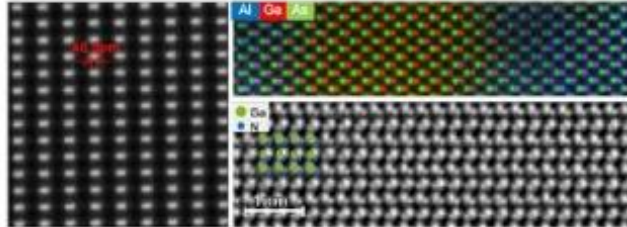
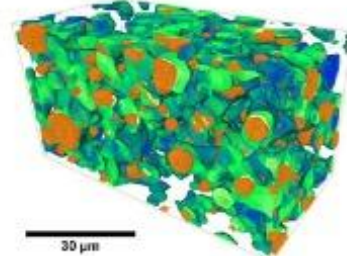


Figure 5. HAADF drift-corrected frame integration (DCFI) STEM image of GaN [212] at 300 kV (left), showing 40.5 pm Ga-Ga dumbbell splitting on a wide-gap pole piece. EDS spectrum imaging of an AlGaAs/GaAs interface using the Ultra-X Detector at 200 kV (top right). GaN [110] imaged with iDPC STEM at 80 kV. Both Ga and N columns are simultaneously revealed (bottom right).

## Scios 2 DualBeam

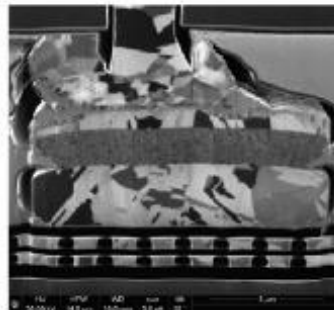
**Focused Ion Beam Scanning Electron Microscope for ultra-high resolution, high quality sample preparation and 3D characterization**

### TEM Sample Prep by DB



Scios 2 DualBeam FIB/SEM for ultra-high resolution sample preparation and 3D characterization. Scios 2 DualBeam FIB/SEM for ultra-high resolution sample preparation and 3D characterization. Scios 2 DualBeam FIB/SEM for ultra-high resolution sample preparation and 3D characterization.

## Helios™ G4 PFIB UXe DualBeam™ Xenon Plasma FIB



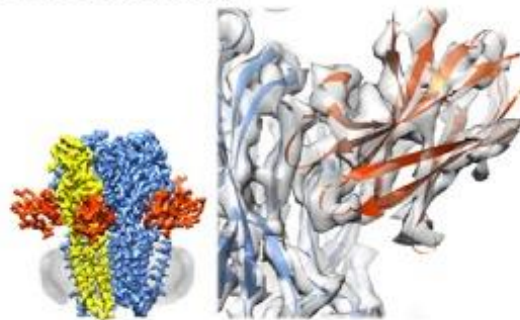
## CRYO - Life Science Systems & Application Workflow

Tomography requires a workflow



**Answer Your Biological Questions**

- 1-) Biochemistry Optimization
- 2-) Vitrification Optimization
- 3-) Structural Determination
  - Protein-protein interaction mapping
  - Ligand binding
  - Model building



**ANATEK**  
Analitik ve Araştırma Cihazları

GABAA receptor Protein interaction mapping

# Mikroskopi Sarf ve Kimyasallarına *Yepyeni Bir Soluk*

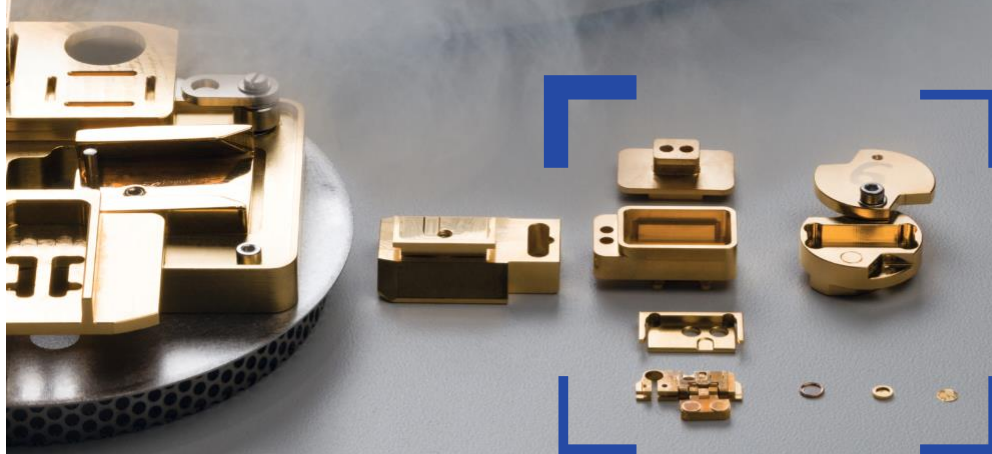
Mikroskopi Sarf ve Kimyasalları konusunda dünyanın en geniş yelpazesine sahip lider **Electron Microscopy Sciences (EMS)**  
Türkiye Yetkili Temsilciliği artık S-TEM'de!

**Electron  
Microscopy  
Sciences**

**S-TEM**

[www.s-tem.com.tr](http://www.s-tem.com.tr)

# Imaging the near-to-native state



## **ZEISS Correlative Cryo Workflow**

Connect widefield, laser scanning, and FIB-SEM microscopes in a seamless and easy-to-use procedure. ZEISS Correlative Cryo Workflow provides hardware and software optimized for the needs of correlative cryogenic microscopy, from localization of fluorescent macromolecules to high-contrast volume imaging and on-grid lamella thinning for cryo electron tomography.

[zeiss.com/cryo](https://zeiss.com/cryo)

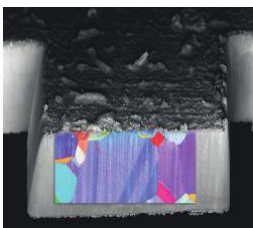


Seeing beyond

# From nano to macro in femtoseconds.



## ZEISS Crossbeam laser



The LaserFIB enhances your *in situ* studies. Gain rapid access to deeply buried structures. Prepare cross-sections up to mm in width and depth for EBSD within minutes. Machine meso-scale large structures for mechanical tests. Minimize sample damage and avoid contamination of your FIB-SEM chamber as you perform work with the femtosecond laser in a dedicated chamber.

[zeiss.com/crossbeam](http://zeiss.com/crossbeam)



Seeing beyond